Comparison of the Stabilities and Solution Structures of Metal Ion Complexes Formed with 5′-di- and 5′-triphosphates of Purine Nucleosides

INAUGURALDISSERTATION

zur Erlangung der Würde eines Doktors der Philosophie
vorgelegt der
Philosophisch-Naturwissenschaftlichen Fakultät
der Universität Basel

von

Emanuela Minari Bianchi
aus Mailand, Italien

Basel, 2003

GENEHMIGT VON DER
PHILOSOPHISCH-NATURWISSENSCHAFTLICHEN FAKULTÄT

auf Antrag der Herren

Prof. Dr. Dr. h.c. Helmut Sigel

und

Prof. Dr. Thomas A. Kaden

Basel, den 18. November, 2003

Prof. Dr. Marcel Tanner

Dekan

To Florian

This work was carried out at the Institute of Inorganic Chemistry, University of Basel, under the guidance of Professor Dr. Dr. h.c. Helmut Sigel.

I am thankful to Professor Sigel for his constant interest in my research, as well as for his encouragement to participate in scientific events.

I owe my gratitude to Professor Dr. Thomas Kaden for taking care of the *Korreferat*.

The Swiss National Science Foundation is gratefully acknowledged for providing the consumables as well as for the scholarships awarded, which were crucial to the completion of this project.

I thank Mrs. Astrid Sigel for reading and correcting my thesis and for her enjoyable presence in the lab, whenever it was mostly needed.

I am also thankful to Dr. Bin Song for his guidance through the secrets of the titration techniques and for his precious help at the beginning of my thesis; to Dr. Claudia Blindauer and Dr. Larisa Kapinos for teaching me how to use the titrino and for the interesting scientific discussions. I owe my sincere gratitude to other past and present members of Professor Sigel's group, in particular to: Dr. Rolf Griesser, Mrs. Jing Zhao, Dr. Marc Lüth, Mr. Alfonso Fernández-Botello, and Dr. Gunnar Kampf, for making my time in Basel as interesting and enjoyable as it could have been.

I had the pleasure of working with Dr. Carla Da Costa and Mrs. Rita Baumbusch, whose presence, constant help, and friendship made these years unforgettable. Thanks.

I am grateful to Dr. Wolfgang Kampf for reading part of my thesis and for his useful suggestions; to Mrs. Anke Kampf for giving me the best of the presents: time. A whole week to finish writing this work, without any external interruptions.

Of course, I owe my sincere gratitude to my parents for their patience, their love and encouragement through all these years.

Finally, I wish to thank my sister (for correcting parts of this thesis, for her constant help through all my life, for being so close no matter how far) and my child Florian (for falling asleep every now and then, giving me a chance to work at this thesis).

Contents

Chapter 1

Introduction

1.1 Nucleotides and metal ions

Genes in all prokaryotic and eukaryotic organisms are made of DNA; in viruses, they are made of either DNA or RNA. Even though nucleic acids had been discovered in 1869 by Friedrich Miescher, who isolated them from the nucleus of leucocytes, the hereditary function of DNA was first established in the 1940s with the work of Avery, MacLead, and McCarty [1–4]. Yet, the realization that nucleic acids are anions and for this reason require cations such as metal ions, protonated amines, or protonated amino acid side chains came about much earlier (already in 1924, E. Hammarsten was aware of the need of cations that should neutralize the negative charge of nucleic acids [5]). Nucleic acids are macromolecules built from nucleotides joined by phosphodiester linkages. A nucleotide is made up of a nucleobase, a cyclic sugar and a phosphate unit. There are mono-heterocyclic bases, pyrimidines (cytosine, C; thymine, T, in DNA; and uracil, U, in RNA) and di-heterocyclic bases, purines (guanine, G, and adenine, A). These bases are attached to the C1′ position of a cyclic sugar, β-D-ribose in RNA, β-D-2′-deoxyribose in DNA. In the corresponding nucleotides, the sugars are phosphorylated in their 5′ position.

The nucleobases carry genetic information while their sugar and phosphate groups perform a structural role in DNA and RNA, in which the bases participate. Modified nucleobases occur at some stage in DNA: for instance, the activity of

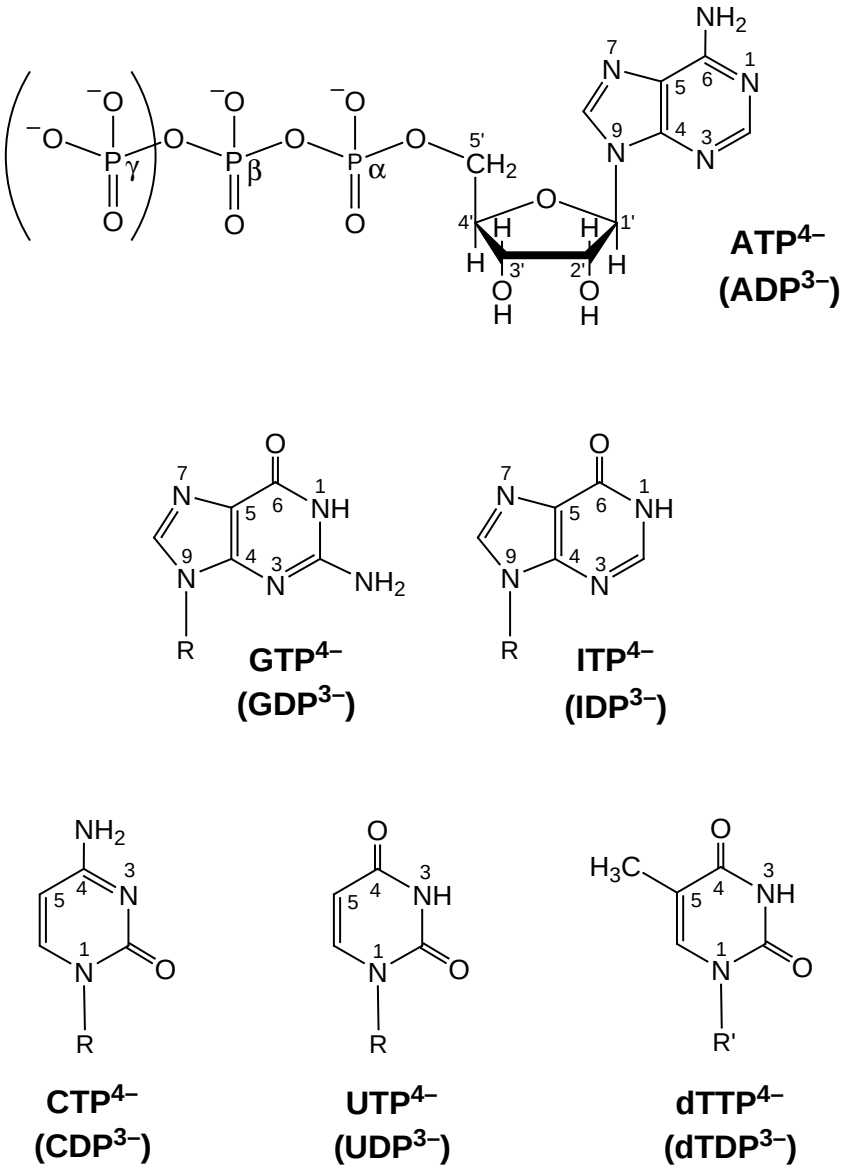

Figure 1.1: Chemical structure of adenosine 5′-triphosphate (ATP^{4-}) and 5′-diphosphate (ADP^{3-}) in their dominating *anti* conformation [6,7]. The structures of the nucleic base residues of purine and pyrimidine nucleotides are illustrated in the lower part of the figure, where R = ribose-5′-triphosphate (or 5′-diphosphate) and R′ = 2′-deoxyribose 5′-triphosphate (or 5′-diphosphate). The other nucleotides shown are: guanosine 5′-di- (GDP^{3-}) and 5′-triphosphate (GTP^{4-}); inosine 5′-di- (IDP^{3-}) and 5′-triphosphate (ITP^{4-}); cytidine 5′-di- (CDP^{3-}) and 5′-triphosphate (CTP^{4-}); uridine 5′-di- (UDP^{3-}) and 5′-triphosphate (UTP^{4-}); and thymidine 5′-di- ($dTDP^{3-}$) and 5′-triphosphate ($dTTP^{4-}$).

gene transcription is regulated by many factors, and among these is the degree of 5′-methylation of cytosine in the dinucleotide sequence $^{5'-\mathrm{CG}-3'}_{3'-\mathrm{GC}-5'}$ [8]. In prokaryotes synthesizing Type *II* restriction endonucleases, methylation of cytosine in the 5′-position and of adenine at N6, protects the cell's own DNA from cleavage by its enzyme [4,8]; many modified forms of the nucleobases are found in tRNAs. The structures of the common nucleoside 5′-di- and triphosphates, as well as the one of inosine (2-deaminoguanosine) 5′-di- and triphosphate, are depicted in Figure 1.1, where R and R′ represent ribose or 2′-deoxyribose phosphate, respectively.

Nucleotides play key roles in nearly all biochemical processes: e.g., they are metabolic regulators and carry energy in their di- and triphosphate chains; nucleoside 5′-triphosphates are activated precursors of DNA and RNA, and nucleoside mono-, di-, and triphosphates are involved in many other biosynthetic processes. ATP and GTP are energy rich molecules, the former is a universal energy carrier while the latter powers movement of macromolecules and supplies energy for gluconeogenesis [4]. Adenine nucleotides are components of three major coenzymes: nicotinamide adenine dinucleotide (NAD^+), flavin adenine dinucleotide (FAD) and coenzyme A (CoA) [9]. IMP is the precursor in the biosynthesis of AMP and GMP; purine-ring formation reactions are driven by hydrolysis of ATP [9] (formed by the pentose phosphate pathway [4,10]). UDP-glucose is the activated intermediate in glycogen synthesis, and hydrolysis of GTP to GDP regulates G-protein activities [4].

As at physiological pH their phosphate groups are deprotonated, nucleotides are present in the cell as anions that readily interact with cations, and virtually all of their reactions involve metal ions [11,12]. NTPs serving as substrates for DNA and RNA polymerases have to be present as complexes of divalent metal ions. It has been shown that a two-metal-ion mechanism is characteristic of many polymerases in the Pol I family and is involved in the synthesis of bacteriophage T7 DNA [13]. During T7 DNA replication, the α-, β-, and γ- phosphates of the incoming dNTP interact with two magnesium ions bound to two aspartic-acid residues (Asp), as

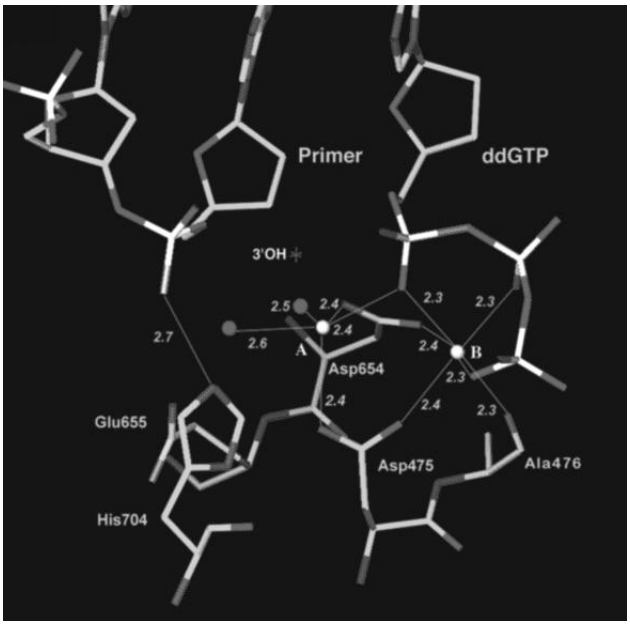

Figure 1.2: Detail of the X-ray crystal structure of the T7 DNA polymerase active site showing two metal ions (A and B) ligating the unesterified oxygen atoms of all three phosphates of the incoming nucleotide. Taken from [13].

shown in Figure 1.2. An identical two-metal-ion polymerase mechanism seems to be used by another, non homologous DNA polymerase — mammalian DNA polymerase β (Pol β) [14,15].

Guanine nucleotide binding proteins, so-called G-proteins, are involved in a variety of key cellular processes, such as cell growth and differentiation, signal transduction, protein synthesis and transport [4,16–19]; their biochemical activities are tightly regulated by the nature of the bound nucleotide, *i.e.*, GTP or GDP. The G-protein Ras is a molecular switch in cellular signal transduction, regulating important processes such as cell differentiation and proliferation: it plays a central role in the transduction of growth signals from the plasma membrane to the nucleus [20]. Oncogenic Ras mutants, being unable to hydrolyze GTP to GDP (and therefore to switch off the signal-cascade), appear to be involved in 25–30% of all human

tumors. In the GTP-bound form, Ras interacts with its effector, Raf, activating a kinase cascade, which transduces the external signal via a series of phosphorylations to the nucleus. The effector binding is terminated by hydrolysis of protein-bound GTP to GDP. In the resting cell, normal Ras exists mainly in the inactive form with GDP bound together with a Mg^{2+} ion in its active center. Interaction of the Mg^{2+} ion with the *pro-R* β-oxygen appears to be the main factor in shifting the charge distribution of this oxygen in such a way that in the GTP educt state it is already GDP-like, thus facilitating hydrolysis [21].

Figure 1.3 shows part of the Ras active center, as derived from crystallographic data on Ras·GDP [22]. In solution, the protein may be able to exist in various conformational states. It has been shown that the metal ion is always coordinated to the β-phosphate group of GDP and to protein residues, with either three or four

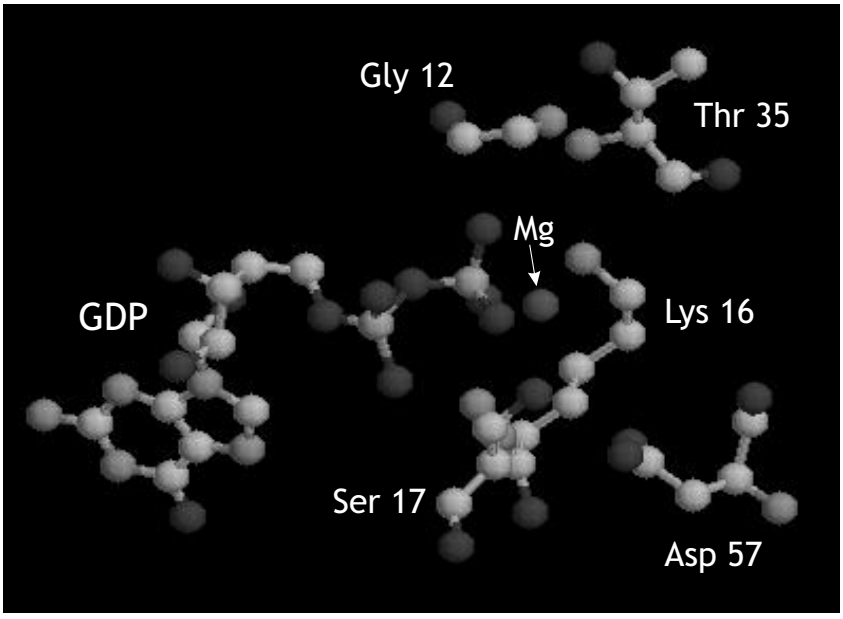

Figure 1.3: Coordination scheme of the metal–nucleotide complex from X-ray data of the Ras·Mg^{2+}·GDP complex. Part of the active site is shown, illustrating Mg^{2+} coordination to the β-phosphate group of GDP and to the hydroxyl group of Ser-17. Four water molecules (not shown) saturate the coordination sphere of the metal ion. Data taken from [22], as deposited in the Protein Data Bank [23].

water molecules saturating the coordination sphere of the metal ion [24].

Furthermore, GTP hydrolysis has been proven to be essential for the insertion of nickel into hydrogenases [25] and for the synthesis of activated sulphate [26], which is an essential step in the metabolic assimilation of sulphur.

The significance of ITP and IDP lies not only in their analogy to GTP and GDP, respectively, they are present in all cells. Hypoxanthine occurs transiently in DNA as a result of spontaneous adenine deamination [27,28]; ITP is generated by pyrophosphorylation of IMP, an essential metabolite of purine biosynthesis. dITP may be generated from dATP, or by reduction of ITP [29]. In human erythrocytes, ITP is continuously synthesized and broken down at a relatively high rate, forming a futile cycle that has been proposed to regulate the concentration of ATP. Additionally, ITP appears to be a substrate (although less efficient than GTP) for receptor/G-proteins, in activating effector systems [30,31].

Normally, the cellular ITP/dITP level is very low and its control has been attributed to the presence of an enzyme, inosine triphosphate pyrophosphatase (ITPase), in the cytoplasm [32,33]. ITPase hydrolyzes ITP/dITP to IMP/dIMP and pyrophosphate, and it has low activity toward other purine nucleoside triphosphates [34]. A divalent metal ion such as Mg^{2+} or Mn^{2+} is an absolute prerequisite for the enzyme activity.

ITP and dITP can be incorporated into RNA and DNA, respectively, by polymerases [35,36]. The deoxyribonucleotide dITP behaves as a dGTP analogue and is incorporated opposite cytosine with about 50% efficiency. Although hypoxanthine DNA glycosylase can remove the base from DNA [37], evidence has been presented that this enzyme only removes a hypoxanthine residue from an I-T base pair efficiently, whereas removal from an I-C base pair is 15–20 times slower [38]. Because of the relative stability of an I-C base pair, inosine can remain incorporated until the next round of DNA replication, increasing the risk of direct mutagenesis. Moreover, inosine di- and triphosphates have been suggested to be a component of the clastogenic factor in the serum of scleroderma patients [39,40].

ATP, as already pointed out, is the universal energy carrier in biological systems: when the energy stored in it is used, the terminal anhydride bond is split, forming ADP and inorganic phosphate. ATP hydrolysis is metal ion facilitated and in the presence of metal ions, proceeds via a dimeric species [41], as schematically shown in Figure 1.4. Under the conditions that normally exist in a cell the ΔG of the reaction is roughly -11 to -13 kcal/mole [42]. ATP is used in the generation of

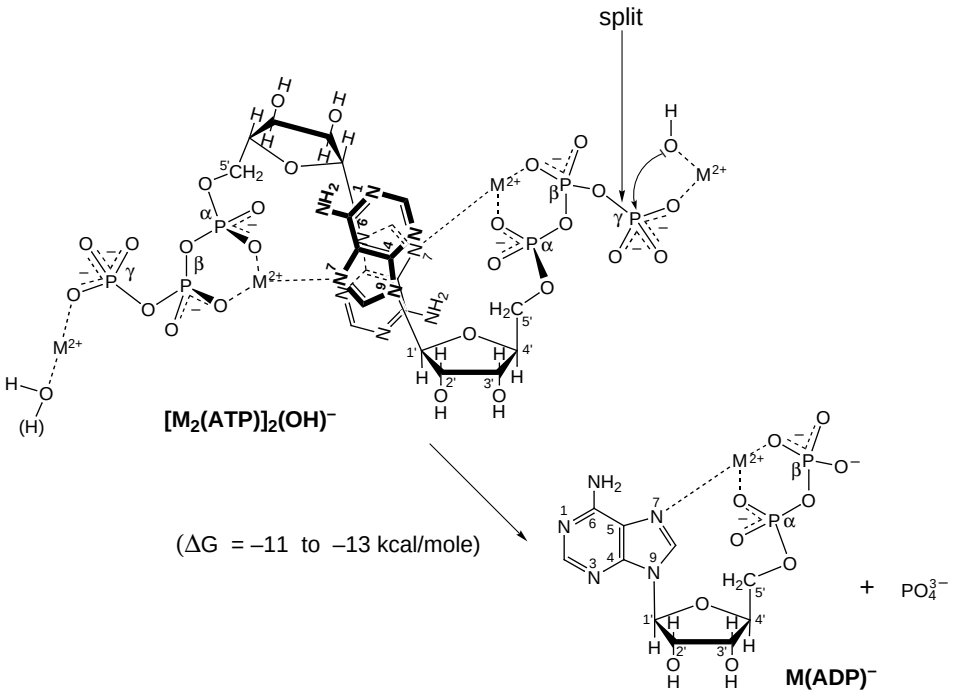

Figure 1.4: Proposed structure of the reactive $[M_2(ATP)]_2(OH)^-$ dimer, which occurs in low concentrations during the metal-ion promoted dephosphorylation of ATP. The intramolecular attack of OH^- is indicated on the right side. The metal ion on the left side stabilizes the dimer by coordination to the α,β phosphate groups of one ATP molecule and to N7 of the other. The second metal ion is ready to transfer into the reactive state by deprotonation of the coordinated water molecule, or to undergo an intramolecular water attack. Adapted from [41].

cell components, muscle contractions, transmission of nerve messages and many other functions [43,44]. Boyer has estimated, based on known metabolic pathways

and the extent of the world's biomass, that ATP, ADP and inorganic phosphate participate in more chemical reactions than any other compound on the Earth's surface, except water [45].

The two nucleotides that usually take part in reactions in form of metal ion complexes, MgADP and MgATP, are the substrates of F_1F_0-ATP synthase [46]; the presence of divalent metal ions is required for phosphoryl or nucleotidyl transfer reactions [11,47]. Structural studies on adenylyl cyclase, an enzyme that converts ATP to cyclic adenine monophosphate, an ubiquitous second messenger that regulates many cellular functions, demonstrate that two metal ions bind to its active site [48]. The reaction catalysed by adenylyl cyclase is analogous with those of DNA polymerases. Both enzymes catalyze the attack of the 3′-hydroxyl group of ribose on the α-phosphate of a nucleoside triphosphate. Moreover, the enzymes have similar active sites, which suggests that the same two-metal-ion mechanism is involved in the reaction [48].

Divalent cations are known to affect the structure of duplex DNA: Mg^{2+}, Ca^{2+}, Ba^{2+}, Mn^{2+}, Co^{2+}, Zn^{2+}, and Cd^{2+} can induce B-to-Z transition of poly[d(G-C)] sequences [49,50]. Binding of Zn^{2+} to DNA can result in strong kinking, most probably caused by joint coordination of Zn^{2+} to the N7 groups of stacked purine residues [51,52]. Indeed, Zn^{2+} plays a catalytic and structural role in a great variety of nucleic acid-binding and gene regulating proteins (zinc fingers); it has been identified as a component of more than 300 enzyme systems [53], and is accepted as an essential element for the growth of most living organisms. In DNA polymerase the tightly bound Zn^{2+} binds the enzyme to DNA [54]. The polymerase is activated by a cation such as Mg^{2+} or Mn^{2+} that ties the NTP substrates to the polymerase itself [14,55,56]. There is evidence that N7 of ATP might interact with Zn^{2+} in *E. coli* DNA-dependent RNA polymerase [57].

Many metal ions, calcium, magnesium, zinc, cobalt, nickel, manganese, iron

and copper among others, are essential for biological systems, taking part in oxygen transport and metabolism, in hydrolytic reactions, in signal transfer, catalyzing electron transfer reactions, and stabilizing the structure of macromolecules. The anionic nature of nucleotides at physiological pH leads to the significance of metal ions in influencing the overall structure and function of the molecules. Understanding metal–nucleotide interactions in solution is a precondition for appreciating their role in the cellular processes in which they are involved. Even though the nucleotide–metal ion interactions of nucleoside 5′-monophosphates have been intensively studied (see, for instance, [58–62]), relatively little is known about nucleoside 5′-diphosphates, and despite some early measurements [63,64], until recently [65] no comprehensive set of stability data was available for nucleoside 5′-triphosphates. The aim of this study was to fill this gap of information by studying the acid-base and metal-ion binding properties of guanosine and inosine 5′-di- and triphosphates, and of adenosine 5′-diphosphate. As far as phosphate metabolism is concerned, magnesium, calcium, manganese and zinc are the most important metals in nature and for this reason their complexes with nucleotides are of primary interest. Nevertheless, the present study deals with complexes formed by the alkaline earth metal ions and the divalent ions of the second half of the 3d-transition series, including Cd^{2+}: most of the mentioned metal ions are present in biological systems and the majority of them have been found to activate one or more enzymes [4].

After dealing with the properties of binary complexes of nucleoside 5′-di- and triphosphates in aqueous solution, the stacking properties of the 5′-diphosphates of adenosine, guanosine and inosine were studied in mixed-ligand complexes, using 2,2′-bipyridine (bpy) and 1,10-phenanthroline (phen) as standards. Some brief information will be given in the next section on the importance of stacking in biological systems.

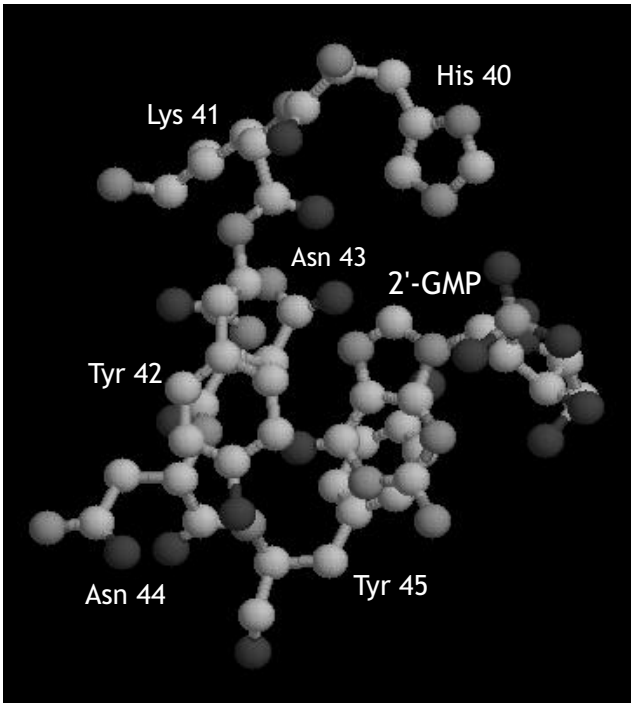

Figure 1.5: Base recognition by RNase T_1. The phenyl ring of Tyr-45 stacks parallel to the guanine plane, at a distance of 3.5 Å. Hydrogen bonds (not shown) between base positions N1 and O6 and the protein backbone (with Asn-44 and Tyr-42), and between the phosphate moiety and the His-40 imidazole, help in correctly positioning of the substrate in the active site cavity. Data taken from [68], as deposited in the Protein Data Bank [23].

1.2 Stacking interactions in biological systems

Noncovalent interactions, such as hydrogen and electrostatic bonding, hydrophobic interactions, and aromatic-ring stacking, govern nucleobase-nucleobase, enzyme-substrate, nucleic acid-protein and other specific interactions in biological systems. The three-dimensional structure and function of DNA are controlled by noncovalent interactions between nucleobases, *i.e.*, the vertical π–π stacking, and the planar hydrogen bonding (Watson-Crick base pairing) [66,67]. The same type of interactions govern the three-dimensional structure of RNA.

Base stacking may be relatively even more important as a stabilizing interaction

for helical structures in looped RNA or DNA that occur, for instance, in hairpins, where hydrogen bonding is less extensive [69].

Recognition processes are governed by hydrogen bonding and nucleobase stacking as well. For example, recognition of a guanine residue by ribonuclease T_1 (RNase T_1, see Figure 1.5), occurs by aromatic-ring stacking with a tyrosine side chain and the formation of several hydrogen bonds involving the enzyme backbone [68].

Similarly, positioning of the template DNA-strain and incoming nucleotide recognition in DNA polymerase β occur by stabilization of the nucleobases through van der Waals interactions (stacking) with an asparagine and a lysine residue in the active site of the enzyme. In more detail: Asp-276 and Lys-280 stack with the bases of the incoming nucleotide and template, respectively. It has been observed that Lys-280 interactions with templating-purines are more important than they are for templating-pyrimidines, which suggests that template positioning and stabilization is unique for each base pair [70].

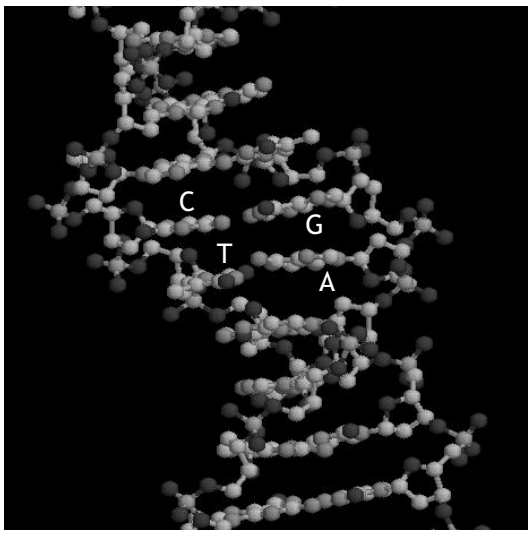

Figure 1.6: X-ray data of a 19Mer DNA, showing the stacking interactions between adjacent nucleobases (G-A and C-T). Data from [71], as deposited in the Protein Data Bank [23].

Considering that base stacking is involved in the stabilization of the DNA double helix (Figure 1.6 shows an example of stacking in a DNA-oligomer), it is not surprising that the self-association of purines and pyrimidines as well as of their nucleosides has long been known.

About 40 years ago it was shown that purines associate much better than pyrimidines [72]. Regarding nucleotides, however, the situation remained unclear for many years. It has been shown that self-association of all these species occurs via base stacking and that it proceeds beyond dimer formation to oligomer formation. The extent of aggregation in these systems is much affected by external conditions, depending on the pH and the presence of metal ions: neutralization of the negative charges at the phosphate groups facilitates self-association [67,73,74]. Certain cell organelles contain rather high concentrations of nucleotides. In the chromaffin granules of the bovine adrenal medulla, for instance, about 0.2 M nucleotide concentrations, largely ATP, and about 0.03 M divalent metal ions, mainly Ca^{2+} and Mg^{2+}, are found [75]. Similar concentrations appear to occur elsewhere, e.g., in the storage organelles of blood platelets [76]. The contents of the chromaffin granule must be brought to osmotic equilibrium with the cytoplasm and the contents of the storage organelles with that of blood. It is therefore assumed that organelle-solute-associations take place. Indeed, it was found that high molecular mass complexes form in the chromaffin granules, and that ATP was crucial for the formation of the aggregates [77,78].

Originally, intramolecular stack formation had first been proven to occur in mixed ligand complexes in aqueous solution nearly 30 years ago [79]; today many examples concerning nucleoside (5′-) mono- or 5′-triphosphates are known [67]. As already mentioned, the ternary complexes formed by purine nucleoside 5′-diphosphates with Cu^{2+} and 1,10-phenanthroline (phen) or 2,2′-bipyridine (bpy) will be dealt with here.

1.3 Influence of the solvent polarity on acidity and stability constants

Solvent polarity is reduced at the surface of proteins [80,81] and in the active-site cavity of enzymes [82]: the so-called "effective" dielectric constant is reduced compared to that of bulky water [83], *i.e.*, the activity of water is decreased due to the presence of aliphatic and aromatic side chains at the protein–water interface. The effective dielectric constant in such locations is estimated to range from $\sim$30 to 70 [82], corresponding to aqueous solutions containing about 10–50% (v/v) of 1,4-dioxane.

There is evidence that complex equilibria are influenced by changing solvent polarity [84]. As at present no data are available regarding nucleoside 5′-diphosphates, it is interesting to study the influence of a reduced solvent polarity on the stability and structure of their complexes. To simulate the situation in the active-site cavities, experiments were carried out by adding 30% or 50% (v/v) 1,4-dioxane to the aqueous reagent mixtures. The acid-base properties of GDP and the stability of its complexes with Cu^{2+}, $Cu(phen)^{2+}$, and $Cu(bpy)^{2+}$ were studied. There are two main reasons for selecting these complexes: (*i*) $Cu(phen)^{2+}$ and $Cu(bpy)^{2+}$ complexes have a very high stability [85,86] and are practically completely formed [87] before the onset of complex formation with the nucleotide. For this reason they can be regarded as simple divalent "metal ions" in the evaluation of the experimental data. (*ii*) These experiments open the possibility of comparing the stability of ternary complexes of GDP in aqueous solution with that in mixed solvents.

1.4 Aims of the study

An understanding of the metal ion binding properties of nucleotides in solution would obviously be desirable, and as information is available only on nucleoside mono- and, partly, triphosphates, this thesis concentrates on the following topics:

1. Determination of the acidity constants of the nucleobase sites (N1 of adenosine 5′-diphosphate, and of guanosine and inosine 5′-di- and 5′-triphosphates) and of the phosphate groups of GTP, ITP, ADP, GDP, and IDP. The corresponding values for ATP are already known [88].

2. Determination of the stability constants of the protonated and deprotonated complexes of the mentioned nucleotides involving Mg^{2+}, Ca^{2+}, Sr^{2+}, Ba^{2+}, Mn^{2+}, Co^{2+}, Ni^{2+}, Cu^{2+}, Zn^{2+}, or Cd^{2+}.

3. Study of the structure of these complexes in aqueous solution, based on comparisons with values expected for a simple phosphate-coordination of the metal ions.

4. Estimation of the influence of a second, heteroaromatic ligand in the coordination sphere of the metal ion on the stability of complexes formed with nucleoside 5′-diphosphates. Study of the stacking properties of the resulting ternary complexes with the aim of comparing them with those of the corresponding nucleoside 5′-mono- and 5′-triphosphate complexes.

5. Evaluation of the mentioned properties for 5′-GDP and its Cu^{2+} complexes in solvents of a polarity lower than that of water [30% and 50% (v/v) 1,4-dioxane–water mixtures].

Chapter 2

Results and Discussion

Nucleotides, as mentioned in the introduction, are composed of three main parts: a nucleobase, a sugar, and a phosphate unit. Each of them has potential proton- or metal ion-binding sites: the nitrogen atoms at the nucleobase, the hydroxy groups at the sugar moiety, which bind a metal ion after deprotonation, and the oxygen atoms at the phosphate group(s).

The hydroxy groups of the sugar moiety have pK_a values in the order of 12 or higher [89] and their interaction with metal ions in the undeprotonated state is very weak [58]. In aqueous solution and at pH values lower than 10, no deprotonation or complex formation involving the ribose moiety is expected, reactions of this kind were therefore not considered here. Hence, only two building blocks are left: the nucleobases and the phosphate group(s), and both will be dealt with in the present study of purine nucleoside 5′-di- and triphosphates. The phosphate residue is well known as the stability determining binding site for metal ions like the alkaline earth ions or those of the 3d transition series [11]. However, the nucleobase moiety influences the structure and stability of several metal ion complexes [59].

Adenosine, inosine and guanosine have several sites which are able to interact with protons or metal ions [6,58]. Their acidity constants are known, and there are no ambiguities in the attribution of the protons. In purine nucleosides and nucleotides, N1 is at least 100 times more basic than N7; the N3 site at least 10^4 times more acidic than the N7 unit [6,89]. The bases of pyrimidine nucleosides

(cytidine, uridine and thymidine), have only one basic site: N3, at least in the pH range of about 2 to 11 [6,90].

Adenosine, inosine, and guanosine can all accept a proton at the nucleobase, adenosine at N1, the other two at N7.

Nucleotides are well known to undergo self-association due to stacking of their heterocyclic ring systems [73]. Equilibrium constants have been determined for the stacking of the nucleotides investigated in this work [74,89,91,92], and it was found that for concentrations lower than 1.5 mM, at least 97% of the species are present in their monomeric form. In the present study, lower nucleotide concentrations, usually in the order of about 0.3 – 0.6 mM, were employed. Self-stacking interactions are therefore negligible and all the results given in the following Sections refer to the monomeric species of the ligands.

2.1 Acid–base properties of GTP and ITP

A comprehensive set of the acidity constants of the three-fold protonated GTP^{4-} and ITP^{4-} species is given in the following Sections (2.1.1 – 2.1.3) [93]. There are several instances where the buffer regions of the deprotonation reactions are overlapping, *i.e.*, the acidity constants are relatively similar. In these instances, micro-acidity-constant analysis were needed to quantify the intrinsic acid–base properties of the various sites.

All potentiometric pH titrations, the results of which are summarized below, were carried out in aqueous solution at 25 °C and I = 0.1 M ($NaNO_3$ or $NaClO_4$) and at ligand concentrations in which no self-stacking occurs (see Section 4.2.1 on page 169) [92].

2.1.1 Acidity constants of $H_3(GTP)^-$ and $H_3(ITP)^-$

Nucleoside 5′-triphosphates can accept four protons at the phosphate groups. Two of the three primary sites at the $–P_3O_{10}H^{3-}$ residue of GTP and ITP are expected to be protonated only at pH <1. This observation is based on the values measured for the acidity constants of the primary protons of 5′-AMP and 5′-UMP ($pK^{H}_{H_3(AMP)}$ = 0.4±0.2 [7] and $pK^{H}_{H_2(UMP)}$ = 0.7±0.3 [94]): those of the triphosphates studied are in the same order of magnitude. In the pH range 1 to 11, $H_3(GTP)^-$ and $H_3(ITP)^-$ undergo four deprotonations. The corresponding pK_a values are listed in Table 2.1 (page 20), together with the acidity constants of some related nucleosides and nucleotides, known from other studies (the references are given in the Table). The values listed in the third column of the Table refer (largely, see below) to the deprotonation of the $(N7)H^+$ unit of the purines, except in the case of the adenines, where the $(N1)H^+$ site is deprotonated, and of $H_2(CTP)^{2-}$, where the proton is at N3 [95] (see Figure 2.1).

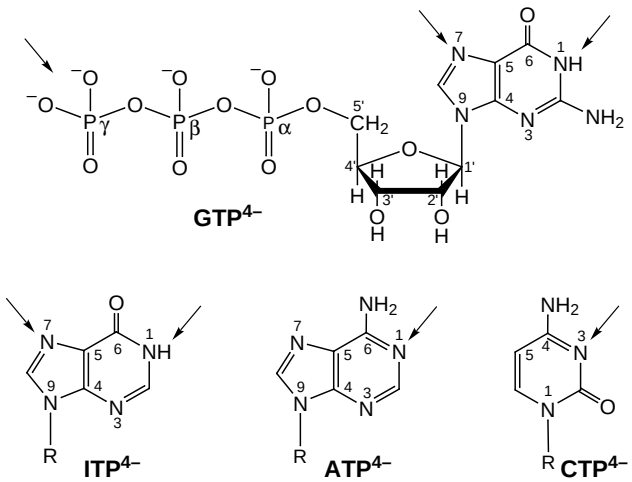

Figure 2.1: Structures of guanosine, inosine, adenosine, and cytidine 5'-triphosphates in their dominating *anti* conformation [6,7]. The arrows show the (de)protonation sites, whose pK_a values are listed in Table 2.1 (page 20).

The (macro) acidity constants determined now *via* potentiometric pH titrations

for equations 2.2–2.4 agree well with a previous tabulation [95]. The acidity constants for the $H_3(NTP)^-$ species are defined in the following equilibria:

$$H_3(NTP)^- \rightleftharpoons H_2(NTP)^{2-} + H^+$$

$$K^H_{H_3(NTP)} = [H_2(NTP)^{2-}][H^+]/[H_3(NTP)^-] \quad (2.1)$$

$$H_2(NTP)^{2-} \rightleftharpoons H(NTP)^{3-} + H^+$$

$$K^H_{H_2(NTP)} = [H(NTP)^{3-}][H^+]/[H_2(NTP)^{2-}] \quad (2.2)$$

$$H(NTP)^{3-} \rightleftharpoons NTP^{4-} + H^+$$

$$K^H_{H(NTP)} = [NTP^{4-}][H^+]/[H(NTP)^{3-}] \quad (2.3)$$

$$NTP^{4-} \rightleftharpoons (NTP-H)^{5-} + H^+$$

$$K^H_{NTP} = [(NTP-H)^{5-}][H^+]/[NTP^{4-}] \quad (2.4)$$

The first proton (equation 2.1) is mainly released from one of the three primary sites of the twofold protonated triphosphate chain (the measured values are listed in column 2 of Table 2.1). $K^H_{H_2(NTP)}$, equation 2.2, is primarily due to proton loss from the (N7)H^+ site. In column 4 of the Table the values of the third constant (eq. 2.3) are given. They refer to the deprotonation of the γ-triphosphate-bound proton in $H(GTP)^{3-}$ or $H(ITP)^{3-}$. These values are identical with the one found for $H(ATP)^{2-}$ ($pK^H_{H(ATP)}$ = 6.47) and closely similar to the ones determined for monoprotonated pyrimidine-nucleoside 5′-triphosphates ($pK^H_{H(PyNTP)}$ = 6.50±0.05 [88]). The highest values in Table 2.1 (eq. 2.4) refer to the ionization of the (N1)H site of the nucleobase in GTP^{4-} and ITP^{4-} (in the case of UTP^{4-} and $dTTP^{4-}$ the (N3)H unit is deprotonated) to give species of an overall -5 charge at pH >10, $(NTP-H)^{5-}$. The site attributions agree with previous conclusions [6,95,96].

Comparison of the acidity constants of the nucleosides with those of their corresponding nucleotides reveals the effect of the 4-fold negatively charged triphosphate chain on the deprotonation of the (N1)H site.

$$pK^{H}_{GTP} - pK^{H}_{Guo} = (9.57 \pm 0.02) - (9.22 \pm 0.01) = 0.35 \pm 0.02$$

$$pK^{H}_{ITP} - pK^{H}_{Ino} = (9.11 \pm 0.03) - (8.76 \pm 0.03) = 0.35 \pm 0.04$$

As one might expect, the release of the proton from (N1)H in $PuNTP^{4-}$ is inhibited by the triphosphate chain and the effect is very similar to that observed with the pyrimidines and their (N3)H site.

$$pK^{H}_{UTP} - pK^{H}_{Urd} = (9.57 \pm 0.02) - (9.19 \pm 0.02; [97]) = 0.38 \pm 0.03$$

$$pK^{H}_{dTTP} - pK^{H}_{Thy} = (10.08 \pm 0.05) - (9.69 \pm 0.03; [97]) = 0.39 \pm 0.06$$

It is interesting to observe that the effect described above operates likewise when a positively charged (N1)H^+ site is involved as in $H_2(ATP)^{2-}$ and H(adenosine)$^+$.

$$pK^{H}_{H_2(ATP)} - pK^{H}_{Ado} = (4.00 \pm 0.01) - (3.61 \pm 0.03) = 0.39 \pm 0.03$$

That the release of this H^+ is inhibited to the same extent by the monoprotonated 3-fold negatively charged triphosphate group as above by the 4-fold negatively charged triphosphate chain is likely to be due to the formation of Na^+ complexes [98] for the latter species, which neutralizes in part the extra charge. Indeed, assuming the stability of the $Na(GTP)^{3-}$ and $Na(ITP)^{3-}$ complexes to be equal to the one of $Na(ATP)^{3-}$, *i.e.*, $\log K^{Na}_{Na(GTP)} = \log K^{Na}_{Na(ITP)} = \log K^{Na}_{Na(ATP)} = 1.31$ [98], one calculates with $pK^{H}_{H(NTP)} = 6.50$, $[PuNTP^{4-}] = 5 \times 10^{-4}$ M, and $[Na^+] = 0.1$ M, that at pH 8.0 two thirds of $PuNTP^{4-}$ are actually present as $Na(PuNTP)^{3-}$.

Table 2.1: Negative logarithms of the acidity constants of several $H_3(PuNTP)^-$ species as determined by potentiometric pH titrations in aqueous solution at 25 °C and I = 0.1 M ($NaNO_3$ or $NaClO_4$) together with some related data that refer to the same conditions[a]

Acid	$pK^H_{H_3(PuNTP)}$ *or* $pK^H_{H_2(PyNTP)}$	$pK^H_{H_2(NTP)}$ *or* $pK^H_{H(Ns)}$	$pK^H_{H(NTP)}$	pK^H_{NTP} *or* pK^H_{Ns}
$H(Guo)^+$		2.11±0.04 [b]		9.22±0.01 [b]
$H(Ino)^+$		1.06±0.06 [b]		8.76±0.03 [b]
$H(Ado)^+$		3.61±0.03 [c,d]		
$H_3(GTP)^-$	1.3±0.2 [e]	2.94±0.02	6.50±0.02	9.57±0.02
$H_3(ITP)^-$	1.0±0.2 [f]	2.19±0.05	6.47±0.02	9.11±0.03
$H_3(ATP)^-$	1.7±0.1 [g]	4.00±0.01 [d,h]	6.47±0.01 [h]	
$H_3(CTP)^-$	1.7 [i]	4.55±0.03 [d,h]	6.55±0.02 [h]	
$H_2(UTP)^{2-}$	2.0±0.1 [j]		6.48±0.02	9.57±0.02 [k]
$H_2(dTTP)^{2-}$	2.0 [h]		6.52±0.02 [h]	10.08±0.05 [k,l]

[a] So-called practical (or mixed) constants are listed [99]. The error limits given are *three times* the standard error of the mean value or the sum of the probable systematic errors, whichever is larger. Those values for which no source is given have been determined in this study. [b] From [89]. [c] From [7]. [d] This value refers to the deprotonation of the $(N1)H^+$ site of the adenine residue; all other values refer (largely; see text) to the deprotonation of the $(N7)H^+$ unit of the purines, except in the case of $H_2(CTP)^{2-}$ where the proton is at N3 [95]. [e] Rounded value from the Scheme of Figure 2.3 (page 23). [f] Rounded value from the Scheme in Figure 2.2 (page 23). [g] From [100]. [h] From [88]; the values for CTP have now been confirmed (see Section 4.2.1). [i] It is assumed that $pK^H_{H_3(ATP)} \simeq pK^H_{H_3(CTP)}$ because the effect of the protonated nucleobase residue on the release of the first proton on the twofold protonated triphosphate chain in $H_3(ATP)^-$ and $H_3(CTP)^-$ is expected to be very similar. [j] From [101]. [k] This value refers to the deprotonation of the (N3)H site of a pyrimidine residue, all other values in this column refer to the deprotonation of a purine-(N1)H site. [l] H. Sigel, unpublished result. The experiments were carried out as those described for UTP in Section 4.2.1 on page 169.

2.1.2 Estimation of some acidity constants in the low pH range

The N7 site is 1.05 log units more basic in guanosine ($pK^{H}_{H(Guo)}$ = 2.11±0.04) than in inosine ($pK^{H}_{H(Ino)}$ = 1.06±0.06, Table 2.1), and this basicity difference is expected to be independent of the presence of the triphosphate chain: the effect of this chain on the acid–base properties of N7 should be the same if calculated for the pK_a values of the two nucleosides [89], or for those of the two NTPs. The value of $pK^{H}_{H_2(ITP)}$ (= 2.19±0.05), measured for the deprotonation of $H_2(ITP)^{2-}$, therefore suggests some contribution from the release of one of the primary phosphate protons and thus does not refer solely to the deprotonation of the $(N7)H^+$ site. A micro acidity constant is therefore estimated for the deprotonation reaction of N7 from phosphate-protonated ITP:

$$(H{\cdot}ITP{\cdot}H)^{2-} \rightleftharpoons (ITP{\cdot}H)^{3-} + H^+$$

where $(H{\cdot}ITP{\cdot}H)^{2-}$ represents a species that carries a proton each at N7 and the terminal γ-phosphate group.

As already pointed out, the *difference* between the pK_a values for the deprotonation of N7 should be identical for Guo and Ino and the two NTPs: ΔpK_a = $pK^{H}_{H(Guo)} - pK^{H}_{H(Ino)}$ = (2.11±0.04) − (1.06±0.06) = 1.05±0.07, from which it follows: $pk^{ITP{\cdot}H}_{H{\cdot}ITP{\cdot}H} = pK^{H}_{H_2(GTP)} - \Delta pK_a$ = (2.94±0.02) − (1.05±0.07) = 1.89±0.07. This micro acidity constant is in excellent agreement with the result of ^{1}H-NMR measurements in D_2O ($pK^{D}_{D_2(ITP)}$ = 2.40±0.15 [92]), if the corresponding value is transformed [102] into H_2O as a solvent: $pk^{ITP{\cdot}H}_{H{\cdot}ITP{\cdot}H}$ = 1.92±0.15. This agreement proves that the above reasoning is correct and that any contribution from a primary phosphate proton towards $pK^{H}_{H_2(GTP)}$ is insignificant, as will further be confirmed below.

The value of $pK^{H}_{H_3(GTP)}$ (eq. 2.1, page 18), referring to the deprotonation of $H_3(GTP)^-$ or the release of the final primary proton from the triphosphate chain, can be estimated. A value for $pK^{H}_{H_3(ATP)}$ is known [100], and this can be used as a basis for the estimation by taking into account the different distances of $(N1)H^+$

in $H_3(ATP)^-$ and $(N7)H^+$ in $H_3(GTP)^-$ from the triphosphate chain. This *distance effect* can be quantified by the difference:
$\Delta\Delta pK_a = \Delta pK_{a/N7} - \Delta pK_{a/N1}$, where $\Delta pK_{a/N7} = pK^{H}_{H_2(GTP)} - pK^{H}_{H(Guo)}$ = (2.94±0.02) − (2.11±0.04) = 0.83±0.04, and $\Delta pK_{a/N1} = pK^{H}_{H_2(ATP)} - pK^{H}_{H(Ado)}$ = (4.00±0.01) − (3.61±0.03) = 0.39±0.03. Hence: $\Delta\Delta pK_a$ = (0.83±0.04) − (0.39±0.03) = 0.44±0.05. From the value of the acidity constant of $H_3(ATP)^-$ one obtains:
$pK^{H}_{H_3(GTP)} = pK^{H}_{H_3(ATP)} - \Delta\Delta pK_a$ = (1.7±0.1) − (0.44±0.05) = 1.26±0.11; this result rounded to 1.3±0.2 is listed in column two of Table 2.1.

The same procedure can be applied to $H_3(ITP)^-$, when considering the deprotonation equilibrium:

$$(H{\cdot}ITP{\cdot}H_2)^- \rightleftharpoons (H{\cdot}ITP{\cdot}H)^{2-} + H^+$$

The species $(H{\cdot}ITP{\cdot}H_2)^-$ carries one proton at N7 and two at the triphosphate chain. The corresponding micro acidity constant is then given by $pk^{H{\cdot}ITP{\cdot}H}_{H{\cdot}ITP{\cdot}H_2} = pK^{H}_{H_3(GTP)}$ = 1.26±0.11.

2.1.3 Micro acidity constant scheme for $H_3(ITP)^-$ and $H_3(GTP)^-$

The equilibrium scheme for $H_3(ITP)^-$ is summarized in Figure 2.2. The micro acidity constants (*k*) and their interrelations with the macro acidity constants (*K*) are defined there. The value of the global acidity constant $pK^{H}_{H_3(ITP)}$ can be calculated using the values deduced in Section 2.1.2 for $pk^{H{\cdot}ITP{\cdot}H}_{H{\cdot}ITP{\cdot}H_2}$ and $pk^{ITP{\cdot}H}_{H{\cdot}ITP{\cdot}H}$ (lower part of the scheme in Fig. 2.2): $pK^{H}_{H_3(ITP)} = pk^{H{\cdot}ITP{\cdot}H}_{H{\cdot}ITP{\cdot}H_2} + pk^{ITP{\cdot}H}_{H{\cdot}ITP{\cdot}H} - pK^{H}_{H_2(ITP)}$ = (1.26±0.11) + (1.89±0.07) − (2.19±0.05) = 0.96±0.14 (equation 2.1 on page 18). This result, rounded to 1.0±0.2 is listed in column two of Table 2.1 on page 20.

In principle, it would now be possible to calculate the values of the micro acidity constants in the upper part of the scheme [103,104], but as the error limits of some of the constants are rather large, a further estimation is preferred. The release of the third primary proton from the triphosphate chain in $H_2(UTP)^{2-}$ is unaffected by

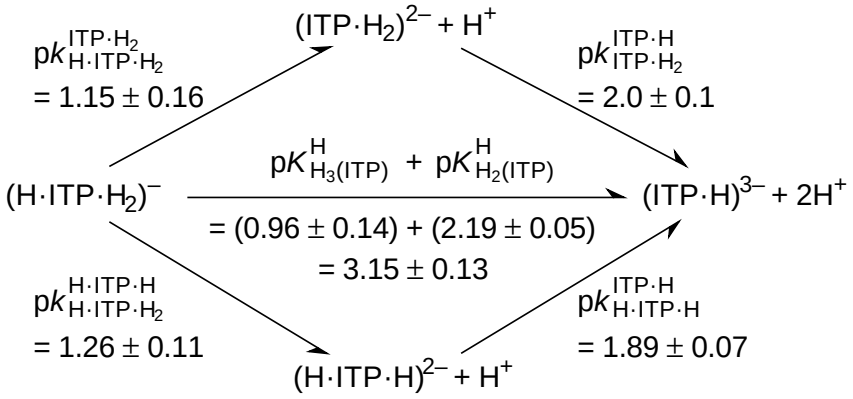

Figure 2.2: Equilibrium scheme for $(H{\cdot}ITP{\cdot}H_2)^-$ defining the micro acidity constants (k) and showing their interrelation with the macro acidity constants (K). In $(ITP{\cdot}H_2)^{2-}$ one proton is at the γ-phosphate group and the other at one of the primary sites at the triphosphate chain, while in $(H{\cdot}ITP{\cdot}H)^{2-}$ one proton is at N7 and the other at the γ-phosphate group. $(H{\cdot}ITP{\cdot}H_2)^-$ is often written as $H_3(ITP)^-$ and carries one proton at N7 and the other two at the triphosphate residue. The arrows indicate the directions for which the constants are defined.

the uridine moiety, as this residue is uncharged. Consequently, the corresponding acidity constant is a good estimate for the microconstant equilibrium:

$$(ITP{\cdot}H_2)^{2-} \rightleftharpoons (ITP{\cdot}H)^{3-} + H^+$$

This means $pk^{ITP{\cdot}H}_{ITP{\cdot}H_2} = pK^{H}_{H_2(UTP)} = 2.0 \pm 0.1$ (Table 2.1 on page 20, [101]). The final micro acidity constant of the upper cycle in the scheme, representing the loss of a proton from N7 when two protons are still bound at the triphosphate chain, can now be calculated due to the properties of a cyclic system.

The micro acidity constant scheme for $H_3(GTP)^-$ is depicted in Figure 2.3. From the result of ^{1}H-NMR shift measurements in D_2O ($pK^{D}_{D_2(GTP)} = 3.41 \pm 0.09$ [92]), the value for $pk^{GTP{\cdot}H}_{H{\cdot}GTP{\cdot}H}$ is calculated [102] to be 2.92 ± 0.09. This result proves that the global constant, $pK^{H}_{H_2(GTP)}$ (2.94 ± 0.02, Table 2.1, column 3) and the micro constant $pk^{GTP{\cdot}H}_{H{\cdot}GTP{\cdot}H}$ are identical within the experimental error. The same applies to $pK^{H}_{H_3(GTP)}$ and the derived micro constant $pk^{H{\cdot}GTP{\cdot}H}_{H{\cdot}GTP{\cdot}H_2}$ (lower cycle in

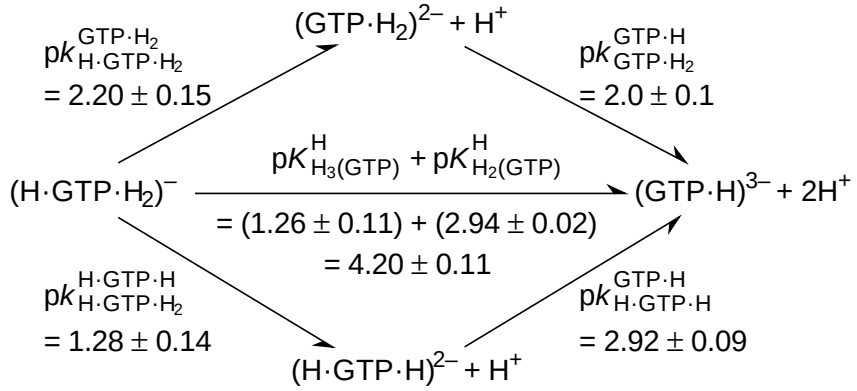

Figure 2.3: Equilibrium scheme for $(H{\cdot}GTP{\cdot}H_2)^-$ defining the micro acidity constants (*k*) and showing their interrelation with the macro acidity constants (*K*). In $(GTP{\cdot}H_2)^{2-}$ one proton is at the γ-phosphate group and the other at one of the primary sites at the triphosphate chain, while in $(H{\cdot}GTP{\cdot}H)^{2-}$ one proton is at N7 and the other at the γ-phosphate group. $(H{\cdot}GTP{\cdot}H_2)^-$ is often written as $H_3(GTP)^-$ and carries one proton at N7 and the other two at the triphosphate residue. The arrows indicate the directions for which the constants are defined.

Figure 2.3).

The same reasons as outlined above for ITP apply to $pk^{GTP{\cdot}H}_{GTP{\cdot}H_2} = pK^{H}_{H_2(UTP)} = 2.0{\pm}0.1$. The remaining constant in the upper pathway can now be calculated. The basicity difference of N7 in GTP and ITP, given by $\Delta pK_{a/N7/NTP} = pk^{GTP{\cdot}H_2}_{H{\cdot}GTP{\cdot}H_2} - pk^{ITP{\cdot}H_2}_{H{\cdot}ITP{\cdot}H_2} = (2.20{\pm}0.15) - (1.15{\pm}0.16) = 1.05{\pm}0.22$ (Figs. 2.2 and 2.3) agrees with the one calculated for the two nucleosides, $\Delta pK_{a/N7/Ns} = pK^{H}_{H(Guo)} - pK^{H}_{H(Ino)} = (2.11{\pm}0.04) - (1.06{\pm}0.06) = 1.05{\pm}0.07$, as expected. Obviously, the relative basicity of N7 in a guanine *versus* that in a hypoxanthine residue has always to be the same. The result of this comparison proves that the micro acidity constants given in the two schemes are self-consistent with each other. The ratios *R* of the twofold protonated and isocharged species $(H{\cdot}NTP{\cdot}H)^{2-}$ and $(NTP{\cdot}H_2)^{2-}$ for ITP and GTP can be estimated by using the micro acidity constant values calculated in the two equilibrium schemes. The two species carry one proton at N7 and one at the terminal γ-phosphate group, or both protons at the triphosphate chain, respectively.

The ratio R_{ITP} is defined below. It corresponds to the approximate percentages of the $(H{\cdot}ITP{\cdot}H)^{2-}$ and $(ITP{\cdot}H_2)^{2-}$ species. The first ratio given in brackets represents the lower limit following from 0.78−0.35 = 0.43, and the second one the upper limit, which follows from 0.78+0.35 = 1.13.

$$R_{ITP} = \frac{[(\mathrm{H{\cdot}ITP{\cdot}H})^{2-}]}{[(\mathrm{ITP{\cdot}H_2})^{2-}]} = \frac{k^{\mathrm{H{\cdot}ITP{\cdot}H}}_{\mathrm{H{\cdot}ITP{\cdot}H_2}}}{k^{\mathrm{ITP{\cdot}H_2}}_{\mathrm{H{\cdot}ITP{\cdot}H_2}}}$$

$$= \frac{10^{-1.26\pm0.11}}{10^{-1.15\pm0.16}} = 10^{-0.11\pm0.19} = \frac{0.78 \pm 0.35}{1}$$

$$= \frac{44}{56}\left(\frac{30}{70};\frac{53}{47}\right)$$

The approximate percentages of the $(H{\cdot}GTP{\cdot}H)^{2-}$ and $(GTP{\cdot}H_2)^{2-}$ species are analogously represented by the ratio R_{GTP}.

$$R_{GTP} = \frac{[(\mathrm{H{\cdot}GTP{\cdot}H})^{2-}]}{[(\mathrm{GTP{\cdot}H_2})^{2-}]} = \frac{k^{\mathrm{H{\cdot}GTP{\cdot}H}}_{\mathrm{H{\cdot}GTP{\cdot}H_2}}}{k^{\mathrm{GTP{\cdot}H_2}}_{\mathrm{H{\cdot}GTP{\cdot}H_2}}}$$

$$= \frac{10^{-1.28\pm0.14}}{10^{-2.20\pm0.15}} = 10^{0.92\pm0.21} = \frac{8.32 \pm 4.02}{1}$$

$$= \frac{89}{11}\left(\frac{81}{19};\frac{93}{7}\right)$$

The results obtained for R_{ITP} and R_{GTP} confirm the assumptions made at the beginning. For the twofold negatively charged $H_2(ITP)^{2-}$ species, which predominates in the pH range 1.3<pH<3.3, the N7 and the phosphate-protonated isomers occur in about equal amounts, while for $H_2(GTP)^{2-}$ the N7-protonated species dominates by about 10:1. Both nucleotides bear a γ-phosphate-bound proton that is not lost until neutral pH values are reached. At the physiological pH of about 7.4 approximately 90% of both nucleotides occur in the form of NTP^{4-}. The (N1)H site begins to lose its proton only at pH>8.5.

2.2 Acid–base properties of purine-nucleoside 5′-diphosphates

All potentiometric titrations, the results of which are summarized in the next sections, were carried in aqueous solution at 25 °C and I = 0.1 M ($NaNO_3$) and at ligand concentrations in which no self-stacking occurs [74]. A comprehensive set of the acidity constants of H_3(ADP) [105], H_3(GDP), and H_3(IDP) is given in Sections 2.2.1 to 2.2.4. In some instances, the buffer regions of the deprotonation reactions are overlapping: to be able to quantify the intrinsic acid–base properties of the various sites, micro-acidity-constant analysis were needed.

Purine-nucleoside 5′-diphosphates are able to accept 3 protons at the diphosphate chain and one at the nucleobase residue; this is located at N7 in GDP and IDP and at the N1 position in ADP. In Figure 2.4 the chemical structures of ADP, GDP, and IDP are depicted. The pK_a values of the sites indicated in the Figure with an arrow, are listed in Table 2.2 on page 28.

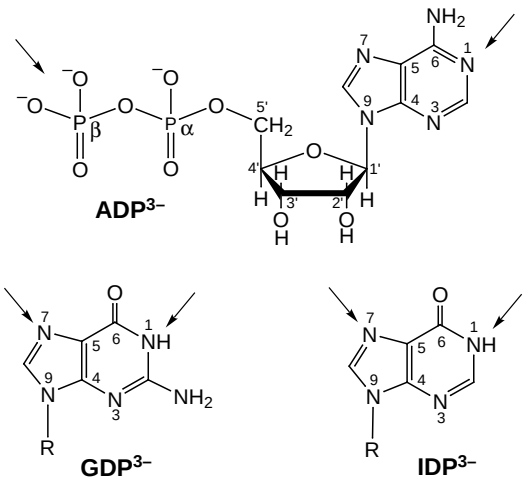

Figure 2.4: Chemical structure of the purine nucleoside 5′-diphosphates: adenosine (ADP^{3-}), guanosine (GDP^{3-}), and inosine (IDP^{3-}) 5′-diphosphates, in their dominating *anti* conformation [6,7]. The arrows show the (de)protonation sites, whose pK_a values are listed in Table 2.2 on page 28.

2.2.1 Acidity constants of $H_4(ADP)^+$

ADP^{3-} is a tetrabasic species: it can accept three protons at the diphosphate chain and one at the N1 site of the adenine moiety [6], to give the acid $H_4(ADP)^+$. First, one of the two primary protons of the diphosphate residue is released; its pK_a is very low (<1). The next proton to be released is the second primary proton from the diphosphate group, and its acidity constant (equation 2.5) was measured [105,106]. Deprotonation of the $(N1)H^+$ site follows. Its equilibrium constant, $K^{\mathrm{H}}_{\mathrm{H_2(ADP)}}$, is defined in equation 2.6. The secondary proton from the terminal β-phosphate group (equation 2.7) is the last one to be released.

$$\mathrm{H_3(ADP)^{\pm} \rightleftharpoons H_2(ADP)^- + H^+}$$

$$K^{\mathrm{H}}_{\mathrm{H_3(ADP)}} = [\mathrm{H_2(ADP)^-}][\mathrm{H^+}]/[\mathrm{H_3(ADP)^{\pm}}] \tag{2.5}$$

$$\mathrm{H_2(ADP)^- \rightleftharpoons H(ADP)^{2-} + H^+}$$

$$K^{\mathrm{H}}_{\mathrm{H_2(ADP)}} = [\mathrm{H(ADP)^{2-}}][\mathrm{H^+}]/[\mathrm{H_2(ADP)^-}] \tag{2.6}$$

$$\mathrm{H(ADP)^{2-} \rightleftharpoons ADP^{3-} + H^+}$$

$$K^{\mathrm{H}}_{\mathrm{H(ADP)}} = [\mathrm{ADP^{3-}}][\mathrm{H^+}]/[\mathrm{H(ADP)^{2-}}] \tag{2.7}$$

The measured acidity constants are summarized in Table 2.2 (page 28) together with some values of related compounds known from previous studies (the references are given in the Table) or measured now and dealt with in the next Sections. The pK_a value measured for $H(ADP)^{2-}$ agrees well with the recommended value given in [61].

A comparison of the pK_a values listed in Table 2.2 confirms that the site attributions given above for the release of the various protons is correct. The basicity-enhancing effect of a second phosphate group on the release of the final primary proton, which is possibly distributed between the α- and β- phosphate groups in the case of ADP, is evident from the difference between the pK_a values of $H_3(ADP)^{\pm}$ and $H_3(AMP)^+$:

$$\Delta \mathrm{p}K_{a/1(ADP-AMP)} = \mathrm{p}K^{\mathrm{H}}_{\mathrm{H_3(ADP)}} - \mathrm{p}K^{\mathrm{H}}_{\mathrm{H_3(AMP)}}$$
$$= (1.02\pm0.20)-(0.4\pm0.2) = 0.62\pm0.28$$

Table 2.2: Negative logarithms of the acidity constants of purine-nucleoside 5′-diphosphates as determined by potentiometric pH titrations in aqueous solution (25 °C; I = 0.1 M, $NaNO_3$), together with some further related data.[a]

Acid	$\mathrm{p}K^{\mathrm{H}}_{\mathrm{H_3(Nu)}}$ [b]	$\mathrm{p}K^{\mathrm{H}}_{\mathrm{H_2(Nu)}}$	$\mathrm{p}K^{\mathrm{H}}_{\mathrm{H(Nu)}}$	$\mathrm{p}K^{\mathrm{H}}_{\mathrm{Nu}}$
$H_3(AMP)^+$	0.4 ±0.2[c]	3.84±0.02[d,e]	6.21±0.01[e]	
$H_3(IMP)^+$	0.45±0.25[f]	1.30±0.10[f]	6.22±0.01[f]	9.02±0.02[f]
$H_3(GMP)^+$	0.3 ±0.2[f]	2.48±0.04[f]	6.25±0.02[f]	9.49±0.02[f]
$H_3(ADP)^{\pm}$	1.02±0.20[e]	3.92±0.02[d,e]	6.40±0.01[e]	
$H_3(IDP)^{\pm}$	0.57±0.21[g]	1.82±0.03	6.38±0.02	9.07±0.02
$H_3(GDP)^{\pm}$	0.77±0.20[h]	2.67±0.02	6.38±0.01	9.56±0.03

[a] So-called practical (or mixed) constants are listed [99]. The error limits given are *three times* the standard error of the mean value or the sum of the probable systematic errors, whichever is larger. [b] $\mathrm{p}K_a$ for the primary phosphate site, *i.e.*, -P(O)$(OH)_2$ for the NMPs, -$P_2(O)_4(OH)_2^-$ for the NDPs. [c] From [7]. [d] This value refers to the deprotonation of the $(N1)H^+$ site; all the other values in this column refer (largely, see text) to the deprotonation of the $(N7)H^+$ unit. [e] From [105]. [f] From [89]. [g] From the scheme of Figure 2.5 on page 36; see Section 2.2.4, page 35. [h] See Section 2.2.2 on page 30.

That the basicity difference between the final primary proton in ADP and that in AMP, $\Delta \mathrm{p}K_{a/(ADP-AMP)}$, is of the same size as the one between ATP and ADP, $\Delta \mathrm{p}K_{a/(ATP-ADP)}$, suggests that the proton released from $H_3(ADP)^{\pm}$ is actually largely located at the α-phosphate group, and therefore addition of a further phosphate group leads to the same effect as observed in the former case:

$$\Delta \mathrm{p}K_{a/2(ATP-ADP)} = \mathrm{p}K^{\mathrm{H}}_{\mathrm{H_3(ATP)}} - \mathrm{p}K^{\mathrm{H}}_{\mathrm{H_3(ADP)}}$$
$$= (1.7\pm0.1)-(1.02\pm0.20) = 0.68\pm0.22$$

Comparing the release of the proton from the terminal phosphate group in ATP, ADP, and AMP, a decrease in the ΔpK_a values is observed, because the additional negative charge is further away:

$$\Delta pK_{a/3(ADP-AMP)} = pK^{H}_{H(ADP)} - pK^{H}_{H(AMP)}$$
$$= (6.40\pm0.01)-(6.21\pm0.01) = 0.19\pm0.01$$

$$\Delta pK_{a/4(ATP-ADP)} = pK^{H}_{H(ATP)} - pK^{H}_{H(ADP)}$$
$$= (6.47\pm0.01)-(6.40\pm0.01) = 0.07\pm0.01$$

The protonated (N1)H^+ site facilitates the release of the primary proton in $H_3(AMP)^+$ ($pK^{H}_{H_3(AMP)} = 0.4\pm0.2$), as it follows from a comparison with the $pK^{H}_{H_2(MeMP)}$ value ($= 1.1\pm0.2$) of $H_2(MeMP)$ [107], where $MeMP^{2-}$ = methyl monophosphate. The effect of a further phosphate group, as described above by $\Delta pK_{a/1(ADP-AMP)}$, remains within the error limits unchanged, as follows from a comparison between methyl diphosphate ($MeDP^{3-}$) [106] and $MeMP^{2-}$ [107]:

$$\Delta pK_{a/(MeDP-MeMP)} = pK^{H}_{H_2(MeDP)} - pK^{H}_{H_2(MeMP)}$$
$$= (1.62\pm0.09)-(1.1\pm0.2) = 0.52\pm0.22$$

The influence that an additional phosphate group exerts on the acid–base properties of the (N1)H^+ site is constant, as follows from the differences in the pK_a values:

$$\Delta pK_{a/5(ADP-AMP)} = pK^{H}_{H_2(ADP)} - pK^{H}_{H_2(AMP)}$$
$$= (3.92\pm0.02)-(3.84\pm0.02) = 0.08\pm0.03$$

$$\Delta pK_{a/6(ATP-ADP)} = pK^{H}_{H_2(ATP)} - pK^{H}_{H_2(ADP)}$$
$$= (4.00\pm0.01)-(3.92\pm0.02) = 0.08\pm0.02$$

These results prove the consistency of the data assembled in Table 2.2 and provide confidence for extrapolations towards values for systems that have not been studied yet.

2.2.2 Acidity constants of $H_3(GDP)^{\pm}$ and $H_3(IDP)^{\pm}$

$H_4(GDP)^+$ and $H_4(IDP)^+$ can release 5 protons: three from the diphosphate chain, one from N7 and, if high enough pH values are reached (pH$\geq$8.5), a further one from the (N1)H site, giving rise to 4-fold negatively charged species. The following equilibria are involved in the deprotonation of the various sites:

$$\mathrm{H_4(NDP)^+ \rightleftharpoons H_3(NDP)^{\pm} + H^+}$$
$$K^{\mathrm{H}}_{\mathrm{H_4(NDP)}} = [\mathrm{H_3(NDP)^{\pm}}][\mathrm{H^+}]/[\mathrm{H_4(NDP)^+}] \tag{2.8}$$

$$\mathrm{H_3(NDP)^{\pm} \rightleftharpoons H_2(NDP)^- + H^+}$$
$$K^{\mathrm{H}}_{\mathrm{H_3(NDP)}} = [\mathrm{H_2(NDP)^-}][\mathrm{H^+}]/[\mathrm{H_3(NDP)^{\pm}}] \tag{2.9}$$

$$\mathrm{H_2(NDP)^- \rightleftharpoons H(NDP)^{2-} + H^+}$$
$$K^{\mathrm{H}}_{\mathrm{H_2(NDP)}} = [\mathrm{H(NDP)^{2-}}][\mathrm{H^+}]/[\mathrm{H_2(NDP)^-}] \tag{2.10}$$

$$\mathrm{H(NDP)^{2-} \rightleftharpoons NDP^{3-} + H^+}$$
$$K^{\mathrm{H}}_{\mathrm{H(NDP)}} = [\mathrm{NDP^{3-}}][\mathrm{H^+}]/[\mathrm{H(NDP)^{2-}}] \tag{2.11}$$

$$\mathrm{NDP^{3-} \rightleftharpoons (NDP-H)^{4-} + H^+}$$
$$K^{\mathrm{H}}_{\mathrm{NDP}} = [\mathrm{(NDP-H)^{4-}}][\mathrm{H^+}]/[\mathrm{NDP^{3-}}] \tag{2.12}$$

In analogy with what is observed with IMP and GMP [89], the first two primary phosphate-bound protons are expected to be released at very low pH (<1), and their constants were not measured here. The first measured constant ($K^{\mathrm{H}}_{\mathrm{H_2(NDP)}}$, equation 2.10) is (mainly, see next Section, page 33) due to the deprotonation of the (N7)H^+ site. The next proton is released from the terminal phosphate group (eq. 2.11), and the last equilibrium, described by $K^{\mathrm{H}}_{\mathrm{NDP}}$ (equation 2.12), refers to the deprotonation of the (N1)H site. These assignments agree with previous conclusions regarding the 5′-mono- [89] and triphosphates [93] of inosine and guanosine. The values of the constants are listed in Table 2.2 on page 28. The measured

values for $pK^{H}_{H_2(GDP)}$, $pK^{H}_{H(GDP)}$, and pK^{H}_{GDP} agree well with a previous tabulation [61,98]. The only constant available for IDP [108] concerns the deprotonation of the β-phosphate group, and the value given there ($pK^{H}_{H(IDP)}$ = 6.69, I = 0.1 M; 25 °C) is somewhat higher than the one measured here. A reason for this discrepancy might be the different medium used. In [108] a tetrapropylammonium salt was used as a background electrolyte (25 °C; I = 0.1 M) and here $NaNO_3$ was employed. If the background electrolyte is changed to a larger, more hydrophobic group, the hydration layers around the ions are decreased, there is less disruption upon adding a proton, and the solvent becomes more non-aqueous in nature, which could explain the higher $pK^{H}_{H(IDP)}$ value measured in the presence of the tetrapropylammonium salt. All other acidity constants measured for IDP have never been determined before [60–62].

The data collected in Table 2.2 allow several comparisons. The presence of a second phosphate group has a basicity-enhancing effect on the release of the final primary proton in $H_3(GDP)^{\pm}$ as is shown by the difference between the pK_a values of $H_3(GDP)^{\pm}$ and $H_3(GMP)^{+}$, $\Delta pK_{a/1(GDP-GMP)}$.

$$\Delta pK_{a/1(GDP-GMP)} = pK^{H}_{H_3(GDP)} - pK^{H}_{H_3(GMP)}$$
$$= (0.77\pm0.20)-(0.3\pm0.2;\ [89]) = 0.47\pm0.28$$

This value has the same size as $\Delta pK_{a/2(GTP-GDP)}$, representing the basicity difference between the final primary proton in GTP and that in GDP, which suggests that the proton released from $H_3(GDP)^{\pm}$ is actually located at the α-phosphate group.

$$\Delta pK_{a/2(GTP-GDP)} = pK^{H}_{H_3(GTP)} - pK^{H}_{H_3(GDP)}$$
$$= (1.26\pm0.11)-(0.77\pm0.20) = 0.49\pm0.23$$

The effect of the presence of a further phosphate group, as described above by $\Delta pK_{a/1(GDP-GMP)}$, remains within the error limits unchanged, as follows from a comparison with the values obtained in the previous section for $\Delta pK_{a/(MeDP-MeMP)}$ ($= 0.52\pm0.22$) and $\Delta pK_{a/1(ADP-AMP)}$ ($= 0.62\pm0.28$).

The values of the acidity constants of the triphosphates are taken from Table 2.1 on page 20; $pK^{H}_{H_3(GDP)}$ (Table 2.2, page 28) is an estimate based on the value of $pK^{H}_{H_3(ADP)}$, see Section 2.2.3, page 33.

Defining now $\Delta pK_{a/(IDP-IMP)} = pK^{H}_{H(IDP)} - pK^{H}_{H(IMP)}$, and $\Delta pK_{a/(ITP-IDP)} = pK^{H}_{H(ITP)} - pK^{H}_{H(IDP)}$, a decrease in their values is observed by $\Delta pK_{a/(IDP-IMP)}$ to $\Delta pK_{a/(ITP-IDP)}$:

$$\Delta pK_{a/(IDP-IMP)} = (6.38\pm0.02)-(6.22\pm0.01) = 0.16\pm0.02$$

$$\Delta pK_{a/(ITP-IDP)} = (6.47\pm0.02)-(6.38\pm0.02) = 0.09\pm0.03$$

Comparison of the acidity constants of the nucleosides with those of their corresponding nucleotides reveals the effect of the 3-fold negatively charged diphosphate chain on the deprotonation of the (N1)H site.

$pK^{H}_{GDP}-pK^{H}_{Guo} = (9.56\pm0.03) - (9.22\pm0.01) = 0.34\pm0.03$
$pK^{H}_{IDP} -pK^{H}_{Ino} = (9.07\pm0.02) - (8.76\pm0.03) = 0.31\pm0.04$

As one might expect, the release of the proton from (N1)H in NDP^{3-} is inhibited by the diphosphate chain and the effect is very similar to that observed with the pyrimidines and their (N3)H site.

$pK^{H}_{UDP} -pK^{H}_{Urd} = (9.47\pm0.02; [106]) - (9.19\pm0.02; [97]) = 0.28\pm0.03$
$pK^{H}_{dTDP}-pK^{H}_{dThy} = (9.93\pm0.02; [106]) - (9.69\pm0.03; [97]) = 0.24\pm0.04$

As already observed in the case of the triphosphates (Section 2.1.1, page 17), the effect described above operates likewise when a positively charged $(N1)H^{+}$ site is involved as in $H_2(ADP)^{2-}$ and $H(adenosine)^{+}$:

$pK^{H}_{H_2(ADP)}-pK^{H}_{Ado} = (3.92\pm0.02) - (3.61\pm0.03) = 0.31\pm0.04$

The same observation can be made in the case of the monophosphates, and using data collected from the literature [89,94,105], one obtains:

$pK^{H}_{GMP}-pK^{H}_{Guo} = (9.49\pm0.02) - (9.22\pm0.01) = 0.27\pm0.02$
$pK^{H}_{IMP} -pK^{H}_{Ino} = (9.02\pm0.02) - (8.76\pm0.03) = 0.26\pm0.04$

$pK^{H}_{UMP} - pK^{H}_{Urd}$ = (9.45±0.02) − (9.19±0.02; [97]) = 0.26±0.03

$pK^{H}_{dTMP} - pK^{H}_{dThy}$ = (9.90±0.03) − (9.69±0.03; [97]) = 0.21±0.04

In the case of AMP and its (N1)H^+ site results:

$pK^{H}_{H_2(AMP)} - pK^{H}_{Ado}$ = (3.84±0.02) − (3.61±0.03) = 0.23±0.04

As it was to be expected, the additional negative charges lead to an increased basicity of the N1 (or N3) sites at the nucleobase.

Comparing the data concerning the influence of the phosphate chain on the basicity of the N1 (or N3) site in nucleoside 5′-mono-, di-, and triphosphates, it is possible to conclude that each additional phosphate group gives rise to an increase in the basicity of the N1 sites of purines or the N3 sites of pyrimidines.

2.2.3 Estimation of the acidity constants for $H_3(GDP)^{\pm}$ and $H_3(IDP)^{\pm}$ in the low pH range

Assuming that the acidity constant of the second primary proton of the diphosphate residue in $H_3(GDP)^{\pm}$ is similar to that of $H_3(ADP)^{\pm}$ (pK_a = 1.02±0.20 [105]), one can observe that the buffer regions of the individual deprotonation steps of $H_3(GDP)^{\pm}$ are separated by about 1.65 (or more) log units, hence there is no significant overlap of the buffer regions and the macro acidity constants are close to the micro acidity constants of the individual sites. This may be different for $H_3(IDP)^{\pm}$, because $pK^{H}_{H_2(IDP)}$ = 1.82±0.03 (Table 2.2, page 28) could well contain a contribution from the release of the second primary proton from the diphosphate group, and thus does not refer to the (N7)H^+ site alone. It is therefore necessary to estimate a micro constant for the equilibrium:

$$(H{\cdot}IDP{\cdot}H)^{-} \rightleftharpoons (IDP{\cdot}H)^{2-} + H^{+}$$

where $(H{\cdot}IDP{\cdot}H)^{-}$ represent a species that carries one proton at N7 and one at the terminal β-phosphate group.

The *difference* between the pK_a values for the deprotonation of the (N7)H^+

site in the guanine and hypoxanthine moieties is expected to be independent of the presence of the diphosphate chain, because the effect of this residue on the acid–base properties of N7 should be identical on both moieties. This difference should therefore be the same if calculated via the pK_a values of the two nucleosides, Ino and Guo, or via those of the two NDPs:

$$\Delta \mathrm{p}K_a = \mathrm{p}K^{\mathrm{H}}_{\mathrm{H(Guo)}} - \mathrm{p}K^{\mathrm{H}}_{\mathrm{H(Ino)}} = (2.11 \pm 0.04) - (1.06 \pm 0.06) = 1.05 \pm 0.07$$

and therefore:

$$\mathrm{p}k^{\mathrm{IDP{\cdot}H}}_{\mathrm{H{\cdot}IDP{\cdot}H}} = \mathrm{p}K^{\mathrm{H}}_{\mathrm{H_2(GDP)}} - \Delta \mathrm{p}K_a = (2.67 \pm 0.02) - (1.05 \pm 0.07) = 1.62 \pm 0.07$$

This value represents the equilibrium constant for the deprotonation of (N7)H^+ of (H·IDP·H)$^-$. This micro constant is relatively close to the macro constant measured in the experiments, p$K^{\mathrm{H}}_{\mathrm{H_2(IDP)}}$ = 1.82±0.03 (Table 2.2, page 28), indicating that the contribution from the deprotonation of the phosphate group to this constant is not very pronounced. A more rigorous evaluation is given in the next section.

In analogy to the procedure adopted for the triphosphates, the value of the macro acidity constant p$K^{\mathrm{H}}_{\mathrm{H_3(GDP)}}$ for the deprotonation of $H_3(GDP)^{\pm}$, or the release of the final primary proton from the diphosphate chain, can be estimated on the basis of the known value [105] of p$K^{\mathrm{H}}_{\mathrm{H_3(ADP)}}$. The different distances of (N7)H^+ and (N1)H^+ from the diphosphate chain must be taken into account (see Figure 2.4, page 26). Indeed, in the predominating *anti* conformation, the (N7)H^+ site of $H_3(GDP)^{\pm}$ is somewhat closer to the diphosphate chain than the (N1)H^+ site of $H_3(ADP)^{\pm}$, therefore it should have a slightly stronger acidifying effect on the diphosphate chain. This *distance effect* can be quantified by the difference:
$\Delta\Delta \mathrm{p}K_a$ = $\Delta \mathrm{p}K_{a/N7} - \Delta \mathrm{p}K_{a/N1}$, where $\Delta \mathrm{p}K_{a/N7}$ = $\mathrm{p}K^{\mathrm{H}}_{\mathrm{H_2(GDP)}} - \mathrm{p}K^{\mathrm{H}}_{\mathrm{H(Guo)}}$ = (2.67±0.02) − (2.11±0.04) = 0.56±0.04, and $\Delta \mathrm{p}K_{a/N1}$ = $\mathrm{p}K^{\mathrm{H}}_{\mathrm{H_2(ADP)}} - \mathrm{p}K^{\mathrm{H}}_{\mathrm{H(Ado)}}$ = (3.92±0.02) − (3.61±0.03) = 0.31±0.04. Hence: $\Delta\Delta \mathrm{p}K_a$ = (0.56±0.04) − (0.31±0.04) = 0.25±0.06. From the value of the acidity constant of $H_3(ADP)^{\pm}$ one obtains:
$\mathrm{p}K^{\mathrm{H}}_{\mathrm{H_3(GDP)}}$ = $\mathrm{p}K^{\mathrm{H}}_{\mathrm{H_3(ADP)}} - \Delta\Delta \mathrm{p}K_a$ = (1.02±0.20) − (0.25±0.06) = 0.77±0.20.

This constant, given in column 2 of Table 2.2, represents the pK_a value for the release of a primary proton from a diphosphate group affected by a protonated (N7)H^+ site. It is thus an estimate for the micro constant p$k^{\mathrm{H\cdot IDP\cdot H}}_{\mathrm{H\cdot IDP\cdot H_2}}$, quantifying the deprotonation of $(H\cdot IDP\cdot H_2)^{\pm}$ according to the following equilibrium:

$$(H\cdot IDP\cdot H_2)^{\pm} \rightleftharpoons (H\cdot IDP\cdot H)^{-} + H^{+}$$

Hence, p$k^{\mathrm{H\cdot IDP\cdot H}}_{\mathrm{H\cdot IDP\cdot H_2}}$ = p$K^{\mathrm{H}}_{\mathrm{H_3(GDP)}}$ = 0.77±0.20.

2.2.4 Micro acidity constant scheme for $H_3(IDP)^{\pm}$

The equilibrium scheme in Figure 2.5 defines the micro constants (*k*) and gives their interrelation with the macro constants (*K*) for $H_3(IDP)^{\pm}$. The sum p$K^{\mathrm{H}}_{\mathrm{H_3(IDP)}}$ + p$K^{\mathrm{H}}_{\mathrm{H_2(IDP)}}$ in Figure 2.5 can be calculated from the values of p$k^{\mathrm{H\cdot IDP\cdot H}}_{\mathrm{H\cdot IDP\cdot H_2}}$ = 0.77±0.20 and p$k^{\mathrm{IDP\cdot H}}_{\mathrm{H\cdot IDP\cdot H}}$ = 1.62±0.07 deduced in Section 2.2.3: p$K^{\mathrm{H}}_{\mathrm{H_3(IDP)}}$ + p$K^{\mathrm{H}}_{\mathrm{H_2(IDP)}}$ = 2.39±0.21. The value of the macro acidity constant p$K^{\mathrm{H}}_{\mathrm{H_3(IDP)}}$, that quantifies the acidity of $H_3(IDP)^{\pm}$ and whose value is listed in the second column of Table 2.2 (page 28), can now be calculated: p$K^{\mathrm{H}}_{\mathrm{H_3(IDP)}}$ = p$k^{\mathrm{H\cdot IDP\cdot H}}_{\mathrm{H\cdot IDP\cdot H_2}}$ + p$k^{\mathrm{IDP\cdot H}}_{\mathrm{H\cdot IDP\cdot H_2}}$ − p$K^{\mathrm{H}}_{\mathrm{H_2(IDP)}}$ = 2.39±0.21 − 1.82±0.03 = 0.57±0.21.

In principle it would now be possible, knowing p$k^{\mathrm{H\cdot IDP\cdot H}}_{\mathrm{H\cdot IDP\cdot H_2}}$, p$k^{\mathrm{IDP\cdot H}}_{\mathrm{H\cdot IDP\cdot H}}$ and the values for the macro constants, to calculate [103,104] the values for the micro constants in the upper part of Figure 2.5. However, as the error limits of some of the constants employed are rather large, a further estimation is preferred in this case.

The micro acidity constant $k^{\mathrm{IDP\cdot H}}_{\mathrm{IDP\cdot H_2}}$ refers to the release of a proton from the diphosphate group of a nucleoside diphosphate which carries a neutral nucleic base residue. Such a value corresponds to the one measured for the release of the second primary proton from the diphosphate chain in $H_2(UDP)^{-}$. The corresponding acidity constant, p$K^{\mathrm{H}}_{\mathrm{H_2(UDP)}}$ = 1.26±0.20 [106], is a good estimate for the micro constant of the equilibrium:

$$(IDP\cdot H_2)^{-} \rightleftharpoons (IDP\cdot H)^{2-} + H^{+}$$

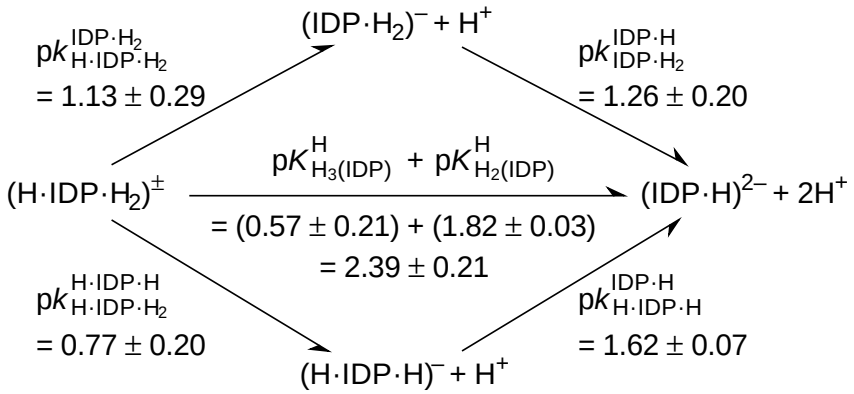

Figure 2.5: Equilibrium scheme for $(H{\cdot}IDP{\cdot}H_2)^{\pm}$ defining the micro acidity constants (*k*) and showing their interrelation with the macro acidity constants (*K*). The interrelation between $(IDP{\cdot}H_2)^-$ and $(H{\cdot}IDP{\cdot}H)^-$ and the other species present are shown as well. In $(IDP{\cdot}H_2)^-$ one proton is at the β-phosphate group and the other at one of the primary sites of the diphosphate chain, while in $(H{\cdot}IDP{\cdot}H)^-$ one proton is at N7 and the other at the β-phosphate group. $(H{\cdot}IDP{\cdot}H_2)^{\pm}$ is often written as $H_3(IDP)^{\pm}$ and carries one proton at N7 and the other two at the diphosphate residue. The arrows indicate the direction for which the acidity constants are defined.

giving: $pk^{IDP{\cdot}H}_{IDP{\cdot}H_2} = pK^{H}_{H_2(UDP)} = 1.26 \pm 0.20$. Employing this value, the last micro acidity constant of the upper cycle in the scheme, $pk^{IDP{\cdot}H_2}_{H{\cdot}IDP{\cdot}H_2}$, can be calculated.

It is now possible to estimate the ratio *R* of the twofold protonated and isocharged species $(H{\cdot}IDP{\cdot}H)^-$ and $(IDP{\cdot}H_2)^-$, that carry one proton at N7 and one at the terminal β-phosphate group, or both protons at the diphosphate chain, respectively.

$$R = \frac{[(H{\cdot}IDP{\cdot}H)^{2-}]}{[(IDP{\cdot}H_2)^{2-}]} = \frac{k^{IDP{\cdot}H}_{IDP{\cdot}H_2}}{k^{IDP{\cdot}H}_{H{\cdot}IDP{\cdot}H}}$$

$$= \frac{10^{-1.26\pm0.20}}{10^{-1.62\pm0.07}} = 10^{0.36\pm0.21}$$

$$R = \frac{2.29 \pm 1.11}{1}$$

The ratio *R* approximately corresponds to the percentages of the $(H{\cdot}IDP{\cdot}H)^-$ and $(IDP{\cdot}H_2)^-$ species formed. Of course, this result must be considered as a rough estimate, but it indicates that both isomers occur in aqueous solution with a possible dominance of the species carrying a proton at the diphosphate residue and one at N7 of the hypoxanthine moiety.

The buffer regions of the $H_2(IDP)^-$ ($pK^{H}_{H_2(IDP)} = 1.82$) and $H_3(IDP)$ ($pK^{H}_{H_3(IDP)} = 0.57$) species are overlapping ($\Delta\ pK_a = 1.25$). In all other systems, overlap of the various equilibria is smaller and therefore not of relevance.

Application of the measured constants listed in Table 2.2 (page 28) allows calculation of the percentages of the species present as a function of pH. A representative example is shown in Figure 2.6 for GDP and IDP.

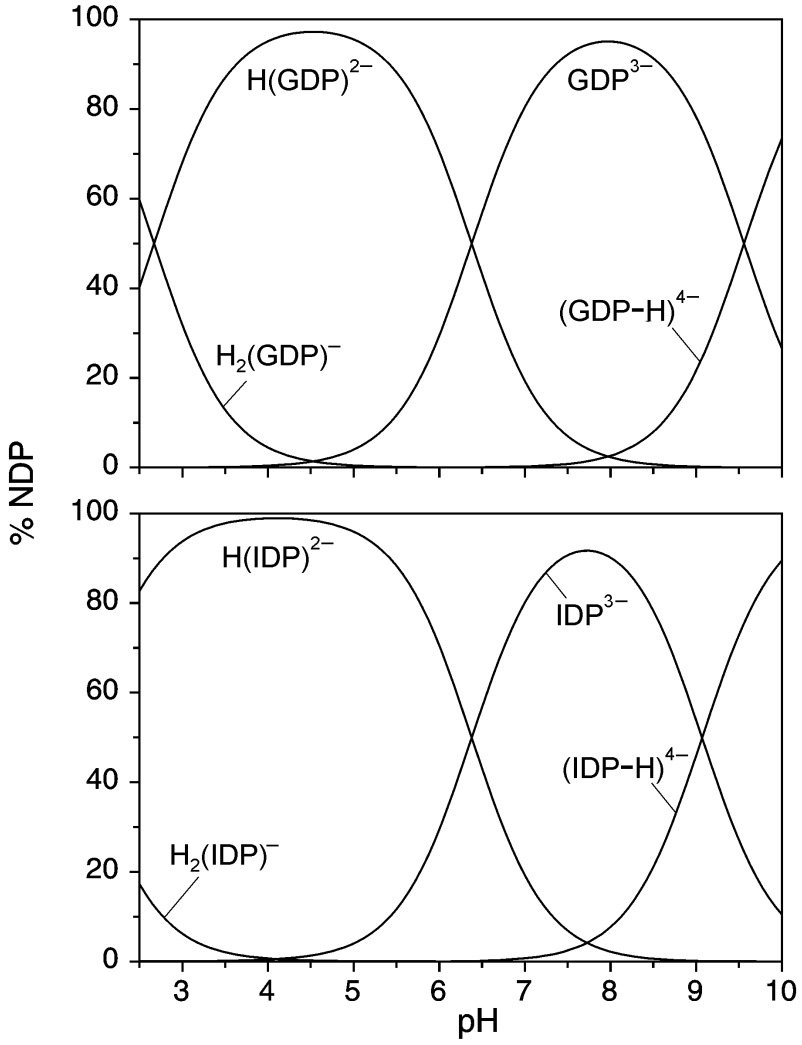

Figure 2.6: Comparison of the distribution curves of the various species present in aqueous solution in dependence on pH for GDP (upper part) and IDP (lower part). The results are given as percentages of the total NDP concentration present. Calculations were carried out using the potentiometrically determined acidity constants listed in Table 2.2, page 28 (25 °C; I = 0.1 M, $NaNO_3$).

2.3 Potential metal binding sites in nucleotides

It is known for several systems that for a series of related ligands metal ion-complex stability increases with ligand basicity [94,106]. Therefore, the acidity constant of each site of a nucleotide can give some information on the possible coordination sites of metal ions. A metal ion may interact with the phosphate group(s) of a nucleotide. In addition, the heterocyclic bases contain oxygen and nitrogen electron donors as potential coordination sites. The hydroxy groups of the sugar moiety have pK_a values of 12 or higher [89], and their interaction with divalent metal ions is weak as long as no deprotonation occurs [58]. Evidence of such weak interactions is given by the two following examples. A X-ray structure study of a polymeric Cu^{2+} complex of guanosine 2′-monophosphate shows an axial Cu–O(5′) bond with the ribose [109]. In the structure, Cu^{2+} has a distorted [4+2]-octahedral coordination sphere, in which the Cu–O(5′) bond (2.474 Å) is 0.138 Å longer than the opposite Cu–O bond to a coordinated water molecule (2.336 Å). Structural studies showed [110] that simple carbohydrates can bind Ca^{2+} only if they can provide *three or more* hydroxy groups in a geometrical arrangement fitting the coordination sphere of the metal ion [111,112]. Solid-state complexes of 3d metal ions with nucleotides only rarely show interactions between the metal ion and the sugar-hydroxy groups [113]. A decrease in solvent polarity favours M^{2+} binding to these weakly coordinating sites, as shown in studies carried out with dihydroxyacetone phosphate, $DHAP^{2-}$, and glycerol 1-phosphate, $G1P^{2-}$, in water and water/1,4-dioxane mixtures [114,115] (Figure 2.7).

In aqueous solutions and at pH lower than 10, no deprotonation or complex formation involving the ribosyl moiety is therefore expected. The data collected from the experiments carried out now with the purine nucleotides in water, and the ones with 5′-GDP in water and water/1,4-dioxane mixtures, were evaluated in a pH range far below the onset of complex formation with the ribose-hydroxy groups. For that reason this kind of interactions are not considered here.

The abundance of electron donor atoms at the phosphate group(s) of nucleotides,

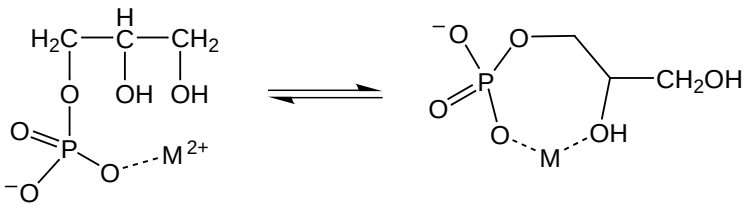

Figure 2.7: Complex formed between $G1P^{2-}$ and a divalent metal ion. Schematic representation of an intramolecular equilibrium between an *open* and a *closed* isomer. In the open form, the metal ion is only phosphate-coordinated, while in the closed one it interacts with the oxygen atom at C2 of $G1P^{2-}$ as well. Such an interaction is only possible in conditions of lower polarity than bulk water, where the -OH group interacts with the metal ion. Such conditions are found in the active site of enzymes. Adapted from [114].

together with the relatively high basicity of the terminal phosphate group, makes of them the preferred binding sites of metal ions: the stability of nucleotide–metal ion complexes with the alkaline earth metal ions or the metals of the 3d transition series is to a very large extent determined by the binding of the metal ion to the phosphate group(s) [58].

However, interactions of the phosphate-bound metal ion with the nucleobase can influence the stability and structure of some nucleotides [59]. Two kinds of interactions are possible: innersphere and outersphere. In an *innersphere* coordination the phosphate-bound metal ion directly interacts with the nucleobase; in an *outersphere* type of interaction, the metal ion is indirectly coordinated to the nucleobase via water molecules. This latter possibility includes H bond formation between aqua ligands bound to the metal ion and suitable acceptors of the nucleobase. Moreover, long range interactions can occur between π-π orbitals of the nucleobase and the metal entity (stacking interactions), if the metal carries heteroaromatic auxiliary ligands [67].

As pointed out at the beginning of this Chapter, in purine nucleotides the N1 position at the nucleobase is the most basic one, followed by N7. The N3 site is the least basic. The structures of the nucleotides (for clarity shown once more

in Figure 2.8) reveal that the base moieties of uridine and thymidine do not offer any strong metal ion-binding sites, apart from the weakly coordinating carbonyl groups, as long as the (N3)H unit is not deprotonated. This reaction will only exceptionally occur in the physiological pH range under the influence of metal ions, as the acidity constants are high [88,94]. A similar situation occurs with inosine and guanosine: the (N1)H sites are in general not available at a pH of about 7 for metal ion binding [89,93]. This leaves N3 and N7 as potential binding sites. Among these, N7 is the predominant site. Adenosine and cytosine show a large degree of ambivalent behaviour.

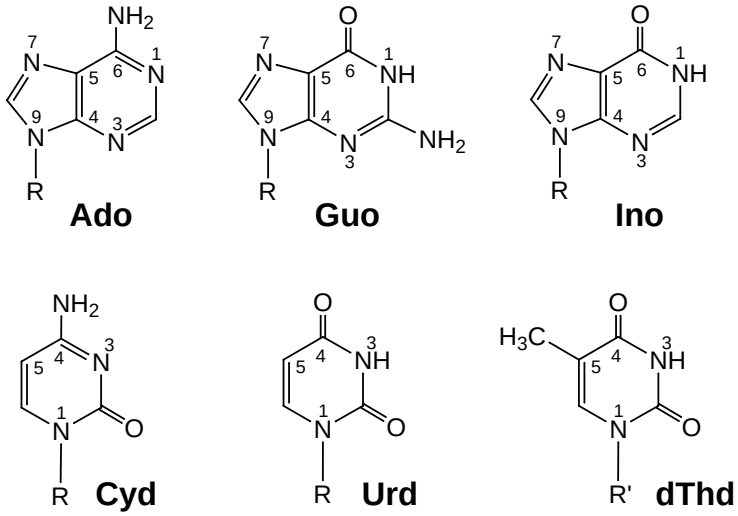

Figure 2.8: Chemical structure of the nucleosides (R = ribose; R′ = 2′-deoxyribose): Ado = adenosine; Guo = guanosine; Ino = inosine; Cyd = cytidine; Urd = uridine; dThd = thymidine; or nucleotides 5′-mono-, di-, or triphosphates (R = ribosyl 5′-mono-, 5′-di-, or 5′-triphosphate; R′ = 2′-deoxyribosyl 5′-mono-, 5′-di-, or 5′-triphosphate, respectively).

The adenine residue offers metal ions N1, N3 (only occasionally, e.g. with adenosine 2′-monophosphate [116]), and N7 as binding sites. Consequently, a dichotomy of metal ion binding of N1 *versus* N7 is left for adenosine. In a detailed study [117], it has been proven that Ni^{2+} and Cu^{2+} (to approximately 70%) and most probably Co^{2+} and Cd^{2+}, prefer to coordinate to adenosine *via* the N7 site. Zn^{2+} showed a more even distribution between the N1 and the N7 sites, while Mn^{2+}

possibly prefers the N1 site, which is strongly predominant for the binding of the proton.

In the case of cytosine, the N3 position is not the only one available for metal ions: the 2-carbonyl group could participate in metal ion binding, together with N3. It has been shown [90] that the carbonyl group does not participate to any appreciable extent in the binding of Co^{2+} and Ni^{2+}, while in the $M(Cyd)^{2+}$ complexes of Zn^{2+}, Cd^{2+}, or Cu^{2+}, chelates involving N3 and a weakly bound O2 are formed, at least in equilibrium. In contrast, the $M(Cyd)^{2+}$ complexes of Mn^{2+}, Mg^{2+}, and Ca^{2+} apparently owe their stability to a large part to the metal ion affinity of the O2-carbonyl group [90].

That a phosphate-coordinated metal ion may form macrochelates by interacting with N7 of the purine moiety of a nucleotide, is an idea that goes back to Szent Györgyi [118] and it has been proven for M(NMP) (*cf.*, e.g., [58,89,104,119–121]) and $M(NTP)^{2-}$ complexes [73,122,123] of several divalent metal ions. By ^{1}H-NMR shift measurements it has been shown to occur [74] in the ADP^{3-} complexes of Zn^{2+} and Cd^{2+}, but a comprehensive evaluation regarding the position of the intramolecular equilibrium shown in Figure 2.9 for the $M(NDP)^{-}$ and $M(NTP)^{2-}$ complexes of purine-nucleoside 5′-di- and 5′-triphosphates is missing.

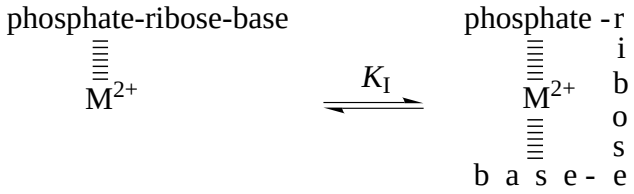

Figure 2.9: Schematic representation of an intramolecular equilibrium between an *open* and a *closed* family of isomers. In the open form, the metal ion is only phosphate-coordinated, while in the closed one it interacts with the nucleobase as well.

In the next Sections, it will be dealt with the stability constants of metal ion coordination to the phosphate groups of these last two classes of ligands. Furthermore, the possibility of metal binding to nucleobase sites and phosphates simultaneously, giving rise to macrochelate formation, as shown in Figure 2.9, will be considered.

2.3.1 Metal ion-coordinating properties of purine-nucleoside 5′-di- and triphosphates

Existence of the described equilibrium between *open* and *closed* isomers for the M(AMP) complexes is well established [58]: the increased stability observed due to macrochelate formation with N7 of the phosphate-coordinated metal ion disappears, as expected, in all the corresponding complexes formed with tubercidin 5′-monophosphate (= 7-deaza-AMP^{2-}) since this ligand lacks N7 [104] (Figure 2.10).

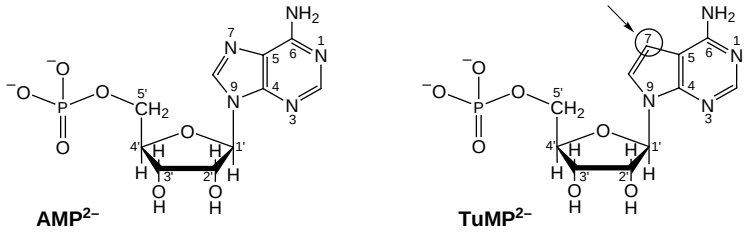

Figure 2.10: Structures of adenosine 5′-monophosphate, AMP^{2-}, and of tubercidin 5′-monophosphate (= 7-deaza-AMP^{2-}), TuMP^{2-}.

Indeed, any kind of chelation [124] must be reflected in an enhanced complex stability [59]. Of course, macrochelates as indicated in equilibrium 2.13 will hardly form to 100%.

$$\mathrm{ML_{op}} \rightleftharpoons \mathrm{ML_{cl}} \tag{2.13}$$

The formation degree of the macrochelated or closed species ($\mathrm{ML_{cl}}$) is *independent* of the total complex concentration because the intramolecular equilibrium constant K_I, as defined by equation 2.14, where $\mathrm{ML_{op}}$ refers to the open species (with only a phosphate-coordinated metal ion) in the equilibrium, is dimensionless:

$$K_\mathrm{I} = [\mathrm{ML_{cl}}]/[\mathrm{ML_{op}}] \tag{2.14}$$

The equilibrium of complex formation can be written as:

$$\mathrm{M^{2+}} + \mathrm{L} \rightleftharpoons \mathrm{ML_{op}} \rightleftharpoons \mathrm{ML_{cl}}$$

and the corresponding equilibrium constant is then defined by:

$$K^{\mathrm{M}}_{\mathrm{ML}} = \frac{[\mathrm{ML_{op}}] + [\mathrm{ML_{cl}}]}{[\mathrm{M^{2+}}][\mathrm{L}]} \tag{2.15}$$

The observed overall stability is the sum of the individual constants for the open and closed forms:

$$K^{\mathrm{M}}_{\mathrm{ML}} = K^{\mathrm{M}}_{\mathrm{ML_{op}}} + K^{\mathrm{M}}_{\mathrm{ML_{cl}}}$$

Any breakdown of the values for $K^{\mathrm{M}}_{\mathrm{ML}}$, which has to reflect the contribution of the various terms necessary for a further interpretation, requires that values for $K^{\mathrm{M}}_{\mathrm{ML_{op}}}$, that cannot be directly measured, are obtainable. In contrast, $K^{\mathrm{M}}_{\mathrm{ML}}$ is experimentally accessible. For families of related ligands, straight lines are observed if log $K^{\mathrm{M}}_{\mathrm{ML}}$ is plotted *versus* p$K^{\mathrm{H}}_{\mathrm{HL}}$ [124]. Indeed, the data pairs log $K^{\mathrm{M}}_{\mathrm{M(R-MP)}}$/ p$K^{\mathrm{H}}_{\mathrm{H(R-MP)}}$ for phenyl phosphate, 4-nitrophenyl phosphate, methyl phosphate, *n*-butyl phosphate, and hydrogen phosphate, for a given metal-ion complex, all fit on a straight line [94]. Complexes formed by methylphosphonate and ethylphosphonate fit on the same straight lines [125]. A linear relationship exists for log $K^{\mathrm{M}}_{\mathrm{M(R-DP)}}$ *versus* p$K^{\mathrm{H}}_{\mathrm{H(R-DP)}}$ [106], where R-DP^{3-} represents a simple diphosphate monoester, *i.e.*, R may be any residue which does not affect complex formation.

The parameters for the corresponding straight-line equations, defined by equation 2.16:

$$\log K^{\mathrm{M}}_{\mathrm{ML}} = m \cdot \mathrm{p}K^{\mathrm{H}}_{\mathrm{HL}} + b \tag{2.16}$$

have been tabulated for L = R-MP^{2-} [94,125] and R-DP^{3-} [106]. Hence, with a known pK_{a} value for the deprotonation of a P(O)$_2$(OH)$^-$ group an expected stability constant can be calculated for any phosph(on)ate- or diphosphate-metal ion complex.

As an example, plots of log $K^{\mathrm{M}}_{\mathrm{M(R-DP)}}$ *versus* p$K^{\mathrm{H}}_{\mathrm{H(R-DP)}}$ are shown in Figure 2.11 for the 1:1 complexes of Mg^{2+}, Co^{2+}, and Zn^{2+}, with the data points (empty circles) of the six (five in the case of Zn^{2+}) simple ligand systems used [106] for

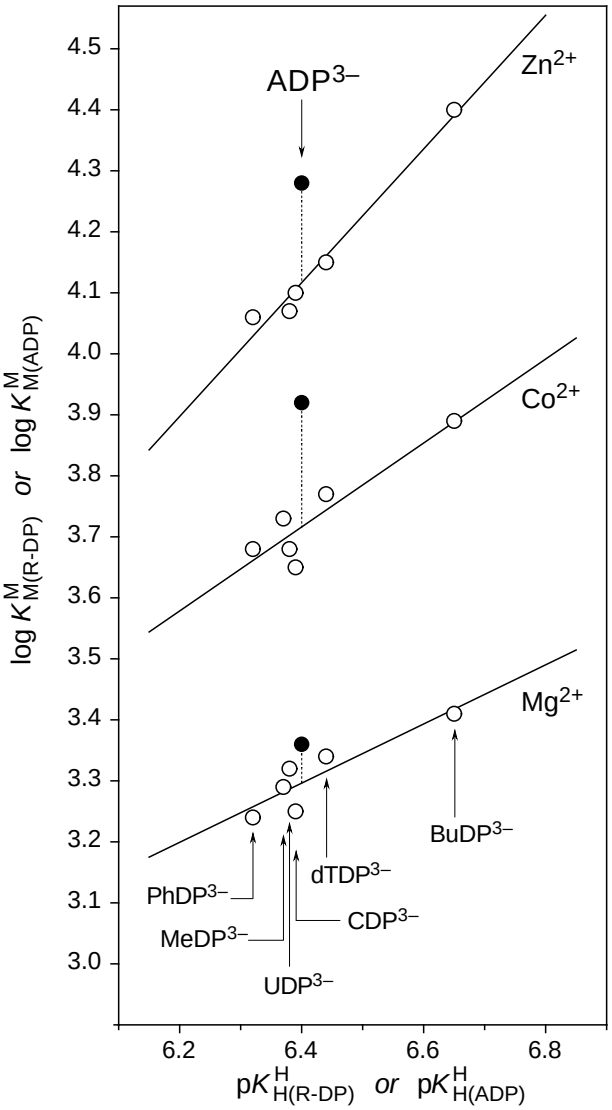

Figure 2.11: Evidence for an enhanced stability of the $Mg(ADP)^{-}$, $Co(ADP)^{-}$ and $Zn(ADP)^{-}$ complexes (•), based on the relationship between log $K^{\mathrm{M}}_{\mathrm{M(R-DP)}}$ and $pK^{\mathrm{H}}_{\mathrm{H(R-DP)}}$ for the simple $M(R\text{-}DP)^{-}$ complexes (○), where $R\text{-}DP^{3-}$ = phenyl diphosphate ($PhDP^{3-}$), methyl diphosphate ($MeDP^{3-}$), uridine 5′-diphosphate (UDP^{3-}), cytidine 5′-diphosphate (CDP^{3-}), thymidine [=1-(2-deoxy-β-D-ribofuranosyl)thymine] 5′-diphosphate ($dTDP^{3-}$) and *n*-butyl diphosphate ($BuDP^{3-}$). The least-square lines are drawn through the six (five in the case of Zn^{2+}) data sets; the corresponding equilibrium constants are from [106]. All the plotted equilibrium constants refer to aqueous solutions at 25 °C and I = 0.1 M ($NaNO_3$).

the determination of the straight reference lines. The solid points refer to the corresponding M(ADP)$^-$ complexes, based on the values listed in Tables 2.2 and 2.9 (on pages 28 and 67, respectively). They are above the reference lines in every instance, proving that macrochelates form. The vertical distances of the solid data points to their reference lines varies, as the extent of macrochelate formation differs for the various systems.

In nucleoside 5′-triphosphates, the terminal γ-phosphate group is relatively far removed from the nucleosidyl residue and consequently its basicity is largely unaffected by the base residues (see Table 2.1 on page 20). To be able to determine the position of the equilibrium and the percentage of macrochelate formation in these systems, the stabilities of those complexes in which the metal ion is coordinated only to the triphosphate chain are needed. Values of $K^{\mathrm{M}}_{\mathrm{ML_{op}}}$ are, in this case, well represented by the stability constants of the complexes of the pyrimidine-nucleoside 5′-triphosphates, PyNTPs (Table 2.4, page 56). Indeed, it has been shown [73,88] that in the PyNTP systems metal ions bind only to the triphosphate chain (see Section 2.4, page 48, for a detailed discussion).

By combining equations 2.14 and 2.15, defining K_{I} and $K^{\mathrm{M}}_{\mathrm{ML}}$, one obtains a new expression for K_{I} (equation 2.17):

$$
\begin{aligned}
K_{\mathrm{I}} &= K^{\mathrm{M}}_{\mathrm{ML_{cl}}} / K^{\mathrm{M}}_{\mathrm{ML_{op}}} \\
K^{\mathrm{M}}_{\mathrm{ML}} &= K^{\mathrm{M}}_{\mathrm{ML_{op}}} + K^{\mathrm{M}}_{\mathrm{ML_{cl}}} \\
&= K^{\mathrm{M}}_{\mathrm{ML_{op}}} + K_{\mathrm{I}} \cdot K^{\mathrm{M}}_{\mathrm{ML_{op}}} \\
&= K^{\mathrm{M}}_{\mathrm{ML_{op}}}(1 + K_{\mathrm{I}})
\end{aligned}
$$

and

$$
K_{\mathrm{I}} = \frac{K^{\mathrm{M}}_{\mathrm{ML}}}{K^{\mathrm{M}}_{\mathrm{ML_{op}}}} - 1 = 10^{\log \Delta} - 1 \tag{2.17}
$$

where the stability difference $\log \Delta$ is defined as:

$$
\log \Delta = \log \Delta_{\mathrm{ML}} = \log K^{\mathrm{M}}_{\mathrm{ML}} - \log K^{\mathrm{M}}_{\mathrm{ML_{op}}}
$$

The equilibrium constant K_I can now be calculated via equation 2.17 and the definition of log Δ: the values for log K^M_{ML} are experimentally accessible and those for $K^M_{ML_{op}}$ can be obtained as indicated above.

The vertical distances indicated by the dotted lines in Figure 2.11 (page 45) are identical with the stability differences log Δ_{ML} as defined above. The reliability of any calculation for K_I depends on the accuracy of the difference log Δ_{ML}, which becomes the more important the more similar the two constants, log K^M_{ML} and log $K^M_{ML_{op}}$, are. Therefore, only well defined error limits allow a quantitative evaluation of the extent of a possibly formed macrochelate. If K_I is known, the percentage of the closed or macrochelated species occurring in the equilibrium can be calculated:

$$\% \, ML_{cl} = 100 \cdot K_I / (1 + K_I)$$

Application of this procedure [104,124] yields the results listed in the various Tables of Sections 2.4 – 2.6.

2.4 Metal ion-binding properties of GTP and ITP

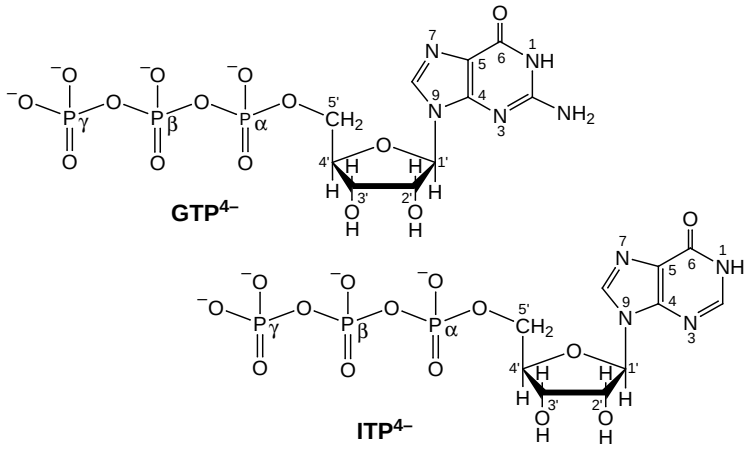

Figure 2.12: Chemical structure of guanosine and inosine (2-deaminoguanosine) 5′-triphosphate in their dominating *anti* conformation [6,7].

The aim of this work was to study the properties of the monomeric complexes formed between Mg^{2+}, Ca^{2+}, Sr^{2+}, Ba^{2+}, Mn^{2+}, Co^{2+}, Ni^{2+}, Cu^{2+}, Zn^{2+}, or Cd^{2+} and GTP or its analogue ITP. Most measurements were done in solutions with a nucleotide concentration of 0.5 mM (see Section 4.3.1, page 176); this low concentration guaranteed [73,89] that indeed the properties of the monomeric species were studied. Potentiometric pH titrations were conducted at pH > 3.0, in fact, mostly at pH > 3.5, so that deprotonation of $H_2(NTP)^{2-}$ is not a main factor. The main ionization is from the triphosphate-bound proton in $H(NTP)^{3-}$ in the pH range up to about neutrality,

$$H_2(NTP)^{2-} \rightleftharpoons H(NTP)^{3-} + H^+$$

$$K^{H}_{H_2(NTP)} = [H(NTP)^{3-}][H^+]/[H_2(NTP)^{2-}] \qquad (2.18)$$

$$H(NTP)^{3-} \rightleftharpoons NTP^{4-} + H^+$$

$$K^{H}_{H(NTP)} = [NTP^{4-}][H^+]/[H(NTP)^{3-}] \qquad (2.19)$$

since this proton is at the γ-phosphate, this species is designated as $(NTP{\cdot}H)^{3-}$. In the presence of metal ions, next to these two equilibria, two more, involving M^{2+} coordination primarily at the triphosphate group, need to be considered:

$$M^{2+} + (NTP{\cdot}H)^{3-} \rightleftharpoons M(NTP{\cdot}H)^{-}$$

$$K^{M}_{M(NTP{\cdot}H)} = [M(NTP{\cdot}H)^{-}]/[M^{2+}][(NTP{\cdot}H)^{3-}] \tag{2.20}$$

$$M^{2+} + NTP^{4-} \rightleftharpoons M(NTP)^{2-}$$

$$K^{M}_{M(NTP)} = [M(NTP)^{2-}]/[M^{2+}][NTP^{4-}] \tag{2.21}$$

These two last equilibria are connected by phosphate deprotonation in the complex via the following equilibrium:

$$M(NTP{\cdot}H)^{-} \rightleftharpoons M(NTP)^{2-} + H^{+}$$

$$K^{M}_{M(NTP{\cdot}H)} = [H^{+}][M(NTP)^{2-}]/[M(NTP{\cdot}H)^{-}] \tag{2.22}$$

Values for $pK^{H}_{M(NTP{\cdot}H)}$ may be calculated from equation 2.23:

$$pK^{H}_{M(NTP{\cdot}H)} = pK^{H}_{H(NTP)} + \log K^{M}_{M(NTP{\cdot}H)} - \log K^{M}_{M(NTP)} \tag{2.23}$$

Table 2.3 lists the results for the two stability constants (equations 2.20 and 2.21) and the values for proton loss from the protonated $M(GTP{\cdot}H)^{-}$ and $M(ITP{\cdot}H)^{-}$ complexes according to equation 2.23. For some of the metal ion-nucleotide systems which appear in the Table, equilibrium constants have been determined before [60–62,64,98] and those for the Mg^{2+} and Ca^{2+} complexes are in fair agreement with the present results. However, the few data previously available for the GTP^{4-} and ITP^{4-} complexes of the divalent 3d-transition metal ions vary widely and are in general somewhat lower than the present results. The reason for this is that the formation of the $M(PuNTP{\cdot}H)^{-}$ complexes had not always been considered. The constants for the M^{2+}/GTP systems with Sr^{2+}, Ba^{2+}, Ni^{2+} or Cd^{2+}, and

those for the M^{2+}/ITP systems with Sr^{2+}, Ba^{2+} or Cd^{2+} have not been determined before.

A comparison of the results obtained for $pK^{H}_{M(PuNTP\cdot H)}$ (listed in the final column in Table 2.3) with $pK^{H}_{H(NTP)}$ = 6.50 $\pm$ 0.05 for the last triphosphate-bound proton in $(GTP\cdot H)^{3-}$ and $(ITP\cdot H)^{3-}$, indicates that a metal ion bound at the triphosphate chain acidifies this proton by about 0.8 to 2.8 log units [65]. The conclusion that in the $M(PuNTP\cdot H)^{-}$ species the proton is at the phosphate chain follows from the comparison of the $pK^{H}_{H_2(GTP)}$ (= 2.94) and $pk^{IDP\cdot H}_{H\cdot ITP\cdot H}$ (= 1.89) values (Table 2.1 on page 20) due to $(N7)H^{+}$ deprotonation with those for $pK^{H}_{M(PuNTP\cdot H)}$ (Table 2.3, column 5). The latter values are considerably higher and hence, H^{+} can not be located in these complexes at the nucleobase residue. Furthermore, since $pK^{H}_{M(PuNTP\cdot H)} \geq 3.7$, H^{+} must be located at the γ-phosphate as this is the only basic triphosphate site remaining at pH > 3 [65]. That the maximum in the distribution curves seen in Figure 2.13 for the $M(GTP\cdot H)^{-}$ species, with Mg^{2+} or Zn^{2+}, occurs in the pH region 3 to 5 confirms the conclusion that the proton must be at the γ-phosphate group. This conclusion agrees with results from solid state studies: Cini *et al.* [126] have studied the crystal structure of the ternary complex $[Mg(H_2O)_6][HBPA]_2[Mg(HATP)_2]\cdot 12\ H_2O$, where BPA = bis(2-pyridyl)amine, and they showed that the two $H(ATP)^{3-}$ ligands each are coordinated via the α-, β-, and γ-phosphate groups to Mg^{2+}.

This means that Mg^{2+} is not only γ-coordinated, but is chelated. The results of Cini *et al.* [126] are also in agreement with a recent solid state ^{25}Mg-NMR study [127].

The above conclusion disagrees with one that places the proton on the β-phosphate and the Mg^{2+} ion preferentially at the terminal γ-group in $Mg(ATP\cdot H)^{-}$ [128]. With the γ-phosphate group monoprotonated, all three phosphate units exhibit comparably weak basicities and it is therefore unlikely that there is a single predominant location for the metal ion in the $(PuNTP\cdot H\cdot M)^{-}$ species in solution;

i.e., α,β,γ as well as β,γ and α,β chelates may be expected to occur in equilibrium depending on the geometry of the coordination sphere of the metal ion involved [65].

Table 2.3: Logarithms of the stability constants of $M(PuNTP{\cdot}H)^{-}$ and $M(PuNTP)^{2-}$ complexes of GTP and ITP as determined by potentiometric pH titrations in aqueous solution, together with the negative logarithms of the acidity constants (eq. 2.23) of the corresponding $M(PuNTP{\cdot}H)^{-}$ complexes (25 °C; I = 0.1 M, $NaNO_3$ or $NaClO_4$)[a,b]

$PuNTP^{4-}$	M^{2+}	$\log K^{M}_{M(PuNTP{\cdot}H)}$	$\log K^{M}_{M(PuNTP)}$	$pK^{H}_{M(PuNTP{\cdot}H)}$
GTP^{4-}	Mg^{2+}	2.6 ±0.3	4.31±0.04	4.8 ±0.3
	Ca^{2+}	2.6 ±0.3	3.96±0.03	5.15±0.3
	Sr^{2+}	2.65±0.2	3.55±0.04	5.6 ±0.2
	Ba^{2+}	2.65±0.2	3.41±0.03	5.75±0.2
	Mn^{2+}	3.36±0.16	5.36±0.03	4.50±0.16
	Co^{2+}	3.50±0.05	5.34±0.05	4.66±0.07
	Ni^{2+}	3.69±0.05	5.42±0.04	4.77±0.07
	Cu^{2+}	4.6 ±0.2	7.38±0.08	3.7 ±0.2
	Zn^{2+}	3.45±0.25	5.52±0.05	4.45±0.25
	Cd^{2+}	3.92±0.08	5.82±0.05	4.60±0.10
ITP^{4-}	Mg^{2+}	2.4 ±0.25	4.29±0.04	4.6 ±0.25
	Ca^{2+}	2.4 ±0.25	3.93±0.05	4.95±0.25
	Sr^{2+}	2.3 ±0.25	3.42±0.10	5.35±0.3
	Ba^{2+}	2.3 ±0.25	3.28±0.09	5.5 ±0.3
	Mn^{2+}	3.1 ±0.3	5.21±0.06	4.35±0.3
	Co^{2+}	3.0 ±0.3	5.08±0.07	4.4 ±0.3
	Ni^{2+}	3.0 ±0.4	5.01±0.10	4.45±0.4
	Cu^{2+}	3.9 ±0.4	6.71±0.10	3.65±0.4
	Zn^{2+}	3.1 ±0.3	5.32±0.06	4.25±0.3
	Cd^{2+}	3.55±0.25	5.62±0.05	4.4 ±0.25

[a] The error limits given are *three times* the standard error of the mean value or the sum of the probable systematic errors, whichever is larger. The error limits of the derived data, in the present case for column 5, were calculated according to the error propagation after Gauss. [b] Many of the values given in the third column are estimates as it is evident from the large error limits.

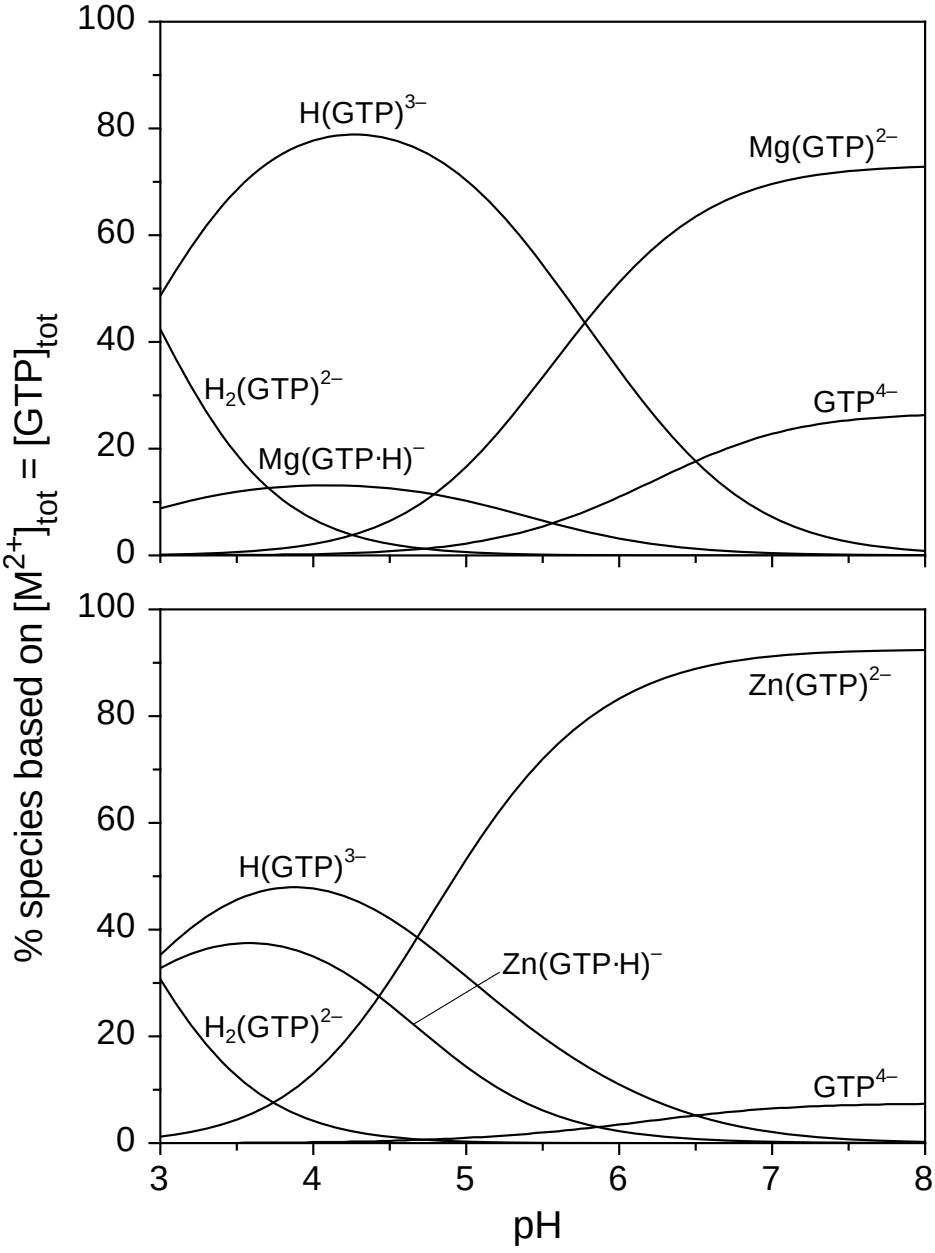

Figure 2.13: Comparison of the effect of pH on the concentration of the species present in aqueous solution of GTP and Mg^{2+} (upper part) or Zn^{2+} (bottom part). The results are given as percentage of total M^{2+} present (= total GTP). Calculations were carried out with the potentiometrically determined acidity and stability constants for concentrations of 5×10^{-4} M for each reactant (25 °C; I = 0.1 M). These conditions are close to those used in the experiments. In the Zn^{2+}/GTP system at pH>7.5 the complexes $Zn(GTP-H)^{3-}$ [p$K^{H}_{Zn(GTP)}$ = 8.4] and $Zn(GTP-H)(OH)^{4-}$ [p$K^{H}_{Zn(GTP-H)(H_2O)}$ = 9.5] [63] are becoming relevant.

2.4.1 Stabilities of pyrimidine-nucleoside 5′-triphosphate complexes

As pointed out before (Section 2.3.1, page 43), the stabilities of those complexes in which the metal ion is coordinated only to the triphosphate chain are needed in order to be able to evaluate the amount of macrochelate formation in the $M(PuNTP{\cdot}H)^{-}$ and $M(PuNTP)^{2-}$ complexes. It has been shown [73,88] that in the PyNTP systems metal ions bind indeed only to the triphosphate group, the single exception being the $Cu(CTP)^{2-}$ complex (for details see Section 8 in [88]). The average values previously [88] obtained for the complexes formed between Mn^{2+}, Co^{2+}, Ni^{2+}, Cu^{2+}, Zn^{2+} or Cd^{2+} and UTP, dTTP, or CTP [except the one for $Cu(CTP)^{2-}$], are listed in entries 5-10 of Table 2.4 (page 56). To complement this set the Sr^{2+} and Ba^{2+} systems with UTP and CTP were now studied and the evaluations for the Mg^{2+} and Ca^{2+} systems with UTP were repeated. The average results valid for the $M(PyNTP{\cdot}H)^{-}$ and $M(PyNTP)^{2-}$ complexes of Mg^{2+}, Ca^{2+}, Sr^{2+}, and Ba^{2+} are given in entries 1-4 of Table 2.4. The averages are based on the following results, that were determined in this work [65]:

$\log K^{\mathrm{Sr}}_{\mathrm{Sr(UTP{\cdot}H)}} = 2.1 \pm 0.3$; $\log K^{\mathrm{Sr}}_{\mathrm{Sr(UTP)}} = 3.38 \pm 0.06$;

$\log K^{\mathrm{Sr}}_{\mathrm{Sr(H;CTP)}} = 2.24 \pm 0.15$; $\log K^{\mathrm{Sr}}_{\mathrm{Sr(CTP)}} = 3.30 \pm 0.04$;

$\log K^{\mathrm{Ba}}_{\mathrm{Ba(UTP{\cdot}H)}} = 2.0 \pm 0.3$; $\log K^{\mathrm{Ba}}_{\mathrm{Ba(UTP)}} = 3.20 \pm 0.06$;

$\log K^{\mathrm{Ba}}_{\mathrm{Ba(H;CTP)}} = 2.15 \pm 0.18$; $\log K^{\mathrm{Ba}}_{\mathrm{Ba(CTP)}} = 3.15 \pm 0.05$.

The stability constants given in Table 2.4 for metal ion binding to a standard pyrimidine-nucleoside 5′-triphosphate, *i.e.*, for complexes in which no nucleobase back-binding resulting in macrochelate formation occurs [65,73,88], allow now comparisons with M^{2+}/PuNTP systems.

A rough comparison of the stability constants of the $M(PyNTP)^{2-}$ complexes for the transition metal ions (Table 2.4) with those of the corresponding $M(GTP)^{2-}$ and $M(ITP)^{2-}$ complexes (Table 2.3, page 52), reveals that the stabilities of these $M(PuNTP)^{2-}$ species are larger and this suggests macrochelate formation in the

purine-nucleotide complexes, as already described for ATP^{4-} [88]. In accord herewith is the acidity of the $M(PyNTP{\cdot}H)^{-}$ species (Table 2.4, column 5) slightly more pronounced than that of the $M(PuNTP{\cdot}H)^{-}$ complexes (Table 2.3, column 5).

In addition, the stability constants of Table 2.4 follow the usual trends observed for phosphate complexes: complex stability of the alkaline earth ions decreases with increasing radius. The stabilities of phosphate-metal ion complexes of the divalent 3d metal ions do not strictly follow the Irving-Williams [129,130] sequence, as previously observed [131,132]. The stability order for the PyNTPs (Table 2.4), is in accordance with that for phosphate monoesters [94] and diphosphate monoesters [106]: $Ba^{2+} < Sr^{2+} < Ca^{2+} < Mg^{2+} < Ni^{2+} < Co^{2+} < Mn^{2+} < Cu^{2+} > Zn^{2+} < Cd^{2+}$, as shown in Figure 2.14 for the series Ba^{2+} through Cd^{2+}.

A view on the constants given in Table 2.3 for the PuNTPs reveals that there this situation is somewhat blurred and this is due to the participation of N7 of the purine moiety in metal ion binding (see Section 2.4.2 on page 57).

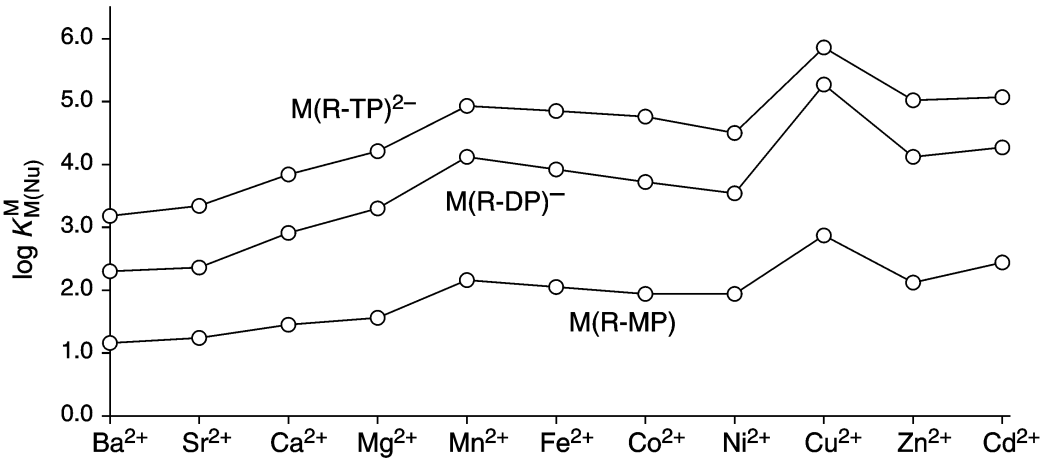

Figure 2.14: Irving-Williams sequence-type plot for the 1:1 complexes of Ba^{2+} through Zn^{2+} formed with mono-, di-, and triphosphate monoesters. The data for the mono- and diphosphates are taken from Table 7 in [106], the ones for the triphosphates are from Table 2.4. The values used for the Fe^{2+} complexes are estimates given in [106].

Table 2.4: Logarithms of the stability constants of $M(PyNTP{\cdot}H)^{-}$ and $M(PyNTP)^{2-}$ complexes of pyrimidine-nucleoside 5′-triphosphates, as determined by potentiometric pH titrations in aqueous solution, together with the negative logarithms of the acidity constants (eq. 2.23) of the corresponding $M(PyNTP{\cdot}H)^{-}$ complexes (25 °C; I = 0.1 M, $NaNO_3$ or $NaClO_4$)[a]

No.[b]	M^{2+}	$\log K^{M}_{M(PyNTP{\cdot}H)}$	$\log K^{M}_{M(PyNTP)}$	$pK^{H}_{M(PyNTP{\cdot}H)}$ [c]
1	Mg^{2+}	2.3 ±0.2[d]	4.21±0.04[e]	4.6 ±0.2
2	Ca^{2+}	2.2 ±0.2[d]	3.84±0.05[e]	4.85±0.2
3	Sr^{2+}	2.15±0.2	3.34±0.05	5.3 ±0.2
4	Ba^{2+}	2.1 ±0.2	3.18±0.04	5.4 ±0.2
5	Mn^{2+}	2.70±0.12	4.93±0.03	4.27±0.13
6	Co^{2+}	2.55±0.24	4.76±0.03	4.3 ±0.25
7	Ni^{2+}	2.51±0.25	4.50±0.03	4.5 ±0.25
8	Cu^{2+}	2.80±0.08	5.86±0.03	3.44±0.10
9	Zn^{2+}	2.73±0.09	5.02±0.02	4.21±0.10
10	Cd^{2+}	2.89±0.06	5.07±0.03	4.32±0.08

[a] The error limits given are *three times* the standard error of the mean value or the sum of the probable systematic errors, whichever is larger. The error limits of the derived data, in the present case for column 4, were calculated according to the error propagation after Gauss. [b] The values for entries 5–10 are for $\log K^{M}_{M(PyNTP{\cdot}H)} = \log K^{M}_{M(UTP{\cdot}H)}$ from Table II of [88], given is an error limit of 3σ, and those for $\log K^{M}_{M(PyNTP)}$ are the averages listed in Table IV of the same reference (with 3σ). [c] Calculated by using the average value $pK^{H}_{H(NTP)}$ = 6.50±0.05 and the constants listed above. [d] Based on $\log K^{Mg}_{Mg(UTP{\cdot}H)}$ = 2.3±0.25 and $\log K^{Ca}_{Ca(UTP{\cdot}H)}$ = 2.2±0.25, estimated now (the values in ref. [88] are too large), and by taking into account the constants given for $\log K^{M}_{M(H;CTP)}$ in Table II of ref. [88]. [e] Based on $\log K^{Mg}_{Mg(UTP)}$ = 4.21±0.05 or $\log K^{Ca}_{Ca(UTP)}$ = 3.82±0.05, which were calculated in this work, as well as on the values listed in Table II of ref. [88] for $\log K^{M}_{M(dTTP)}$ and $\log K^{M}_{M(CTP)}$ by using the number of titrations as weighting factor.

2.4.2 Proof of an enhanced stability for the M(PuNTP·H)$^{-}$ and M(PuNTP)$^{2-}$ complexes

Monoprotonated complexes of the purine 5′-triphosphates, M(PuNTP·H), show an enhanced stability, when the values of their stability constants are compared to the corresponding ones of the pyrimidine 5′-triphosphates, M(PyNTP·H). Analogously to what was done for the deprotonated complexes (see Section 2.3.1, page 43), an equation representing the stability enhancement due to macrochelate formation in the complexes of the protonated species can be written as:

$$\log \Delta_{\mathrm{M(PuNTP\cdot H)}} = \log K^{\mathrm{M}}_{\mathrm{M(PuNTP\cdot H)}} - \log K^{\mathrm{M}}_{\mathrm{M(PyNTP\cdot H)}}$$

The $\log \Delta_{\mathrm{M(PuNTP\cdot H)}}$ values are summarized in Table 2.5 for the GTP and ITP systems. In all instances, values larger than zero are observed. It is remarkable, that the corresponding values for the monoprotonated M(PuNTP·H)$^{-}$ complexes (Table 2.5, column 5) are quite similar, in fact, in most instances they are identical within the error limits with those for M(PuNTP)$^{2-}$ (Tables 2.6 and 2.7, column 4). This shows that intramolecular chelate formation occurs to about the same extent in both types of complexes. However, because of the large error limits of the $\log \Delta_{\mathrm{M(PuNTP\cdot H)}}$ values, further evaluations shall be centred on the M(PuNTP)$^{2-}$ systems.

From the values calculated for $\log \Delta_{\mathrm{M(PuNTP)}}$, it is possible, following the procedure illustrated in Section 2.3.1 (page 43), to determine the value of K_{I} for each system, and to calculate the percentage of macrochelates formed in the various complexes. Tables 2.6 and 2.7 (pages 59 and 60) list the results for $\log \Delta_{\mathrm{M(PuNTP)}}$, K_{I}, and % M(PuNTP)$^{2-}_{\mathrm{cl}}$ of the GTP^{4-} and ITP^{4-} complexes formed with each of the ten metal ions studied [65]. The previous results for M(ATP)$^{2-}$ complexes [88] are given in a revised form for comparison in Table 2.8 on page 61. In the last mentioned Table, the values for $\log \Delta_{\mathrm{M(ATP)}}$ of the Mg^{2+} and Ca^{2+} systems are based on $\log K^{\mathrm{M}}_{\mathrm{M(ATP)}}$ of Table II in ref. [88] (here given with an error limit corresponding to 3σ) and on the revised values for $\log K^{\mathrm{M}}_{\mathrm{M(PyNTP)}}$ given in column 4 of Table 2.4.

Table 2.5: Comparison of the stability constants of the $M(PuNTP{\cdot}H)^{-}$ complexes with those of the corresponding $M(PyNTP{\cdot}H)^{-}$ species having only M^{2+}-phosphate coordination, together with the resulting stability differences $\log \Delta_{M(PuNTP{\cdot}H)}$ (aq. sol., 25 °C; I = 0.1 M, $NaNO_3$ or $NaClO_4$)[a]

Ligand	M^{2+}	$\log K^{M}_{M(PuNTP{\cdot}H)}$ [b]	$\log K^{M}_{M(PyNTP{\cdot}H)}$ [b]	$\log \Delta_{M(PuNTP{\cdot}H)}$
GTP^{4-}	Mg^{2+}	2.6 ±0.3	2.3 ±0.2	0.3 ±0.35
	Ca^{2+}	2.6 ±0.3	2.2 ±0.2	0.4 ±0.35
	Sr^{2+}	2.65±0.2	2.15±0.2	0.5 ±0.3
	Ba^{2+}	2.65±0.2	2.1 ±0.2	0.55±0.3
	Mn^{2+}	3.36±0.16	2.70±0.12	0.66±0.20
	Co^{2+}	3.50±0.05	2.55±0.24	0.95±0.25
	Ni^{2+}	3.69±0.05	2.51±0.25	1.2 ±0.25
	Cu^{2+}	4.6 ±0.2	2.80±0.08	1.8 ±0.2
	Zn^{2+}	3.45±0.25	2.73±0.09	0.7 ±0.25
	Cd^{2+}	3.92±0.08	2.89±0.06	1.03±0.10
ITP^{4-}	Mg^{2+}	2.4 ±0.25	2.3 ±0.2	0.1 ±0.3
	Ca^{2+}	2.4 ±0.25	2.2 ±0.2	0.2 ±0.3
	Sr^{2+}	2.3 ±0.25	2.15±0.2	0.15±0.3
	Ba^{2+}	2.3 ±0.25	2.1 ±0.2	0.2 ±0.3
	Mn^{2+}	3.1 ±0.3	2.70±0.12	0.4 ±0.3
	Co^{2+}	3.0 ±0.3	2.55±0.24	0.45±0.4
	Ni^{2+}	3.0 ±0.4	2.51±0.25	0.5 ±0.45
	Cu^{2+}	3.9 ±0.4	2.80±0.08	1.1 ±0.4
	Zn^{2+}	3.1 ±0.3	2.73±0.09	0.35±0.3
	Cd^{2+}	3.55±0.25	2.89±0.06	0.65±0.25

[a] The error limits given are *three times* the standard error of the mean value or the sum of the probable systematic errors, whichever is larger. The error limits of the derived data, in the present case for column 5, were calculated according to the error propagation after Gauss. [b] Many of the values given are estimates, as shown by the large error limits.

The situation where log $\Delta_{\mathrm{M(NTP)}}$ and K_{I} both equal zero, indicating that no macrochelate forms, does not occur. The greatest amount of macrochelate is formed in the complexes of Cu^{2+} followed (usually) by Ni^{2+}.

Tables 2.6, 2.7, and 2.8 show that for the four alkaline earth metal ions the closed or macrochelated forms are lower in percentage than those of the transition metal ions; this is especially true for $M(ITP)^{2-}$ and $M(ATP)^{2-}$. For $M(GTP)^{2-}$ Ba^{2+} forms the macrochelate to about 40% whereas that of Mg^{2+} occurs only to about 20%.

Table 2.6: Comparison of the measured stability constants of the $M(GTP)^{2-}$ complexes with those of the corresponding $M(PyNTP)^{2-}$ species, having a sole M^{2+}-phosphate coordination, together with the stability differences, log Δ, reflecting an increased stability, and the extent of intramolecular macrochelate formation as quantified by the dimension-less equilibrium constant K_{I} for aqueous solutions at 25 °C and I = 0.1 M ($NaNO_3$ or $NaClO_4$).[a]

M^{2+}	log $K^{\mathrm{M}}_{\mathrm{M(GTP)}}$	log $K^{\mathrm{M}}_{\mathrm{M(PyNTP)}}$	log Δ	K_{I}	% $M(GTP)^{-}_{\mathrm{cl}}$
Mg^{2+}	4.31±0.04	4.21±0.04	0.10±0.06	0.26±0.17	21±11
Ca^{2+}	3.96±0.03	3.84±0.05	0.12±0.06	0.32±0.18	24±10
Sr^{2+}	3.55±0.04	3.34±0.05	0.21±0.06	0.62±0.22	38± 9
Ba^{2+}	3.41±0.03	3.18±0.04	0.23±0.05	0.70±0.20	41± 7
Mn^{2+}	5.36±0.03	4.93±0.03	0.43±0.04	1.69±0.25	63± 3
Co^{2+}	5.34±0.05	4.76±0.03	0.58±0.06	2.80±0.53	74± 4
Ni^{2+}	5.42±0.04	4.50±0.03	0.92±0.05	7.32±0.96	88± 1
Cu^{2+}	7.38±0.08	5.86±0.03	1.52±0.08	32.11±6.10	97± 1
Zn^{2+}	5.52±0.05	5.02±0.02	0.50±0.05	2.16±0.36	68± 4
Cd^{2+}	5.82±0.05	5.07±0.03	0.75±0.06	4.62±0.78	82± 2

[a] The error limits given are *three times* the standard error of the mean value or the sum of the probable systematic errors, whichever is larger. The error limits of the derived data were calculated according to the error propagation after Gauss.

A similar high formation degree is observed for Ba(GMP) [59]. This might have to do with the availability of (C6)O in GTP^{4-} allowing the formation of outersphere hydrogen bonds with a coordinated water molecule [89].

Table 2.7: Comparison of the measured stability constants of the $M(ITP)^{2-}$ complexes with those of the corresponding $M(PyNTP)^{2-}$ species, having a sole M^{2+}-phosphate coordination, together with the stability differences, log Δ, reflecting an increased stability, and the extent of intramolecular macrochelate formation as quantified by the dimension-less equilibrium constant K_{I} for aqueous solutions at 25 °C and I = 0.1 M ($NaNO_3$ or $NaClO_4$).[a]

M^{2+}	log $K^{\mathrm{M}}_{\mathrm{M(ITP)}}$	log $K^{\mathrm{M}}_{\mathrm{M(PyNTP)}}$	log Δ	K_{I}	% $M(ITP)^{-}_{\mathrm{cl}}$
Mg^{2+}	4.29±0.04	4.21±0.04	0.08±0.06	0.20±0.17	17±11
Ca^{2+}	3.93±0.05	3.84±0.05	0.09±0.07	0.23±0.20	19±13
Sr^{2+}	3.42±0.10	3.34±0.05	0.08±0.11	0.20±0.30	17±21
Ba^{2+}	3.28±0.09	3.18±0.04	0.10±0.10	0.26±0.29	21±18
Mn^{2+}	5.21±0.06	4.93±0.03	0.28±0.07	0.91±0.31	48± 8
Co^{2+}	5.08±0.07	4.76±0.03	0.32±0.08	1.09±0.38	52± 9
Ni^{2+}	5.01±0.10	4.50±0.03	0.51±0.10	2.24±0.75	69± 7
Cu^{2+}	6.71±0.10	5.86±0.03	0.85±0.10	6.08±1.63	86± 3
Zn^{2+}	5.32±0.06	5.02±0.02	0.30±0.06	1.00±0.28	50± 7
Cd^{2+}	5.62±0.05	5.07±0.03	0.55±0.06	2.55±0.49	72± 4

[a] The error limits given are *three times* the standard error of the mean value or the sum of the probable systematic errors, whichever is larger. The error limits of the derived data were calculated according to the error propagation after Gauss.

For the six transition metal ions considered, substantial amounts of macrochelate occur; e.g., up to 97% macrochelate and only 3% open forms are observed for $Cu(GTP)^{2-}$. Generally, for a given metal ion the percentage of macrochelate falls

off in the order $M(GTP)^{2-}_{cl}$ > $M(ITP)^{2-}_{cl}$ > $M(ATP)^{2-}_{cl}$. This order corresponds to the decreasing N7 basicity of GTP and ITP [93].

The N7 basicities of the inosine and adenosine residues are comparable [95], but M^{2+} binding at the N7 site of adenosine is hampered by the steric influence of the (C6)NH_2 group [117,133]. Hence, the above order is understandable and also in accord with the observations made for the complexes of nucleoside 5'-monophosphates [59,89].

Table 2.8: Comparison of the measured stability constants, $K^{M}_{M(ATP)}$, of the $M(ATP)^{2-}$ complexes with those of the corresponding $M(PyNTP)^{2-}$ species, $K^{M}_{M(PyNTP)}$, having a sole M^{2+}-phosphate coordination, together with the stability differences, log Δ, reflecting an increased stability, and extent of intramolecular macrochelate formation as quantified by the dimension-less equilibrium constant K_I, in the $M(ATP)^{2-}$ complexes (aq. solution, 25 °C; I = 0.1 M, $NaNO_3$)[a]

M^{2+}	log $K^{M}_{M(ATP)}$	log $K^{M}_{M(PyNTP)}$	log Δ	K_I	% $M(ATP)^{2-}_{cl}$
Mg^{2+}	4.29±0.04	4.21±0.04	0.08±0.05	0.20±0.14	17±10
Ca^{2+}	3.93±0.05	3.84±0.05	0.07±0.06	0.17±0.16	15±12
Mn^{2+}	5.21±0.06	4.93±0.03	0.08±0.08	0.20±0.22	17±15
Co^{2+}	5.08±0.07	4.76±0.03	0.21±0.09	0.62±0.34	38±13
Ni^{2+}	5.01±0.10	4.50±0.03	0.36±0.06	1.29±0.32	56± 6
Cu^{2+}	6.71±0.10	5.86±0.03	0.48±0.04	2.02±0.28	67± 3
Zn^{2+}	5.32±0.06	5.02±0.02	0.14±0.06	0.38±0.19	28±10
Cd^{2+}	5.62±0.05	5.07±0.03	0.27±0.04	0.86±0.17	46± 5

[a] The error limits given are *three times* the standard error of the mean value or the sum of the probable systematic errors, whichever is larger. The error limits of the derived data were calculated according to the error propagation after Gauss.

2.4.3 Considerations on the structure of the M(PuNTP)$^{2-}$ complexes

Comparison of the present results obtained for the M(GTP)$^{2-}$ and M(ITP)$^{2-}$ complexes, including the ones for M(ATP)$^{2-}$ (Tables 2.6, 2.7, 2.8, respectively) with those obtained earlier [59,89] for M(GMP), M(IMP), and M(AMP) reveals that the formation degrees of the macrochelates are astonishingly similar for a given metal ion and purine-nucleobase residue. This is somewhat surprising considering that the triphosphate complexes are by about 2 to 3 log units more stable than the monophosphate ones. On the other hand, it indicates that for the extent of macrochelate formation mainly the properties of the N7 site are responsible, at least as long as the coordination sphere of the metal ion considered is not yet saturated.

From the studies of M(ATP)$^{2-}$ complexes it is well known that (at least) two types of macrochelates can form, [58,59,88] one in which the phosphate-coordinated metal ion binds innersphere to N7 of the adenine residue and one where this interaction is of an outersphere type, *i.e.*, with a water molecule between N7 and M^{2+}, see Figure 2.15.

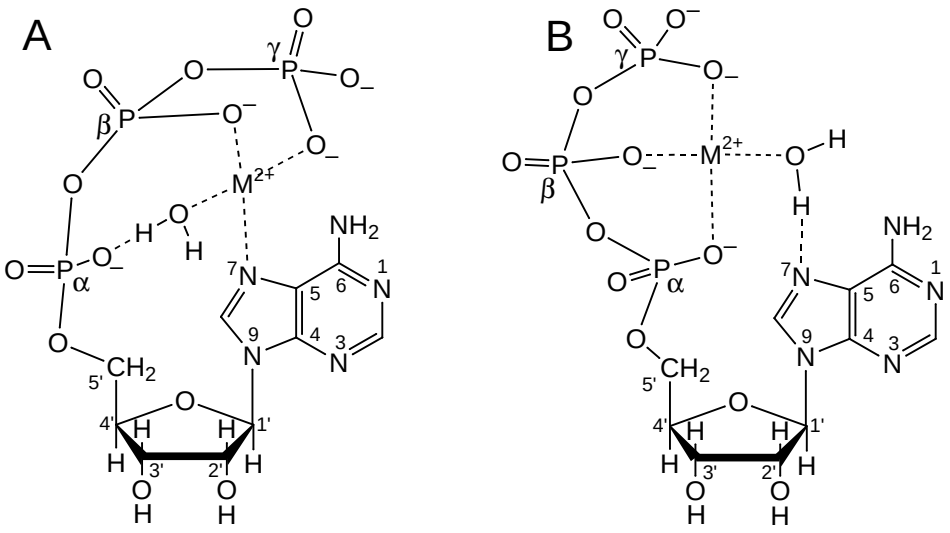

Figure 2.15: Tentative and simplified structures for the macrochelated innersphere (A) and outersphere (B) isomers of M(ATP)$^{2-}$. From [134].

A similar situation also occurs for $M(GTP)^{2-}$ and $M(ITP)^{2-}$: ^{1}H-NMR shift experiments of the corresponding Mg^{2+} systems [73] gave no indication for macrochelate formation, which is on the other hand proven to occur by the present results and in accord with those for $Mg(ATP)^{2-}$; hence, one has to conclude that $Mg(GTP)^{2-}_{cl}$ and $Mg(ITP)^{2-}_{cl}$ are of an outersphere type and this is most probably also true for the other alkaline earth ions [65]. From an early line-broadening study [135] for the Mn^{2+}/ITP system follows that at least to some extent innersphere binding occurs with N7. There, it is concluded that in approximately 11% of the $Mn(ITP)^{2-}$ species, Mn^{2+}-nucleobase innersphere binding occurs. The problem with that study is, that high concentrations of ITP were used (up to 0.3 M), and under these conditions self-stacking occurs [73]. Comparisons of the present results [65] for the Zn^{2+} and Cd^{2+} complexes of GTP^{4-} and ITP^{4-} with those of the cited ^{1}H-NMR shift study [73], indicate that macrochelate formation for the $M(GTP)^{2-}_{cl}$ and $M(ITP)^{2-}_{cl}$ species with these two metal ions is largely innersphere. In Figure 2.13 one of the possible isomers of $M(GTP)^{2-}$ with a hexa-coordinating metal ion is shown. The depicted M^{2+}-triphosphate coordination follows an earlier suggestion [6].

If intramolecular direct M^{2+}-N7 coordination occurs, then it is sterically more favorable to have a water molecule between M^{2+} and the α-phosphate group, though a simultaneous innersphere binding of both N7 and the α-phosphate group in complexes of purine-NMPs is possible [89]. Of course, other isomers that differ in the phosphate coordination are possible: for example, direct β,γ-phosphate and N7 coordination, which leaves the α group free. In the depicted structure, the equatorial positions of an octahedral coordination sphere could have been used, thus giving rise to further isomers. In the present context, it is only distinguished between macrochelated and open species, in which the metal ion is only phosphate-coordinated. In addition, it should be noted that the (C6)O carbonyl group may also participate in outersphere metal ion binding as discussed in detail [89] for M(GMP) complexes.

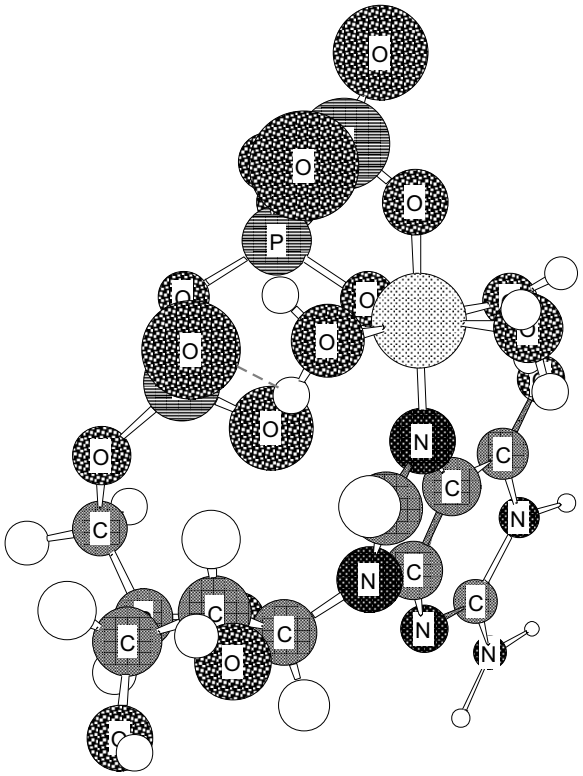

Figure 2.16: Simplified structure of one of the macrochelated innersphere $M(GTP)^{2-}$ isomers with a hexa-coordinating metal ion. The metal ion is shown in pearl-grey; all the other unlabelled spheres are H atoms. The above structure was drawn with Chem3D Pro (Version 5.0) from Cambridge Scientific Computing Inc.; the minimized and relaxed form is shown.

The above conclusions concerning the M(NMP) and $M(NTP)^{2-}$ complexes showing that N7 of the guanine residue is an especially vivid metal ion-binding site are confirmed by observations made with nucleic acids. For example, cis-$(NH_3)_2Pt^{2+}$ interacts preferably with guanine-N7 sites of DNA [136–139]. That this also applies to labile metal ions like Mn^{2+} or Zn^{2+} follows from observations made with nucleic acids [140], including ribozymes [141–143].

2.5 Stability and structure of M^{2+}-nucleoside 5′-diphosphate complexes in aqueous solution

2.5.1 Metal ion-binding properties of ADP

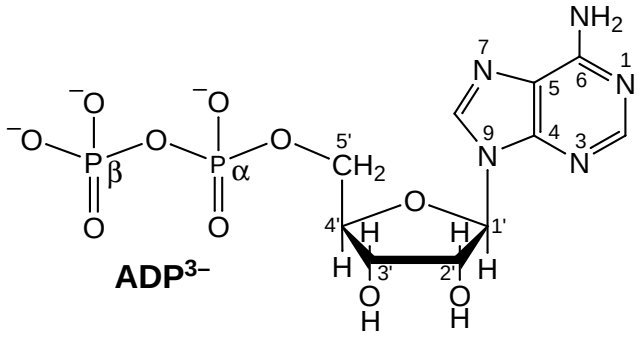

Figure 2.17: Chemical structure of adenosine 5′-diphosphate in the dominating *anti* conformation [6,7].

It is well known [67,92,144–146], that nucleotides undergo self association due to stacking of their nucleobase aromatic-ring systems. To make sure that the monomeric properties of the M^{2+}/ADP complexes (with M^{2+} = Mg^{2+}, Ca^{2+}, Sr^{2+}, Ba^{2+}, Mn^{2+}, Co^{2+}, Ni^{2+}, Cu^{2+}, Zn^{2+} or Cd^{2+}) were studied [105], all the potentiometric pH titrations were carried out at ligand concentrations of 0.3 and 0.6 mM, where the self stacking of ADP is negligible [74] (see Section 4.3.2 on page 179). In fact, with the self-association constant K = 15 M^{-1}, which holds for adenosine [73], one calculates that in a 10^{-3} M solution about 97% of the species are present in their monomeric form.

If the evaluation is not carried out into the pH range where formation of hydroxo complexes occurs (see Section 4.3.2 on page 179), the experimental data collected *via* potentiometric pH titrations for these systems [105] can be described by four equilibrium constants. Two of them represent the deprotonation equilibria 2.6 and 2.7 (on page 27) and are for clarity rewritten here as equation 2.24 and 2.25, respectively:

$$H_2(ADP)^- \rightleftharpoons H(ADP)^{2-} + H^+$$

$$K^{H}_{H_2(ADP)} = [H(ADP)^{2-}][H^+]/[H_2(ADP)^-] \quad (2.24)$$

$$H(ADP)^{2-} \rightleftharpoons ADP^{3-} + H^+$$

$$K^{H}_{H(ADP)} = [ADP^{3-}][H^+]/[H(ADP)^{2-}] \quad (2.25)$$

The next two equations, 2.26 and 2.27, refer to the complex-formation reactions:

$$M^{2+} + H(ADP)^{2-} \rightleftharpoons M(H;ADP)$$

$$K^{M}_{M(H;ADP)} = [M(H;ADP)]/[M^{2+}][H(ADP)^{2-}] \quad (2.26)$$

$$M^{2+} + ADP^{3-} \rightleftharpoons M(ADP)^-$$

$$K^{M}_{M(ADP)} = [M(ADP)]/[M^{2+}][ADP^{3-}] \quad (2.27)$$

The acidity constant $K^{H}_{M(H;ADP)}$ (equation 2.28), refers to the deprotonation reaction of the M(H;ADP) complex and can be calculated from equation 2.29:

$$M(H;ADP) \rightleftharpoons M(ADP)^- + H^+$$

$$K^{H}_{M(H;ADP)} = [M(ADP)^-][H^+]/[M(H;ADP)] \quad (2.28)$$

$$pK^{H}_{M(H;ADP)} = pK^{H}_{H(ADP)} + \log K^{M}_{M(H;ADP)} - \log K^{M}_{M(ADP)} \quad (2.29)$$

The results obtained for the stability constants 2.26, 2.27, and 2.29 are listed in columns 2, 3, and 4 of Table 2.9, respectively.

From the earlier values determined for the stabilities of the $M(ADP)^-$ complexes [61,98,147], those of Taqui Kahn and Martell [147] agree in several instances well with the present results. For the complexes Mg(H;ADP), Ca(H;ADP), Co(H;ADP), Ni(H;ADP), $Ca(ADP)^-$, $Ba(ADP)^-$, $Mn(ADP)^-$, and $Zn(ADP)^-$, the log stability constants agree within ± 0.1 log unit; however, for other complexes rather large errors are observed. The biggest discrepancy is observed for the value of $Ni(ADP)^-$, that is 0.57 log unit higher in the former tabulation [147]. On the

other hand, the value of Frey and Stuehr [148,149], log $K^{\mathrm{Ni}}_{\mathrm{Ni(ADP)}}$ = 4.18, which was determined at 15 °C (I = 0.1 M, $NaNO_3$) is in reasonable agreement with the present result if one takes into account the difference in temperature at which the experiments were carried out. This holds as well for log $K^{\mathrm{Ni}}_{\mathrm{Ni(H;ADP)}}$ = 2.30 from the same source.

In the calculation of the very recently published stability constants of $M(ADP)^-$ complexes [150] the formation of protonated complexes was ignored. Those results should therefore not be taken into consideration.

Table 2.9: Logarithms of the stability constants of M(H;ADP) and $M(ADP)^-$ complexes as determined by potentiometric pH titrations in aqueous solution [105], together with the negative logarithms of the acidity constants (eq. 2.29) of the corresponding M(H;ADP) complexes (25 °C; I = 0.1 M, $NaNO_3$)[a]

M^{2+}	log $K^{\mathrm{M}}_{\mathrm{M(H;ADP)}}$	log $K^{\mathrm{M}}_{\mathrm{M(ADP)}}$	p$K^{\mathrm{H}}_{\mathrm{M(H;ADP)}}$
Mg^{2+}	1.68±0.10	3.36±0.03	4.72±0.10
Ca^{2+}	1.5 ±0.25[b]	2.95±0.02	4.95±0.25
Sr^{2+}	1.2 ±0.25[b]	2.42±0.03	5.18±0.25
Ba^{2+}	1.12±0.16	2.37±0.06	5.15±0.17
Mn^{2+}	2.38±0.22	4.22±0.02	4.56±0.22
Co^{2+}	2.07±0.14	3.92±0.02	4.55±0.14
Ni^{2+}	2.26±0.15	3.93±0.02	4.73±0.15
Cu^{2+}	2.77±0.16	5.61±0.03	3.56±0.16
Zn^{2+}	2.31±0.20	4.28±0.05	4.43±0.21
Cd^{2+}	2.57±0.12	4.63±0.04	4.34±0.13

[a] The error limits given are *three times* the standard error of the mean value or the sum of the probable systematic errors, whichever is larger. The error limits of the derived data, in the present case for column 4, were calculated according to the error propagation after Gauss. [b] These values are estimates.

2.5.2 M(H;ADP) complexes: location of H^+ and M^{2+}

Potentiometric pH titrations allow determination of the stability constants of the M(H;ADP) complexes, but further information is needed in order to locate the binding sites of the proton and the metal ion in these species. First, the proton will be considered because binding of a metal ion to a protonated ligand commonly leads to an acidification of the ligand-bound proton [151,152]. Indeed, the average value for the deprotonation constants of the M(H;ADP) complexes, listed in column 4 of Table 2.9, $pK^{H}_{M(H;ADP)} \simeq 4.7 \pm 0.4$, ignoring the one for Cu(H;ADP), is about 1.7 p*K* units below $pK^{H}_{H(ADP)}$ (= 6.40; Table 2.2 on page 28), and about 0.8 p*K* unit *above* $pK^{H}_{H_2(ADP)}$ (= 3.92), which quantifies the release of the proton from the $(N1)H^+$ site. Hence, in all the M(H;ADP) complexes, except Cu(H;ADP), the proton must be located at the diphosphate chain, and here at the terminal β-phosphate group because this is the most basic site in this residue. That the maximum of the Co(H;ADP) speciation curve occurs in the pH range between 4 and 5, as shown in Figure 2.18, confirms that the proton must be at the β-phosphate group.

One question still needs to be answered: *Where is the metal ion?* Tentatively, one might argue that as the proton is at the phosphate residue, the metal ion must be at the nucleobase. But the irregular order observed for the stabilities of the M(H;ADP) complexes (Table 2.9), when they are compared with the Irving-Williams sequence [129,130], suggests that in these instances the metal ion is located at the monoprotonated diphosphate residue. This observation is confirmed by the following evaluations.

In the case of Cu(H;ADP), $pK^{H}_{Cu(H;ADP)} = 3.56 \pm 0.16$ (Table 2.9) is lower than $pK^{H}_{H_2(ADP)} = 3.92 \pm 0.02$ (Table 2.2, page 28). This means that an isomer with the proton at N1 is a possibility. In principle, four isomeric species are possible: (*i*) In ADP·Cu·H the proton and Cu^{2+} are located at the diphosphate group; (*ii*) H·ADP·Cu carries the proton at N1 and Cu^{2+} at the diphosphate residue, whereas (*iii*) in Cu·ADP·H the proton is at the terminal β-phosphate group and the metal ion at the nucleobase residue. Finally, (*iv*) the ADP·Cu·H species (or the Cu·ADP·H

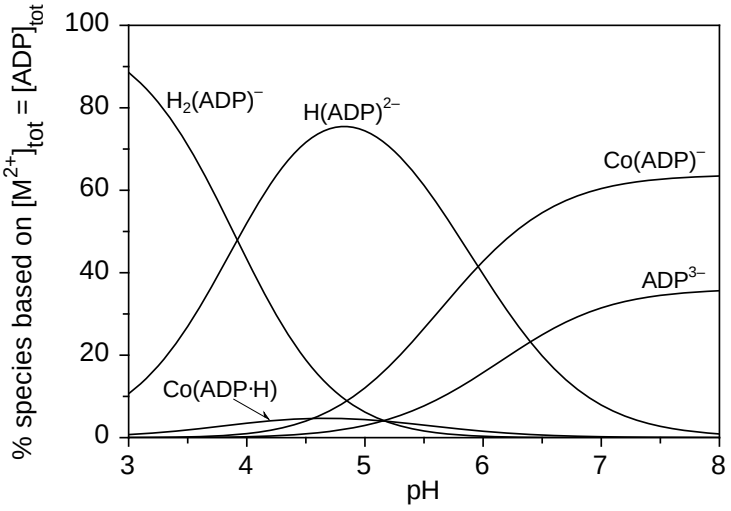

Figure 2.18: Effect of pH on the concentration of the species present in an aqueous solution of ADP and Co^{2+}. The results are given as percentage of the total M^{2+} present (= total ADP). The calculations were carried out with the potentiometrically determined acidity and stability constants for concentrations of 6×10^{-4} M for each reactant (25 °C; I = 0.1 M, $NaNO_3$).

one, with Cu^{2+} at N7) could to some extent form a closed (=cl) or macrochelated species involving N7, thus giving rise to the $(ADP{\cdot}Cu{\cdot}H)_{cl}$ isomer. Hence, $K^{Cu}_{Cu(H;ADP)}$ (eq. 2.26) may be redefined as given in equation 2.30:

$$K^{Cu}_{Cu(H;ADP)} = \frac{[ADP{\cdot}Cu{\cdot}H] + [H{\cdot}ADP{\cdot}Cu] + [Cu{\cdot}ADP{\cdot}H] + [(ADP{\cdot}Cu{\cdot}H)_{cl}]}{[Cu^{2+}][H(ADP)^{2-}]} \tag{2.30}$$

Therefore the experimentally accessible overall equilibrium constant $K^{Cu}_{Cu(H;ADP)}$ is actually composed of the four microconstants:

$$K^{Cu}_{Cu(H;ADP)} = k^{Cu}_{ADP{\cdot}Cu{\cdot}H} + k^{Cu}_{H{\cdot}ADP{\cdot}Cu} + k^{Cu}_{Cu{\cdot}ADP{\cdot}H} + k^{Cu}_{(ADP{\cdot}Cu{\cdot}H)_{cl}}$$

The microconstant $k^{Cu}_{ADP{\cdot}Cu{\cdot}H}$ is certainly well represented by the stability of the Cu(H;UDP) complex in which both, H^+ and Cu^{2+} are bound at the diphosphate residue, since the uracil moiety cannot be protonated, *i.e.*, $\log k^{Cu}_{ADP{\cdot}Cu{\cdot}H} = \log$

$K^{\mathrm{Cu}}_{\mathrm{Cu(H;UDP)}}$ = 2.4±0.25 [87].

A value for $k^{\mathrm{Cu}}_{\mathrm{Cu\cdot ADP\cdot H}}$ can be estimated by correcting the stability of the Cu(adenosine)$^{2+}$ complex for the difference in N1 basicity between Ado and H(ADP)$^{2-}$, as well as for the charge effect that the twofold negatively charged diphosphate residue exerts on the adenine-bound Cu^{2+}. The following procedure was adopted: the stability of the Cu(adenosine)$^{2+}$ complex is given by log $K^{\mathrm{Cu}}_{\mathrm{Cu(Ado)}}$ = 0.80±0.12 [117]. This value first needs to be corrected for the difference in basicity of the N1 sites, which is defined by $\Delta \mathrm{p}K_{\mathrm{a}} = \mathrm{p}K^{\mathrm{H}}_{\mathrm{H_2(ADP)}} - \mathrm{p}K^{\mathrm{H}}_{\mathrm{Ado}}$ = (3.92±0.02) − (3.61±0.03; [7]) = 0.31±0.04. Assuming a slope of m = 0.46 (average of the values given in [117]) for the log $K^{\mathrm{M}}_{\mathrm{ML}}$ *versus* p$K^{\mathrm{H}}_{\mathrm{HL}}$ plot, one obtains a $\Delta\log K$ = 0.14±0.04 correction for the complex stability, and a corrected complex stability of (0.80±0.12) + (0.14±0.04) = 0.94±0.13. The charge effect which the -P(O)$_2^-$-O-PO$_3$H$^-$ residue exerts on the Cu^{2+} located at the nucleobase needs to be further taken into account. Based on the experience with the effect of 2+/1− or 2−/1+ charges, where the distances are of a comparable size, and which amounts to 0.40±0.15 log unit [153], the charge effect of the twofold negatively charged residue is estimated as being 0.7±0.2 log unit. Hence, the stability constant of the Cu·ADP·H isomer is given by log $k^{\mathrm{Cu}}_{\mathrm{Cu\cdot ADP\cdot H}}$ = (0.94±0.13) + (0.7±0.2) = 1.64±0.24.

The microconstant $k^{\mathrm{Cu}}_{(\mathrm{ADP\cdot Cu\cdot H})_{\mathrm{cl}}}$ is given by the expression:

$$k^{\mathrm{Cu}}_{(\mathrm{ADP\cdot Cu\cdot H})_{\mathrm{cl}}} = K_{\mathrm{I/P}} \cdot k^{\mathrm{Cu}}_{\mathrm{ADP\cdot Cu\cdot H}}$$

where $K_{\mathrm{I/P}}$ refers to the constant of the intramolecular equilibrium:

$$\mathrm{ADP\cdot Cu\cdot H} \rightleftharpoons (\mathrm{ADP\cdot Cu\cdot H})_{\mathrm{cl}}$$

$$K_{\mathrm{I/P}} = [(\mathrm{ADP\cdot Cu\cdot H})_{\mathrm{cl}}]/[\mathrm{ADP\cdot Cu\cdot H}] \qquad (2.31)$$

Assuming [88] that the intramolecular equilibrium constant for macrochelate formation is the same in the protonated and unprotonated complexes, and that $K_{\mathrm{I/P}}$ = $K_{\mathrm{I/N7}}$ = 1.19±0.25 (Table 2.11 on page 77), one obtains: $k^{\mathrm{Cu}}_{(\mathrm{ADP\cdot Cu\cdot H})_{\mathrm{cl}}} = K_{\mathrm{I/P}} \cdot k^{\mathrm{Cu}}_{\mathrm{ADP\cdot Cu\cdot H}}$ = (1.19±0.25) × $10^{(2.4\pm0.25)}$ = $10^{(2.48\pm0.27)}$.

The only remaining unknown constant is $k^{\mathrm{Cu}}_{\mathrm{H\cdot ADP\cdot Cu}}$, that may now be calculated from $K^{\mathrm{Cu}}_{\mathrm{Cu(H;ADP)}}$ (Table 2.9, page 67):

$$k^{\mathrm{Cu}}_{\mathrm{H\cdot ADP\cdot Cu}} = K^{\mathrm{Cu}}_{\mathrm{Cu(H;ADP)}} - k^{\mathrm{Cu}}_{\mathrm{ADP\cdot Cu\cdot H}} - k^{\mathrm{Cu}}_{\mathrm{Cu\cdot ADP\cdot H}} - k^{\mathrm{Cu}}_{(\mathrm{ADP\cdot Cu\cdot H})_{\mathrm{cl}}} =$$

$$= 10^{(2.77\pm0.16)} - 10^{(2.4\pm0.25)} - 10^{(1.64\pm0.24)} - 10^{(2.48\pm0.27)} =$$

$$= (589\pm217) - (251\pm145) - (44\pm24) - (302\pm188) = -8\pm300(3\sigma)$$

This means that the micro stability constant of the H·ADP·Cu isomer is zero within the error limits [154] and thus this species does not occur in significant amounts. With this result in mind, and by setting the right hand sides of equation 2.26 (page 66) equal to that of eq. 2.30 (page 69), one obtains:

$$[\mathrm{Cu(H;ADP)}] = [\mathrm{ADP\cdot Cu\cdot H}] + [\mathrm{Cu\cdot ADP\cdot H}] + [(\mathrm{ADP\cdot Cu\cdot H})_{\mathrm{cl}}]$$

$$10^{(2.77\pm0.16)} = 10^{(2.4\pm0.25)} + 10^{(1.64\pm0.24)} + 10^{(2.48\pm0.27)}$$

$$1 = 10^{-(0.37\pm0.30)} + 10^{-(1.13\pm0.29)} + 10^{-(0.29\pm0.31)}$$

$$1 = (0.427\pm0.294) + (0.074\pm0.050) + (0.513\pm0.366)$$

$$100\% = (43\pm29)\% + (7\pm5)\% + (51\pm37)\%$$

Since all error limits refer to three times the standard error of the mean value (3σ) (see footnote *a* of Table 2.9), it might be helpful to rewrite this last equation with only 1σ:

$$100\% = (43\pm10)\% + (7\pm2)\% + (51\pm12)\%$$

From this equation follows that the species Cu·ADP·H occurs only in low concentration. The dominating isomers of the Cu(H;ADP) complex are clearly those where *both the metal ion and the proton are bound to the diphosphate residue*. Both the open ADP·Cu·H and the chelated isomer $(\mathrm{ADP\cdot Cu\cdot H})_{\mathrm{cl}}$ occur in about equal concentrations with nearly 50% each. Figure 2.19 shows a schematic representation of the mentioned equilibrium.

How is the situation with the M(H;ADP) complexes of the other metal ions studied? Clearly, here the H·ADP·M isomer is of no relevance, as concluded above on the basis of the measured $\mathrm{p}K^{\mathrm{H}}_{\mathrm{M(H;ADP)}}$ values (see Table 2.9, page 67). This is true for the M·ADP·H species as well, since it occurs only in very low concentration already with Cu^{2+}, which has by far the highest affinity toward the adenine residue of all the metal ions considered here. Hence, only the open ADP·M·H and

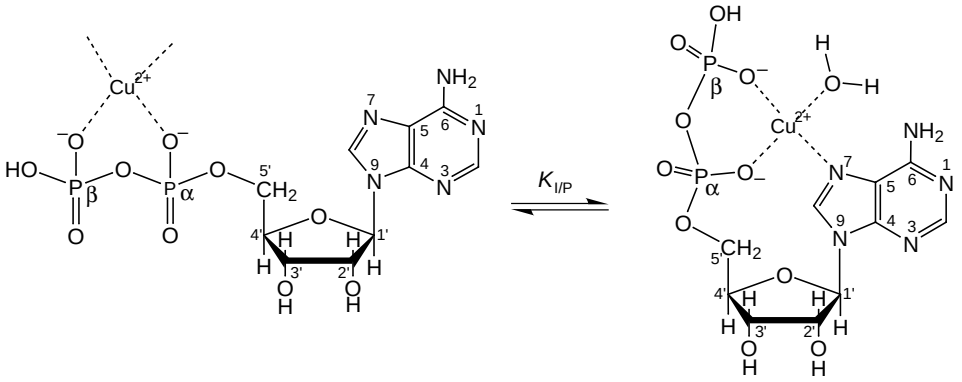

Figure 2.19: Schematic representation of the equilibrium between an *open* and a *closed* isomer of the monoprotonated complex Cu(H;ADP). The equatorial plane of the Jahn-Teller distorted Cu^{2+} octahedron is shown. Two additional water molecules are bound to the central metal ion, pointing out of the page's plane, in the direction to the reader and opposite to it; these waters have been omitted for clarity. In the *open* form, the metal ion and the proton sit at the diphosphate group, while in the *closed* isomer, the phosphate-bound Cu^{2+} interacts with N7 of the nucleobase as well. The two isomers occur in about equal concentrations with nearly 50% each.

the closed $(ADP{\cdot}M{\cdot}H)_{cl}$ isomers are left. To be able to quantify the isomeric ratio in these cases, values for the stability constant of the open isomer, $k^{M}_{ADP{\cdot}M{\cdot}H}$, are needed. By ^{1}H-NMR studies [74] and by stability constant comparisons [106], it has been proven that in the $M(UDP)^{-}$ complexes the uridine residue does not participate in metal ion binding. The same may be assumed for its monoprotonated complexes, therefore it can be assumed that $k^{M}_{ADP{\cdot}M{\cdot}H} = K^{M}_{M(H;UDP)}$. The stability constants of the M(H;ADP) complexes (from column 2 of Table 2.9) and those previously estimated for the M(H;UDP) species [106], are listed in Table 2.10 to facilitate comparisons. The values measured now for M(H;ADP) are identical within the error limits with the ones of the M(H;UDP) species, the only exception being Cu^{2+}. This means that the open ADP·M·H isomer is the dominating species for these M(H;ADP) complexes. As the error limits of the considered stability constants are large (see Table 2.10), one cannot exclude that the chelated isomer

$(ADP{\cdot}M{\cdot}H)_{cl}$ occurs to some extent in an intramolecular equilibrium. Indeed, stability differences between log $K^{M}_{M(H;ADP)}$ and log $K^{M}_{M(H;UDP)}$ of 0.1 or 0.2 log unit, which are within the error limits, correspond to a formation degree of 21 and 37% of the macrochelated isomer, respectively.

Table 2.10: Comparison of the logarithms of the stability constants of M(H;ADP) and M(H;UDP) complexes, the latter having only a M^{2+}-diphosphate coordination, together with the resulting stability difference, log $\Delta_{M(H;ADP)}$ (pot. pH titrations, aq. sol.; 25 °C; I = 0.1 M, $NaNO_3$)[a]

M^{2+}	log $K^{M}_{M(H;ADP)}$ [b]	log $K^{M}_{M(H;UDP)}$ [c,d]	log $\Delta_{M(H;ADP)}$
Mg^{2+}	1.68±0.10	1.6±0.3	0.08±0.3
Ca^{2+}	1.5 ±0.25[c]	1.5±0.3	0.0 ±0.4
Sr^{2+}	1.2 ±0.25[c]	1.2±0.3	0.0 ±0.4
Ba^{2+}	1.12±0.16	1.1±0.3	0.02±0.3
Mn^{2+}	2.38±0.22	2.3±0.3	0.08±0.4
Co^{2+}	2.07±0.14	2.0±0.3	0.07±0.3
Ni^{2+}	2.26±0.15	2.2±0.3	0.06±0.3
Cu^{2+}	2.77±0.16	2.4±0.3	0.37±0.3
Zn^{2+}	2.31±0.20	2.3±0.3	0.01±0.4
Cd^{2+}	2.57±0.12	2.5±0.3	0.07±0.3

[a] The error limits given are *three times* the standard error of the mean value or the sum of the probable systematic errors, whichever is larger. [b] From column 2, Table 2.9. [c] These values are estimates. [d] From [106].

2.5.3 Proof of an enhanced stability of several M(ADP)$^-$ complexes

Applying the procedure described in Section 2.3.1 (page 46) for the determination of log Δ and K_{I} in the case of the M^{2+} complexes of ADP^{3-}, one obtains the results summarized in Table 2.11 on page 77. In Figure 2.11 (page 45) and in Figure 2.20 (page 75) plots of log $K^{\mathrm{M}}_{\mathrm{M(R-DP)}}$ *versus* p$K^{\mathrm{H}}_{\mathrm{H(R-DP)}}$ are shown, where the solid points represent the 1:1 complexes of Mg^{2+}, Co^{2+}, or Zn^{2+}, and of Mg^{2+}, Ni^{2+}, or Cu^{2+} and ADP^{3-}, respectively. They are always above their reference line, proving that macrochelates form. Their distance from the lines is proportional to the degree of macrochelate formation, and represents the log Δ values listed in Table 2.11. The values in the final column of the same Table show that within the error limits, there is no macrochelate formation for the M(ADP)$^-$ complex of Ba^{2+} and possibly not for the one with Sr^{2+} either, yet for Mg(ADP)$^-$ significant amounts in the order of 10% are formed (Figure 2.20). This agrees with results obtained for the M(NMP) [59,89], M(NDP)$^-$ (Section 2.5.6, page 94), and M(NTP)$^{2-}$ (Section 2.4.2, page 57; [65]) complexes of the four alkaline earth ions, where especially with the guanine residue the formation degree is remarkable in all instances. The results obtained for the Ca(ADP)$^-$ complex are at the limit of the accuracy of the data ($Ca(ADP)^-_{cl}$ = 9$\pm$8%, Table 2.11), nevertheless, it is very likely that macrochelates form to some extent. Indeed, the Ca(ATP)$^{2-}$ complex forms macrochelates (15$\pm$12%) [65] (see Table 2.8 on page 61, and Section 2.4.2). It is therefore likely that the result obtained for the Ca(ADP)$^-$ species shows that macrochelates exist, even though there is no evidence of the existence of a closed $Ca(AMP)_{cl}$ species [59,105]. It is not possible to draw similar conclusions about the existence of a $Sr(ADP)^-_{cl}$ complex: the obtained result ($Sr(ADP)^-_{cl}$ = 13$\pm$10%, Table 2.11) is at the limit of data accuracy, and no data are available that would allow such kind of comparisons. Indeed, the corresponding Sr(ATP)$^{2-}$ complex has not yet been investigated, while there is no evidence of macrochelate formation in the Sr(AMP) species [59,105].

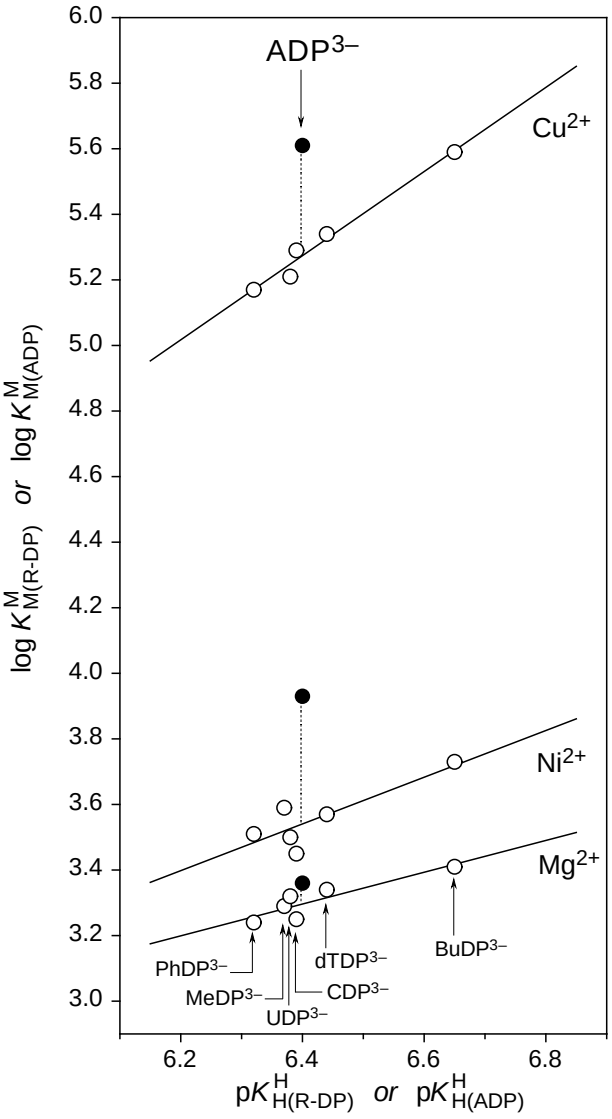

Figure 2.20: Evidence for an enhanced stability of the $Mg(ADP)^{-}$, $Cu(ADP)^{-}$ and $Ni(ADP)^{-}$ complexes (•), based on the relationship between log $K^{\mathrm{M}}_{\mathrm{M(R-DP)}}$ and p$K^{\mathrm{H}}_{\mathrm{H(R-DP)}}$ for the simple $M(R\text{-}DP)^{-}$ complexes (○), where $R\text{-}DP^{3-}$ = phenyl diphosphate ($PhDP^{3-}$), methyl diphosphate ($MeDP^{3-}$), uridine 5′-diphosphate (UDP^{3-}), cytidine 5′-diphosphate (CDP^{3-}), thymidine [=1-(2-deoxy-β-D-ribofuranosyl)thymine] 5′-diphosphate ($dTDP^{3-}$) and *n*-butyl diphosphate ($BuDP^{3-}$). The least-square lines are drawn through the six (five in the case of Cu^{2+}) data sets; the corresponding equilibrium constants are from [106]. All the plotted equilibrium constants refer to aqueous solutions at 25 °C and I = 0.1 M ($NaNO_3$).

Evidently, for all the 3d-transition elements, including Zn^{2+} and Cd^{2+}, the formation degree of the $M(ADP)^{-}_{cl}$ species is high.

By ^{1}H-NMR shift experiments it has previously been proven that macrochelates involving N7 form with the $Zn(ADP)^{-}$ and $Cd(ADP)^{-}$ systems in solution [74]. From kinetic experiments carried out by Frey and Stuehr [148,149] at 15 °C and I = 0.1 M (KNO_3) a formation degree of 80% follows for $Ni(ADP)^{-}_{cl}$; if one considers the difference in temperature, this result is in fair agreement with the 59±6% determined now. For this system macrochelate formation has also been proven by Mariam and Martin [155] by spectrophotometric experiments.

If one considers the results obtained for the complexes of the 3d series, it is evident from the log Δ values (column 4, Table 2.11) that these follow the Irving-Williams series [129,130], as one would expect [131] for a metal ion-imidazole-type interaction. The fact that the maximum stability increase and consequently the highest formation degree of the macrochelates is observed for $Ni(ADP)^{-}$ and not for the corresponding Cu^{2+} complexes can be explained by taking into account the different coordination spheres of Ni^{2+} and Cu^{2+} and by statistical considerations connected with these differences [104].

The results obtained for $Mg(ADP)^{-}$ clearly show that outersphere interactions are of relevance for the $M(ADP)^{-}_{cl}$ species, in analogy to what is observed for the $M(ATP)^{2-}$ complexes [58,59,88,134]. ^{1}H-NMR shift measurements [74], that are sensitive to innersphere binding only, provide no evidence for a Mg^{2+}-N7 interaction, yet macrochelate formation in the order of about 10% is certain (Table 2.11) and must thus occur in an outersphere manner. Most probably, the same is true for the $Ca(ADP)^{-}$ complex. According to the same ^{1}H-NMR experiments, $Zn(ADP)^{-}_{cl}$ and $Cd(ADP)^{-}_{cl}$ reach formation degrees of about 20 and 40%, respectively. Yet, the data from the potentiometric pH titrations, that measure the overall stability increase and which do not distinguish between inner- and outersphere binding, provide formation degrees of about 30 and 55%, respectively. Hence, about one third of $Zn(ADP)^{-}_{cl}$ and $Cd(ADP)^{-}_{cl}$ is formed by outersphere binding to N7 and the other

two thirds by innersphere coordination. Mariam and Martin [155] concluded, based on their spectrophotometric measurements, that about one part of $Ni(ADP)^{-}_{cl}$ is outersphere and that about four parts are innersphere.

Table 2.11: Comparison of the measured stability constants, $K^{M}_{M(ADP)}$, of the $M(ADP)^{-}$ complexes with the stability constants, $K^{M}_{M(ADP)_{op}}$, of the isomers with a sole diphosphate coordination of M^{2+}, together with the stability differences, log Δ, reflecting an increased stability. Extent of intramolecular macrochelate formation as quantified by the dimension-less equilibrium constant K_I in the $M(ADP)^{-}$ complexes (aq. solution, 25 °C; I = 0.1 M, $NaNO_3$)[a]

M^{2+}	log $K^{M}_{M(ADP)}$	log $K^{M}_{M(ADP)_{op}}$ [b]	log Δ	K_I	% $M(ADP)^{-}_{cl}$
Mg^{2+}	3.36±0.03	3.30±0.03	0.06±0.04	0.15±0.11	13± 9
Ca^{2+}	2.95±0.02	2.91±0.03	0.04±0.04	0.10±0.09	9± 8
Sr^{2+}	2.42±0.03	2.36±0.04	0.06±0.05	0.15±0.13	13±10
Ba^{2+}	2.37±0.06	2.30±0.03	0.07±0.07	0.17±0.18	15±13
Mn^{2+}	4.22±0.02	4.12±0.03	0.10±0.04	0.26±0.10	21± 7
Co^{2+}	3.92±0.02	3.72±0.05	0.20±0.05	0.58±0.20	37± 8
Ni^{2+}	3.93±0.02	3.54±0.06	0.39±0.06	1.45±0.36	59± 6
Cu^{2+}	5.61±0.03	5.27±0.04	0.34±0.05	1.19±0.25	54± 5
Zn^{2+}	4.28±0.05	4.12±0.03	0.16±0.06	0.44±0.19	31± 9
Cd^{2+}	4.63±0.04	4.27±0.03	0.36±0.05	1.29±0.26	56± 5

[a] The error limits given are *three times* the standard error of the mean value or the sum of the probable systematic errors, whichever is larger. [b] Values calculated with $pK^{H}_{H(ADP)}$ = 6.40±0.01 and the reference-line equations defined in [106].

In Table 2.12 the formation degrees of $M(AMP)_{cl}$ (from [105]), $M(ADP)^{-}_{cl}$ (from Table 2.11), and the ones of $M(ATP)^{2-}_{cl}$ (from Table 2.8, page 61) are summarized. Comparing these values with each other, one observes that for nearly all the metal

ions studied, the formation degrees of the macrochelated species of a given metal ion are identical within the error limits, independently of the number of phosphate groups present in the ligands. There are only two exceptions: for Co^{2+} and Ni^{2+} one observes the series $M(AMP)_{cl} > M(ADP)^{-}_{cl} \sim M(ATP)^{2-}_{cl}$.

This observation is more astonishing when one considers the overall stabilities of the complexes, that are determined to the largest part by the coordination of the metal ions to the phosphate residues. The stability differences between the M(AMP) and $M(ADP)^{-}$ complexes amount to about 1.2 to 2.4 log units, those between the $M(ADP)^{-}$ and $M(ATP)^{2-}$ complexes are in the order of about 1 log unit. For instance, the log stability constants for Mn(AMP), $Mn(ADP)^{-}$ and $Mn(ATP)^{2-}$ are about 2.2, 4.2, and 5.0; those for the corresponding Mg^{2+} complexes are about 1.6, 3.4 and 4.3, and for Zn^{2+}, 2.4, 4.3 and 5.2, respectively.

One might recall that 1 log unit of a stability constant corresponds approximately to a change in free energy (ΔG°) of 6 kJ/mol at 25 °C [115]. The binding sites of the phosphate residue are high-energy ones, while the structuring interactions that occur at the N7 of the adenine moiety are weak ones. A stability difference log Δ of 0.1 log unit gives rise to a formation degree of about 20% for the macrochelated species ML_{cl}, yet the change in free energy involved in creating the special structure, corresponds only to about 0.6 kJ/mol. It is evident that if 20% of a substrate exists in the correct conformation/orientation needed by the enzyme for a reaction, this is more than enough, especially as with all these metal ions equilibration is fast.

Table 2.12: Comparison of the extent of intramolecular macrochelate formation in the M(AMP), $M(ADP)^{-}$, and $M(ATP)^{2-}$ complexes (aq. solution, 25 °C; I = 0.1 M, $NaNO_3$)[a]

M^{2+}	% $M(AMP)_{cl}$[b]	% $M(ADP)^{-}_{cl}$	% $M(ATP)^{2-}_{cl}$[c]
Mg^{2+}	13±10	13± 9	17±10
Ca^{2+}	7±13	9± 8	15±12
Sr^{2+}	5±10	13±10	–
Ba^{2+}	5±12	15±13	–
Mn^{2+}	15±11	21± 7	17±15
Co^{2+}	56± 7	37± 8	38±13
Ni^{2+}	75± 4	59± 6	56± 6
Cu^{2+}	50± 7	54± 5	67± 3
Zn^{2+}	44±12	31± 9	28±10
Cd^{2+}	50± 8	56± 5	46± 5

[a] The error limits given are *three times* the standard error of the mean value or the sum of the probable systematic errors, whichever is larger. [b] From [105]. [c] From Table 2.8, page 61

2.5.4 Metal ion-binding properties of GDP and IDP

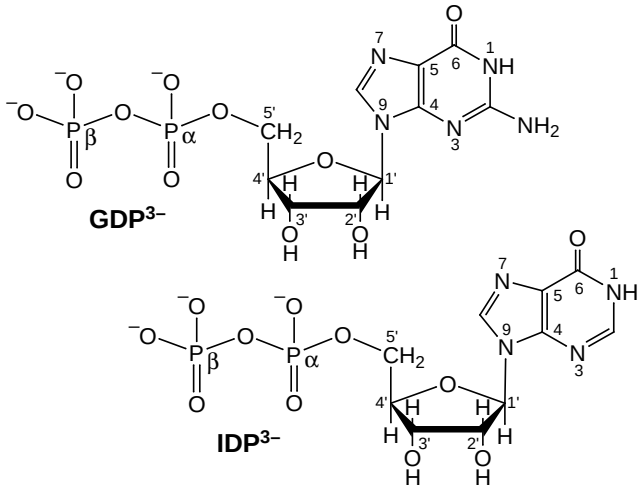

Figure 2.21: Chemical structure of guanosine and inosine (2-deaminoguanosine) 5′-diphosphate in the dominating *anti* conformation [6,7].

All potentiometric pH titrations (25 °C; I = 0.1 M, $NaNO_3$), the results of which are summarized below and in the next sections, were carried out at ligand concentrations of 0.6 mM (Section 4.3.2, page 179) at which self-stacking of GDP and IDP is negligible [74]; *i.e.*, the results presented refer definitely to the monomeric species.

If the evaluation of the experimental data for the M^{2+}/GDP and M^{2+}/IDP systems (M^{2+} = Mg^{2+}, Ca^{2+}, Sr^{2+}, Ba^{2+}, Mn^{2+}, Co^{2+}, Ni^{2+}, Cu^{2+}, Zn^{2+} or Cd^{2+}) is not carried out into the pH range where formation of hydroxo complexes occurs (Section 4.3.2), they are completely described by the four following equilibria and their constants:

The two deprotonation equilibria 2.10 and 2.11, are rewritten here as equations 2.32 and 2.33, respectively:

$$H_2(NDP)^- \rightleftharpoons H(NDP)^{2-} + H^+$$

$$K^{\mathrm{H}}_{\mathrm{H_2(NDP)}} = [\mathrm{H(NDP)^{2-}}][\mathrm{H^+}]/[\mathrm{H_2(NDP)^-}] \tag{2.32}$$

$$\mathrm{H(NDP)^{2-}} \rightleftharpoons \mathrm{NDP^{3-}} + \mathrm{H^+}$$

$$K^{\mathrm{H}}_{\mathrm{H(NDP)}} = [\mathrm{NDP^{3-}}][\mathrm{H^+}]/[\mathrm{H(NDP)^{2-}}] \tag{2.33}$$

The two complex-formation equilibria and their stability constants are defined by equations 2.34 and 2.35:

$$\mathrm{M^{2+}} + \mathrm{H(NDP)^{2-}} \rightleftharpoons \mathrm{M(H;NDP)}$$

$$K^{\mathrm{M}}_{\mathrm{M(H;NDP)}} = [\mathrm{M(H;NDP)}]/[\mathrm{M^{2+}}][\mathrm{H(NDP)^{2-}}] \tag{2.34}$$

$$\mathrm{M^{2+}} + \mathrm{NDP^{3-}} \rightleftharpoons \mathrm{M(NDP)^-}$$

$$K^{\mathrm{M}}_{\mathrm{M(NDP)}} = [\mathrm{M(NDP)^-}]/[\mathrm{M^{2+}}][\mathrm{NDP^{3-}}] \tag{2.35}$$

The acidity constant of the equilibrium describing the loss of the proton from the M(H;NDP) complex, $K^{\mathrm{H}}_{\mathrm{M(H;NDP)}}$ (eq. 2.36), can be calculated with equation 2.37:

$$\mathrm{M(H;NDP)} \rightleftharpoons \mathrm{M(NDP)^-} + \mathrm{H^+}$$

$$K^{\mathrm{H}}_{\mathrm{M(H;NDP)}} = [\mathrm{M(NDP)^-}][\mathrm{H^+}]/[\mathrm{M(H;NDP)}] \tag{2.36}$$

$$\mathrm{p}K^{\mathrm{H}}_{\mathrm{M(H;NDP)}} = \mathrm{p}K^{\mathrm{H}}_{\mathrm{H(NDP)}} + \log K^{\mathrm{M}}_{\mathrm{M(H;NDP)}} - \log K^{\mathrm{M}}_{\mathrm{M(NDP)}} \tag{2.37}$$

Moreover, just like $\mathrm{GDP^{3-}}$ and $\mathrm{IDP^{3-}}$, the $\mathrm{M(GDP)^-}$ and $\mathrm{M(IDP)^-}$ complexes can dissociate a proton from the (N1)H site (see Figure 2.21). This deprotonation is defined by the following equilibrium together with its acidity constant (eq. 2.38):

$$\mathrm{M(NDP)^-} \rightleftharpoons \mathrm{M(NDP{-}H)^{2-}} + \mathrm{H^+}$$

$$K^{\mathrm{H}}_{\mathrm{M(NDP)}} = [\mathrm{M(NDP{-}H)^{2-}}][\mathrm{H^+}]/[\mathrm{M(NDP)^-}] \tag{2.38}$$

The acidity constant referring to proton loss from the (N1)H site of the $\mathrm{M(GDP)^-}$ and $\mathrm{M(IDP)^-}$ complexes, $\mathrm{p}K^{\mathrm{H}}_{\mathrm{M(NDP)}}$, can be calculated from the stability of the corresponding $\mathrm{M(GDP{-}H)^{2-}}$ and $\mathrm{M(IDP{-}H)^{2-}}$ complexes, as given in equation 2.39. Here, $\mathrm{p}K^{\mathrm{H}}_{\mathrm{NDP}}$ represents the acidity constant of the (N1)H site, as given by equation 2.12 (page 30):

$$\mathrm{p}K^{\mathrm{H}}_{\mathrm{M(NDP)}} = \log K^{\mathrm{M}}_{\mathrm{M(NDP)}} - \log K^{\mathrm{M}}_{\mathrm{M(NDP-H)}} + \mathrm{p}K^{\mathrm{H}}_{\mathrm{NDP}} \qquad (2.39)$$

The values of the equilibrium constants (2.34)–(2.39) are listed in Table 2.13.

Comparison of these values with the ones measured for the corresponding complexes of ADP (Table 2.9, page 67) shows that complex stability increases in the series $\mathrm{M(ADP)}^- \leq \mathrm{M(IDP)}^- < \mathrm{M(GDP)}^-$.

For the $\mathrm{M(ADP)}^-$ complexes with the 3d transition metal ions it had been proven [105] (Section 2.5.3 on page 74) that macrochelates involving N7 of the purine nucleobase are formed; the above series demonstrates that this is true for the $\mathrm{M(GDP)}^-$ and $\mathrm{M(IDP)}^-$ complexes as well. A quantitative evaluation of the percentages of macrochelate formation with these complexes will be given in Section 2.5.6 (page 94).

Of all the constants measured here, only $\log K^{\mathrm{Mg}}_{\mathrm{Mg(GDP)}}$ and $\log K^{\mathrm{Mg}}_{\mathrm{Mg(IDP)}}$ had been determined before [60–62,98]. Despite the different methods and conditions employed, the value measured now for $\log K^{\mathrm{Mg}}_{\mathrm{Mg(GDP)}}$ agrees well with the calorimetrically determined one, $\log K^{\mathrm{Mg}}_{\mathrm{Mg(GDP)}} = 3.42$ [156].

The only stability constant value available for the $\mathrm{Mg(IDP)}^-$ complex [157], seems to be too high ($\log K^{\mathrm{Mg}}_{\mathrm{Mg(IDP)}} = 3.76$) compared with the values determined for $\log K^{\mathrm{Mg}}_{\mathrm{Mg(ADP)}}$ and $\log K^{\mathrm{Mg}}_{\mathrm{Mg(GDP)}}$. The temperature at which the spectroscopic measurements were performed is not specified. This value should therefore not be taken into account.

2.5.5 Considerations on the structure of the M(H;GDP) and M(H;IDP) complexes in solution

Via potentiometric pH titrations it was possible to determine the stability constants of the metal ion complexes of $\mathrm{(H;GDP)}^{2-}$ and to estimate the ones of the corresponding complexes formed with $\mathrm{(H;IDP)}^{2-}$.

Table 2.13: Logarithms of the stability constants of M(H;NDP) and M(NDP)$^-$ (NDP = GDP^{3-} or IDP^{3-}) complexes, together with the negative logarithms of the acidity constants of the corresponding M(H;NDP) (eq. 2.37) and M(NDP)$^-$ complexes (eq. 2.38) as determined by potentiometric pH titrations in aqueous solution (25 °C; I = 0.1 M, $NaNO_3$)[a]

NDP^{3-}	M^{2+}	$\log K^{M}_{M(H;NDP)}$	$\log K^{M}_{M(NDP)}$	$pK^{H}_{M(H;NDP)}$	$pK^{H}_{M(NDP)}$
GDP^{3-}	Mg^{2+}	1.6 ±0.3[b]	3.39±0.04	4.59±0.3	9.32±0.04
	Ca^{2+}	1.5 ±0.3[b]	3.05±0.05	4.83±0.3	9.36±0.05
	Sr^{2+}	1.2 ±0.3[b]	2.47±0.04	5.11±0.3	9.36±0.10
	Ba^{2+}	1.2 ±0.3[b]	2.39±0.04	5.19±0.3	9.36±0.08
	Mn^{2+}	2.3 ±0.25	4.35±0.06	4.33±0.26	9.06±0.03
	Co^{2+}	2.4 ±0.25	4.31±0.05	4.47±0.25	8.58±0.05
	Ni^{2+}	2.92±0.13	4.51±0.03	4.79±0.13	8.50±0.04
	Cu^{2+}	3.39±0.19	5.85±0.04	3.92±0.19	–
	Zn^{2+}	2.60±0.07	4.52±0.03	4.46±0.08	8.32±0.10
	Cd^{2+}	3.00±0.10	4.86±0.03	4.52±0.10	8.37±0.07
IDP^{3-}	Mg^{2+}	1.6 ±0.3[b]	3.33±0.03	4.65±0.3	8.89±0.06
	Ca^{2+}	1.5 ±0.3[b]	2.96±0.06	4.92±0.3	8.90±0.03
	Sr^{2+}	1.2 ±0.3[b]	2.42±0.08	5.16±0.3	8.87±0.07
	Ba^{2+}	1.1 ±0.3[b]	2.33±0.07	5.15±0.3	8.86±0.05
	Mn^{2+}	2.3 ±0.25[b]	4.22±0.04	4.46±0.25	8.61±0.05
	Co^{2+}	2.2 ±0.25[b]	4.16±0.05	4.42±0.25	8.13±0.08
	Ni^{2+}	2.4 ±0.3[c]	4.27±0.05	4.51±0.30	7.95±0.06
	Cu^{2+}	3.1 ±0.2[b]	5.69±0.10	3.79±0.22	–
	Zn^{2+}	2.4 ±0.2[b]	4.34±0.05	4.44±0.21	8.05±0.10
	Cd^{2+}	2.7 ±0.2[b]	4.63±0.06	4.45±0.21	8.04±0.06

[a] The error limits given are *three times* the standard error of the mean value or the sum of the probable systematic errors, whichever is larger. The error limits of the derived data, in the present case for column 5, were calculated according to the error propagation after Gauss. [b] These values are estimates. [c] Estimated value, confirmed by experimental results.

One question is now open: *Where are H^+ and the metal ion located?* It is well known that binding of a metal ion to a protonated ligand commonly leads to an acidification of the ligand-bound proton [151,152]. The average value of the deprotonation constants of the M(H;GDP) and M(H;IDP) complexes, listed in column 5 of Table 2.13 (page 83), $pK^{H}_{M(H;NDP)_{av}} \simeq 4.6 \pm 0.4$, is about 1.8 p$K$ units below $pK^{H}_{H(GDP)}$ and $pK^{H}_{H(IDP)}$ (= 6.38; Table 2.2, page 28). Moreover, this value lies about 1.9 pK units *above* $pK^{H}_{H_2(GDP)}$ = 2.67±0.02 (Table 2.2), and about 3 pK units *above* $pk^{IDP\cdot H}_{H\cdot IDP\cdot H}$ = 1.62±0.07 (from Figure 2.5, page 36), that quantify the deprotonation of the (N7)H^+ site in $(H;GDP)^{2-}$ and $(H;IDP)^{2-}$, respectively. Hence, in all the M(H;GDP) and M(H;IDP) complexes, the proton must be located at the diphosphate chain, and there at the terminal β-phosphate group, because this is the most basic site. The label M(NDP·H) indicates that in the M(H;NDP) complexes of IDP and GDP the proton sits at the diphosphate chain. That the maximum of the distribution curves for the Mg(GDP·H), Zn(GDP·H), Ca(IDP·H), and Ni(IDP·H) complexes occurs in the pH region 3 to 5, as shown in Figures 2.22 and 2.23, confirms that the proton must be bound at the β-phosphate group.

But where is the metal ion? As the proton is at the diphosphate residue, one might argue that the metal ion should be located at the nucleobase. Examining the stability constants given in the third column of Table 2.13, one observes that the complex stability of the alkaline earth ions decreases with increasing radius, as expected for their phosphate complexes, indicating that in these instances, both the proton and the metal ion must sit at the diphosphate residue.

As far as the divalent 3d metal ions are concerned, the situation is more complicated. The Cu(H;GDP) and Cu(H;IDP) complexes will be considered first, as Cu^{2+} has the highest affinity towards the guanine and inosine residues of all the metal ions studied here. A further evaluation of the possible isomers of the protonated complexes of GDP and IDP with this metal ion will be carried out. Considerations on the structure of the M(H;GDP) and M(H;IDP) complexes with the other metal ions studied here, will follow.

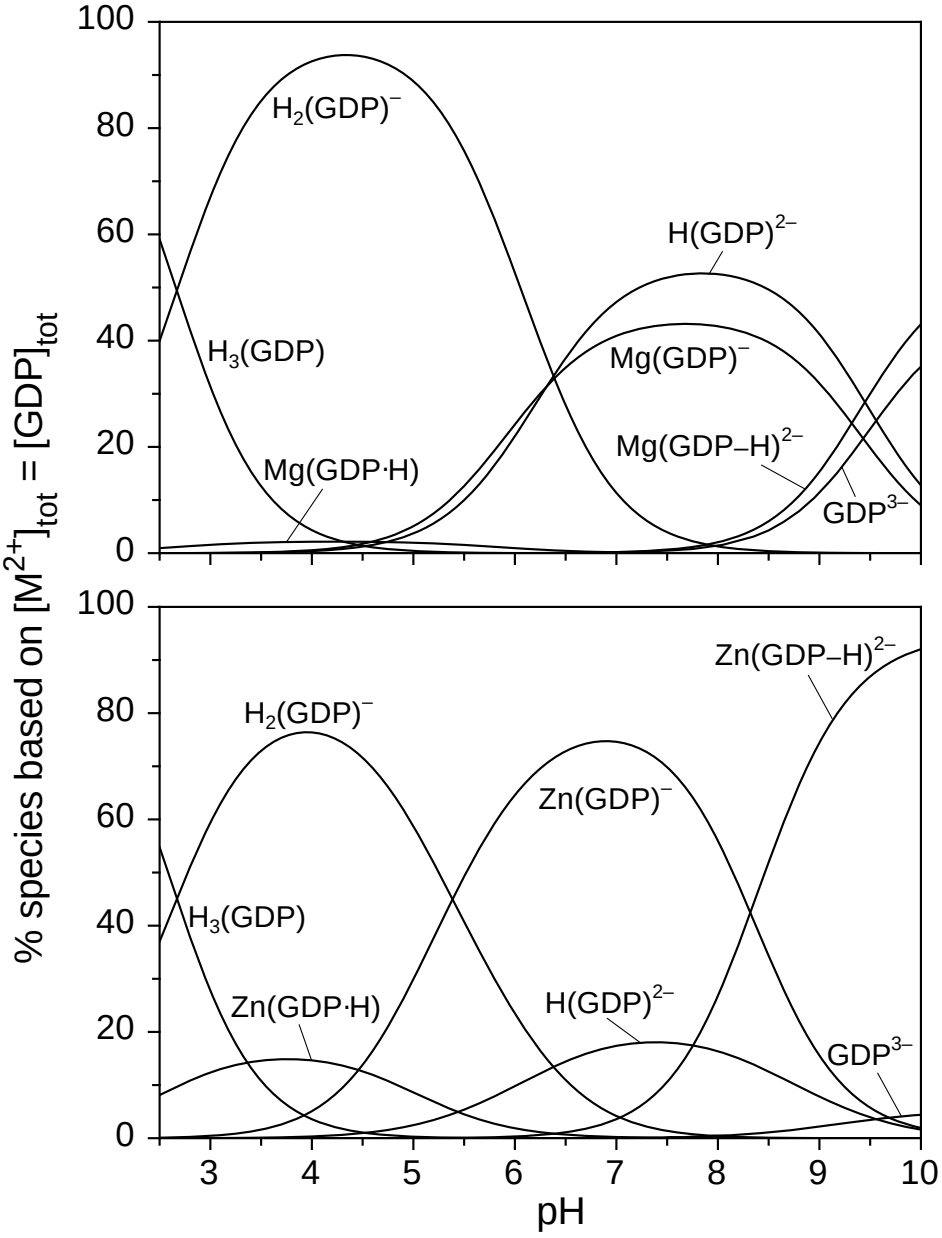

Figure 2.22: Comparison of the effect of pH on the concentration of the species present in aqueous solution of GDP and Mg^{2+} (upper part) or Zn^{2+} (bottom part). The results are given as percentage of the total M^{2+} present (= total GDP). Calculations were carried out with the potentiometrically determined acidity and stability constants for concentrations of 6×10^{-4} M for each reactant (25 °C; I = 0.1 M, $NaNO_3$). These conditions are used in the experiments.

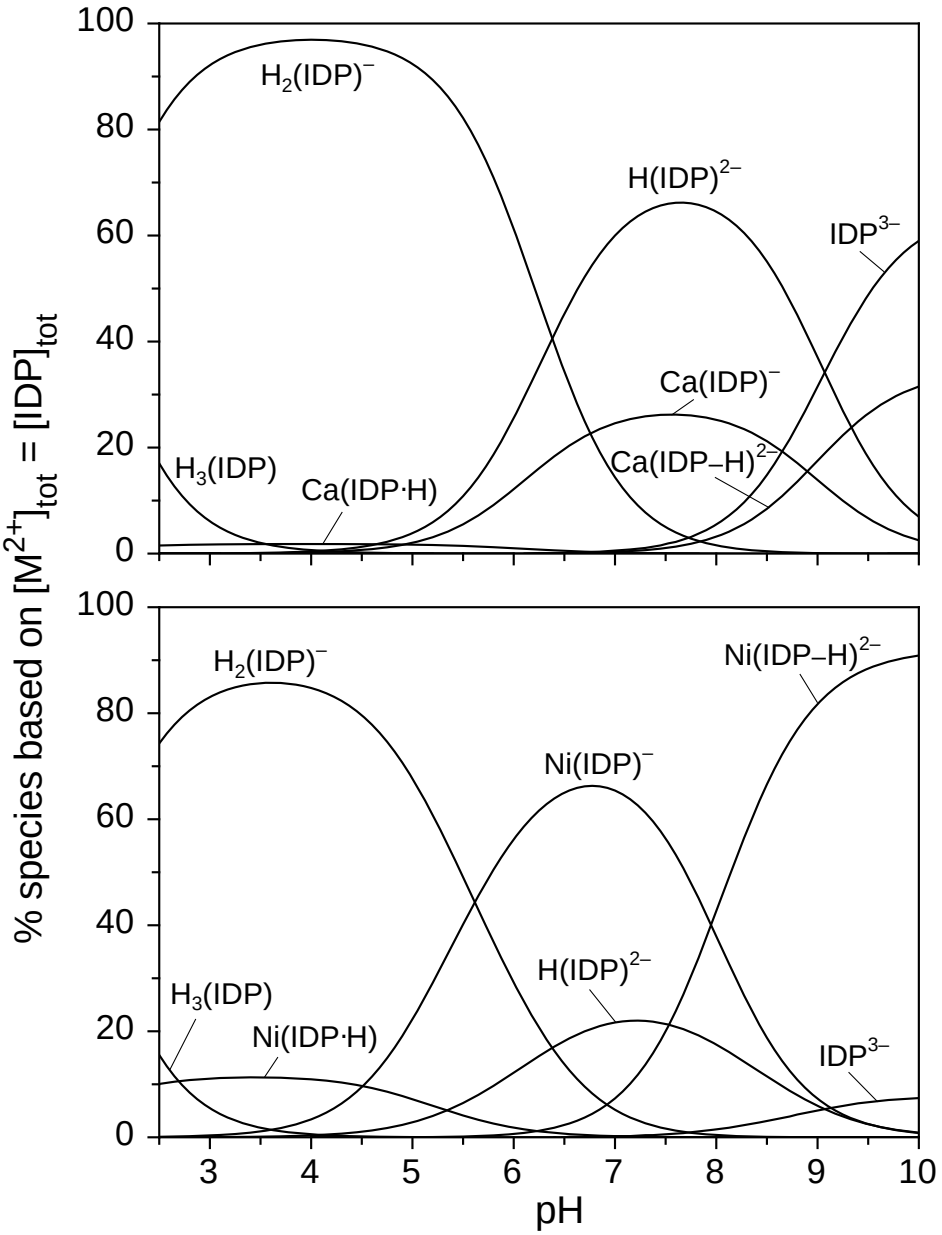

Figure 2.23: Comparison of the effect of pH on the concentration of the species present in aqueous solution of IDP and Ca^{2+} (upper part) or Ni^{2+} (bottom part). The results are given as the percentage of total M^{2+} present (= total IDP). Calculations were carried out with the potentiometrically determined acidity and stability constants for concentrations of 6×10^{-4} M for each reactant (25 °C; I = 0.1 M, $NaNO_3$). These conditions are used in the experiments.

An isomer carrying the proton at the nucleobase and Cu^{2+} at the diphosphate residue, H·NDP·Cu, is clearly of no relevance, as concluded above on the basis of the $pK^{H}_{Cu(H;NDP)}$ values (Table 2.13, page 83).

Considering the Cu(GDP·H) complex, three isomers are therefore possible: (*i*) in GDP·Cu·H the metal ion and the proton sit at the diphosphate chain; (*ii*) Cu·GDP·H carries the metal ion at the nucleobase (N7) and H^+ at the terminal β-phosphate group; (*iii*) both species could to some extent form a closed one, with Cu^{2+} bound at the phosphate residue and at N7, giving rise to the $(GDP{\cdot}Cu{\cdot}H)_{cl}$ isomer. The stability constant of the Cu(H;GDP) complex, $K^{Cu}_{Cu(H;GDP)}$, may be redefined as:

$$K^{Cu}_{Cu(H;GDP)} = \frac{[GDP{\cdot}Cu{\cdot}H] + [Cu{\cdot}GDP{\cdot}H] + [(GDP{\cdot}Cu{\cdot}H)_{cl}]}{[Cu^{2+}][H(GDP)^{2-}]} \qquad (2.40)$$

Hence, the experimentally accessible overall equilibrium constant $K^{Cu}_{Cu(H;GDP)}$ is composed of the three microconstants:

$$K^{Cu}_{Cu(H;GDP)} = k^{Cu}_{GDP{\cdot}Cu{\cdot}H} + k^{Cu}_{Cu{\cdot}GDP{\cdot}H} + k^{Cu}_{(GDP{\cdot}Cu{\cdot}H)_{cl}}$$

The isomeric distribution of the Cu(H;GDP) species can be determined in analogy to what was done in the case of Cu(H;ADP) (see Section 2.5.2 on page 68) [154]. The microconstant $k^{Cu}_{GDP{\cdot}Cu{\cdot}H}$ can be represented by the stability constant of the Cu(H;UDP) complex, in which both, H^+ and Cu^{2+} are bound at the diphosphate residue, *i.e.*, $\log k^{Cu}_{GDP{\cdot}Cu{\cdot}H} = \log K^{Cu}_{Cu(H;UDP)} = 2.4 \pm 0.25$ [87].

The microconstant $k^{Cu}_{(GDP{\cdot}Cu{\cdot}H)_{cl}}$ is given by the expression:

$$k^{Cu}_{(GDP{\cdot}Cu{\cdot}H)_{cl}} = K_{I/P} \cdot k^{Cu}_{GDP{\cdot}Cu{\cdot}H}$$

where $K_{I/P}$ refers to the constant of the intramolecular equilibrium:

$$GDP{\cdot}Cu{\cdot}H \rightleftharpoons (GDP{\cdot}Cu{\cdot}H)_{cl}$$

$$K_{I/P} = [(GDP{\cdot}Cu{\cdot}H)_{cl}]/[GDP{\cdot}Cu{\cdot}H] \qquad (2.41)$$

Assuming [88] that the intramolecular equilibrium constant for macrochelate formation is the same in the protonated and unprotonated complexes, and therefore $K_{I/P} = K_{I/N7} = 2.98 \pm 0.52$ (Table 2.16, page 97), one obtains:

$$k^{Cu}_{(GDP\cdot Cu\cdot H)_{cl}} = K_{I/P} \cdot k^{Cu}_{GDP\cdot Cu\cdot H} = (2.98 \pm 0.52) \times 10^{(2.4\pm0.25)} = 10^{(2.87\pm0.26)}.$$

The only unknown constant is now $k^{Cu}_{Cu\cdot GDP\cdot H}$, that may be calculated from $K^{Cu}_{Cu(H;GDP)}$ (Table 2.13, page 83):

$$\begin{aligned} k^{Cu}_{Cu\cdot GDP\cdot H} &= K^{Cu}_{Cu(H;GDP)} - k^{Cu}_{GDP\cdot Cu\cdot H} - k^{Cu}_{(GDP\cdot Cu\cdot H)_{cl}} \\ &= 10^{(3.39\pm0.19)} - 10^{(2.4\pm0.25)} - 10^{(2.87\pm0.26)} \\ &= (2455 \pm 1074) - (251 \pm 145) - (741 \pm 444) = 1463 \pm 1171\ (3\sigma) \\ k^{Cu}_{Cu\cdot GDP\cdot H} &= 10^{(3.165\pm0.35)} \end{aligned}$$

Setting the right hand side of equation 2.34 equal to that of equation 2.40, gives:

$$\begin{aligned} [Cu(H;GDP)] &= [GDP\cdot Cu\cdot H] + [Cu\cdot GDP\cdot H] + [(GDP\cdot Cu\cdot H)_{cl}] \\ 10^{(3.39\pm0.19)} &= 10^{(2.4\pm0.25)} + 10^{(3.165\pm0.35)} + 10^{(2.87\pm0.26)} \\ 1 &= 10^{-(0.99\pm0.31)} + 10^{-(0.225\pm0.398)} + 10^{-(0.52\pm0.32)} \\ 1 &= (0.102 \pm 0.073) + (0.596 \pm 0.546) + (0.302 \pm 0.222) \\ 100\% &= (10 \pm 7)\% + (60 \pm 55)\% + (30 \pm 22)\% \end{aligned}$$

Since all error limits refer to three times the standard error of the mean value (3σ) (see footnote *a* of Table 2.13), it might be helpful to rewrite this last equation with only 1σ:

$$100\% = (10 \pm 2)\% + (60 \pm 18)\% + (30 \pm 7)\%$$

From this equation follows that the species GDP·Cu·H, where both Cu^{2+} and the proton sit at the diphosphate residue, occurs only in low concentration. The dominating isomer of the Cu(H;GDP) complex is the one carrying the proton at the diphosphate group and the metal ion at the nucleobase. The chelated $(GDP\cdot Cu\cdot H)_{cl}$ isomer occurs in high concentrations, as well.

The different behaviours of the Cu(H;GDP) and Cu(H;ADP) complexes (in the last species, the dominating isomers are those carrying both, the metal ion and the

proton, at the diphosphate residue), might be explained on the basis of the higher basicity of the N7 position of the guanosine compared to the adenosine residue.

The same procedure can be applied in the case of the Cu(H;IDP) complex. Considering the possibility of three different isomers, $K^{\mathrm{Cu}}_{\mathrm{Cu(H;IDP)}}$ can be written as:

$$K^{\mathrm{Cu}}_{\mathrm{Cu(H;IDP)}} = \frac{[\mathrm{IDP{\cdot}Cu{\cdot}H}] + [\mathrm{Cu{\cdot}IDP{\cdot}H}] + [(\mathrm{IDP{\cdot}Cu{\cdot}H})_{\mathrm{cl}}]}{[\mathrm{Cu^{2+}}][\mathrm{H(IDP)^{2-}}]} \tag{2.42}$$

Where IDP·Cu·H represents the isomer carrying both, the proton and the metal ion, at the diphosphate residue; in the Cu·IDP·H species, Cu^{2+} sits at the nucleobase, while H^+ is bound at the terminal β-phosphate group; and finally, the $(IDP{\cdot}Cu{\cdot}H)_{cl}$ isomer represents the macrochelated species that can be formed either by the IDP·Cu·H, or by the Cu·IDP·H isomer, the latter one carrying the Cu^{2+} at N7. The experimentally accessible overall equilibrium constant $K^{\mathrm{Cu}}_{\mathrm{Cu(H;IDP)}}$ is therefore composed of the three microconstants:

$$K^{\mathrm{Cu}}_{\mathrm{Cu(H;IDP)}} = k^{\mathrm{Cu}}_{\mathrm{IDP{\cdot}Cu{\cdot}H}} + k^{\mathrm{Cu}}_{\mathrm{Cu{\cdot}IDP{\cdot}H}} + k^{\mathrm{Cu}}_{\mathrm{(IDP{\cdot}Cu{\cdot}H)_{cl}}}$$

The first microconstant, $k^{\mathrm{Cu}}_{\mathrm{IDP{\cdot}Cu{\cdot}H}}$, refers to the *open* isomer, carrying both the metal ion and the proton at the diphosphate residue, and as already discussed in the cases of ADP and GDP, might be represented by the stability constant of the Cu(H;UDP) complex: $\log k^{\mathrm{Cu}}_{\mathrm{IDP{\cdot}Cu{\cdot}H}} = \log K^{\mathrm{Cu}}_{\mathrm{Cu(H;UDP)}} = 2.4 \pm 0.25$ [87].

$k^{\mathrm{Cu}}_{\mathrm{(IDP{\cdot}Cu{\cdot}H)_{cl}}}$ is given by the expression:

$$k^{\mathrm{Cu}}_{\mathrm{(IDP{\cdot}Cu{\cdot}H)_{cl}}} = K_{\mathrm{I/P}} \cdot k^{\mathrm{Cu}}_{\mathrm{IDP{\cdot}Cu{\cdot}H}}$$

where $K_{\mathrm{I/P}}$ refers to the constant of the intramolecular equilibrium:

$$\mathrm{IDP{\cdot}Cu{\cdot}H} \rightleftharpoons \mathrm{(IDP{\cdot}Cu{\cdot}H)_{cl}}$$

$$K_{\mathrm{I/P}} = [\mathrm{(IDP{\cdot}Cu{\cdot}H)_{cl}}]/[\mathrm{IDP{\cdot}Cu{\cdot}H}] \tag{2.43}$$

Assuming once again that $K_{\mathrm{I/P}} = K_{\mathrm{I/N7}}$ (= 1.75±0.68; Table 2.17, page 99), one obtains: $k^{\mathrm{Cu}}_{\mathrm{(IDP{\cdot}Cu{\cdot}H)_{cl}}} = K_{\mathrm{I/P}} \cdot k^{\mathrm{Cu}}_{\mathrm{IDP{\cdot}Cu{\cdot}H}} = (1.75 \pm 0.68) \times 10^{(2.4 \pm 0.25)} = 10^{(2.64 \pm 0.30)}$.

The constant $k^{\mathrm{Cu}}_{\mathrm{Cu{\cdot}IDP{\cdot}H}}$, may now be calculated from $K^{\mathrm{Cu}}_{\mathrm{Cu(H;IDP)}}$ (Table 2.13, page 83):

$$k^{Cu}_{Cu\cdot IDP\cdot H} = K^{Cu}_{Cu(H;IDP)} - k^{Cu}_{IDP\cdot Cu\cdot H} - k^{Cu}_{(IDP\cdot Cu\cdot H)_{cl}} =$$

$$= 10^{(3.1\pm0.2)} - 10^{(2.4\pm0.25)} - 10^{(2.64\pm0.30)}$$

$$k^{Cu}_{Cu\cdot IDP\cdot H} = 10^{(2.76\pm0.51)}$$

By setting the right hand sides of equation 2.34 (page 81) equal to that of equation 2.42, one obtains:

$$[Cu(H;IDP)] = [IDP\cdot Cu\cdot H] + [Cu\cdot IDP\cdot H] + [(IDP\cdot Cu\cdot H)_{cl}]$$

$$10^{(3.1\pm0.2)} = 10^{(2.4\pm0.25)} + 10^{(2.76\pm0.51)} + 10^{(2.64\pm0.30)}$$

$$1 = 10^{-(0.70\pm0.32)} + 10^{-(0.34\pm0.55)} + 10^{-(0.46\pm0.36)}$$

$$1 = 0.200(0.095/0.420) + 0.457(0.128/1.62) + 0.347(0.151/0.794)$$

The values given between brackets provide the lower and the upper limits based on the logarithmic errors (3σ).

$$100\% = 20(10/42)\% + 46(13/162)\% + 35(15/79)\%$$

And, considering only 1σ for the error limits of the logarithmic results, one obtains:

$$100\% = 20(16/26)\% + 46(30/70)\% + 35(26/46)\%$$

The dominating isomers of the Cu(H;IDP) complex are those where the proton is bound to the diphosphate residue and the metal ion sits at the nucleobase, with the open Cu·IDP·H and the chelated $(IDP\cdot Cu\cdot H)_{cl}$ isomers occurring in high concentrations.

The percentage of isomeric species carrying the metal ion at the nucleobase residue and the proton at the phosphate group in the Cu(H;NDP) complexes increases in the series ADP<IDP<GDP (see above and Section 2.5.2 on page 68), corresponding to the increase in N7 basicity. Even though the acidity constants of the N7 site for the adenosine and inosine residues are comparable [95], metal ion binding at the N7 site of the nucleobase in adenine is sterically hindered by the presence of the $(C6)NH_2$ group [117,133].

It has been shown (as already pointed out in the previous sections), via ^{1}H-NMR studies [74] and by stability constant comparisons [106], that the uridine residue does not participate in metal ion binding in the $M(UDP)^-$ complexes, and

the same can be assumed for its monoprotonated complexes. The log $K^{\mathrm{M}}_{\mathrm{M(H;UDP)}}$ values represent the stability constant for a phosphate-coordinated metal ion that doesn't interact with the nucleobase, therefore $k^{\mathrm{M}}_{\mathrm{GDP\cdot M\cdot H}} = k^{\mathrm{M}}_{\mathrm{IDP\cdot M\cdot H}} = K^{\mathrm{M}}_{\mathrm{M(H;UDP)}}$.

Comparing the stability constant values of the M(H;GDP) and the M(H;IDP) complexes with the corresponding ones previously estimated [106] for the M(H; UDP) systems (see Table 2.14), one observes that they are identical within the error limits. There are four exceptions: the Ni(H;GDP), Cu(H;GDP), Cd(H;GDP), and Cu(H;IDP) systems. The Cu^{2+} systems with both the ligands have already been analysed. Applying the same procedure to the Ni(H;GDP) and Cd(H;GDP) systems, it can be shown that the micro stability constants for the Ni·GDP·H and Cd·GDP·H isomers, $k^{\mathrm{M}}_{\mathrm{M\cdot GDP\cdot H}}$, in which the metal ion sits at the nucleobase and the proton at the diphosphate group, are zero within the error limits. This means that one is left with only two possible isomers for the Ni(H;GDP) and Cd(H;GDP) species: (*i*) GDP·M·H, carrying both, the metal ion and the proton at the diphosphate chain, the metal ion being solely phosphate-coordinated, and (*ii*) $(\mathrm{GDP\cdot M\cdot H})_{\mathrm{cl}}$, a *closed* isomer, in which an interaction occurs between the phosphate-bound metal ion and the N7 at the nucleobase. From the log $\Delta_{\mathrm{M(H;GDP)}}$ values (Table 2.14) for the Ni(H;GDP) and Cd(H;GDP) complexes, an equilibrium between the *open* and *closed* forms is expected, with a considerable formation of macrochelates.

In all other instances, the open GDP·M·H and IDP·M·H isomers are the dominating species, as it can be concluded on the basis of the log $\Delta_{\mathrm{M(H;GDP)}}$ and log $\Delta_{\mathrm{M(H;IDP)}}$ values. As the error limits of the considered stability constants are large, one cannot exclude that chelated isomers, $(\mathrm{GDP\cdot M\cdot H})_{\mathrm{cl}}$ or $(\mathrm{IDP\cdot M\cdot H})_{\mathrm{cl}}$, occur to some extent in an intramolecular equilibrium. Indeed, stability differences log $\Delta_{\mathrm{M(H;NDP)}}$ of 0.1 or 0.2 log unit, which are within the error limits of the data given, correspond to a formation degree of 21 and 37% of the macrochelated isomer, respectively.

In conclusion, with the exception of the Cu(H;GDP) and Cu(H;IDP) complexes,

where the metal ion is preferentially located at the nucleobase, in all other complexes of GDP and IDP both the metal ion and the proton sit at the diphosphate group. It could be proven that macrochelates form with Ni(H;GDP), Cd(H;GDP), Cu(H;GDP), and Cu(H;IDP).

Table 2.14: Comparison of the logarithms of the stability constants of M(H;GDP), M(H;IDP), and M(H;UDP) complexes, the latter having only a M^{2+}-phosphate coordination, together with the resulting stability difference, log $\Delta_{M(H;NDP)}$ (pot. pH titrations, aq. sol.; 25 °C; I = 0.1 M, $NaNO_3$)[a]

NDP^{3-}	M^{2+}	log $K^{M}_{M(H;NDP)}$ [b]	log $K^{M}_{M(H;UDP)}$ [c,d]	log $\Delta_{M(H;NDP)}$
GDP^{3-}	Mg^{2+}	1.6 ±0.3[c]	1.6±0.3	0.0 ±0.4
	Ca^{2+}	1.5 ±0.3[c]	1.5±0.3	0.0 ±0.4
	Sr^{2+}	1.2 ±0.3[c]	1.2±0.3	0.0 ±0.4
	Ba^{2+}	1.2 ±0.3[c]	1.1±0.3	0.1 ±0.4
	Mn^{2+}	2.3 ±0.25	2.3±0.3	0.0 ±0.4
	Co^{2+}	2.4 ±0.25	2.0±0.3	0.4 ±0.4
	Ni^{2+}	2.92±0.13	2.2±0.3	0.72±0.3
	Cu^{2+}	3.39±0.19	2.4±0.3	0.99±0.4
	Zn^{2+}	2.60±0.07	2.3±0.3	0.3 ±0.3
	Cd^{2+}	3.00±0.10	2.5±0.3	0.5 ±0.3
IDP^{3-}	Mg^{2+}	1.6 ±0.3[c]	1.6±0.3	0.0 ±0.4
	Ca^{2+}	1.5 ±0.3[c]	1.5±0.3	0.0 ±0.4
	Sr^{2+}	1.2 ±0.3[c]	1.2±0.3	0.0 ±0.4
	Ba^{2+}	1.1 ±0.3[c]	1.1±0.3	0.0 ±0.4
	Mn^{2+}	2.3 ±0.25[c]	2.3±0.3	0.0 ±0.4
	Co^{2+}	2.2 ±0.25[c]	2.0±0.3	0.2 ±0.4
	Ni^{2+}	2.4 ±0.3[c]	2.2±0.3	0.2 ±0.4
	Cu^{2+}	3.1 ±0.2[c]	2.4±0.3	0.7 ±0.4
	Zn^{2+}	2.4 ±0.2[c]	2.3±0.3	0.1 ±0.4
	Cd^{2+}	2.7 ±0.2[c]	2.5±0.3	0.2 ±0.4

[a] The error limits given are *three times* the standard error of the mean value or the sum of the probable systematic errors, whichever is larger. The error limits of the derived data, in this case for column 5, were calculated according to the error propagation after Gauss. [b] From column 3, Table 2.13. [c] These values are estimates. [d] From [106].

2.5.6 Proof of an enhanced stability for some M^{2+} complexes of GDP^{3-} and IDP^{3-}

The results of the potentiometric pH titrations of metal ion complexes formed between the alkaline earth metal ions and several of the divalent metal ions of the 3d series and IDP or GDP are listed in Table 2.15, together with the ones of ADP [105,154]. Analogously to what was observed in the case of purine-nucleoside mono- [89] and triphosphates [65], the stability of $M(NDP)^-$ complexes increases for all the metal ions considered in the series $M(ADP)^- < M(IDP)^- < M(GDP)^-$. As macrochelate formation has been proven to occur with $M(ADP)^-$ complexes, and as it is reflected in an enhanced stability, macrochelates are expected to form with the $M(IDP)^-$ and $M(GDP)^-$ complexes as well. Of course, they will hardly form to 100%, *i.e.*, the equilibrium between an *open* and a *closed* family of isomers (see Figure 2.24, which reproduces Figure 2.9) must be considered:

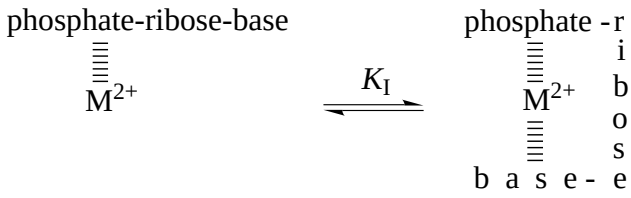

Figure 2.24: Schematic representation of an intramolecular equilibrium between an *open* and a *closed* family of isomers. In the open form, the metal ion is only phosphate-coordinated, while in the closed one it interacts with the nucleobase as well.

Moreover, just like IDP^{3-} and GDP^{3-}, also the $M(IDP)^-$ and $M(GDP)^-$ complexes can dissociate a proton from their (N1)H site (see Figure 2.21 on page 80). The constant describing this deprotonation equilibrium, $pK^{H}_{M(NDP)}$, is defined in equation 2.39 on page 82. The corresponding values for those systems where deprotonation takes place before the onset of the hydrolysis of $M(aq)^{2+}$ could be determined and these results are listed in columns 5 and 6 of Table 2.15.

So far, practically none of the stability constants of the IDP and GDP complexes measured here had been determined before (see Section 2.5.4, page 80).

Table 2.15: Logarithms of the stability constants of $M(ADP)^-$, $M(IDP)^-$, and $M(GDP)^-$ complexes together with the negative logarithms of the acidity constants for some of the $M(IDP)^-$ and $M(GDP)^-$ complexes as determined by potentiometric pH titrations (aq. solution, 25 °C; I = 0.1 M, $NaNO_3$)[a]

M^{2+}	$\log K^{M}_{M(ADP)}$ [b]	$\log K^{M}_{M(IDP)}$ [c]	$\log K^{M}_{M(GDP)}$ [c]	$pK^{H}_{M(IDP)}$ [c]	$pK^{H}_{M(GDP)}$ [c]
Mg^{2+}	3.36±0.03	3.33±0.03	3.39±0.04	8.89±0.06	9.32±0.04
Ca^{2+}	2.95±0.02	2.96±0.06	3.05±0.05	8.90±0.03	9.36±0.05
Sr^{2+}	2.42±0.03	2.42±0.08	2.47±0.04	8.87±0.07	9.36±0.10
Ba^{2+}	2.37±0.06	2.33±0.07	2.39±0.04	8.86±0.05	9.36±0.08
Mn^{2+}	4.22±0.02	4.22±0.04	4.35±0.06	8.61±0.05	9.06±0.03
Co^{2+}	3.92±0.02	4.16±0.05	4.31±0.05	8.13±0.08	8.58±0.05
Ni^{2+}	3.93±0.02	4.27±0.05	4.51±0.03	7.95±0.06	8.50±0.04
Cu^{2+}	5.61±0.03	5.69±0.10	5.85±0.04	–	–
Zn^{2+}	4.28±0.05	4.34±0.05	4.52±0.03	8.05±0.10	8.32±0.10
Cd^{2+}	4.63±0.04	4.63±0.06	4.86±0.03	8.04±0.06	8.37±0.07

[a] The error limits given are *three times* the standard error of the mean value or the sum of the probable systematic errors, whichever is larger. [b] From Table 2.9 on page 67. [c] From Table 2.13 on page 83.

The position of the equilibrium between an *open* and a *closed* form of the $M(GDP)^-$ and $M(IDP)^-$ complexes (Figure 2.24), can be determined once its equilibrium constant, K_I, is known. K_I has been defined in Section 2.3.1 (equation 2.17, page 46), as given again in equation 2.44:

$$K_I = \frac{K^{M}_{ML}}{K^{M}_{ML_{op}}} - 1 = 10^{\log \Delta} - 1 \qquad (2.44)$$

where

$$\log \Delta = \log \Delta_{ML} = \log K^{M}_{ML} - \log K^{M}_{ML_{op}}$$

A quantitative evaluation of the increase in stability of the $M(NDP)^{-}$ complexes, $\log \Delta$, is possible by calculating with the base-line equations [106] and the acidity constant of the diphosphate group, $pK^{H}_{H(NDP)}$, the expected stability for the $M(NDP)^{-}$ complexes with a sole phosphate coordination, *i.e.*, of the *open* isomer, $\log K^{M}_{ML_{op}}$.

Once K_I is known, the percentage of macrochelates formed can be calculated:

$$\% ML_{cl} = 100 \cdot K_I / (1 + K_I)$$

Application of this procedure yields the results listed in Table 2.16 for GDP, and in Table 2.17 on page 99 for IDP.

From the results listed in Table 2.16, it is clear that substantial amounts of macrochelates are formed for all the $M(GDP)^{-}$ species, including the complexes of the alkali earth metal ions. This latter point is remarkable and the most evident difference to the $M(ADP)^{-}$ complexes, where the only alkali earth metal ion that forms macrochelates is Mg^{2+} (see Table 2.11, on page 77).

^{1}H-NMR shift measurements [74] provide no evidence for a Mg^{2+}-N7 interaction in the $Mg(GDP)^{-}$ complexes, yet macrochelate formation in the order of about 20% is certain. This means that an outersphere interaction must occur between the phosphate-bound metal ion and N7 of the nucleobase. This kind of interaction cannot be quantified via ^{1}H-NMR measurements, as this kind of experiment is sensitive only to innersphere binding. Most probably the same kind of outersphere interaction operates with the other alkaline earth metal ions, where there is substantial evidence for macrochelate formation. According to the same ^{1}H-NMR shift study, the $Zn(GDP)^{-}_{cl}$ and $Cd(GDP)^{-}_{cl}$ species should mainly form *via* innersphere coordination to the N7 site.

Table 2.16: Comparison of the measured stability constants, $K^{M}_{M(GDP)}$, of the $M(GDP)^{-}$ complexes with the stability constants, $K^{M}_{M(GDP)_{op}}$, of the isomers with a sole diphosphate coordination of M^{2+}, together with the stability differences, log Δ, reflecting an increased stability, and extent of intramolecular macrochelate formation in the $M(GDP)^{-}$ complexes, as quantified by the dimension-less equilibrium constant K_I (aq. solution, 25 °C; I = 0.1 M, $NaNO_3$)[a]

M^{2+}	log $K^{M}_{M(GDP)}$	log $K^{M}_{M(GDP)_{op}}$ [b]	log Δ	K_I	% $M(GDP)^{-}_{cl}$
Mg^{2+}	3.39±0.04	3.29±0.03	0.10±0.05	0.26±0.14	21± 9
Ca^{2+}	3.05±0.05	2.90±0.03	0.15±0.06	0.41±0.19	29±10
Sr^{2+}	2.47±0.04	2.36±0.04	0.11±0.06	0.29±0.17	22±10
Ba^{2+}	2.39±0.04	2.30±0.03	0.09±0.05	0.23±0.14	19± 9
Mn^{2+}	4.35±0.06	4.11±0.03	0.24±0.07	0.74±0.27	42± 9
Co^{2+}	4.31±0.05	3.70±0.05	0.61±0.07	3.07±0.66	75± 4
Ni^{2+}	4.51±0.03	3.52±0.06	0.99±0.07	8.77±1.51	90± 2
Cu^{2+}	5.85±0.04	5.25±0.04	0.60±0.06	2.98±0.52	75± 3
Zn^{2+}	4.52±0.03	4.09±0.03	0.43±0.04	1.69±0.26	63± 4
Cd^{2+}	4.86±0.03	4.25±0.03	0.61±0.04	3.07±0.40	75± 2

[a] The error limits given are *three times* the standard error of the mean value or the sum of the probable systematic errors, whichever is larger. The error limits of the derived data were calculated according to the error propagation after Gauss. [b] These values were calculated with the reference line equations of Table 4 in [106] and $pK^{H}_{H(GDP)}$ = 6.38±0.01.

Three examples for plots of log $K^{M}_{M(R-DP)}$ versus $pK^{H}_{H(R-DP)}$ are shown in Figure 2.25. The values for the $Mg(GDP)^{-}$ and for the $M(GDP)^{-}$ and the $M(IDP)^{-}$ complexes with Ni^{2+} and Cu^{2+} are clearly above the reference lines. This proves the enhanced stability for these $M(NDP)^{-}$ species.

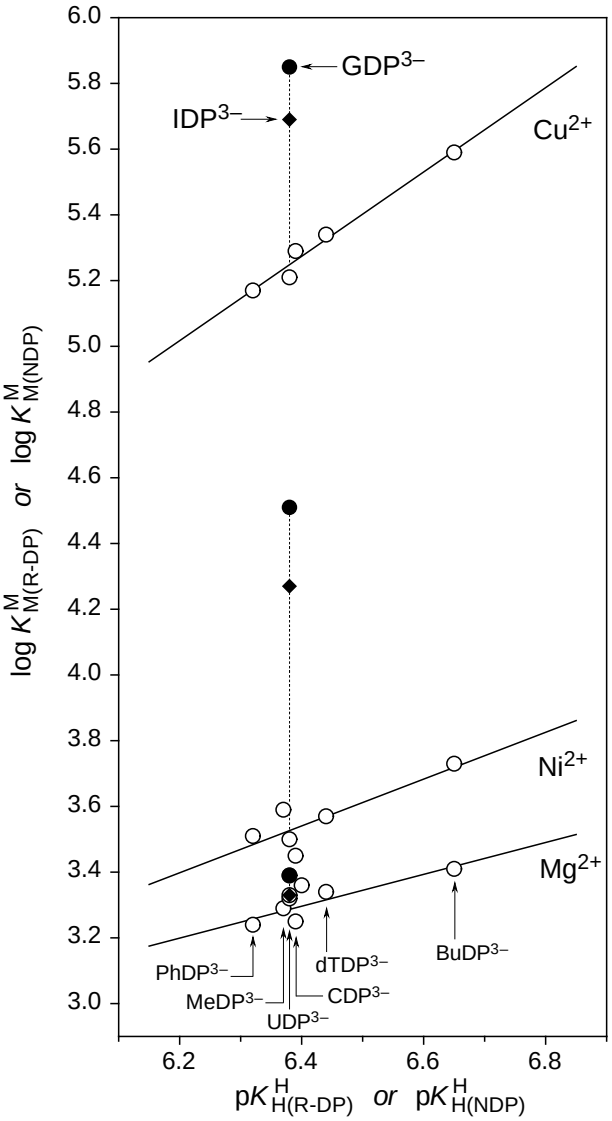

Figure 2.25: Evidence for an enhanced stability of the $M(IDP)^-$ (♦) and $M(GDP)^-$ (•) complexes of Mg^{2+}, Ni^{2+}, and Cu^{2+}, based on the relationship between log $K^{\mathrm{M}}_{\mathrm{M(R-DP)}}$ and p$K^{\mathrm{H}}_{\mathrm{H(R-DP)}}$ for the 1:1 complexes of some simple diphosphate monoester ligands, $R\text{-}DP^{3-}$: phenyl diphosphate ($PhDP^{3-}$), methyl diphosphate ($MeDP^{3-}$), uridine 5′-diphosphate (UDP^{3-}), cytidine 5′-diphosphate (CDP^{3-}), thymidine [=1-(2-deoxy-β-D-ribofuranosyl)thymine] 5′-diphosphate ($dTDP^{3-}$) and *n*-butyl diphosphate ($BuDP^{3-}$). The least-square lines are drawn through the six (five in the case of Cu^{2+}) data sets; the corresponding equilibrium constants are from [106]. All the plotted equilibrium constants refer to aqueous solutions at 25 °C and I = 0.1 M ($NaNO_3$).

In each case the vertical distance between the point due to a certain $M(NDP)^-$ complex and the base line is a reflection of its increased stability.

The values measured for the stability constants of the $M(IDP)^-$ complexes, log $K^{M}_{M(IDP)}$, are listed in Table 2.17, together with the stability constants of the *open* isomers having a sole diphosphate coordination of M^{2+}; the log Δ and K_I values, and the percentages of macrochelation are also given.

Table 2.17: Comparison of the measured stability constants, $K^{M}_{M(IDP)}$, of the $M(IDP)^-$ complexes with the stability constants, $K^{M}_{M(IDP)_{op}}$, of the isomers with a sole diphosphate coordination of M^{2+}, together with the stability differences, log Δ, reflecting an increased stability, and extent of intramolecular macrochelate formation in the $M(IDP)^-$ complexes, as quantified by the dimension-less equilibrium constant K_I (aq. solution, 25 °C; I = 0.1 M, $NaNO_3$)[a]

M^{2+}	log $K^{M}_{M(IDP)}$	log $K^{M}_{M(IDP)_{op}}$	log Δ	K_I	% $M(IDP)^-_{cl}$
Mg^{2+}	3.33±0.03	3.29±0.03	0.04±0.04	0.10±0.11	9± 9
Ca^{2+}	2.96±0.06	2.90±0.03	0.06±0.07	0.15±0.18	13±13
Sr^{2+}	2.42±0.08	2.36±0.04	0.06±0.09	0.15±0.24	13±18
Ba^{2+}	2.33±0.07	2.30±0.03	0.03±0.08	0.07±0.19	7±16
Mn^{2+}	4.22±0.04	4.11±0.03	0.11±0.05	0.29±0.15	22± 9
Co^{2+}	4.16±0.05	3.70±0.05	0.46±0.07	1.88±0.47	65± 6
Ni^{2+}	4.27±0.05	3.52±0.06	0.75±0.08	4.62±1.01	82± 3
Cu^{2+}	5.69±0.10	5.25±0.04	0.44±0.11	1.75±0.68	64± 9
Zn^{2+}	4.34±0.05	4.09±0.03	0.25±0.06	0.78±0.24	44± 8
Cd^{2+}	4.63±0.06	4.25±0.03	0.38±0.07	1.40±0.37	58± 6

[a] The error limits given are *three times* the standard error of the mean value or the sum of the probable systematic errors, whichever is larger. The error limits of the derived data were calculated according to the error propagation after Gauss. [b] These stability constants were calculated with the reference line equations of Table 4 in [106] and $pK^{H}_{H(IDP)}$ = 6.38±0.02.

The result for $Mg(IDP)^-$ is just at the limit of accuracy of the data; without knowing the formation degrees of the closed species in $Mg(ADP)^-$ and $Mg(GDP)^-$, one would probably conclude that $Mg(IDP)^-_{cl}$ doesn't form any macrochelates. Yet, with this knowledge, one may conclude that small amounts of this species exist. This agrees with the results obtained for Mg(IMP) and $Mg(ITP)^{2-}$, that occur to 22±10% [59] and 17±11% ([65], see Section 2.4.2 on page 57) as macrochelates, respectively. The same reasoning applies to the $Ca(IDP)^-$ complex: even though the result is just at the limit of accuracy of the data, the comparison of this value with the ones measured for the Ca(IMP) and $Ca(ITP)^{2-}$ complexes (13±12% and 19±13%, respectively), shows that at least some amounts of macrochelates are likely to be formed with $Ca(IDP)^-$. Most probably, as in these other cases, the metal ion interacts outer-sphere, *i.e.*, via a water molecule, with N7 [134]. This kind of interaction is likely to occur since there is no evidence of innersphere macrochelation from ^{1}H-NMR shift experiments [74]. The formation degree of macrochelates between IDP^{3-} and the other alkali earth ions is zero within the error limits.

From the same ^{1}H-NMR shift study [74], one may conclude, that analogously to $Zn(GDP)^-_{cl}$ and $Cd(GDP)^-_{cl}$, the complexes of the corresponding metal ions with IDP^{3-} mainly form innersphere macrochelates.

Analogously to what has been observed in the case of the M(IMP) and M(GMP) [89] complexes, the highest macrochelate formation degree is observed for the $Ni(IDP)^-$ and $Ni(GDP)^-$ species. The smaller stability enhancements observed for $Cu(IDP)^-$ and $Cu(GDP)^-$ in comparison with those of $Ni(IDP)^-$ and $Ni(GDP)^-$, respectively, indicate that the geometry of the coordination sphere of the metal ion is probably playing a role [104]. Assuming for Cu^{2+} a Jahn-Teller distorted octahedral coordination sphere with a strong tendency to coordinate donor atoms equatorially [158], there are *two* equatorial positions available at Cu^{2+} in a diphosphate coordinated complex, but only one of these is sterically accessible for an interaction with N7. In the octahedral coordination sphere of Ni^{2+} there are *four* positions left

after diphosphate coordination, and three of these are sterically suitable for N7 coordination. Hence, Cu^{2+} back-binding to N7 is statistically disfavoured by a factor of $1/3$, corresponding to -0.48 log unit. This value is indeed close to the reduced enhancement of -0.31 log unit ($= \log \Delta_{\mathrm{Cu/IDP}} - \log \Delta_{\mathrm{Ni/IDP}} = 0.44 - 0.75$; Table 2.17) observed for the $Cu(IDP)^-$ complex in comparison with the $Ni(IDP)^-$ one, and to -0.39 log unit ($= \log \Delta_{\mathrm{Cu/GDP}} - \log \Delta_{\mathrm{Ni/GDP}} = 0.60 - 0.99$; Table 2.16) for the $Cu(GDP)^-$ species, compared with the $Ni(GDP)^-$ one.

The affinity of Mn^{2+} toward imidazole nitrogen is considerably lower than that of the other 3d ions studied here, but at the same time, considerably larger than that of the alkaline earth ions [131], and this is reflected in its log Δ values.

The values of log $\Delta_{\mathrm{M(NDP)}}$ collected in Table 2.18 confirm that the stability increase follows the series $M(ADP)^- \leq M(IDP)^- < M(GDP)^-$ for all 10 metal ions studied.

Table 2.18: Comparison of the log $\Delta_{\mathrm{M(NDP)}}$ values for the metal ion complexes of ADP^{3-}, IDP^{3-}, and GDP^{3-}[a]

M^{2+}	log $\Delta_{\mathrm{M(ADP)}}$[b]	log $\Delta_{\mathrm{M(IDP)}}$[c]	log $\Delta_{\mathrm{M(GDP)}}$[d]
Mg^{2+}	0.06±0.04	0.04±0.04	0.10±0.05
Ca^{2+}	0.04±0.04	0.06±0.07	0.15±0.06
Sr^{2+}	0.06±0.05	0.06±0.09	0.11±0.06
Ba^{2+}	0.07±0.07	0.03±0.08	0.09±0.05
Mn^{2+}	0.10±0.04	0.11±0.05	0.24±0.07
Co^{2+}	0.20±0.05	0.46±0.07	0.61±0.07
Ni^{2+}	0.39±0.06	0.75±0.08	0.99±0.07
Cu^{2+}	0.34±0.05	0.44±0.11	0.60±0.06
Zn^{2+}	0.16±0.06	0.25±0.06	0.43±0.04
Cd^{2+}	0.36±0.05	0.38±0.07	0.61±0.04

[a] See footnote *a* of Table 2.15 regarding the error limits. [b] The values are taken from column 4 of Table 2.11 on page 77. [c] From Table 2.17 on page 99. [d] From Table 2.16 on page 97.

2.5.7 Evidence of macrochelation in several M(IDP−H)$^{2-}$ and M(GDP−H)$^{2-}$ complexes

What happens to a macrochelated species $M(NDP)^{-}_{cl}$, if the (N1)H position at the nucleobase is deprotonated? Of course, any interaction in addition to the phosphate group coordination must be reflected in an increased stability. To know whether any kind of such interactions occurs, one needs to determine the difference (if any) between the overall stability constants that are measured and the stability of an *open* species, in which no additional interaction occurs. This difference is

quantified by log $\Delta^{\star}$:

$$\log \Delta^{\star}_{\mathrm{M(NDP-H)}} = \log K^{\mathrm{M}}_{\mathrm{M(NDP-H)}} - \log K^{\mathrm{M}}_{\mathrm{M(NDP-H)_{op}}}$$

The values for $\log K^{\mathrm{M}}_{\mathrm{M(NDP-H)}}$ are connected to $\mathrm{p}K^{\mathrm{H}}_{\mathrm{M(NDP)}}$ via equation 2.39 (page 82), which is here rewritten as equation 2.45 for clarity,

$$\log K^{\mathrm{M}}_{\mathrm{M(NDP-H)}} = \log K^{\mathrm{M}}_{\mathrm{M(NDP)}} + \mathrm{p}K^{\mathrm{H}}_{\mathrm{NDP}} - \mathrm{p}K^{\mathrm{H}}_{\mathrm{M(NDP)}} \tag{2.45}$$

and log $\Delta^{\star}$ can then be written as (for details see [89]):

$$\begin{aligned}\log \Delta^{\star}_{\mathrm{M(NDP-H)}} &= \mathrm{p}K^{\mathrm{H}}_{\mathrm{M(NDP)_{op}}} - \mathrm{p}K^{\mathrm{H}}_{\mathrm{M(NDP)}} \\ &= (\mathrm{p}K^{\mathrm{H}}_{\mathrm{NDP}} - \mathrm{p}K^{\mathrm{H}}_{\mathrm{M(NDP)}}) - (\mathrm{p}K^{\mathrm{H}}_{\mathrm{NDP}} - \mathrm{p}K^{\mathrm{H}}_{\mathrm{M(NDP)_{op}}})\end{aligned}$$

$$\log \Delta^{\star}_{\mathrm{M(NDP-H)}} = \Delta\ \mathrm{p}K_{\mathrm{a}} - \Delta\ \mathrm{p}K_{\mathrm{a/op}} \tag{2.46}$$

The $\Delta\ \mathrm{p}K_{\mathrm{a}}$ values that appear in equation 2.46 are listed in column 4 of Table 2.19. Indeed, $\mathrm{p}K^{\mathrm{H}}_{\mathrm{NDP}}$ could be determined for both nucleotides, and the $\mathrm{p}K^{\mathrm{H}}_{\mathrm{M(NDP)}}$ values are experimentally accessible for those complexes which undergo hydrolysis only at high enough pH values. The only systems whose constants could not be determined, are the Cu^{2+} complexes of GDP and IDP, for which not enough experimental data points were available before the onset of hydrolysis.

A value for $\Delta\ \mathrm{p}K_{\mathrm{a/op}}$ is needed: this constant quantifies the acidification that affects the proton bound at the N1 position of the nucleobase, when a divalent metal ion is solely coordinated to the diphosphate group. It has been proven [89] that there is no significant macrochelation in any of the $\mathrm{M(GMP-H)}^{-}$ and $\mathrm{M(IMP-H)}^{-}$ complexes of the alkaline earth metal ions, as the acidification of these ions on the (N1)H site corresponds to the electrostatic effect expected for a divalent metal ion bound to the phosphate group of the nucleotide. From the values of $\Delta\ \mathrm{p}K_a$ ($= \mathrm{p}K^{\mathrm{H}}_{\mathrm{NDP}} - \mathrm{p}K^{\mathrm{H}}_{\mathrm{M(NDP)}}$) listed in column 4 of Table 2.19, it is clear that with both IDP^{3-} and GDP^{3-}, an acidification of $\mathrm{p}K^{\mathrm{H}}_{\mathrm{NDP}}$ of about 0.20 log unit is observed with the earth alkaline ions (on average, $\Delta\ \mathrm{p}K_{\mathrm{a/op}} = 0.20 \pm 0.06$).

Table 2.19: Negative logarithms of the acidity constants for the $M(NDP-H)^{2-}$ complexes of IDP and GDP, together with the Δ pK_a and the log $\Delta^{\star}_{M(NDP-H)}$ values defined in equation 2.46[a]

NDP^{3-}	M^{2+}	p$K^{H}_{M(NDP)}$ [b]	Δ pK_a [c]	log $\Delta^{\star}_{M(NDP-H)}$ [d]
IDP^{3-}	Mg^{2+}	8.89±0.06	0.18±0.06	–
	Ca^{2+}	8.90±0.03	0.17±0.04	–
	Sr^{2+}	8.87±0.07	0.20±0.07	–
	Ba^{2+}	8.86±0.05	0.21±0.05	–
	Mn^{2+}	8.61±0.05	0.46±0.05	0.26±0.08
	Co^{2+}	8.13±0.08	0.94±0.08	0.74±0.10
	Ni^{2+}	7.95±0.06	1.12±0.06	0.92±0.08
	Cu^{2+}	–	–	–
	Zn^{2+}	8.05±0.10	1.02±0.10	0.82±0.12
	Cd^{2+}	8.04±0.06	1.03±0.06	0.83±0.08
GDP^{3-}	Mg^{2+}	9.32±0.04	0.24±0.05	–
	Ca^{2+}	9.36±0.05	0.20±0.06	–
	Sr^{2+}	9.36±0.10	0.20±0.10	–
	Ba^{2+}	9.36±0.08	0.20±0.09	–
	Mn^{2+}	9.06±0.03	0.50±0.04	0.30±0.07
	Co^{2+}	8.58±0.05	0.98±0.06	0.78±0.08
	Ni^{2+}	8.50±0.04	1.06±0.05	0.86±0.08
	Cu^{2+}	–	–	–
	Zn^{2+}	8.32±0.10	1.24±0.10	1.04±0.12
	Cd^{2+}	8.37±0.07	1.19±0.08	0.99±0.10

[a] See footnote *a* of Table 2.13 regarding the error limits. [b] The values are taken from column 6 of Table 2.13 on page 83. [c] Δ pK_a = pK^{H}_{NDP} − p$K^{H}_{M(NDP)}$, where pK^{H}_{GDP} = 9.56±0.03 and pK^{H}_{IDP} = 9.07±0.02 (from Table 2.2 on page 28). [d] log $\Delta^{\star}_{M(NDP-H)}$ = Δ pK_a − Δ p$K_{a/op}$, with Δ p$K_{a/op}$ = 0.20±0.06, see text in this Section.

As there is no reason to expect any kind of additional interaction of these metal ions with the deprotonated nucleobase, in analogy to what was observed with the corresponding M(GMP−H)$^-$ and M(IMP−H)$^-$ complexes, this value can be assumed to be due to a pure electrostatic repulsion between the phosphate-coordinated M^{2+} and the proton at N1. This can then be a good estimation for the value of Δ p$K_{\mathrm{a/op}}$. Therefore, assuming Δ p$K_{\mathrm{a/op}} = 0.20 \pm 0.06$, log $\Delta^{\star}_{\mathrm{M(NDP-H)}}$ (equation 2.46) can now be calculated (Table 2.19, column 5).

Defining $K_{\mathrm{I}}^{\star}$ in analogy to K_{I} (equation 2.14, page 43) as the equilibrium constant between an *open* isomer (phosphate-bound metal ion with N1 being deprotonated), and a *closed* isomer, where the metal ion does interact with the N1-deprotonated nucleobase (not necessarily with (N1)$^-$ itself: see Figure 2.26 on page 108), gives:

$$K_{\mathrm{I}}^{\star} = [\mathrm{M(NDP-H)}^{2-}_{\mathrm{cl}}]/[\mathrm{M(NDP-H)}^{2-}_{\mathrm{op}}] \tag{2.47}$$

Knowing the values of log $\Delta^{\star}_{\mathrm{M(NDP-H)}}$, it is possible to calculate $K_{\mathrm{I}}^{\star}$ and the percentage of macrochelates formed, %M(NDP−H)$^{2-}_{\mathrm{cl}}$. These results are listed in columns 4 and 5 of Table 2.20; they were calculated according to equations 2.48 and 2.49:

$$K_{\mathrm{I}}^{\star} = \frac{K^{\mathrm{M}}_{\mathrm{M(NDP-H)}}}{K^{\mathrm{M}}_{\mathrm{M(NDP-H)_{op}}}} - 1 = 10^{\log\ \Delta^{\star}_{\mathrm{M(NDP-H)}}} - 1 \tag{2.48}$$

$$\%\mathrm{M(NDP-H)}^{2-}_{\mathrm{cl}} = 100 \cdot K_{\mathrm{I}}^{\star}/(1 + K_{\mathrm{I}}^{\star}) \tag{2.49}$$

Comparison of the results listed in Table 2.20 with the corresponding ones for the M(NDP)$^-$ species given in columns 4-6 of Table 2.16 (page 97) and Table 2.17 (page 99), provides two observations: (*i*) There is no indication for a significant macrochelation in any of the M(NDP−H)$^{2-}$ complexes of the alkaline earth metal ions; the acidification of these ions on (N1)H corresponds to the electrostatic effect. This result contrasts somewhat with what was obtained for the corresponding M(GDP)$^-$ complexes, where *closed* species form: if at all, there are only traces ($\leq$ 20%) of macrochelates formed with the M(NDP−H)$^{2-}$ complexes.

(*ii*) Macrochelate formation in $M(IDP-H)^{2-}$ and $M(GDP-H)^{2-}$, where $M^{2+} = Mn^{2+}$, Co^{2+}, Ni^{2+}, Zn^{2+}, and Cd^{2+} is quite pronounced and larger than in the undeprotonated $M(NDP)^{-}$ complexes.

Table 2.20: Extent of macrochelate formation in the $M(NDP-H)^{2-}$ complexes of GDP and IDP as calculated from the stability enhancement, log $\Delta^{\star}_{M(NDP-H)}$ defined in equation 2.46. The resulting intramolecular equilibrium constant $K^{\star}_{I}$ and the percentage of the macrochelates formed quantify the situation in aqueous solution at 25 °C and I = 0.1 M ($NaNO_3$)[a]

NDP^{3-}	M^{2+}	log $\Delta^{\star}_{M(NDP-H)}$ [b]	$K^{\star}_{I}$	% $M(NDP-H)^{2-}_{cl}$
IDP^{3-}	Mg^{2+}	–	∼0	∼0 (<29)
	Ca^{2+}	–	∼0	∼0 (<24)
	Sr^{2+}	–	∼0	∼0 (<21)
	Ba^{2+}	–	∼0	∼0 (<20)
	Mn^{2+}	0.26±0.08	0.82±0.34	45±10
	Co^{2+}	0.74±0.10	4.50±1.27	82± 4
	Ni^{2+}	0.92±0.08	7.32±1.53	88± 2
	Zn^{2+}	0.82±0.12	5.61±1.83	85± 4
	Cd^{2+}	0.83±0.08	5.76±1.24	85± 3
GDP^{3-}	Mg^{2+}	–	∼0	∼0 (<26)
	Ca^{2+}	–	∼0	∼0 (<18)
	Sr^{2+}	–	∼0	∼0 (<28)
	Ba^{2+}	–	∼0	∼0 (<25)
	Mn^{2+}	0.30±0.07	1.00±0.32	50± 8
	Co^{2+}	0.78±0.08	5.03±1.11	83± 3
	Ni^{2+}	0.86±0.08	6.24±1.33	86± 3
	Zn^{2+}	1.04±0.12	9.96±3.03	91± 3
	Cd^{2+}	0.99±0.10	8.77±2.25	90± 2

[a] See footnote *a* of Table 2.13 on page 83 regarding the error limits. [b] The values are taken from column 5 of Table 2.19 on page 104.

In addition, for a given 3d metal ion there is hardly a significant difference in base back-binding between the complexes of $M(IDP-H)^{2-}$ and $M(GDP-H)^{2-}$, whereas the corresponding $M(GDP)^{-}_{cl}$ and $M(IDP)^{-}_{cl}$ species form to different extents.

These two points suggest an interaction of the diphosphate bound metal ion with the N1-deprotonated nucleobase. But how is the structure of these macrochelates affected by the deprotonation of the (N1)H site? Analogously to what was observed in the case of this kind of complexes formed with GMP and IMP [89], one would assume that O6 is participating in the metal ion coordination. In fact, in the Mn^{2+}, Co^{2+}, Ni^{2+}, Zn^{2+}, or Cd^{2+} complexes formed with xanthosinate, where N1 is deprotonated, the coordination of M^{2+} still occurs to a significant extent at N7, thought the N1 bound isomer exists in equilibrium [159]. The question, whether a metal ion bound to N7 does or does not interact with O6, which is expected to carry part of the negative charge created upon deprotonation of (N1)H, has been positively answered [89]. Here follows a short summary of the considerations that led to this conclusion:

(*i*) In a ^{13}C NMR study [160] of guanosine and inosine (basic conditions, in dimethyl sulfoxide) some evidence was shown for O6 participation in metal ion coordination. However, the N7/O6 bite is quite large, the N7-C5-C6 angle being about 132 ° [161,162] and in fact, the crystal structure of *trans*-tetraaqua-bis-(xanthosinato)zinc(II) dihydrate [161] shows a direct coordination of Zn^{2+} to N7, but an outer-sphere (hydrogen bond formation via a metal ion coordinated water molecule) coordination to O6.

(*ii*) Evidence of innersphere coordination of metal ions with a N,O donor set in systems whose structures are close to the one of the purine rings comes, for instance, from the crystal structures of pterin derivatives [163,164] and of the anionic 8-hydroxyquinoline [165]. Here the bite between the N and O donor sites is smaller, because the angle around the carbon (in an analogous position as C5 in the purines, but now between two six-membered rings) is close to 120 ° and this allows the

formation of unstrained five-membered rings. This evidences that the outersphere chelation observed in the Zn(xanthosinate)$_2$ system has to do with the wide N7/O6 angle.

In conclusion, upon deprotonation of the (N1)H site, an additional interaction next to the one with N7, is observed between the diphosphate-bound metal ion and the nucleobase. In analogy to what was shown in the case of the corresponding M(GMP) and M(IMP) complexes, an interaction between the (C6)O and the metal ion is expected to be responsible for the additionally enhanced stability of the 3d metal ion complexes. This interaction could be of an innersphere or an outersphere kind. A schematic and tentative representation of the possible structure of these complexes is shown in Figure 2.26.

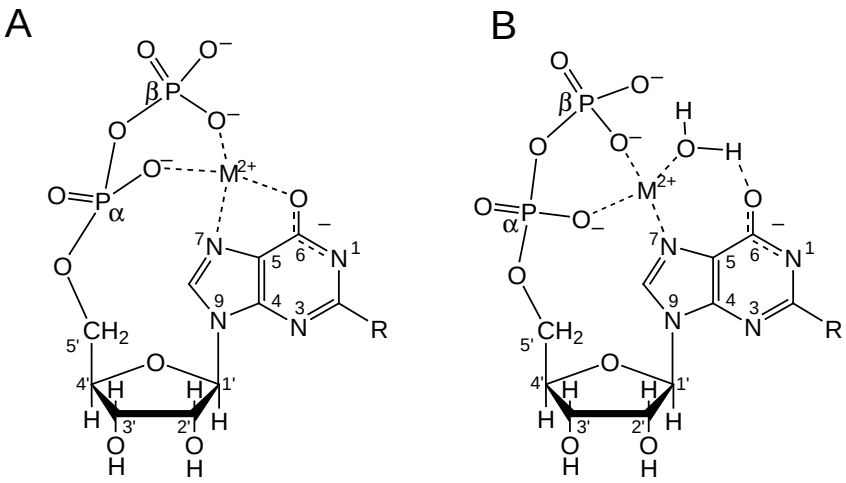

Figure 2.26: Schematic and simplified structures for the macrochelated N1-deprotonated innersphere (A) and outersphere (B) isomers of M(GDP−H)$^{2-}$ (R = NH_2) and M(IDP−H)$^{2-}$ (R = H).

2.6 Equilibrium constants of ternary complexes of ADP, GDP, and IDP

The aim of this study was to quantify the stacking tendency of structurally different purine nucleoside 5′-diphosphates in mixed-ligand complexes, using 2,2′-bipyridine (bpy) and 1,10-phenanthroline (phen) (see Figure 2.27) as standards. As already mentioned in the previous sections, purine derivatives are known to undergo self-association due to stacking of their nucleobase ring systems [67,144]. To make sure that the properties of the monomeric species were indeed studied, all potentiometric pH titrations (25 °C; I = 0.1 M, $NaNO_3$) were carried out at nucleotide concentrations of 0.6 mM. Under these conditions self stacking of ADP, IDP and GDP is negligible [74].

Phen and bpy were chosen as they are easy to handle and still provide generalizable information: the coordinating and π-accepting qualities of the pyridyl group are similar to those of the imidazole moiety [166], an important binding site in natural systems. Moreover, a number of studies exists (see, e.g. [64,87,167–169]) providing a detailed quantification of the stacking interactions of several systems with these two ligands.

Metal ions can coordinate to the diphosphate residue of the nucleotide, as well as to the nitrogen atoms of the heteroaromatic amines (= arm = bpy or phen) and thus, form a bridge between the aromatic rings which undergo the stacking interaction. From earlier studies it is known [67,145,170] that such links facilitate stack formation.

Because of the high stability of the $Cu(arm)^{2+}$ complexes [85,86], that are practically completely formed [87] before the onset of complex formation with the nucleotides, it is possible to treat ternary complexes between $Cu(arm)^{2+}$ and ADP^{3-}, GDP^{3-}, or IDP^{3-} as simple binary ones, by defining M^{2+} = $Cu(bpy)^{2+}$ or $Cu(phen)^{2+}$. Here and in the next sections, N represents any of the three nucleobases.

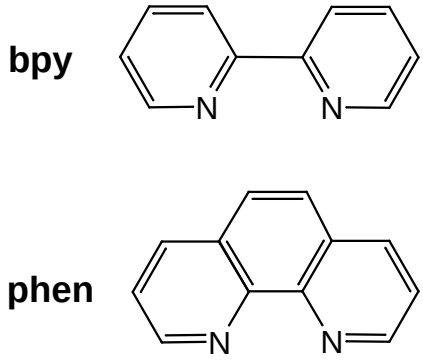

Figure 2.27: Structures of 2,2′-bipyridine (bpy) and 1,10-phenanthroline (phen).

For the studied nucleotides, stack formation in Cu(arm)$(NDP)^{-}$ slightly decreases in the order $GDP^{3-} > IDP^{3-} > ADP^{3-}$. This differs from what is observed for self-stacking of the corresponding base moieties, which decreases in the series adenine $>$ guanine $\geq$ hypoxanthine [74].

2.6.1 Equilibrium constants measured

Under the present experimental conditions the data of the potentiometric pH titrations may be fully described by the acidity (equations 2.50 and 2.51) and by the stability constants 2.52 and 2.53, accounting for the corresponding equilibria, provided the evaluation of the potentiometric data is restricted to the pH range below the onset of hydroxo complex formation. M^{2+} represents below Cu(arm)$^{2+}$:

$$\mathrm{H_2(NDP)^-} \rightleftharpoons \mathrm{H(NDP)^{2-}} + \mathrm{H^+}$$

$$K^{\mathrm{H}}_{\mathrm{H_2(NDP)}} = [\mathrm{H(NDP)^{2-}}][\mathrm{H^+}]/[\mathrm{H_2(NDP)^-}] \tag{2.50}$$

$$\mathrm{H(NDP)^{2-}} \rightleftharpoons \mathrm{NDP^{3-}} + \mathrm{H^+}$$

$$K^{\mathrm{H}}_{\mathrm{H(NDP)}} = [\mathrm{NDP^{3-}}][\mathrm{H^+}]/[\mathrm{H(NDP)^{2-}}] \tag{2.51}$$

$$\mathrm{M^{2+}} + \mathrm{H(NDP)^{2-}} \rightleftharpoons \mathrm{M(H;NDP)}$$

$$K^{\mathrm{M}}_{\mathrm{M(H;NDP)}} = [\mathrm{M(H;NDP)}]/[\mathrm{M^{2+}}][\mathrm{H(NDP)^{2-}}] \tag{2.52}$$

$$M^{2+} + NDP^{3-} \rightleftharpoons M(NDP)^{-}$$

$$K^{M}_{M(NDP)} = [M(NDP)^{-}]/[M^{2+}][NDP^{3-}] \quad (2.53)$$

The last two equilibria are connected via equilibrium 2.54, and the corresponding acidity constant, equation 2.55, may be calculated with equation 2.56:

$$M(H;NDP) \rightleftharpoons M(NDP)^{-} + H^{+} \quad (2.54)$$

$$K^{H}_{M(H;NDP)} = [M(NDP)^{-}][H^{+}]/[M(H;NDP)] \quad (2.55)$$

$$pK^{H}_{M(H;NDP)} = pK^{H}_{H(NDP)} + \log K^{M}_{M(H;NDP)} - \log K^{M}_{M(NDP)} \quad (2.56)$$

The values of the constants 2.52–2.56, determined *via* potentiometric pH titrations (25 °C; I = 0.1 M, $NaNO_3$), are listed in Table 2.21. To facilitate comparisons, the corresponding values measured for the binary Cu^{2+}/NDP systems, already given in Tables 2.9 (page 67) and 2.13 (page 83), are again listed here. The constants, which refer to the binary Cu^{2+}/ADP system are in fair agreement with previous values [60–62]. None of the other stability constants given in the Table have been previously determined.

Table 2.21: Logarithms of the stability constants of M(H;NDP) (equation 2.52) and $M(NDP)^-$ (equation 2.53), together with the negative logarithms of the acidity constants of the corresponding M(H;NDP) (equation 2.56) complexes, where M^{2+} = Cu^{2+}, $Cu(bpy)^{2+}$, or $Cu(phen)^{2+}$, as determined by potentiometric pH titrations in aqueous solution (25 °C; I = 0.1 M, $NaNO_3$)[a,b]

NDP^{3-}	M^{2+}	$\log K^{M}_{M(H;NDP)}$	$\log K^{M}_{M(NDP)}$	$pK^{H}_{M(H;NDP)}$
ADP^{3-}	Cu^{2+}	2.77±0.16[c]	5.61±0.03[c]	3.56±0.16[c]
	$Cu(bpy)^{2+}$	3.62±0.05	6.39±0.03	3.63±0.06
	$Cu(phen)^{2+}$	3.75±0.11	6.52±0.04	3.63±0.12
GDP^{3-}	Cu^{2+}	3.39±0.19[d]	5.85±0.04[d]	3.92±0.19[d]
	$Cu(bpy)^{2+}$	3.94±0.18	6.79±0.05	3.53±0.19
	$Cu(phen)^{2+}$	4.13±0.25	7.00±0.05	3.51±0.26
IDP^{3-}	Cu^{2+}	3.1 ±0.2[d,e]	5.69±0.04[d]	3.79±0.20[d]
	$Cu(bpy)^{2+}$	3.8 ±0.2[e]	6.58±0.04	3.60±0.20
	$Cu(phen)^{2+}$	3.95±0.25[e]	6.72±0.03	3.61±0.25

[a] The acidity constants of $H_2(ADP)^-$ are $pK^{H}_{H_2(ADP)}$ = 3.92±0.02 (equation 2.50) and $pK^{H}_{H(ADP)}$ = 6.40±0.01 (equation 2.51); the ones of $H_2(GDP)^-$ are $pK^{H}_{H_2(GDP)}$ = 2.67±0.02 and $pK^{H}_{H(GDP)}$ = 6.38±0.01, and the corresponding values for $H_2(IDP)^-$ are: $pK^{H}_{H_2(IDP)}$ = 1.82±0.03 and $pK^{H}_{H(IDP)}$ = 6.38±0.02. These acidity constants are from Table 2.2 on page 28. [b] The error limits given are *three times* the standard error of the mean value or the sum of the probable systematic errors, whichever is larger. The error limits (3σ) of the derived data, in the present case for column 5, were calculated according to the error propagation after Gauss. [c] From Table 2.9 on page 67. [d] From Table 2.13 on page 83. [e] Estimated value.

2.6.2 Proof of an increased stability due to stacking in the mixed ligand Cu(arm)(NDP)$^-$ complexes

One way to quantify the stability of mixed ligand complexes [166,171,172] is to consider the following equilibrium, the constant (equation 2.57) of which is calculated with equation 2.58:

$$\mathrm{Cu(arm)^{2+} + Cu(NDP)^- \rightleftharpoons Cu(arm)(NDP)^- + Cu^{2+}}$$

$$10^{\Delta \log K} = [\mathrm{Cu(arm)(NDP)^-}][\mathrm{Cu^{2+}}]/[\mathrm{Cu(arm)^{2+}}][\mathrm{Cu(NDP)^-}] \qquad (2.57)$$

$$\Delta \log K = \log K^{\mathrm{Cu(arm)}}_{\mathrm{Cu(arm)(NDP)}} - \log K^{\mathrm{Cu}}_{\mathrm{Cu(NDP)}} \qquad (2.58)$$

In case a further identification of $\Delta \log K$ for a certain equilibrium is needed, this will be given by additional subscripts, like $\Delta \log K_{\mathrm{Cu/arm/NDP}}$.

According to the general rule for complex stabilities, $K_1 > K_2$, one expects this equilibrium to lie on the left with negative values for $\Delta \log K$. This agrees with statistical considerations obtained for a Jahn-Teller distorted octahedral coordination sphere of Cu^{2+} to which two bidentate ligands A and B are coordinated, *i.e.*, $\Delta \log K_{\mathrm{Cu/statist}} \simeq -0.9$ was estimated [166].

The values for the corresponding bpy and phen systems with ADP [154] according to equation 2.58, are:

$$\Delta \log K_{\mathrm{Cu/bpy/ADP}} = (6.39 \pm 0.03) - (5.61 \pm 0.03) = 0.78 \pm 0.04$$
$$\Delta \log K_{\mathrm{Cu/phen/ADP}} = (6.52 \pm 0.04) - (5.61 \pm 0.03) = 0.91 \pm 0.05$$

The $\Delta \log K_{\mathrm{Cu/arm/ADP}}$ values are larger than zero and the equilibrium is displaced to its right-hand side! What about the Cu(arm)(GDP)$^-$ and Cu(arm)(IDP)$^-$ systems? Also in these instances, the equilibrium is displaced far to its right-hand side:

$$\Delta \log K_{\mathrm{Cu/bpy/GDP}} = (6.79 \pm 0.05) - (5.85 \pm 0.04) = 0.94 \pm 0.06$$
$$\Delta \log K_{\mathrm{Cu/phen/GDP}} = (7.00 \pm 0.05) - (5.85 \pm 0.04) = 1.15 \pm 0.06$$

$$\Delta \log K_{\mathrm{Cu/bpy/IDP}} = (6.58 \pm 0.04) - (5.69 \pm 0.04) = 0.89 \pm 0.06$$
$$\Delta \log K_{\mathrm{Cu/phen/IDP}} = (6.72 \pm 0.03) - (5.69 \pm 0.04) = 1.03 \pm 0.05$$

Indeed, from previous experience an increased stability is actually expected for mixed ligand complexes formed by a divalent 3d metal ion, a heteroaromatic N base and an O donor ligand [166,171–176].

The expected stability increase resulting from the arm/O,O-ligand combination is certainly well represented by the Cu^{2+}/arm/$MePP^{3-}$ system, where $MePP^{3-}$ represents methylphosphonylphosphate (CH_3-P(O)$_2^-$-O-PO_3^{2-}) [177], because the equatorial coordination sphere of Cu^{2+}, Cu(arm)$(O,O)^-$, is identical in all these mixed ligand complexes. Hence, the results for the $MePP^{3-}$ systems [177] may be used as a basis for comparison with the present results:

$$\mathrm{Cu(bpy)^{2+} + Cu(MePP)^- \rightleftharpoons Cu(bpy)(MePP)^- + Cu^{2+}}$$
$$\Delta \log K_{\mathrm{Cu/bpy/MePP}} = 0.42 \pm 0.05 \tag{2.59}$$

$$\mathrm{Cu(phen)^{2+} + Cu(MePP)^- \rightleftharpoons Cu(phen)(MePP)^- + Cu^{2+}}$$
$$\Delta \log K_{\mathrm{Cu/phen/MePP}} = 0.45 \pm 0.05 \tag{2.60}$$

The only significant difference between $MePP^{3-}$ and any of the NDPs considered, is the presence of the base residue in the latter species; hence, any extra stability increase $\Delta\Delta \log K_{\mathrm{arm/NDP}}$, as defined by equation 2.61,

$$\Delta\Delta \log K_{\mathrm{arm/NDP}} = \Delta \log K_{\mathrm{Cu/arm/NDP}} - \Delta \log K_{\mathrm{Cu/arm/MePP}} \tag{2.61}$$

has to be attributed to the nucleobase moiety.

In fact, the results of equations 2.62–2.67 prove that a further interaction must occur within the Cu(arm)$(NDP)^-$ complexes.

$$\Delta\Delta \log K_{\mathrm{bpy/ADP}} = (0.78 \pm 0.04) - (0.42 \pm 0.05) = 0.36 \pm 0.06 \tag{2.62}$$

$$\Delta\Delta \log K_{\mathrm{phen/ADP}} = (0.91 \pm 0.05) - (0.45 \pm 0.05) = 0.46 \pm 0.07 \tag{2.63}$$

$$\Delta\Delta \log K_{\mathrm{bpy/GDP}} = (0.94 \pm 0.06) - (0.42 \pm 0.05) = 0.52 \pm 0.08 \tag{2.64}$$

$$\Delta\Delta \log K_{\mathrm{phen/GDP}} = (1.15 \pm 0.05) - (0.45 \pm 0.05) = 0.70 \pm 0.07 \tag{2.65}$$

$$\Delta\Delta \log K_{\mathrm{bpy/IDP}} = (0.89 \pm 0.06) - (0.42 \pm 0.05) = 0.47 \pm 0.08 \tag{2.66}$$

$$\Delta\Delta \log K_{\mathrm{phen/IDP}} = (1.03 \pm 0.05) - (0.45 \pm 0.05) = 0.58 \pm 0.07 \tag{2.67}$$

In other words, there must be an intramolecular ligand-ligand interaction between the aromatic-ring systems of arm and the nucleobase residue. Hence, these results provide convincing evidence for the occurrence of the intramolecular equilibrium shown in Figure 2.28, involving stack formation.

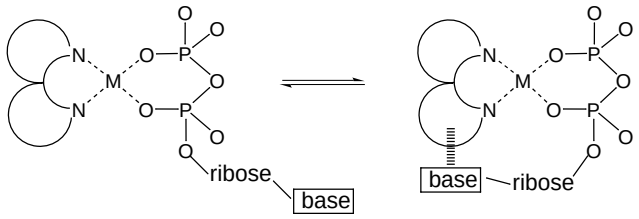

Figure 2.28: Schematic representation of an intramolecular equilibrium between an *open* and a *stacked* isomer. In the *open* form, the metal ion bound to an aromatic ligand is only phosphate-coordinated, while in the stacked one the aromatic residue interacts with the nucleobase.

Certainly, this intramolecular stacking interaction could in addition be proven via spectrophotometric (charge transfer) and ^{1}H-NMR shift measurements (upfield shift), as done before for other related mixed ligand systems with nucleotides [67, 169,170,178,179]. However, such attempts were considered as superfluous in the present case, especially as intramolecular stack formation for the ternary Cu^{2+}, bpy, ADP system has already been proven to occur in the solid state by a crystal structure study [180]. Here, gathering quantitative information about the actual position of the stacking equilibrium in the six systems seemed to be more important.

In the next sections these interactions will further be analysed and quantified.

2.6.3 Structural considerations on the monoprotonated ternary Cu(arm)(H;ADP) complexes

Based on the results discussed for the binary Cu(H;ADP) system in Section 2.5.2 (page 68), it is evident that the species H·ADP·Cu(arm) [154], in which

the proton is located at N1 and Cu(arm)$^{2+}$ at the diphosphate residue, is not expected to play any role. This conclusion agrees with the fact that the acidity constants p$K^{\mathrm{H}}_{\mathrm{Cu(arm)(H;ADP)}}$ and p$K^{\mathrm{H}}_{\mathrm{Cu(H;ADP)}}$ are identical within the error limits (see Table 2.21 on page 112). Similarly, since the concentration of the Cu·ADP·H isomer in the binary system is very low, the formation degree of the ternary species Cu(arm)·ADP·H is expected to be insignificant because the coordination of arm to Cu^{2+} is known [166,172–176] to drastically reduce the affinity of this metal ion toward further N binding sites. This agrees with observations made [169] for the Cu(arm)(dGMP) complexes.

Another species one might think to be of importance for the Cu(arm)(H;ADP) systems is an unbridged mixed ligand complex in which arm undergoes a stacking interaction with the adenine residue. However, the stability constant for the stack between phen or Cu(phen)$^{2+}$ and an adenine residue [181] amounts only to $K \simeq 40\pm6$ M^{-1}, *i.e.*, log K = 1.60±0.07, and even if one takes into account a possible coulombic contribution resulting from the diphosphate residue, *i.e.*, a 2+/2− interaction, not a very high stability of this unbridged stack results because the indicated effect amounts only to 0.7±0.2 log units [106] giving an overall stability of log K = (1.60±0.07) + (0.7±0.2) = 2.30±0.21. Since this value is still far away from the measured stability constant log $K^{\mathrm{Cu(phen)}}_{\mathrm{Cu(phen)(H;ADP)}}$ = 3.75±0.11 (Table 2.21, page 112), a contribution from the unbridged stack to the overall stability constant of this monoprotonated mixed ligand complex is certainly negligible.

The corresponding estimation for the stability of the unbridged Cu(bpy)$^{2+}$/ H(ADP)$^{2-}$ stack leads to the same conclusion. The stability of a bpy/adenine-residue stack amounts to $K = 20\pm5$ M^{-1} [169,181] and by taking into account the charge effect this gives then an estimated stability of the above mentioned unbridged stack: log K = (1.30±0.11) + (0.7±0.2) = 2.00±0.23. Again, this value is far away from the actually measured stability constant log $K^{\mathrm{Cu(bpy)}}_{\mathrm{Cu(bpy)(H;ADP)}}$ = 3.62±0.05 (Table 2.21).

Hence, in the Cu(arm)(H;ADP) systems two possible equilibria have to be taken

into account: the intramolecular stacking equilibrium shown in Figure 2.28 (page 115), between an unstacked and a stacked isomer and the possible existence of the equilibrium between an *open* and a *closed* species (see Figure 2.29), involving the formation of a macrochelated $(ADP{\cdot}Cu(arm){\cdot}H)_{cl}$ isomer.

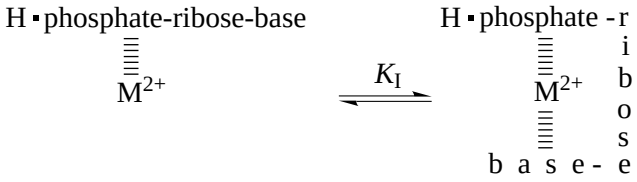

Figure 2.29: Schematic representation of an intramolecular equilibrium between an *open* and a *closed* isomer. In the *open* form, the metal ion is only phosphate-coordinated, while in the *closed* one it interacts with the nucleobase as well.

The stability of the latter may be estimated based on $\log k^{Cu}_{(ADP{\cdot}Cu{\cdot}H)_{cl}} = 2.48\pm0.27$ obtained in Section 2.5.2 for the corresponding binary and macrochelated species, $(ADP{\cdot}Cu{\cdot}H)_{cl}$. Since the affinity of $Cu(arm)^{2+}$, compared with that of Cu^{2+}, is reduced towards N donor binding sites [166,172–176], the stability constant of the binary complex needs to be corrected for this effect. The reduced affinity of $Cu(arm)^{2+}$ towards an unhindered N7, if compared with that of Cu^{2+}, was determined to be $-(0.40\pm0.06)$ log unit and by taking into account the steric hindrance an overall reduction of the affinity of $-(0.80\pm0.25)$ log unit was obtained [169] (and this value must be considered as an upper limit, since there is evidence that the steric inhibition is larger [182]). The estimated micro stability constant for $(ADP{\cdot}Cu(arm){\cdot}H)_{cl}$ amounts to $\log k^{Cu(arm)}_{(ADP{\cdot}Cu(arm){\cdot}H)_{cl}} = (2.48\pm0.27) - (0.80\pm0.25) = 1.68\pm0.37$. This value is clearly much smaller than the two measured macro stability constants, $\log K^{Cu(bpy)}_{Cu(bpy)(H;ADP)} = 3.62\pm0.05$ and $\log K^{Cu(phen)}_{Cu(phen)(H;ADP)} = 3.75\pm0.11$ (Table 2.21, page 112), and therefore one may conclude that the formation of macrochelates is insignificant in the monoprotonated ternary Cu(arm)(H;ADP) systems.

At this point only the $(ADP{\cdot}Cu(arm){\cdot}H)_{op}$ and $(ADP{\cdot}Cu(arm){\cdot}H)_{st}$ isomers are

left, *i.e.*, the equilibrium shown in Figure 2.28 on page 114 in its monoprotonated form, the proton being located in both instances at the terminal β-phosphate group. This then means, $K^{\mathrm{Cu}}_{\mathrm{Cu(arm)(H;ADP)}}$ has to be redefined as given in equation 2.68:

$$K^{\mathrm{Cu(arm)}}_{\mathrm{Cu(arm)(H;ADP)}} = [\mathrm{Cu(arm)(H;ADP)}]/[\mathrm{Cu(arm)}^{2+}][\mathrm{H(ADP)}^{2-}]$$

$$= \frac{[(\mathrm{ADP{\cdot}Cu(arm){\cdot}H})_{\mathrm{op}}]}{[\mathrm{Cu(arm)}^{2+}][\mathrm{H(ADP)}^{2-}]} + \frac{[(\mathrm{ADP{\cdot}Cu(arm){\cdot}H})_{\mathrm{st}}]}{[\mathrm{Cu(arm)}^{2+}][\mathrm{H(ADP)}^{2-}]}$$

Therefore:

$$K^{\mathrm{Cu(arm)}}_{\mathrm{Cu(arm)(H;ADP)}} = k^{\mathrm{Cu(arm)}}_{(\mathrm{ADP{\cdot}Cu(arm){\cdot}H})_{\mathrm{op}}} + k^{\mathrm{Cu(arm)}}_{(\mathrm{ADP{\cdot}Cu(arm){\cdot}H})_{\mathrm{st}}} \tag{2.68}$$

One of the two micro stability constants of equation 2.68 has to be estimated. Since the coordination sphere, Cu(arm)(O,O/H), in the $(\mathrm{ADP{\cdot}Cu(arm){\cdot}H})_{\mathrm{op}}$ and Cu(arm)-(H;MePP) complexes is identical, in both types of complexes $\mathrm{Cu(arm)}^{2+}$ and H^{+} being bound at a -P(O)$_2^-$-O-P(O)$_3^{2-}$ residue, one may assume that the corresponding stability constants are identical and therefore the earlier estimations [177] for the stability of Cu(arm)(H;MePP) are used now. Hence, one can define

$$\log k^{\mathrm{Cu(arm)}}_{(\mathrm{ADP{\cdot}Cu(arm){\cdot}H})_{\mathrm{op}}} = \log K^{\mathrm{Cu(arm)}}_{\mathrm{Cu(arm)(H;MePP)}}$$
$$= 2.5{\pm}0.3$$

The $\Delta \log K$ value obtained as follows, leads to the conclusion that the estimated $\log k^{\mathrm{Cu(arm)}}_{(\mathrm{ADP{\cdot}Cu(arm){\cdot}H})_{\mathrm{op}}}$ value is reasonable:

$$\Delta \log K_{(\mathrm{ADP/Cu(arm)/H})_{\mathrm{op}}} = \log k^{\mathrm{Cu(arm)}}_{(\mathrm{ADP{\cdot}Cu(arm){\cdot}H})_{\mathrm{op}}} - \log k^{\mathrm{Cu}}_{\mathrm{ADP{\cdot}Cu{\cdot}H}}$$
$$= (2.5{\pm}0.3) - (2.4{\pm}0.25) \text{ (bottom of page 69)}$$
$$= 0.1{\pm}0.4$$

This result agrees well with values listed in [177].

The second microconstant of equation 2.68 can now be calculated:

$$k^{\mathrm{Cu(arm)}}_{(\mathrm{ADP{\cdot}Cu(arm){\cdot}H})_{\mathrm{st}}} = K^{\mathrm{Cu(arm)}}_{\mathrm{Cu(arm)(H;ADP)}} - k^{\mathrm{Cu(arm)}}_{(\mathrm{ADP{\cdot}Cu(arm){\cdot}H})_{\mathrm{op}}}$$

and the bpy and phen systems can be evaluated:

$$k^{\mathrm{Cu(bpy)}}_{(\mathrm{ADP{\cdot}Cu(bpy){\cdot}H})_{\mathrm{st}}} = 10^{(3.62{\pm}0.05)} - 10^{(2.5{\pm}0.3)} = 3852.5{\pm}527.3$$

$$k^{\mathrm{Cu(phen)}}_{(\mathrm{ADP{\cdot}Cu(phen){\cdot}H})_{\mathrm{st}}} = 10^{(3.75\pm0.11)} - 10^{(2.5\pm0.3)} = 5307.2\pm1441.0$$

The intramolecular equilibrium between the open and the stacked isomers,

$$(\mathrm{ADP{\cdot}Cu(arm){\cdot}H})_{\mathrm{op}} \rightleftharpoons (\mathrm{ADP{\cdot}Cu(arm){\cdot}H})_{\mathrm{st}}$$

contributes to the value of $K^{\mathrm{Cu(arm)}}_{\mathrm{Cu(arm)(H;ADP)}}$, and from

$$K^{\mathrm{Cu(arm)}}_{\mathrm{Cu(arm)(H;ADP)}} = \frac{[(\mathrm{ADP{\cdot}Cu(arm){\cdot}H})_{\mathrm{op}}]}{[\mathrm{Cu(arm)}^{2+}][\mathrm{H(ADP)}^{2-}]} + \frac{[(\mathrm{ADP{\cdot}Cu(arm){\cdot}H})_{\mathrm{st}}]}{[\mathrm{Cu(arm)}^{2+}][\mathrm{H(ADP)}^{2-}]}$$

follows:

$$[\mathrm{Cu(arm)(H;ADP)}] = [(\mathrm{ADP{\cdot}Cu(arm){\cdot}H})_{\mathrm{op}}] + [(\mathrm{ADP{\cdot}Cu(arm){\cdot}H})_{\mathrm{st}}]$$

Consequently, the dimensionless equilibrium constant, $K_{\mathrm{I/P/st}}$, for the intramolecular stacking equilibrium may be defined, by using equation 2.68, as:

$$K_{\mathrm{I/P/st}} = [(\mathrm{ADP{\cdot}Cu(arm){\cdot}H})_{\mathrm{st}}] \,/\, [(\mathrm{ADP{\cdot}Cu(arm){\cdot}H})_{\mathrm{op}}]$$

$$K_{\mathrm{I/P/st}} = k^{\mathrm{Cu(arm)}}_{(\mathrm{ADP{\cdot}Cu(arm){\cdot}H})_{\mathrm{st}}} / k^{\mathrm{Cu(arm)}}_{(\mathrm{ADP{\cdot}Cu(arm){\cdot}H})_{\mathrm{op}}} \tag{2.69}$$

Once $K_{\mathrm{I/P/st}}$ is known, the percentage of stacked species may be calculated [167,181] according to:

$$\%(\mathrm{ADP{\cdot}Cu(arm){\cdot}H})_{\mathrm{st}} = 100 \cdot K_{\mathrm{I/P/st}}/(1 + K_{\mathrm{I/P/st}}) \tag{2.70}$$

The results for equations 2.69 and 2.70 are summarized in Table 2.22. From the final column in this table it is evident that the stacking equilibrium is displaced far to the right and that the stacked isomer strongly dominates.

Table 2.22: Extent of intramolecular stack formation in monoprotonated ternary M(H;ADP) (M^{2+} = $Cu(arm)^{2+}$) complexes as calculated from stability constant comparisons, and percentage in which these species occur in the stacking equilibrium in aqueous solution (25 °C; I = 0.1 M, $NaNO_3$)[a]

M(H;ADP)[b]	$k^{M}_{(ADP\cdot M\cdot H)_{st}}$	$k^{M}_{(ADP\cdot M\cdot H)_{op}}$	$K_{I/P/st}$	% $(ADP\cdot M\cdot H)_{st}$
Cu(bpy)(H;ADP)	3852.5± 527.3	316.2±218.4	12.2± 9.2	92±5
Cu(phen)(H;ADP)	5307.2±1441.0	316.2±218.4	16.8±13.1	94±4

[a] The error limits given are *three times* the standard error of the mean value or the sum of the probable systematic errors, whichever is larger. [b] $Cu(arm)^{2+}$ and H^+ are both bound to the diphosphate residue of ADP^{3-}.

2.6.4 Structural considerations on the monoprotonated ternary Cu(arm)(H;GDP) and Cu(arm)(H;IDP) complexes

At which sites are the proton and the metal ion bound in the Cu(arm)(H;NDP) (NDP = GDP or IDP) complexes?

As far as the location of the proton is concerned, the same arguments as given for the corresponding binary Cu(H;NDP) systems (Section 2.5.5, page 82) hold; *i.e.*, comparing the acidity constants $pK^{H}_{Cu(arm)(H;NDP)}$ (Table 2.21, page 112), and the $pK^{H}_{H_2(NDP)}$ and $pK^{H}_{H(NDP)}$ values listed in Table 2.2 (page 28) of the corresponding NDPs, follows that the proton must sit at the terminal β-phosphate group in all of the Cu(arm)(NDP) species considered here. Indeed, metal-ion coordination must give rise to an acidification [152], and this is actually observed for the β-phosphate bound proton.

Considering that the proton is at the diphosphate group, the Cu(arm)(NDP·H) complexes may still exist as different isomers.

An unbridged mixed ligand complex in which arm undergoes a stacking interaction with the nucleobase residue is a species that might be thought of importance. In another possible form, $Cu(arm)^{2+}$ is simply coordinated either to N7 of the nucleobase residue, ((arm)Cu·NDP·H), or to the diphosphate group, which already carries the proton, (NDP·H·Cu(arm)). The former species, for steric reasons, cannot lead to intramolecular stacks, while the latter one could do so. In $(Cu(arm)(NDP{\cdot}H))_{cl}$, the arm-bound metal ion interacts with both, the diphosphate group and the N7 site of the nucleobase, forming an intramolecular macrochelate. A further species that needs to be investigated, is $(Cu(arm)(NDP{\cdot}H))_{st}$, in which both the proton and the metal ion are bound to the diphosphate group, and the aromatic-ring system of arm undergoes a stacking interaction with the nucleobase residue (see Figure 2.28, page 115). How much of these isomers is actually formed?

First the species will be considered, in which a pure-stacking interaction takes place.

Adducts formed between phenanthroline and guanosine have about the same stability [183] as those formed between phenanthroline and adenine derivatives [181], *i.e.*, $K \simeq 40\pm6$ M^{-1}, or $\log K = 1.60\pm0.07$. A similar estimation can be made for the corresponding bipyridine/guanosine system. The bpy/adenine stacks are about half as stable as the phen/adenine ones [169,181]: assuming the same to be true for the corresponding guanosine systems, one obtains $K \simeq 20\pm5$ M^{-1}, or $\log K = 1.30\pm0.11$ for bpy/guanosine. It can be presumed that these values hold for the arm/IDP complexes as well. Applying the same procedure as for the Cu(arm)(ADP) systems (see Section 2.6.3 on page 115), taking into account the coulombic interactions (−2/+2) between the diphosphate residue and the $Cu(arm)^{2+}$ ion, overall stabilities of $\log K_{stack/phen} = 2.30\pm0.21$ and $\log K_{stack/bpy} = 2.00\pm0.23$ are found for a pure-stacking interaction between a purine-nucleobase and the phenanthroline or bipyridine aromatic-ring systems, respectively. Since these values are far away from the measured stability constants ($\log K^{Cu(phen)}_{Cu(phen)(H;GDP)}$

= 4.13±0.25 and log $K^{\mathrm{Cu(bpy)}}_{\mathrm{Cu(bpy)(H;GDP)}}$ = 3.94±0.18 for the Cu(arm)(H;GDP) complexes, as well as from log $K^{\mathrm{Cu(phen)}}_{\mathrm{Cu(phen)(H;IDP)}}$ = 3.95±0.25 and log $K^{\mathrm{Cu(bpy)}}_{\mathrm{Cu(bpy)(H;IDP)}}$ = 3.8±0.2 for the Cu(arm)(H;IDP) systems, Table 2.21, page 112), a contribution from the unbridged stack to the overall stability constant of these monoprotonated mixed ligand complexes is certainly negligible.

One is therefore left with the equilibria shown in Figure 2.30:

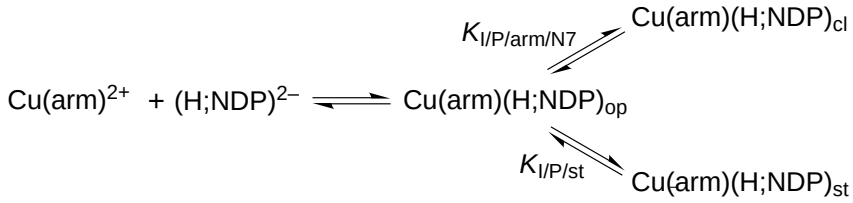

Figure 2.30: Equilibrium scheme for the possible isomers of the Cu(arm)(H;GDP) and Cu(arm)(H;IDP) complexes. The species ((arm)Cu·NDP·H) and (NDP·H·Cu(arm)) are designated together as Cu(arm)(H;NDP)$_{\mathrm{op}}$. Of these two, only the latter isomer, carrying both the proton and the Cu(arm)$^{2+}$ ion at the diphosphate group, can undergo a stacking interaction, according to the equilibrium shown in the lower part of the figure.

One must consider the possible existence of an equilibrium between an *open* and a *closed* form, involving the formation of an intramolecular macrochelate, in which Cu(arm)$^{2+}$ interacts with N7 and the diphosphate group, as shown in the upper part of Figure 2.30. (Cu(arm)(NDP·H))$_{\mathrm{op}}$ consists of two isomers: (NDP·H·Cu(arm)) and ((arm)Cu·NDP·H). The former one could lead to intramolecular stacking interactions between the arm species and the nucleobase, giving rise to the equilibrium shown in the lower part of the Figure. The latter species is of importance in the Cu(H;NDP) complexes of GDP and IDP. Due to the coordination of arm to Cu^{2+}, the affinity of this metal ion toward further N binding sites is reduced [166,172–176], and its formation degree is expected to be lower than in the corresponding Cu(H;NDP) complexes. Nevertheless, this species might still play a role in determining the overall stability of the protonated ternary complexes.

The overall stability constant, $K^{\mathrm{Cu(arm)}}_{\mathrm{Cu(arm)(H;GDP)}}$, measured for the monoprotonated ternary complexes of GDP, can therefore be rewritten according to equation 2.71, where the contribution of the single isomers is taken into account (M^{2+} = $Cu(arm)^{2+}$; [M·GDP·H] and [GDP·H·M] represent the concentrations of the *open* species, as specified above):

$$K^{\mathrm{M}}_{\mathrm{M(H;GDP)}} = \frac{[\mathrm{M{\cdot}GDP{\cdot}H}] + [\mathrm{GDP{\cdot}H{\cdot}M}] + [(\mathrm{GDP{\cdot}H{\cdot}M})_{\mathrm{cl}}] + [(\mathrm{GDP{\cdot}H{\cdot}M})_{\mathrm{st}}]}{[\mathrm{M}^{2+}][\mathrm{H(GDP)}^{2-}]} \tag{2.71}$$

The experimentally accessible overall equilibrium constant $K^{\mathrm{Cu(arm)}}_{\mathrm{Cu(arm)(H;GDP)}}$ is actually composed of the four microconstants summarized in equation 2.72:

$$K^{\mathrm{M}}_{\mathrm{M(H;GDP)}} = k^{\mathrm{M}}_{\mathrm{M{\cdot}GDP{\cdot}H}} + k^{\mathrm{M}}_{\mathrm{GDP{\cdot}H{\cdot}M}} + k^{\mathrm{M}}_{(\mathrm{GDP{\cdot}H{\cdot}M})_{\mathrm{cl}}} + k^{\mathrm{M}}_{(\mathrm{GDP{\cdot}H{\cdot}M})_{\mathrm{st}}} \tag{2.72}$$

Estimations of the micro stability constants $k^{\mathrm{M}}_{\mathrm{M{\cdot}GDP{\cdot}H}}$ (with M^{2+} = $Cu(arm)^{2+}$) may be made by using available stability constants of the corresponding dGMP complexes [169]. Indeed, it has been proven [169] that the $Cu(arm)^{2+}$ ion binds predominantly to N7 at the nucleobase in the Cu(arm)(H;dGMP) complexes: their stability constants can therefore be taken as good approximations for the stability of an isomer carrying the proton at the diphosphate residue, the $Cu(arm)^{2+}$ species at the nucleobase, and where no stacking interactions occur.

Considering the M(H;GDP) systems, log $k^{\mathrm{M}}_{(\mathrm{M{\cdot}dGMP{\cdot}H})_{\mathrm{op}}}$ should be corrected (*i*) for the different basicities of the N7 site in $(H;GDP)^{2-}$ and $(H;dGMP)^{-}$; and (*ii*) for the charge effect that the additional -PO_3^- group exerts on the M^{2+} bound to the base residue in [M·NDP·H].

(*i*) The basicity of the N7 position in GDP and dGMP is within the error limits, identical: $\Delta \mathrm{p}K_a = \mathrm{p}K^{\mathrm{H}}_{\mathrm{H_2(GDP)}} - \mathrm{p}K^{\mathrm{H}}_{\mathrm{H_2(dGMP)}} = (2.67 \pm 0.02) - (2.65 \pm 0.03) = 0.02 \pm 0.04$ ($\mathrm{p}K^{\mathrm{H}}_{\mathrm{H_2(GDP)}}$ is taken from Table 2.2 on page 28; $\mathrm{p}K^{\mathrm{H}}_{\mathrm{H_2(dGMP)}}$ from [169]), and therefore no basicity-correction is needed in this case.

(*ii*) The log $k^{\mathrm{M}}_{(\mathrm{M{\cdot}dGMP{\cdot}H})_{\mathrm{op}}}$ values must then be corrected for the charge effect, that is different in the $Cu(arm)^{2+}/H(dGMP)^{-}$ and the $Cu(arm)^{2+}/H(NDP)^{2-}$ systems. The $+2/-1$ interaction in the former complexes is replaced by a $+2/-2$ in

the last species. Based on previous experience with distant charge effects [153,169, 184], the promoting effect of a $+2/-1$ coulombic interaction is estimated to be of 0.40±0.15 log unit. This effect should be subtracted from log $k^{\mathrm{M}}_{(\mathrm{M{\cdot}dGMP{\cdot}H})_{\mathrm{op}}}$ and the one due to a $+2/-2$ interaction, which amounts to 0.7±0.2 log unit, added to it. The corrected values are: log $k^{\mathrm{Cu(bpy)}}_{(\mathrm{Cu(bpy){\cdot}GDP{\cdot}H})} = (2.60{\pm}0.10)$ [169] $-$ (0.40±0.15) + (0.7±0.2) = 2.90±0.27 for a bipyridine/GDP interaction, and log $k^{\mathrm{Cu(phen)}}_{(\mathrm{Cu(phen){\cdot}GDP{\cdot}H})}$ = (2.60±0.12) [169] − (0.40±0.15) + (0.7±0.2) = 2.90±0.28, for a GDP N7-bound Cu(phen)$^{2+}$ ion.

In the binary Cu(H;GDP) complex, the isomer carrying both the proton and the metal ion at the diphosphate group occurred only in relatively low concentrations, and the predominant species was the one where the proton was bound at the diphosphate residue and the metal ion at the N7 site. The presence of the arm group is known [166,172,173,176] to considerably reduce the affinity of the Cu^{2+} ion toward further N binding sites. Therefore, the contribution of the (GDP·H·Cu(arm)) isomer to the overall stability of the Cu(arm)(H;GDP) complexes still needs to be considered. Analogously to what was done for the (ADP·H·Cu(arm)) complexes, one may assume that the stability of the (GDP·H·Cu(arm)) isomer is identical with the one of the Cu(arm)(H;MePP) complexes. Indeed, the coordination sphere, Cu(arm)(O,O/H), in the (GDP·H·Cu(arm)) and Cu(arm)(H;MePP) complexes is identical, in both types of complexes Cu(arm)$^{2+}$ and H^+ being bound at a -P(O)$_2^-$-O-P(O)$_3^{2-}$ residue. Hence, one can define:

$$\log k^{\mathrm{Cu(arm)}}_{(\mathrm{GDP{\cdot}Cu(arm){\cdot}H})} = \log K^{\mathrm{Cu(arm)}}_{\mathrm{Cu(arm)(H;MePP)}} = 2.5{\pm}0.3 \text{ [177]}$$

The possible formation of an intramolecular macrochelate involving the diphosphate group and N7 at the nucleobase, as shown by the upper equilibrium in Figure 2.30 on page 122 (see also Figure 2.29, page 117), could give some contribution to the value of $K^{\mathrm{Cu(arm)}}_{\mathrm{Cu(arm)(H;GDP)}}$. The stability constant of the macrochelate formed, log $k^{\mathrm{M}}_{(\mathrm{GDP{\cdot}H{\cdot}M})_{\mathrm{cl}}}$, can be estimated. For the corresponding binary and macrochelated species, (GDP·Cu·H)$_{\mathrm{cl}}$, log $k^{\mathrm{Cu}}_{(\mathrm{GDP{\cdot}Cu{\cdot}H})_{\mathrm{cl}}}$ = 2.87±0.26 was obtained (page 88, see

Section 2.5.5, page 82). Since the affinity of Cu(arm)$^{2+}$ compared with that of Cu^{2+}, is reduced towards further N donor binding sites, the stability constant of the binary complex needs to be corrected for this effect. The affinity-reduction due to the presence of the arm group amounts to $-(0.80\pm0.25)$ log unit [169, 182] (see Section 2.6.3, page 115). The estimated micro stability constant for (Cu(arm)(GDP·H))$_{cl}$ is then $\log k^{M}_{(GDP\cdot H\cdot M)_{cl}} = (2.87\pm0.26) - (0.80\pm0.25) = 2.07\pm0.36$.

At this point, the only unknown micro stability constant contributing to the measured stability of Cu(arm)(H;GDP), is $k^{Cu(arm)}_{Cu(arm)(H;GDP)_{st}}$, the others having been estimated. This micro stability constant can be calculated from the equation defining $K^{Cu(arm)}_{Cu(arm)(H;GDP)}$ (equation 2.72 on page 123), as given in equation 2.73:

$$k^{M}_{(GDP\cdot H\cdot M)_{st}} = K^{M}_{M(H;GDP)} - k^{M}_{M\cdot GDP\cdot H} - k^{M}_{GDP\cdot H\cdot M} - k^{M}_{(GDP\cdot H\cdot M)_{cl}} \qquad (2.73)$$

In the case of the Cu(phen)(H;GDP) complexes, $\log K^{Cu(phen)}_{Cu(phen)(H;GDP)} = 4.13\pm0.25$ (Table 2.21 on page 112), and $k^{Cu(phen)}_{(GDP\cdot H\cdot Cu(phen))_{st}}$ is then given by:

$$\begin{aligned} k^{Cu(phen)}_{(GDP\cdot H\cdot Cu(phen))_{st}} &= 10^{4.13\pm0.25} - 10^{2.90\pm0.28} - 10^{2.5\pm0.3} - 10^{2.07\pm0.36} \\ &= (13490\pm7765) - (794\pm512) - (316\pm218) - (117\pm97) \\ &= (12263\pm7786) \end{aligned}$$

from which, $\log k^{Cu(phen)}_{(GDP\cdot H\cdot Cu(phen))_{st}} = 4.09\pm0.28$.

Remembering the definition of $K^{M}_{M(H;GDP)}$,

$$K^{M}_{M(H;GDP)} = [M(H;GDP)]/[M^{2+}][(H;GDP)^{2-}]$$

and setting its right-hand side equal to the one in equation 2.71 on page 123, one obtains:

$$[M(H;GDP)] = [M\cdot GDP\cdot H] + [GDP\cdot H\cdot M] + [(GDP\cdot H\cdot M)_{cl}] + [(GDP\cdot H\cdot M)_{st}]$$

$$\begin{aligned} 10^{4.13\pm0.25} &= 10^{2.90\pm0.28} + 10^{2.5\pm0.3} + 10^{2.07\pm0.36} + 10^{4.09\pm0.28} \\ 1 &= 10^{-(1.23\pm0.38)} + 10^{-(1.63\pm0.39)} + 10^{-(2.06\pm0.44)} + 10^{-(0.04\pm0.38)} \\ 1 &= 0.059(0.024/0.141) + 0.023(0.010/0.058) + 0.0087(0.0031/0.024) \\ &\quad + 0.91(0.380/2.188) \end{aligned}$$

The values in parentheses provide the lower and the upper limits based on the logarithmic errors (3σ).

$$100\% = 6(3/14)\% + 2(1/6)\% + 1(0.3/2)\% + 91(38/219)\% \tag{2.74}$$

Since the error limits of the logarithmic results refer to three times the standard error of the mean value (3σ), it might be helpful to rewrite equation 2.74 with only 1σ, as given in equation 2.75:

$$100\% = 6(4/8)\% + 2(1.7/3)\% + 1(0.6/1.2)\% + 91(68/122)\% \tag{2.75}$$

From equations 2.74 and 2.75, it follows that $(GDP{\cdot}H{\cdot}Cu(phen))_{cl}$ occurs only in very low concentration. The dominating isomer of the Cu(phen)(H;GDP) complex is clearly the stacked one, $(GDP{\cdot}H{\cdot}Cu(phen))_{st}$, occurring with a concentration of about 90%.

The same approach can be used to determine the isomeric distribution in the case of the Cu(bpy)(H;GDP) complex. For the intramolecular-stacking microconstant, $k^{Cu(bpy)}_{(GDP{\cdot}H{\cdot}Cu(bpy))_{st}}$, applying equation 2.73 (with M^{2+} = $Cu(bpy)^{2+}$ and $K^{Cu(bpy}_{Cu(bpy)(H;GDP)}$ = 3.94±0.18, Table 2.21, page 112), one obtains:

$$\begin{aligned} k^{Cu(bpy)}_{(GDP{\cdot}H{\cdot}Cu(bpy))_{st}} &= 10^{3.94\pm0.18} - 10^{2.90\pm0.28} - 10^{2.5\pm0.3} - 10^{2.07\pm0.36} \\ &= (8710\pm3610) - (794\pm512) - (316\pm218) - (117\pm97) \\ &= (7483\pm3654) \end{aligned}$$

and thus log $k^{Cu(bpy)}_{(GDP{\cdot}H{\cdot}Cu(bpy))_{st}}$ = 3.87±0.21.

Going through the same procedure as done for the Cu(phen)(H;GDP) complex, one obtains:

$$[M(H;GDP)] = [M{\cdot}GDP{\cdot}H] + [GDP{\cdot}H{\cdot}M] + [(GDP{\cdot}H{\cdot}M)_{cl}] + [(GDP{\cdot}H{\cdot}M)_{st}]$$

$$\begin{aligned} 10^{3.94\pm0.18} &= 10^{2.90\pm0.28} + 10^{2.5\pm0.3} + 10^{2.07\pm0.36} + 10^{3.87\pm0.21} \\ 1 &= 10^{-(1.04\pm0.33)} + 10^{-(1.44\pm0.35)} + 10^{-(1.87\pm0.40)} + 10^{-(0.07\pm0.28)} \\ 1 &= 0.091(0.043/0.195) + 0.036(0.016/0.081) + 0.013(0.0054/0.034) \\ &\quad + 0.85(0.45/1.62) \end{aligned}$$

The values given in brackets provide the lower and the upper limits based on the logarithmic errors (3σ). It is:

$$100\% = 9(4/20)\% + 4(2/8)\% + 1(0.5/3)\% + 85(45/162)\% \qquad (2.76)$$

In equation 2.76 the error limits of the logarithmic results refer to three times the standard error of the mean value (3σ); considering only 1σ, one obtains equation 2.77:

$$100\% = 9(7/12)\% + 4(3/5)\% + 1(1/2)\% + 85(69/106)\% \qquad (2.77)$$

It is evident, that the dominating isomer is the one in which an intramolecular stacking interaction occurs between the bipyridine-aromatic ring of the phosphate-bound Cu(bpy)$^{2+}$ ion and the nucleobase. This isomer occurs in a concentration of about 85%. The *closed* isomer, in which the Cu(bpy)$^{2+}$ ion interacts with the diphosphate group and the N7 of the nucleobase occurs only to a very low extent.

In the Cu(phen)(H;GDP) and Cu(bpy)(H;GDP) complexes, the equilibrium shown in the lower part of Figure 2.30 (page 122) lies to its right hand side, while the formation of a closed isomer (upper equilibrium in the Figure) is in both instances negligible.

What about the Cu(arm)(H;IDP) complexes? It has been shown above that a pure (open) stacking interaction between the aromatic-ring systems of bipyridine or phenanthroline with the purine residue of the nucleotide could not justify the high stability constants measured for these complexes. One is then left with the two equilibria shown in Figure 2.30 on page 122, *i.e.*, the possibility of an intramolecular equilibrium between an *open* and a *closed* form, or that between the *open* isomer, and a stacked one, in which an intramolecular stacking interaction takes place between the aromatic-ring system of the Cu^{2+}-bound arm and the nucleobase, the Cu(arm)$^{2+}$ being phosphate-bound. The stabilities of all the species involved must then be considered.

The open species, (Cu(arm)(IDP·H))$_{\mathrm{op}}$, consists of the two isomers ((arm)Cu·IDP·H), carrying the proton at the terminal β-phosphate group and the Cu(arm)$^{2+}$

ion at N7 of the nucleobase, and (IDP·H·Cu(arm)), where both the proton and the $Cu(arm)^{2+}$ ion sit at the diphosphate residue. Its stability constant, $k^{M}_{(M(IDP\cdot H))_{op}}$, is given by the sum of the stabilities of the two isomers: $k^{M}_{(M(IDP\cdot H))_{op}} = k^{M}_{(M\cdot IDP\cdot H)} + k^{M}_{(IDP\cdot H\cdot M)}$.

An estimation of the micro stability constant of the ((arm)Cu·IDP·H) isomer, $k^{M}_{(M\cdot IDP\cdot H)}$, can be made on the basis of $k^{M}_{(M\cdot GDP\cdot H)}$, as determined for the corresponding Cu(arm)(H;GDP) systems, and of the stability constant determined for the binary (Cu·IDP·H) isomer, $k^{Cu}_{(Cu\cdot IDP\cdot H)}$ (Section 2.5.5 on page 82). It can be assumed that the difference in stability, $\Delta \log k_{Cu(arm)}$, observed for the (Cu(arm)·GDP·H) isomers compared to the corresponding isomer of the binary system, (Cu·GDP·H), is the same for IDP:

$$\begin{aligned}\Delta \log k_{Cu(arm)} &= \log k^{Cu}_{(Cu\cdot GDP\cdot H)} - \log k^{Cu(arm)}_{((arm)Cu\cdot GDP\cdot H)} \\ &= \log k^{Cu}_{(Cu\cdot IDP\cdot H)} - \log k^{Cu(arm)}_{((arm)Cu\cdot IDP\cdot H)} \\ \Delta \log k_{Cu(arm)} &= (3.165\pm0.35) - (2.90\pm0.28) = (0.265\pm0.44)\end{aligned}$$

$\log k^{Cu}_{(Cu\cdot GDP\cdot H)}$ is from Section 2.5.5 on page 82; $\log k^{Cu(arm)}_{((arm)Cu\cdot GDP\cdot H)}$ is taken from above. Despite the large error limit, this value can be used to get an estimation of the stability constant of ((arm)Cu·IDP·H), $\log k^{Cu(arm)}_{((arm)Cu\cdot IDP\cdot H)}$:

$$\log k^{Cu(arm)}_{((arm)Cu\cdot IDP\cdot H)} = (2.76\pm0.51) - (0.265\pm0.44) = 2.495\pm0.67 \simeq 2.50\pm0.67$$

The stability constant of the (IDP·H·Cu(arm)) species can be assumed to be equal to the one of Cu(arm)(H;MePP), as their coordination spheres are identical (see Section 2.6.3 on page 115, and above the discussion on GDP). Hence, one can define:

$$\begin{aligned}\log k^{Cu(arm)}_{(IDP\cdot H\cdot Cu(arm))} &= \log K^{Cu(arm)}_{(Cu(arm)(H;MePP))} \\ &= 2.5\pm0.3 \text{ [177]}\end{aligned}$$

The possibility of an intramolecular equilibrium between the *open* and a *closed* isomer, in which the arm-bound metal ion interacts with both, the diphosphate group and the N7 site at the nucleobase (upper part of Figure 2.30 on page 122), will be considered next. Its stability may be estimated based on $\log k^{Cu}_{(IDP\cdot Cu\cdot H)_{cl}} =$

2.64±0.30 obtained for the corresponding binary macrochelated species, $(IDP{\cdot}Cu{\cdot}H)_{cl}$ (see Section 2.5.5 on page 82). As it has already been recalled (see above), the affinity of Cu^{2+} towards N binding sites is reduced upon coordination to the arm systems [169,182] by −(0.80±0.25) log unit (see above). The estimated micro stability constant for $(IDP{\cdot}H{\cdot}Cu(arm))_{cl}$ amounts then to $\log k^{Cu(arm)}_{(IDP{\cdot}Cu(arm){\cdot}H)_{cl}}$ = (2.64±0.30) − (0.80±0.25) = 1.84±0.39.

Dealing with the data in an analogous way to what was done for the Cu(arm)(H;GDP) complexes, one can rewrite the experimentally determined overall stability constant, $K^{Cu(arm)}_{Cu(arm)(H;IDP)}$, according to equation 2.78, where the contribution of the single isomers is taken into account (M^{2+} = $Cu(arm)^{2+}$; [M·IDP·H] and [IDP·H·M] represent the concentrations of the *open* species):

$$K^{M}_{M(H;IDP)} = \frac{[M{\cdot}IDP{\cdot}H] + [IDP{\cdot}H{\cdot}M] + [(IDP{\cdot}H{\cdot}M)_{cl}] + [(IDP{\cdot}H{\cdot}M)_{st}]}{[M^{2+}][H(IDP)^{2-}]} \tag{2.78}$$

$K^{Cu(arm)}_{Cu(arm)(H;IDP)}$ is actually composed of the four microconstants summarized in equation 2.79:

$$K^{M}_{M(H;IDP)} = k^{M}_{M{\cdot}IDP{\cdot}H} + k^{M}_{IDP{\cdot}H{\cdot}M} + k^{M}_{(IDP{\cdot}H{\cdot}M)_{cl}} + k^{M}_{(IDP{\cdot}H{\cdot}M)_{st}} \tag{2.79}$$

All the micro stability constants that contribute to the value of $K^{Cu(arm)}_{Cu(arm)(H;IDP)}$ have been estimated above, leaving $k^{Cu(arm)}_{(IDP{\cdot}H{\cdot}Cu(arm))_{st}}$ as the only unknown in equation 2.79. It is then possible to calculate it, via equation 2.80:

$$k^{M}_{(IDP{\cdot}H{\cdot}M)_{st}} = K^{M}_{M(H;IDP)} - k^{M}_{M{\cdot}IDP{\cdot}H} - k^{M}_{IDP{\cdot}H{\cdot}M} - k^{M}_{(IDP{\cdot}H{\cdot}M)_{cl}} \tag{2.80}$$

For the Cu(phen)(H;IDP) complex, $\log K^{Cu(phen)}_{Cu(phen)(H;IDP)}$ = 3.95±0.25 (Table 2.21 on page 112), and $k^{Cu(phen)}_{(IDP{\cdot}H{\cdot}Cu(phen))_{st}}$ is then given by:

$$\begin{aligned} k^{Cu(phen)}_{(IDP{\cdot}H{\cdot}Cu(phen))_{st}} &= 10^{3.95\pm0.25} - 10^{2.50\pm0.67} - 10^{2.5\pm0.3} - 10^{1.84\pm0.39} \\ &= (8913\pm5130) - (316\pm488) - (316\pm218) - (69\pm62) \\ &= (8212\pm5158) \end{aligned}$$

and $\log k^{Cu(phen)}_{(IDP{\cdot}H{\cdot}Cu(phen))_{st}}$ = 3.91±0.27.

From the definition of $K^{\mathrm{M}}_{\mathrm{M(H;IDP)}}$,

$$K^{\mathrm{M}}_{\mathrm{M(H;IDP)}} = [\mathrm{M(H;IDP)}]/[\mathrm{M}^{2+}][(\mathrm{H;IDP})^{2-}]$$

and setting its right-hand side equal to the one in equation 2.78, one obtains:

$$[\mathrm{M(H;IDP)}] = [\mathrm{M{\cdot}IDP{\cdot}H}] + [\mathrm{IDP{\cdot}H{\cdot}M}] + [(\mathrm{IDP{\cdot}H{\cdot}M})_{\mathrm{cl}}] + [(\mathrm{IDP{\cdot}H{\cdot}M})_{\mathrm{st}}]$$

$$\begin{aligned} 10^{3.95\pm0.25} &= 10^{2.50\pm0.67} + 10^{2.5\pm0.3} + 10^{1.84\pm0.39} + 10^{3.91\pm0.27} \\ 1 &= 10^{-(1.45\pm0.72)} + 10^{-(1.45\pm0.39)} + 10^{-(2.11\pm0.46)} + 10^{-(0.04\pm0.37)} \\ 1 &= 0.035(0.0068/0.186) + 0.035(0.014/0.087) + 0.0078(0.0027/0.022) \\ &\quad + 0.91(0.39/2.14) \end{aligned}$$

again, the values given in parentheses provide the lower and the upper limits based on the logarithmic errors (3σ). it follows:

$$100\% = 4(1/19)\% + 4(1/9)\% + 1(0.3/2)\% + 91(39/214)\% \qquad (2.81)$$

Since all error limits refer to three times the standard error of the mean value (3σ), it might be helpful to rewrite equation 2.81 with only 1σ, as given in equation 2.82:

$$100\% = 4(2/6)\% + 4(3/5)\% + 1(0.5/1.1)\% + 91(69/121)\% \qquad (2.82)$$

From equations 2.81 and 2.82, follows that $(\mathrm{IDP{\cdot}H{\cdot}Cu(phen)})_{\mathrm{cl}}$ occurs only in very low concentration. Analogously to what was observed for the Cu(phen)(H;GDP) complex, the dominating isomer of the Cu(phen)(H;IDP) complex is the stacked one, $(\mathrm{IDP{\cdot}H{\cdot}Cu(phen)})_{\mathrm{st}}$, occurring with a concentration of about 90%.

$K^{\mathrm{Cu(bpy)}}_{\mathrm{Cu(bpy)(H;IDP)}}$ can be analysed in an analogous way, and the value for $k^{\mathrm{Cu(bpy)}}_{(\mathrm{IDP{\cdot}H{\cdot}Cu(bpy)})_{\mathrm{st}}}$ can be determined applying equation 2.80 (with $\log K^{\mathrm{Cu(bpy)}}_{\mathrm{Cu(bpy)(H;IDP)}}$ = 3.8±0.2; Table 2.21, page 112):

$$\begin{aligned} k^{\mathrm{Cu(bpy)}}_{(\mathrm{IDP{\cdot}H{\cdot}Cu(bpy)})_{\mathrm{st}}} &= 10^{3.8\pm0.2} - 10^{2.50\pm0.67} - 10^{2.5\pm0.3} - 10^{1.84\pm0.39} \\ &= (5609\pm2955) \end{aligned}$$

and $\log k^{\mathrm{Cu(bpy)}}_{(\mathrm{IDP{\cdot}H{\cdot}Cu(bpy)})_{\mathrm{st}}}$ = 3.75±0.23.

Again considering the definition of $K^{\mathrm{M}}_{\mathrm{M(H;IDP)}}$,

$$K^{\mathrm{M}}_{\mathrm{M(H;IDP)}} = [\mathrm{M(H;IDP)}]/[\mathrm{M}^{2+}][(\mathrm{H;IDP})^{2-}]$$

and setting its right-hand side equal to the one in equation 2.78 (page 129), one obtains:

$$[\mathrm{M(H;IDP)}] = [\mathrm{M{\cdot}IDP{\cdot}H}] + [\mathrm{IDP{\cdot}H{\cdot}M}] + [(\mathrm{IDP{\cdot}H{\cdot}M})_{\mathrm{cl}}] + [(\mathrm{IDP{\cdot}H{\cdot}M})_{\mathrm{st}}]$$

$$10^{3.8\pm0.2} = 10^{2.50\pm0.67} + 10^{2.5\pm0.3} + 10^{1.84\pm0.39} + 10^{3.75\pm0.23}$$

$$1 = 10^{-(1.3\pm0.7)} + 10^{-(1.3\pm0.4)} + 10^{-(1.96\pm0.44)} + 10^{-(0.05\pm0.30)}$$

$$1 = 0.050(0.010/0.251) + 0.050(0.020/0.126) + 0.011(0.0040/0.030) + 0.89(0.45/1.78)$$

and:

$$100\% = 5(1/25)\% + 5(2/13)\% + 1(0.4/3)\% + 89(45/173)\% \qquad (2.83)$$

Since all error limits of the logarithmic results given in brackets refer to three times the standard error of the mean value (3σ), it might be helpful to rewrite equation 2.83 with only 1σ, as given in equation 2.84:

$$100\% = 5(3/9)\% + 5(4/7)\% + 1(0.8/1.5)\% + 89(71/112)\% \qquad (2.84)$$

From equations 2.83 and 2.84, follows that $(\mathrm{IDP{\cdot}H{\cdot}Cu(bpy)})_{\mathrm{cl}}$ occurs only in very low concentration. Analogously to what was observed for the Cu(phen)(H;IDP) complex, one of the isomers strongly dominates, and this is the one in which an intramolecular stack occurs between the bipyridine aromatic ring and the nucleobase, $(\mathrm{IDP{\cdot}H{\cdot}Cu(bpy)})_{\mathrm{st}}$, occurring with a concentration of about 90%.

The percentages of stacked species formed in the six Cu(arm)(H;NDP) complexes studied are identical within the error limits, as it can easily be seen in the last column of Table 2.23.

Table 2.23: Stability constants of the stacked isomers formed in monoprotonated ternary M(H;NDP) complexes (M^{2+} = $Cu(arm)^{2+}$), and percentages at which these species occur in equilibrium in aqueous solution (25 °C; *I* = 0.1 M, $NaNO_3$)[a]

M(H;NDP)	log $k^{M}_{(NDP\cdot M\cdot H)_{st}}$	% $(NDP\cdot M\cdot H)_{st}$
Cu(bpy)(H;ADP)	3.59±0.06	92± 2
Cu(phen)(H;ADP)	3.72±0.12	94± 1
Cu(bpy)(H;GDP)	3.87±0.07	85±18
Cu(phen)(H;GDP)	4.09±0.09	91±27
Cu(bpy)(H;IDP)	3.75±0.08	89±21
Cu(phen)(H;IDP)	3.91±0.09	91±26

[a] The error limits given are *one time* the standard error of the mean value or the sum of the probable systematic errors, whichever is larger.

2.6.5 Calculation of the formation degree of the intramolecular stack in the $Cu(arm)(NDP)^{-}$ complexes

In Section 2.6.2 it was shown that the mixed ligand complexes $Cu(arm)(NDP)^{-}$ (NDP^{3-} = ADP^{3-}, IDP^{3-}, or GDP^{3-}) possess an increased stability and that an intramolecular equilibrium between an open and a stacked form actually exists. This means, a stacked isomer is formed, a schematic and simplified structure of the $Cu(phen)(ADP)^{-}$ species is shown in Figure 2.31.

The stability constants log $K^{Cu}_{Cu(NDP)}$ (from Section 2.5.3 on page 74, and from Section 2.5.6 on page 94) and log $K^{Cu(arm)}_{Cu(arm)(NDP)}$ *versus* p$K^{H}_{H(NDP)}$ are plotted in Figure 2.32 (page 134), together with the reference line derived from equation 2.86 (page 135). The data points for the binary $Cu(NDP)^{-}$ and the ternary $Cu(arm)(NDP)^{-}$

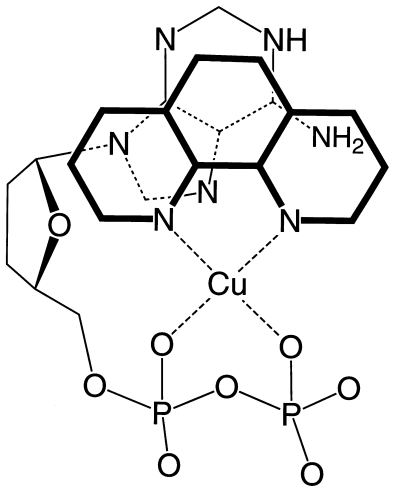

Figure 2.31: Schematic and simplified structure of the species with an intramolecular stack for Cu(phen)(ADP)$^-$ [154]. In solution certainly a whole series of stacked complexes occur in which the orientation of the aromatic-ring planes toward each other differs somewhat; of course, the expression Cu(arm)(ADP)$^-_{\mathrm{st}}$ and the quantifications given for it (Table 2.26 on page 139) encompass all of these species.

complexes shown in the Figure, are far above the reference line, proving an increased complex stability in all these instances. This means [124,170] that aside from the diphosphate-Cu^{2+} coordination further interactions occur within the complexes, namely, a N7 interaction of the phosphate-bound Cu^{2+} in the binary Cu(NDP)$^-$ complexes (see Section 2.5.1 on page 65, and Section 2.5.6, page 94), and stack formation in the ternary Cu(arm)(NDP)$^-$ systems, as it will be shown in detail below.

Moreover, from Figure 2.32, it is evident that the Cu(arm)(NDP)$^-$ complexes are considerably more stable than the binary Cu(NDP)$^-$ ones. The stability of all these complexes is overwhelmingly determined by the metal ion affinity of the diphosphate residue and the observed stability enhancement must result from an additional interaction with the nucleobase residue. For principle reasons there are two possibilities for further interactions in the open isomers Cu(arm)(NDP)$^-_{\mathrm{op}}$: (*i*) A macrochelate could be formed with N7, *i.e.*, Cu(arm) (NDP)$^-_{\mathrm{cl/N7}}$, as is known for the binary Cu(NDP)$^-$ complexes.

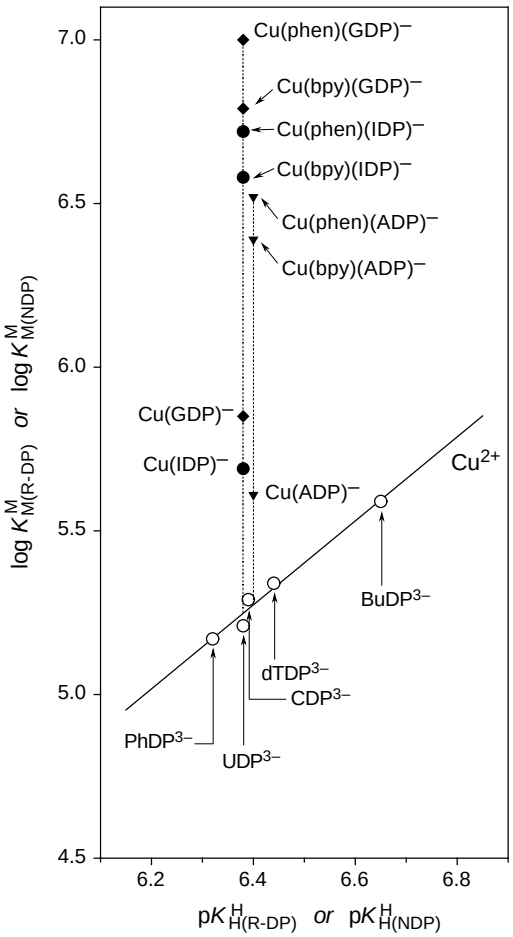

Figure 2.32: Evidence for an increased stability of the binary Cu(ADP)$^{-}$, Cu(IDP)$^{-}$, and Cu(GDP)$^{-}$ and of the ternary Cu(bpy)(ADP)$^{-}$, Cu(phen)(ADP)$^{-}$, Cu(bpy)(IDP)$^{-}$, Cu(phen)(IDP)$^{-}$, Cu(bpy)(GDP)$^{-}$, and Cu(phen)(GDP)$^{-}$ complexes based on the relationship between log $K^{\mathrm{M}}_{\mathrm{M(NDP)}}$ (where M^{2+} = Cu^{2+}, $Cu(bpy)^{2+}$, or $Cu(phen)^{2+}$) or log $K^{\mathrm{Cu}}_{\mathrm{Cu(R-DP)}}$ and p$K^{\mathrm{H}}_{\mathrm{H(NDP)}}$ or p$K^{\mathrm{H}}_{\mathrm{H(R-DP)}}$ in aqueous solution at 25 °C and I = 0.1 M ($NaNO_3$). The plotted data for the binary NDP complexes are from Table 2.11 (page 77) and from Table 2.13 (page 83); the ones for the ternary systems, are from Table 2.21 on page 112. The reference line (see equation 2.86) represents the log $K^{\mathrm{Cu}}_{\mathrm{Cu(R-DP)}}$ *versus* p$K^{\mathrm{H}}_{\mathrm{H(R-DP)}}$ relationship for the binary Cu(R-DP)$^{-}$ complexes, where R-DP^{3-} = phenyl diphosphate (PhDP^{3-}), uridine 5′-diphosphate (UDP^{3-}), cytidine 5′-diphosphate (CDP^{3-}), thymidine [= 1-(2-deoxy-β-D-ribofuranosyl)thymine] 5′-diphosphate (dTDP^{3-}) and *n*-butyl diphosphate (BuDP^{3-}) (from left to right). The least-squares line was calculated [106] through the indicated five data sets; the corresponding equilibrium constants are listed in Tables 1 and 3 of [106] (25 °C; I = 0.1 M, $NaNO_3$).

(*ii*) The other possibility is the formation of an intramolecular stack, $Cu(arm)(NDP)^{-}_{st}$, as it has been shown to occur in the ternary Cu(arm)(H;NDP) systems (see Table 2.22 on page 120).

Based on the above considerations, the following equilibrium scheme may be written:

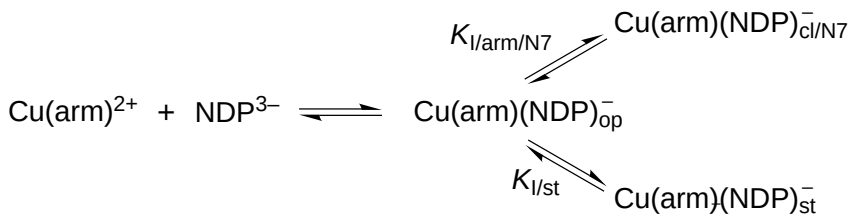

At this point it needs to be emphasized that already the $Cu(arm)(NDP)^{-}_{op}$ isomers have an increased stability, compared to the corresponding $Cu(NDP)^{-}_{op}$, due to the arm/O,O ligand combination [166,172–177]; however, this effect is well quantified by equations 2.59 and 2.60 (page 114) via the $Cu(arm)^{2+}$/$MePP^{3-}$ systems, as already discussed in Section 2.6.2 on page 113. Hence, the calculated stability of the open complex, $Cu(arm)(NDP)^{-}_{op}$, is given by equation 2.85:

$$\log K^{\mathrm{Cu(arm)}}_{\mathrm{Cu(arm)(NDP)_{op}}} = \log K^{\mathrm{Cu}}_{\mathrm{Cu(NDP)_{op}}} + \Delta \log K_{\mathrm{Cu/arm/MePP}} \qquad (2.85)$$

The stability constant of the $Cu(NDP)^{-}_{op}$ complex can be calculated from the straight-line correlation that was established [106] for the $\log K^{\mathrm{Cu}}_{\mathrm{Cu(R-DP)}}$ *versus* $\mathrm{p}K^{\mathrm{H}}_{\mathrm{H(R-DP)}}$ plot (equation 2.86, see Figure 2.32), where $R-DP^{3-}$ represents diphosphate-monoester ligands in which the residue R is unable to interact with Cu^{2+}:

$$\log K^{\mathrm{Cu}}_{\mathrm{Cu(R-DP)}} = 1.283 \times \mathrm{p}K^{\mathrm{H}}_{\mathrm{H(R-DP)}} - 2.939 \qquad (2.86)$$

The error limits of log stability constants calculated with given $\mathrm{p}K^{\mathrm{H}}_{\mathrm{H(NDP)}}$ values and equation 2.86, are 0.04 (3σ) in the $\mathrm{p}K_a$ range 6.2–6.7. The $\mathrm{p}K^{\mathrm{H}}_{\mathrm{H(NDP)}}$ values for ADP, GDP, and IDP, are listed in Table 2.2 on page 28.

Values for $\Delta \log K_{\mathrm{Cu/arm/MePP}}$ are given in equations 2.59 and 2.60 on page 114.

Consequently, the actual (*actl*) stability increase due to any intramolecular interaction with the nucleobase residue in the ternary Cu(arm)(NDP)$^-$ complexes is given by:

$$\log \Delta_{\mathrm{Cu/arm/NDP/}\textit{actl}} = \log K^{\mathrm{Cu(arm)}}_{\mathrm{Cu(arm)(NDP)}} - \log K^{\mathrm{Cu(arm)}}_{\mathrm{Cu(arm)(NDP)_{op}}}$$
$$= \log \Delta_{\mathrm{Cu/arm/NDP}} - \Delta \log K_{\mathrm{Cu/arm/MePP}}$$

where $\log \Delta_{\mathrm{Cu/arm/NDP}} = \log K^{\mathrm{Cu(arm)}}_{\mathrm{Cu(arm)(NDP)}} - \log K^{\mathrm{Cu}}_{\mathrm{Cu(NDP)_{op}}}$

The results for $\log \Delta_{\mathrm{Cu/arm/NDP}}$ are listed in column 4 of Table 2.24, while the values calculated for $\log \Delta_{\mathrm{Cu/arm/NDP/}\textit{actl}}$ are summarized, with the data they are based on, in Table 2.25 on page 138.

Table 2.24: Proof of an enhanced stability of the Cu(arm)(NDP)$^-$ complexes in aqueous solution, based on the positive values obtained for $\log \Delta_{\mathrm{Cu/arm/NDP}}$ (25 °C; I = 0.1 M, $NaNO_3$) (see also Figure 2.32)[a]

Cu(arm)(NDP)$^-$	$\log K^{\mathrm{Cu(arm)}}_{\mathrm{Cu(arm)(NDP)}}$ [b]	$\log K^{\mathrm{Cu}}_{\mathrm{Cu(NDP)_{op}}}$ [c]	$\log \Delta_{\mathrm{Cu/arm/NDP}}$
Cu(bpy)(ADP)$^-$	6.39±0.03	5.27±0.04	1.12±0.05
Cu(phen)(ADP)$^-$	6.52±0.04	5.27±0.04	1.25±0.06
Cu(bpy)(GDP)$^-$	6.79±0.05	5.25±0.04	1.54±0.06
Cu(phen)(GDP)$^-$	7.00±0.05	5.25±0.04	1.75±0.06
Cu(bpy)(IDP)$^-$	6.58±0.04	5.25±0.04	1.33±0.06
Cu(phen)(IDP)$^-$	6.72±0.03	5.25±0.04	1.47±0.05

[a] The error limits given are *three times* the standard error of the mean value or the sum of the probable systematic errors, whichever is larger. [b] Experimentally determined values; from column 4 of Table 2.21 on page 112. [c] Calculated with equation 2.86 and $pK^{\mathrm{H}}_{\mathrm{H(ADP)}}$ = 6.40±0.01, $pK^{\mathrm{H}}_{\mathrm{H(GDP)}}$ = 6.38±0.01, and $pK^{\mathrm{H}}_{\mathrm{H(IDP)}}$ = 6.38±0.02 (Table 2.2 on page 28).

The question which needs to be answered next is: Are both equilibrium branches of the scheme shown on page 135, the one involving macrochelate formation with

the N7 site, and the one describing a stacking interaction between the nucleobase and the aromatic ring of bpy or phen, of comparable importance? In Section 2.6.3 (page 115) it was shown that a N7 interaction of diphosphate-coordinated Cu(arm)$^{2+}$ is inhibited by $-(0.80\pm0.25)$ log unit compared with the same interaction of Cu^{2+} (see also [169]). In fact, this value is an upper limit since the steric inhibition is actually more pronounced [182]. In any case, the enhanced stability of the binary Cu(NDP)$^{-}$ complexes is solely due to macrochelate formation (see Section 2.5.1 on page 65, and Section 2.5.6 on page 94), and therefore, the expected stability of the ternary $Cu(arm)(NDP)^{-}_{cl/N7}$ complexes can be calculated as follows, under the assumption that only macrochelate formation (and no stacking) occurs:

$$\log K^{\mathrm{Cu(arm)}}_{\mathrm{Cu(arm)(NDP)_{cl/N7}}} = \log K^{\mathrm{Cu}}_{\mathrm{Cu(NDP)}} + \Delta \log K_{\mathrm{Cu/arm/MePP}} - (0.80\pm0.25)$$

The second term on the right-hand side, $\Delta \log K_{\mathrm{Cu/arm/MePP}}$, appears since the arm/O,O ligand combination (the average of equations 2.59 and 2.60 on page 114 is used) leads to an enhanced complex stability (see above and in Section 2.5.1) which must be taken into account in the calculation for $K^{\mathrm{Cu(arm)}}_{\mathrm{Cu(arm)(NDP)_{cl/N7}}}$.

Applying the above-given equation to the experimental data of the Cu(arm)(NDP)$^{-}$ complexes studied, one obtains:

$$\log K^{\mathrm{Cu(arm)}}_{\mathrm{Cu(arm)(ADP)_{cl/N7}}} = (5.61\pm0.03) + (0.44\pm0.06) - (0.80\pm0.25)$$
$$= 5.25\pm0.26$$

$$\log K^{\mathrm{Cu(arm)}}_{\mathrm{Cu(arm)(GDP)_{cl/N7}}} = (5.85\pm0.04) + (0.44\pm0.06) - (0.80\pm0.25)$$
$$= 5.49\pm0.26$$

$$\log K^{\mathrm{Cu(arm)}}_{\mathrm{Cu(arm)(IDP)_{cl/N7}}} = (5.69\pm0.04) + (0.44\pm0.06) - (0.80\pm0.25)$$
$$= 5.33\pm0.26$$

The above results show that the calculated stability for $Cu(arm)(NDP)^{-}_{cl/N7}$ is at least 1.1 log units less stable than the stability constants measured for the ternary Cu(arm)(NDP)$^{-}$ complexes (see Table 2.21 on page 112); hence, one may conclude that the upper branch of the equilibrium scheme on page 135 does not contribute

significantly to the overall stability of these complexes. In other words, the concentration of Cu(arm)$(NDP)^{-}_{cl/N7}$ is negligible. Therefore, only the lower branch of the equilibrium scheme is left, and this then means that the total actual stability increase as defined by log $\Delta_{Cu/arm/ADP/actl}$ (see Table 2.25, column 4) has to be attributed to the intramolecular stack formation according to the stacking equilibrium as shown in Figure 2.28 (page 115).

Table 2.25: Quantification of the stability increase of the ternary $M(NDP)^{-}$ complexes (M^{2+} = $Cu(arm)^{2+}$), which is *actually* (*actl*) due to an interaction involving the nucleobase moiety of NDP^{3-} in aqueous solution (25 °C; *I* = 0.1 M, $NaNO_3$)[a]

$M(NDP)^{-}$	log $\Delta_{M/NDP}$[b]	Δ log $K_{M/MePP}$[c]	log $\Delta_{M/NDP/actl}$
Cu(bpy)$(ADP)^{-}$	1.12±0.05	0.42±0.05	0.70±0.07
Cu(phen)$(ADP)^{-}$	1.25±0.06	0.45±0.05	0.80±0.08
Cu(bpy)$(GDP)^{-}$	1.54±0.06	0.42±0.05	1.12±0.08
Cu(phen)$(GDP)^{-}$	1.75±0.06	0.45±0.05	1.30±0.08
Cu(bpy)$(IDP)^{-}$	1.33±0.06	0.42±0.05	0.91±0.08
Cu(phen)$(IDP)^{-}$	1.47±0.05	0.45±0.05	1.02±0.07

[a] The error limits given are *three times* the standard error of the mean value or the sum of the probable systematic errors, whichever is larger. [b] From Table 2.24. [c] From equations 2.59 and 2.60 on page 114 [177].

The values for log $\Delta_{Cu/arm/NDP/actl}$ allow a quantification of the position of this equilibrium by application of equation 2.87 [167,181,185], where log Δ represents log $\Delta_{Cu/arm/NDP/actl}$:

$$K_{I/st} = [Cu(arm)(NDP)^{-}_{st}]/[Cu(arm)(NDP)^{-}_{op}] = 10^{\log \Delta} - 1 \qquad (2.87)$$

Once $K_{I/st}$ is known, the percentage of the stacked isomer in the equilibrium can be calculated with equation 2.88, in analogy to equation 2.70. From the results assembled in Table 2.26 it is evident that the formation degree of the stacked isomers is large.

$$\% \, \mathrm{Cu(arm)(NDP)_{st}} = 100 \cdot K_{\mathrm{I/st}}/(1 + K_{\mathrm{I/st}}) \qquad (2.88)$$

Table 2.26: Extent of intramolecular stack formation in ternary Cu(arm)(NDP)$^-$ complexes as calculated from the stability enhancement, log Δ (= log $\Delta_{\mathrm{Cu/arm/ADP/}actl}$). The resulting intramolecular dimensionless equilibrium constant $K_{\mathrm{I/st}}$ and the percentage of the stacked Cu(arm)(NDP)$^-_{\mathrm{st}}$ species quantify the situation in aqueous solution (25 °C; I = 0.1 M, $NaNO_3$)[a]

Cu(arm)(NDP)$^-$	log Δ[b]	$K_{\mathrm{I/st}}$	% Cu(arm)(NDP)$^-_{\mathrm{st}}$
Cu(bpy)(ADP)$^-$	0.70±0.07	4.01±0.81	80±3
Cu(phen)(ADP)$^-$	0.80±0.08	5.31±1.16	84±3
Cu(bpy)(GDP)$^-$	1.12±0.08	12.18±2.43	92±1
Cu(phen)(GDP)$^-$	1.30±0.08	18.95±3.67	95±1
Cu(bpy)(IDP)$^-$	0.91±0.08	7.12±1.50	88±2
Cu(phen)(IDP)$^-$	1.02±0.07	9.47±1.69	90±2

[a] The error limits given are *three times* the standard error of the mean value or the sum of the probable systematic errors, whichever is larger. The error limits (3σ) of the derived data were calculated according to the error propagation after Gauss. [b] From column 4 of Table 2.25 on page 138.

2.6.6 Some conclusions on the Cu(arm)(H;NDP) and Cu(arm)(NDP)$^-$ complexes studied here

From a coordination chemistry point of view the evaluation of the protonated complexes regarding the location of the metal ion and the proton was an interesting challenge and the determination of the various intramolecular equilibria is revealing in various ways. It has been shown that in all the Cu(arm)(H;NDP) complexes, the proton is located at the terminal β-phosphate group. In the Cu(arm)(H;ADP), and, at least to some extent, in the Cu(arm)(H;IDP) and Cu(arm)(H;GDP) complexes, the metal ion is located at the diphosphate residue as well as the proton. This result is of general importance because it demonstrates that several positively

charged species can be accommodated at the diphosphate group; this is of special interest with regard to the metal ion facilitated hydrolysis or group transfer reactions [41,47,186,187] in which this residue is involved [47,144]. However, the pK_a values of all these monoprotonated complexes are such that these species are of no relevance in the usual physiological pH range though in certain cell organelles with pH about 5.5 [188,189] they could play a role [146], especially if the local intrinsic dielectric constant [170] should be low [80–82] because then the tendency of phosphate groups to hold a proton increases [58,59].

That intramolecular stacks between the aromatic rings of arm and the purine residue of ADP, IDP, and GDP can be formed not only in the Cu(arm)(NDP)$^-$ complexes but also in their monoprotonated Cu(arm)(H;NDP) species, where the proton is at the terminal β-phosphate group, is an interesting observation though not a big surprise; indeed, the stacking tendency of the nucleobase residue remains practically unaffected by the phosphate protonation (*cf.* Table 2.27). Of considerably more interest is a comparison of the stacking tendency of NMP^{2-}, NDP^{3-}, and NTP^{4-} (= Nu) in M(arm)(Nu) complexes; to this end the results summarized in Tables 2.27 and 2.28 were collected.

Comparison of the data gathered in the two Tables reveals that the length of the phosphate residue has little effect on the formation degree of the intramolecular stacks; of course, the absolute stabilities of the complexes differ significantly [58, 59,106], but the position of the intramolecular-stacking equilibria is very similar. If the K_{I} values of the Cu(phen)(Nu) complexes are compared to the ones of the Cu(bpy)(Nu) systems (column 3 of Table 2.27) the tendency becomes evident that stack formation in the Cu(phen)(Nu) complexes is slightly favored over that in the Cu(bpy)(Nu) complexes; considering the structures of phen and bpy (Figure 2.27 on page 110) this is easily understandable. The same applies to the Cu(arm)(H;Nu) complexes. The values of $K_{\mathrm{I/st}}$ determined for these systems, despite the in some instances large error limits, reflect the expected trend: the larger phen is able to stack somewhat better with the purine residue than bpy.

Table 2.27: Comparison of the extent of intramolecular stack formation in ternary Cu(arm)(Pu) complexes (Pu = purine-nucleotide) as calculated from stability constants determined by potentiometric pH titrations (aq. sol.; 25 °C; I = 0.1 M, $NaNO_3$). The stability enhancements, log Δ, the intramolecular equilibrium constants, $K_{\mathrm{I/st}}$ (see equation 2.87), and the percentages of the stacked species (see equation 2.88 on page 139) are listed[a]

Cu(arm)(Pu)	log Δ	$K_{\mathrm{I/st}}$	% Cu(arm)(Pu)$_{\mathrm{st}}$	ref.
Cu(bpy)(AMP)	0.73±0.08	4.37±1.02	81± 4	[167]
Cu(phen)(AMP)	0.99±0.08	8.77±1.81	90± 2	[167]
Cu(bpy)(ADP)$^-$	0.70±0.07	4.01±0.81	80± 3	[154]
Cu(phen)(ADP)$^-$	0.80±0.08	5.31±1.16	84± 3	[154]
Cu(bpy)(H;ADP)	1.12±0.30	12.2±9.2	92± 5	[154]
Cu(phen)(H;ADP)	1.25±0.32	16.8±13.1	94± 4	[154]
Cu(bpy)(ATP)$^{2-}$	0.84±0.15	5.92±2.39	86± 5	[67,101]
Cu(phen)(ATP)$^{2-}$	1.07±0.15	10.7±4.1	91± 3	[67,101]
Cu(bpy)(H;ATP)$^-$	0.45±0.22	1.82±1.43	65±18	[67,101]
Cu(phen)(H;ATP)$^-$	0.78±0.24	5.03±3.33	83± 9	[67,101]
Cu(bpy)(GMP)	0.82±0.08	5.61±1.25	85± 3	[168]
Cu(bpy)(GDP)$^-$	1.12±0.08	12.18±2.43	92± 1	*b*
Cu(phen)(GDP)$^-$	1.30±0.08	18.95±3.67	95± 1	*b*
Cu(bpy)(H;GDP)	1.04±0.32	10.0±8.2	91± 7	*c*
Cu(phen)(H;GDP)	1.23±0.38	16.0±14.7	94± 5	*c*
Cu(bpy)(IMP)	0.56±0.08	2.63±0.69	72± 5	[168]
Cu(bpy)(IDP)$^-$	0.91±0.08	7.12±1.50	88± 2	*b*
Cu(phen)(IDP)$^-$	1.02±0.07	9.47±1.69	90± 2	*b*
Cu(bpy)(H;IDP)	1.30±0.45	19.0±20.5	95± 5	*c*
Cu(phen)(H;IDP)	1.45±0.47	27.2±30.6	96± 4	*c*

[a] The error limits given are *three times* the standard error of the mean value or the sum of the probable systematic errors, whichever is larger. The error limits (3σ) of the derived data were calculated according to the error propagation after Gauss. [b] From Table 2.26 on page 139. [c] From Table 2.22 on page 120.

Such a tendency does not exist in the Cu(arm)(Py) complexes, where Py = UMP^{2-}, UDP^{3-} or UTP^{4-} (Table 2.28); since the uracil residue consists only of a single ring which may stack with bpy as well as with phen. However, that the stacking tendency of the one-ring uracil residue is considerably smaller than that of the two-ring purine residues is clearly borne out from a comparison of the data collected in the two Tables.

Table 2.28: Comparison of the extent of intramolecular stack formation in ternary Cu(arm)(Py) complexes (Py = pyrimidine-nucleotide) as calculated from stability constants determined by potentiometric pH titrations (aq. sol.; 25 °C; I = 0.1 M, $NaNO_3$). The stability enhancements, log Δ, $K_{\mathrm{I/st}}$ (see equation 2.87) and the percentages of the stacked species (see equation 2.88 on page 139) are listed[a]

Cu(arm)(Py)	log Δ	$K_{\mathrm{I/st}}$	% Cu(arm)(Py)$_{\mathrm{st}}$	ref.
Cu(bpy)(UMP)	0.23±0.07	0.70±0.26	41± 9	[190]
Cu(phen)(UMP)	0.33±0.07	1.14±0.34	53± 7	[190]
Cu(bpy)$(UDP)^{-}$	0.36±0.10	1.29±0.54	56±10	[87]
Cu(phen)$(UDP)^{-}$	0.29±0.10	0.95±0.46	49±12	[87]
Cu(bpy)$(UTP)^{2-}$	0.45±0.22	1.82±1.43	65±18	[67,101]
Cu(phen)$(UTP)^{2-}$	0.46±0.22	1.88±1.46	65±18	[67,101]

[a] The error limits given are *three times* the standard error of the mean value or the sum of the probable systematic errors, whichever is larger. The error limits (3σ) of the derived data were calculated according to the error propagation after Gauss.

To conclude, the most interesting result of this study is most probably the fact that the stacking tendency of a nucleobase moiety in a nucleotide complex mainly depends on the nature of the nucleobase (see Tables 2.27 and 2.28). However, the relevance of this kind of adduct formation for recognition reactions in nature is evident; e.g., in protein-nucleotide/nucleic acid interactions the role of bpy or phen may be taken over by the phenyl or indole moieties of phenylalanyl or tryptophanyl residues, respectively.

2.7 Influence of a decreasing solvent polarity on the stability of the Cu^{2+} complexes formed with GDP

The influence of 1,4-dioxane on the complex equilibria involving GDP and Cu^{2+} has been determined. The acidity constants of $H_2(GDP)^-$ and the stability constants of the binary Cu(H;GDP) and $Cu(GDP)^-$ complexes have been measured by potentiometric pH titrations in water (see Section 2.5.4 on page 80), as well as in 30 and 50% (v/v) dioxane-water solutions.

There is good evidence that the equivalent solution dielectric constant is reduced at the surface of proteins and in the active-site cavities of enzymes [82], and that complex equilibria are influenced by changing the solvent polarity [84,101,114, 172,191,192]. It is therefore interesting to study the influence of a reduced solvent polarity on the stability and structure of a nucleotide complex.

The polarity of an aqueous solution may be reduced by the addition of a miscible organic solvent, e.g. ethanol or 1,4-dioxane, and the latter one was used here.

The collected results were used to determine the position of the intramolecular equilibrium already shown in Figure 2.9 and given here again in Figure 2.33.

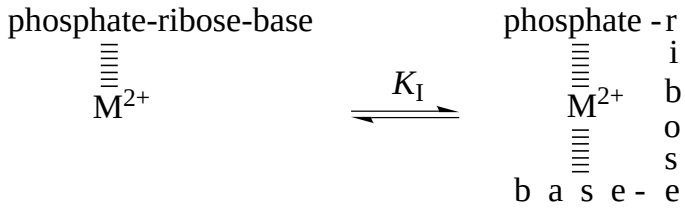

Figure 2.33: Schematic representation of the equilibrium between an *open* and a *closed* isomer. In the latter, the phosphate-bound metal ion interacts with N7 at the nucleobase, forming an intramolecular macrochelate.

To make sure that the properties of the monomeric species were indeed studied, all potentiometric pH titrations (25 °C; I = 0.1 M, $NaNO_3$) were carried out at nucleotide concentrations of 0.6 mM. In water, under these conditions self-stacking of

GDP is negligible [74]. Organic solvents inhibit the formation of unbridged stacking adducts [192–194]. Moreover, it has been proven [101], that addition of dioxane to an aqueous solution considerably inhibits the self-stacking tendency of 2,2′-bipyridine and 1,10-phenanthroline. In water the self-stacking tendency of GDP is considerably smaller than that of bpy or phen [74,101]. It therefore appears to be safe to assume that the addition of dioxane to an aqueous solution of GDP will at least not favour its self-association.

2.7.1 Equilibrium constants measured

The equilibrium constants are defined according to equations 2.89 to 2.93. In the pH range 2.5–11, the experimental data for H_2GDP^- may be completely described by the following deprotonation equilibria and their acidity constants (equations 2.89–2.91), in all solvents employed.

$$\mathrm{H_2(GDP)^-} \rightleftharpoons \mathrm{H(GDP)^{2-} + H^+}$$
$$K^{\mathrm{H}}_{\mathrm{H_2(GDP)}} = [\mathrm{H(GDP)^{2-}}][\mathrm{H^+}]/[\mathrm{H_2(GDP)^-}] \tag{2.89}$$

$$\mathrm{H(GDP)^{2-}} \rightleftharpoons \mathrm{GDP^{3-} + H^+}$$
$$K^{\mathrm{H}}_{\mathrm{H(GDP)}} = [\mathrm{GDP^{3-}}][\mathrm{H^+}]/[\mathrm{H(GDP)^{2-}}] \tag{2.90}$$

$$\mathrm{GDP^{3-}} \rightleftharpoons \mathrm{(GDP-H)^{4-} + H^+}$$
$$K^{\mathrm{H}}_{\mathrm{GDP}} = [\mathrm{(GDP-H)^{4-}}][\mathrm{H^+}]/[\mathrm{GDP^{3-}}] \tag{2.91}$$

The measured acidity constants are listed in Table 2.29 (page 147), together with some related data taken from the literature [84,89,101] and used for comparison.

The experimental data of the potentiometric pH titrations for the Cu^{2+}/GDP 1:1 system are completely described in the pH range below hydroxo complex formation by the stability constants defined in equations 2.92 and 2.93. The results are listed in columns 4 and 5 of Table 2.30 on page 151:

$$\mathrm{Cu^{2+} + H(GDP)^{2-}} \rightleftharpoons \mathrm{Cu(H;GDP)}$$

$$K^{\mathrm{Cu}}_{\mathrm{Cu(H;GDP)}} = [\mathrm{Cu(H;GDP)}]/[\mathrm{Cu}^{2+}][\mathrm{H(GDP)}^{2-}] \tag{2.92}$$

$$\mathrm{Cu}^{2+} + \mathrm{GDP}^{3-} \rightleftharpoons \mathrm{Cu(GDP)}^{-}$$

$$K^{\mathrm{Cu}}_{\mathrm{Cu(GDP)}} = [\mathrm{Cu(GDP)}]/[\mathrm{Cu}^{2+}][\mathrm{GDP}^{3-}] \tag{2.93}$$

The acidity constant of the equilibrium describing the loss of the proton from the Cu(H;GDP) complex, $K^{\mathrm{H}}_{\mathrm{Cu(H;GDP)}}$ (equation 2.94), can be calculated using equation 2.95:

$$\mathrm{Cu(H;GDP)} \rightleftharpoons \mathrm{Cu(GDP)}^{-} + \mathrm{H}^{+}$$

$$K^{\mathrm{H}}_{\mathrm{Cu(H;GDP)}} = [\mathrm{Cu(GDP)}^{-}][\mathrm{H}^{+}]/[\mathrm{Cu(H;GDP)}] \tag{2.94}$$

$$\mathrm{p}K^{\mathrm{H}}_{\mathrm{Cu(H;GDP)}} = \mathrm{p}K^{\mathrm{H}}_{\mathrm{H(GDP)}} + \log K^{\mathrm{Cu}}_{\mathrm{Cu(H;GDP)}} - \log K^{\mathrm{Cu}}_{\mathrm{Cu(GDP)}} \tag{2.95}$$

The calculated $\mathrm{p}K^{\mathrm{H}}_{\mathrm{Cu(H;GDP)}}$ values are given in column 6 of Table 2.30.

2.7.2 Acidity constants of $H_2(GDP)^-$ in water-dioxane mixtures

From the data in Table 2.29 on page 147, it is evident that the negative logarithms of the acidity constants of $H_2(GDP)^-$ increase considerably with increasing amounts of dioxane present in the aqueous solvent mixtures.

In water, the first proton of $H_2(GDP)^-$, equation 2.89, is released from the $(N7)H^+$ site. The value of the acidity constant of this site is expected to decrease with increasing amounts of dioxane. Indeed, the basicity of (neutral) N-ligands decreases as the polarity of the solvent decreases [131]. From the data collected in Table 2.29 on page 147, it is evident that the values measured for $\mathrm{p}K^{\mathrm{H}}_{\mathrm{H_2(GDP)}}$ increase with decreasing solvent polarity, in contrast to the behaviour expected for a N-bound proton. This means that in water-dioxane mixtures, $\mathrm{p}K^{\mathrm{H}}_{\mathrm{H_2(GDP)}}$ must not only refer to the release of the proton from the $(N7)H^+$ site, but another proton must contribute to its value as well. As decreasing solvent polarity increases the basicity of negatively charged O-ligands [82,131], one may expect this contribution to be due to the release of the second primary proton of the diphosphate group, whose $\mathrm{p}K_a$ is expected to increase with increasing dioxane concentration. Thus,

the value of $pK^{H}_{H_2(GDP)}$ must result from the contribution of the two microconstants $pk^{GDP\cdot H}_{H\cdot GDP\cdot H}$, due to the release of the proton from the (N7)H^+ site, and $pk^{GDP\cdot H}_{GDP\cdot H_2}$, due to the loss of the second primary proton from the diphosphate group. This second constant could well be represented by $pK^{H}_{H_2(UDP)}$, as both of them refer to the release of the second primary proton from the diphosphate chain of a nucleoside diphosphate which carries a neutral nucleic base residue. It is known [106] that $pK^{H}_{H_2(UDP)}$ = 1.26±0.20 in water, and assuming $pK^{H}_{H_2(UDP)} \simeq 2.0$ in 50% dioxane, it is evident that one needs to consider the possibility of an overlap between the two microconstants $pk^{GDP\cdot H}_{H\cdot GDP\cdot H}$ and $pk^{GDP\cdot H}_{GDP\cdot H_2}$ ($pK^{H}_{H_2(GDP)}$ = 2.89 in 50% dioxane, Table 2.29). It is therefore well possible, that with decreasing polarity $pk^{GDP\cdot H}_{H\cdot GDP\cdot H}$ actually decreases, while $pk^{GDP\cdot H}_{GDP\cdot H_2}$ increases, leading to increasing values of the measured acidity constant, $pK^{H}_{H_2(GDP)}$. More data on related systems would be needed for precise evaluations of the values of the microconstants.

The deprotonation of the terminal β-phosphate group is quantified by $K^{H}_{H(GDP)}$ (equation 2.90), whose values are listed in column 6 of Table 2.29. Addition of dioxane to the solvent leads to an inhibition of the release of this last phosphate-bound proton, and this effect is much more pronounced compared to the one observed for $K^{H}_{H_2(GDP)}$. This trend is in agreement with the observation that decreasing solvent polarity increases the basicity of negatively charged O-ligands [82,131,195].

The third constant, K^{H}_{GDP} (equation 2.91), given in column 7 of Table 2.29, refers to the ionization of the (N1)H site of the nucleobase in GDP^{3-}, to yield species of an overall -4 charge, *i.e.*, $(GDP-H)^{4-}$. As is to be expected, a decrease in the solvent polarity leads to an inhibition of the release of the proton from the (N1)H site.

The same trend is observed for the constants measured for $H_2(GMP)^{\pm}$. The location of the protons is analogous to the one described for $H_2(GDP)^{-}$: in water, the first proton is released from the (N7)H^+ site, but most probably, analogously to what is observed with $H_2(GDP)^{-}$, a contribution from the primary proton of the

phosphate group becomes more important with increasing dioxane concentration, leading to $pK^{H}_{H_2(GMP)}$ values that increase with decreasing solvent polarity.

Table 2.29: Negative logarithms of the acidity constants of $H_2(GDP)^-$ and some related ligands in dependence on the amount of dioxane (D) added to water (W), as determined by potentiometric pH titrations at 25 °C; I = 0.1 M, $NaNO_3$[a]

ligand	solvent	%D (v/v)	mole fraction	$pK^{H}_{H_2(Nu)}$	$pK^{H}_{H(Nu)}$	pK^{H}_{Nu}
GDP^{3-}	W [b]	0	0	2.67±0.02[c]	6.38±0.01	9.56±0.03
	D/W	30	0.083	2.75±0.02[c]	6.89±0.02	9.97±0.02
	D/W	50	0.175	2.89±0.04[c]	7.09±0.02	10.25±0.04
GMP^{2-}	W [d]	0	0	2.48±0.04[c]	6.25±0.02	9.49±0.02
	D/W [e]	30	0.083	2.57±0.03[c]	7.02±0.04	9.96±0.02
	D/W [e]	50	0.175	2.69±0.04[c]	7.48±0.06	10.30±0.03
AMP^{2-}	W [f]	0	0	3.84±0.02[g]	6.21±0.01	–
	D/W [f]	30	0.083	3.47±0.02[g]	7.00±0.01	–
	D/W [f]	50	0.175	3.42±0.02[g]	7.48±0.01	–
ATP^{4-}	W [h]	0	0	4.01±0.01[g]	6.49±0.01	–
	D/W [h]	30	0.083	3.68±0.02[g]	6.82±0.01	–
	D/W [h]	50	0.175	3.59±0.02[g]	6.90±0.02	–
UTP^{4-}	W [h]	0	0	2.0 ±0.1[i]	6.46±0.01	–
	D/W [h]	30	0.083	2.37±0.06[i]	6.84±0.01	–
	D/W [h]	50	0.175	2.60±0.05[i]	6.92±0.01	–

[a] The error limits given are *three times* the standard error of the mean value or the sum of the probable systematic errors, whichever is larger. [b] From Table 2.2 on page 28. [c] This value is mainly due to deprotonation of the $(N7)H^+$ site in water. With increasing dioxane concentrations, the deprotonation of the (second) primary proton released from the (di)phosphate group increasingly contributes to it. [d] From [89]. [e] H. Sigel and B. Song, unpublished results. [f] From [84]. [g] This value refers to the deprotonation of the $(N1)H^+$ site. [h] From [101]. [i] Both protons in $H_2(UTP)^{2-}$ are located at the triphosphate chain and one of them is at the terminal γ-phosphate group. To this latter one corresponds $pK^{H}_{H(UTP)}$.

The second proton is released from the phosphate group, and its constant is $K^{\mathrm{H}}_{\mathrm{H(GMP)}}$; $K^{\mathrm{H}}_{\mathrm{GMP}}$ is due to the ionization of the (N1)H site.

With both ligands, the basicity linearly increases with the increasing amount of dioxane added to the solution: the p$K^{\mathrm{H}}_{\mathrm{H_2(Nu)}}$ values measured in the different solvent mixtures fit on straight lines, and the same is true for the p$K^{\mathrm{H}}_{\mathrm{H(Nu)}}$ and p$K^{\mathrm{H}}_{\mathrm{Nu}}$ values. For instance, a plot of p$K^{\mathrm{H}}_{\mathrm{H_2(GDP)}}$ *vs* dioxane mole fraction, gives a straight line with a slope of 1.26 [$\pm$0.48(3σ)] (see Figure 2.34); all three points fit within 0.02 pK unit on this line.

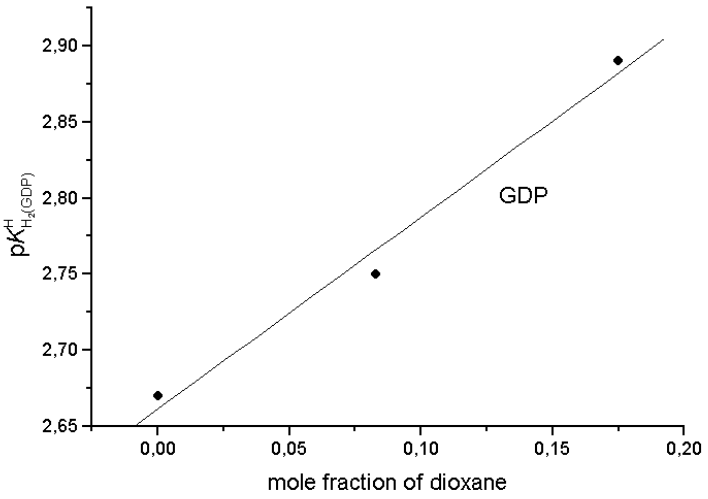

Figure 2.34: Relationship between p$K^{\mathrm{H}}_{\mathrm{H_2(GDP)}}$ and dioxane mole fraction in the solvent. The straight (regression) line is p$K^{\mathrm{H}}_{\mathrm{H_2(GDP)}}$ = $m_{\mathrm{H_2(GDP)}}\cdot$ (dioxane-mole fraction) + $b_{\mathrm{H_2(GDP)}}$. Its parameters are: $m_{\mathrm{H_2(GDP)}} = 1.262\pm0.160$ (1σ); the intercept is $b_{\mathrm{H_2(GDP)}} = 2.661\pm0.018$ (1σ), and the correlation coefficient is $R = 0.992$. The plotted data are from Table 2.29.

An analogous behaviour is observed in the case of $H_2(UTP)^{2-}$, while a decrease in the p$K^{\mathrm{H}}_{\mathrm{H_2(Nu)}}$ values with decreasing solvent polarity is observed with $H_2(AMP)^{\pm}$ and $H_2(ATP)^{2-}$ (Table 2.29). In $H_2(UTP)^{2-}$, p$K^{\mathrm{H}}_{\mathrm{H_2(UTP)}}$ is due to proton loss from one of the phosphate groups in the triphosphate chain, while in $H_2(AMP)^{\pm}$ and

$H_2(ATP)^{2-}$, the acidity constant refers to proton loss from the $(N1)H^+$ site, the basicity of which is known to decrease as the polarity of the solvent decreases [101, 131].

The $pK^{H}_{H(Nu)}$ values show the same trend with all the nucleotides considered: they all refer to the release of the last phosphate-bound proton, and as to be expected, the basicity of phosphate groups increases with decreasing solvent polarity [82,131].

2.7.3 Some considerations on the protonated Cu(H;GDP) complex

The different behaviour of $H_2(ATP)^{2-}$, $H_2(GDP)^-$, $H_2(GMP)$, and $H_2(UTP)^{2-}$, is reflected in the stability of the binary Cu(H;Nu) complexes. The stability [101] of $Cu(H;ATP)^-$ is, within experimental error, the same in all three solvents studied (Table 2.30), whereas the stability of $Cu(H;UTP)^-$, Cu(H;GDP), and $Cu(H;GMP)^+$ increases considerably with increasing amounts of dioxane in the solvent. Indeed, plots of log $K^{Cu}_{Cu(H;Nu)}$ (with Nu = GMP, GDP, or UTP) *vs* $pK^{H}_{H_2(Nu)}$ give straight lines. A plot of log $K^{Cu}_{Cu(H;UTP)}$ *vs* $pK^{H}_{H_2(UTP)}$ gives a straight line with a slope of 1.62±0.19 (1σ) [101]; the slopes of log $K^{Cu}_{Cu(H;GDP)}$ *vs* $pK^{H}_{H_2(GDP)}$ and log $K^{Cu}_{Cu(H;GMP)}$ *vs* $pK^{H}_{H_2(GMP)}$ are $m_{Cu(H;GDP)}$ = 1.895±0.200 (1σ) and $m_{Cu(H;GMP)}$ = 5.784±0.889 (1σ), respectively (see Figure 2.35). All three points measured for the Cu(H;GDP) complexes fit within 0.03 log unit on the line; the ones measured for $Cu(H;GMP)^+$ fit within 0.15 log unit on the corresponding line.

Comparing the $pK^{H}_{Cu(H;Nu)}$ values measured for the deprotonation of the Cu(H;Nu) complexes (column 6, Table 2.30), with $pK^{H}_{H_2(Nu)}$ and $pK^{H}_{H(Nu)}$ (columns 5 and 6 of Table 2.29 on page 147), it is evident that in the Cu(H;GMP) and Cu(H;GDP) complexes the proton is located at the phosphate residue (in the case of GDP, at the β-phosphate group, this being the only basic site available for GDP^{3-}).

For these species, carrying the proton at the phosphate residue, there exists the possibility of an equilibrium between an open and a macrochelated form, in which

the (di)phosphate-bound metal ion interacts with N7 of the nucleobase; this is analogous to the equilibrium shown in Figure 2.33 (page 143).

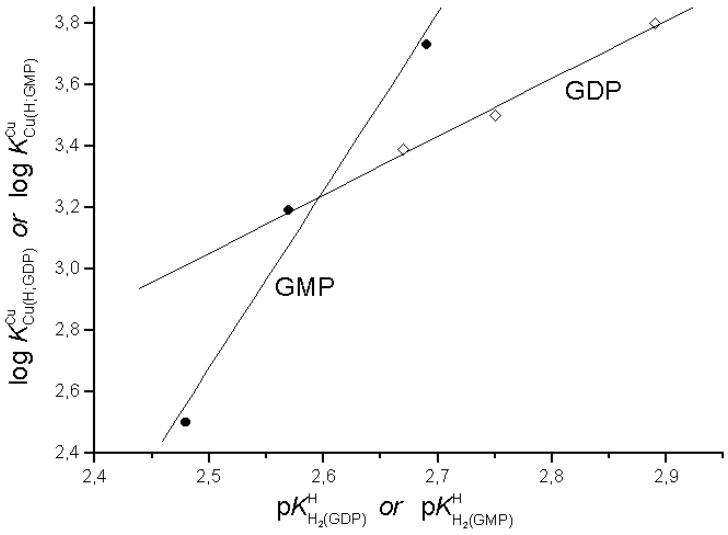

Figure 2.35: Relationship between log $K^{H}_{H_2(Nu)}$ and $pK^{H}_{H_2(Nu)}$ for the Cu(H;GDP) (♢) and Cu(H;GMP)$^{+}$ (•) complexes resulting from the addition of increasing amounts of dioxane to the solvent (I = 0.1 M, $NaNO_3$; 25 °C). The parameters of the straight (regression) lines are $m_{Cu(H;GDP)}$ = 1.895±0.200 (1σ); $b_{Cu(H;GDP)}$ = −1.686±0.555 (1σ), and R = 0.994, for the Cu(H;GDP) complex. For the Cu(H;GMP) complex, the straight-line slope is $m_{Cu(H;GMP)}$ = 5.784±0.889 (1σ); its intercept is $b_{Cu(H;GMP)}$ = −11.782±2.296 (1σ), and the regression coefficient is R = 0.988. The plotted equilibrium constants are from Table 2.30, the corresponding acidity constants are from Table 2.29 on page 147.

2.7.4 Proof of an increased stability of the Cu(GDP)$^{-}$ complexes

In water, the Cu(GDP)$^{-}$ complex shows an enhanced stability compared to that expected on the basis of a pure Cu^{2+}-diphosphate interaction (see Section 2.5.6 on page 94). This enhancement has been attributed to an intramolecular macrochelate formation, where the diphosphate-bound metal ion interacts with N7 at the nucleobase, as schematically represented by the equilibrium shown in Figure 2.33 on page 143.

Table 2.30: Logarithms of the stability constants of Cu^{2+}/GDP complexes and some complexes with related ligands in dependence on the amount of dioxane (D) added to water (W), as determined by potentiometric pH titrations at 25 °C and I = 0.1 M ($NaNO_3$), together with the negative logarithms of the acidity constants of the corresponding Cu(H;Nu) complexes (equation 2.95 on page 145)[a]

ligand	solvent	%D (v/v)	$\log K^{Cu}_{Cu(H;Nu)}$	$\log K^{Cu}_{Cu(Nu)}$	$pK^{H}_{Cu(H;Nu)}$
GDP^{3-}	W [b]	0	3.39±0.19	5.85±0.04	3.92±0.19
	D/W	30	3.50±0.08	6.18±0.18	4.21±0.20
	D/W	50	3.80±0.13	6.36±0.05	4.53±0.14
GMP^{2-}	W [c]	0	2.5 ±0.3	3.86±0.04	4.89±0.09
	D/W [d]	30	3.19±0.03	4.90±0.06	5.31±0.08
	D/W [d]	50	3.73±0.05	5.85±0.09	5.36±0.12
AMP^{2-}	W [e]	0	–	3.14±0.01	–
	D/W [e]	30	–	3.86±0.02	–
	D/W [e]	50	–	4.73±0.04	–
ATP^{4-}	W [f]	0	3.57±0.08	6.32±0.04	3.74±0.09
	D/W [f]	30	3.53±0.06	6.40±0.05	3.95±0.08
	D/W [f]	50	3.64±0.05	6.34±0.05	4.20±0.07
UTP^{4-}	W [f]	0	2.8 ±0.2	5.81±0.06	3.45±0.20
	D/W [f]	30	3.31±0.09	6.16±0.05	3.99±0.10
	D/W [f]	50	3.79±0.07	6.24±0.03	4.47±0.08

[a] The error limits given are *three times* the standard error of the mean value or the sum of the probable systematic errors, whichever is larger. The error limits of the derived data, in the present case for column 6, were calculated according to the error propagation after Gauss. [b] From Table 2.13 on page 83. [c] From [89]. [d] H. Sigel and B. Song, unpublished results. [e] From [84]. [f] From [101].

To be able to quantify the extent of the metal ion-nucleobase interaction, the position of the intramolecular equilibrium (shown in Figure 2.33) between the *open*, $Cu(GDP)^{-}_{op}$, and the *closed*, $Cu(GDP)^{-}_{cl}$, isomers has to be considered. The dimensionless intramolecular equilibrium constant, K_I can be deduced, as already shown (see Section 2.3.1 on page 43) [119,149,155,169], from the experimentally accessible overall stability constant $K^{Cu}_{Cu(GDP)}$ (equation 2.93 on page 145), provided that the stability constant of the open isomer, $K^{Cu}_{Cu(GDP)_{op}}$, is known. In such a case, K_I is given by equation 2.17 (page 46), as rewritten here in equation 2.96, to facilitate reading:

$$K_I = \frac{K^{M}_{ML}}{K^{M}_{ML_{op}}} - 1 = 10^{\log \Delta} - 1 \tag{2.96}$$

In the case of an aqueous solution, straight lines have been determined [106], that allow the calculation of the expected stability for a simple M^{2+}-diphosphate interaction ($K^{M}_{ML_{op}}$), once the pK_a of the phosphate group is known. Such a straight line has not yet been determined for complexes of diphosphate monoesters in water-dioxane solvent mixtures. It is therefore necessary to make some extrapolations to be able to estimate the stability constant of the $Cu(GDP)^{-}_{op}$ complex in 30 and 50% (v/v) water-dioxane.

The influence of decreasing solvent polarity on the stability of metal ion (Cu^{2+} or Zn^{2+}) complexes formed with six different phosphate monoester ligands ($NPhP^{2-}$, 4-nitrophenyl phosphate; PhP^{2-}, phenyl phosphate; $RibMP^{2-}$, D-ribose 5′-monophosphate; UTP^{4-}; $HCOO^{-}$; and Ac^{-}, acetate) have been studied [195], and it has been shown that for all eight systems the slope of the straight lines is very close to one. This indicates that the solvent effect on proton binding and on metal ion binding is approximately of the same size. The importance of this result is pointed out by the fact that the studied ligands carry different charges: the phosphate ligands, R-MP^{2-}, have a twofold negative charge; UTP^{4-} is fourfold negatively charged, while the two carboxylate ligands carry only a single charge, and still in all the cases, a slope of about one is observed [195]. This allows one to predict that most

probably the same slope would be obtained if the stability constants of Cu^{2+} complexes of simple diphosphate monoester ligands, R-DP^{3-} (R is a non-coordinating residue), measured in water-dioxane mixtures, would be plotted *versus* their acidity constants (measured in the same solvent). It thus seems to be reasonable to assume that the slope of the straight reference line for these Cu^{2+}/R-DP^{3-} systems is equal to one: $m_{\mathrm{H_2O/dioxane}} = 1$. The value of the intercept for this straight line must now be estimated.

A straight line has been determined for the Cu^{2+}/ R-DP^{3-} systems in water [106]:

$$\log K^{\mathrm{Cu}}_{\mathrm{Cu(R-DP)}} = 1.283 \cdot \mathrm{p}K^{\mathrm{H}}_{\mathrm{H(R-DP)}} - 2.939 \tag{2.97}$$

Applying this equation to the $Cu(GDP)^{-}_{\mathrm{op}}$ complex in water, one obtains log $K^{\mathrm{Cu}}_{\mathrm{Cu(GDP)_{op}}}$ = 5.25±0.03 (3σ) (p$K^{\mathrm{H}}_{\mathrm{H(GDP)}}$ = 6.38±0.01, Table 2.29 on page 147).

To calculate the intercept, $b_{\mathrm{H_2O/dioxane}}$, of the straight reference line in water-dioxane, one needs now to insert the known variables (log $K^{\mathrm{Cu}}_{\mathrm{Cu(GDP)_{op}}}$ = log $K^{\mathrm{Cu}}_{\mathrm{Cu(R-DP)}}$, $m_{\mathrm{H_2O/dioxane}}$, and p$K^{\mathrm{H}}_{\mathrm{H(GDP)}}$) in the general definition of a straight line:

$$\log K^{\mathrm{Cu}}_{\mathrm{Cu(R-DP)}} = m_{\mathrm{H_2O/dioxane}} \cdot \mathrm{p}K^{\mathrm{H}}_{\mathrm{H(R-DP)}} + b_{\mathrm{H_2O/dioxane}} \tag{2.98}$$

From equation 2.98 follows

$$b_{\mathrm{H_2O/dioxane}} = -1.13 \tag{2.99}$$

and the straight-line equation, defining the relationship between the stability constant of a solely-diphosphate bound Cu^{2+} ion and the pK_a value of the β-phosphate group in a water-dioxane mixture, is given by:

$$\log K^{\mathrm{Cu}}_{\mathrm{Cu(GDP)_{op}}} = 1 \cdot \mathrm{p}K^{\mathrm{H}}_{\mathrm{H(GDP)}} - 1.13 \tag{2.100}$$

Once log $K^{\mathrm{Cu}}_{\mathrm{Cu(GDP)_{op}}}$ is known (equation 2.100), K_{I} becomes accessible, and the percentage of macrochelated species formed at the equilibrium can be calculated as follows:

$$\%\ \mathrm{ML_{cl}} = 100 \cdot K_{\mathrm{I}} / (1 + K_{\mathrm{I}})$$

Straight lines are available [115] for the calculation of log $K^{\mathrm{Cu}}_{\mathrm{Cu(GMP)_{op}}}$ in the three solvents used, and their data are listed in Table 2.31.

Table 2.31: Straight-line correlations for Cu^{2+}-phosphate monoester or -phosphonate complex stabilities and phosph(on)ate group basicities[a]

% (v/v) dioxane	*m*	*b*	S.D.	ref.
0	0.465±0.025	−0.015±0.164	0.057	[125]
30	0.559±0.015	−0.089±0.106	0.03	[191]
50	0.571±0.022	0.190±0.160	0.03	[191]

[a] Slopes (*m*) and intercepts (*b*) for the straight-line plots of log $K^{\mathrm{M}}_{\mathrm{ML}}$ *vs* p$K^{\mathrm{H}}_{\mathrm{HL}}$ as calculated by the least-square procedure from the equilibrium constants for simple R-$PO_3^{2-}/H^+/Cu^{2+}$ systems (R = non coordinating residue) obtained in aqueous solutions and in water containing 30 or 50% (v/v) 1,4-dioxane at 25 °C and I = 0.1 M ($NaNO_3$). The listed S.D. values (3σ) are considered as reasonable error limits for any stability constant calculation in the p$K^{\mathrm{H}}_{\mathrm{HL}}$ range 5–8 for aqueous solution, 6–8.5 for 30%, and 6.5–9 for 50% (v/v) dioxane-water mixtures. From [115].

Application of equations 2.96, 2.100, and of the definition of % $\mathrm{ML_{cl}}$, leads to the results summarized in Table 2.32, where log $K^{\mathrm{Cu}}_{\mathrm{Cu(GMP)_{op}}}$ was calculated with the data given in Table 2.31. From the data collected in column 7 of Table 2.32, it is evident that addition of dioxane to the aqueous solution of the nucleotide complexes considerably alters the extent of macrochelate formation, but not in an easily predictable way. $\mathrm{Cu(GMP)_{cl}}$ increases with decreasing solvent polarity, while the concentration of $\mathrm{Cu(GDP)^-_{cl}}$ decreases in going from an aqueous solution to a water-dioxane one and reaches an apparently constant value of about 60% (in 30

and 50% (v/v) dioxane mixtures). A minimum is reached for $Cu(AMP)_{cl}$ in 30% (v/v) dioxane-water, while the extent of $Cu(ATP)^{2-}_{cl}$ decreases with increasing dioxane concentrations [84,101].

Table 2.32: Solvent influence on the extent of the intramolecular macrochelate formation in Cu(Nu) complexes (potentiometric pH titrations; 25 °C; I = 0.1 M, $NaNO_3$)[a]

ligand	%D (v/v)	$\log K^{Cu}_{Cu(Nu)}$	$\log K^{Cu}_{Cu(Nu)_{op}}$	$\log \Delta$	K_I	$\%Cu(Nu)_{cl}$
GDP^{3-}	0	5.85±0.04	5.25±0.04	0.60±0.06	2.98±0.52	75± 3
	30	6.18±0.18	5.76	0.42±0.18[b]	1.63±1.12	62±16
	50	6.36±0.05	5.96	0.40±0.06[b]	1.51±0.37	60± 6
[c] GMP^{2-}	0	3.86±0.04	2.89±0.06	0.97±0.07	8.33±1.55	89± 2
	30	4.90±0.06	3.84±0.03	1.06±0.07	10.48±1.77	91± 1
	50	5.85±0.09	4.46±0.03	1.39±0.10	23.55±5.36	96± 1
[d] AMP^{2-}	0	3.14±0.01	2.87±0.08	0.27±0.08	0.86±0.35	46±10
	30	3.86±0.02	3.82±0.03	0.04±0.04	0.10±0.09	9± 8
	50	4.73±0.04	4.45±0.02	0.28±0.04	0.91±0.20	48± 5
[e] ATP^{4-}	0	6.32±0.04	5.83	0.49±0.05[b]	2.09±0.36	68± 4
	30	6.40±0.05	6.14	0.26±0.05[b]	0.82±0.21	45± 6
	50	6.34±0.05	6.22	0.12±0.05[b]	0.32±0.15	24± 9

[a] The error limits given are *three times* the standard error of the mean value or the sum of the probable systematic errors, whichever is larger. [b] The range of error given with these values is estimated. [c] H. Sigel and B. Song, unpublished results. The data for the straight lines of phosphate monoesters in 30 and 50% dioxane were taken from [115]. [d] From [84]. [e] From [101].

The different influences of dioxane on the formation of the macrochelates must be due to a combination of effects. Two in particular, might play an important role: (*i*) alterations of the metal ion affinity of the binding sites due to the decreasing solvent polarity; (*ii*) hydrophobic solvation of the purine moiety of the nucleotide by the ethylene groups of 1,4-dioxane might shield a binding site, e.g. N7, in a certain concentration range of dioxane.

It should finally be noted that not only the nucleobase residues alter their coordinating properties but also the metal ion affinity of the phosphate residues increases drastically with a decreasing solvent polarity (see column 3 of Table 2.32).

In those cases in which with increasing amounts of dioxane, the concentrations of the macrochelated isomers decrease [in $Cu(ATP)^{2-}$ and, partly, in $Cu(GDP)^{-}$], the prevailing effect is probably an increasing hydrophobic solvation of the nucleobase moiety by dioxane, which renders the coordination of N7 due to increasing steric shielding more difficult.

Chapter 3

Conclusions

The present study deals with the acid–base and metal ion-binding properties of purine nucleoside 5′-di- and 5′-triphosphates (= Nu) with the alkaline earth ions and the second half of the divalent 3d transition metal ions and Cd^{2+}, providing an overview on the stabilities and structures of their complexes in aqueous solution.

It is shown that in the M(Nu) complexes formed between one of the metal ions studied and GTP^{4-}, ITP^{4-}, or GDP^{3-}, the phosphate-bound metal ion interacts with the N7 site of the guanine or hypoxanthine residues by forming macrochelates (see Section 2.4 on page 48, and Section 2.5.6 on page 94) [65]. One of the possible structures of a macrochelated complex, $M(GDP)^{-}_{cl}$, is shown in Figure 3.1.

The same kind of interaction is observed in the case of the complexes formed with ADP^{3-} [105] or IDP^{3-} and Mg^{2+}, Ca^{2+}, Mn^{2+}, Co^{2+}, Ni^{2+}, Cu^{2+}, Zn^{2+}, or Cd^{2+}.

From potentiometric pH titrations only overall (global) stability constants can be obtained, and hence different types of macrochelates cannot be distinguished. What is measured is the concentration of all complexes formed, including the sum of all possible macrochelated isomers. However, for $M(ATP)^{2-}$ complexes evidence has accumulated [58,59,65,88,134] that at least two types of macrochelates can form, one in which the γ,β,(α)-triphosphate-coordinated metal ion [6,47,58,134] binds *innersphere* to N7 of the adenine residue and one in which this interaction is of the *outersphere* type, that is, with a water molecule between N7 and M^{2+} (see Figure

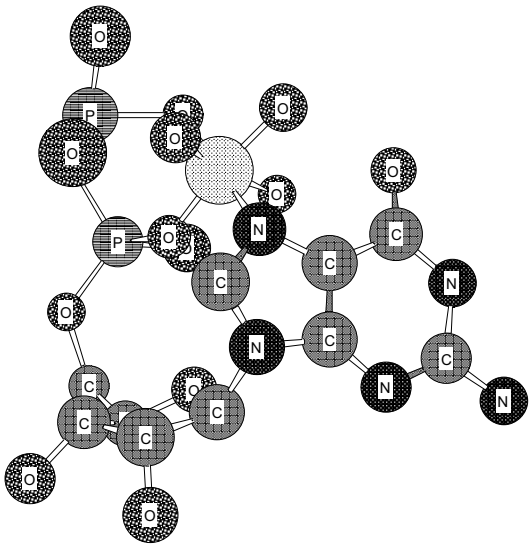

Figure 3.1: Example of a structure of a macrochelated $M(GDP)^{-}$ isomer with a hexacoordinating M^{2+} innersphere bound to the diphosphate group and to N7 of the guanine residue. The metal ion is shown in pearl-grey; H atoms are omitted for clarity.

2.15 on page 62).

A similar situation occurs for $M(GTP)^{2-}$ and $M(ITP)^{2-}$ (see Tables 2.6, 2.7, and 2.8 on pages 59–61) [65]. As no indication of a Mg^{2+}-nucleobase interaction was obtained from ^{1}H-NMR shift experiments [73], $Mg(GTP)^{2-}$ and $Mg(ITP)^{2-}$ must form outersphere macrochelates, and this is most probably also true for the other alkaline earth ions. From an early line-broadening study [135] of the Mn^{2+}/ITP system it follows that at least some innersphere binding occurs with N7. It is evident that further detailed studies by NMR and/or spectrophotometry are desirable to reveal the ratios of the innersphere/outersphere macrochelated isomers for other metal ions as well. In addition, it should be noted that the (C6)O carbonyl group may also participate in outersphere metal ion binding [89].

Comparing the results obtained now for the purine-nucleoside 5′-diphosphate/M^{2+} systems via potentiometric pH titrations with the literature data that were collected from ^{1}H-NMR shift measurements [74], one may conclude that Mg^{2+}-N7 interactions in the $Mg(ADP)^{-}$ and $Mg(GDP)^{-}$ complexes must occur in an outersphere

manner. The stability constant comparison for the $M(ADP)^-$ and $M(IDP)^-$ complexes of the other alkaline earth metal ions give little evidence of macrochelate formation, while it is very likely that some amounts of $Ca(ADP)^-_{cl}$ (9±8%), of $Mg(IDP)^-_{cl}$ (9±9%), and of $Ca(IDP)^-_{cl}$ (13±13%) exist (and most probably as an outersphere-N7 macrochelate), even if the results obtained are at the limit of the accuracy of the data. This agrees with the results obtained for $Mg(IMP)_{cl}$ [59] and $Mg(ITP)^{2-}_{cl}$ [65], which amount to 17±11% and 22±10%, respectively, and with what was obtained for the $Ca(IMP)_{cl}$ [59] and $Ca(ITP)^{2-}_{cl}$ [65] complexes, amounting to 13±12% and 19±13%, respectively (see Table 3.1 and Section 2.5.6 on page 94). Even though there is no evidence of the existence of a closed $Ca(AMP)_{cl}$ species [59], the $Ca(ATP)^{2-}$ complex forms macrochelates to some extent (15±12%) [65] (see Table 3.1 on page 161, and Section 2.4.2 on page 57). It is therefore likely that the result obtained for the $Ca(ADP)^-_{cl}$ species (9±8%) is actually indicative of some macrochelate formation.

Moreover, proceeding in the same way, it becomes evident that about one third of $Zn(ADP)^-_{cl}$ and $Cd(ADP)^-_{cl}$, corresponding to about 10% and 19% of the macrochelate, respectively, is formed by outersphere binding to N7 and the other two thirds (about 20% and 37% of the total $Zn(ADP)^-_{cl}$ and $Cd(ADP)^-_{cl}$ formed, respectively) by innersphere coordination [74] (see Section 2.5.3 on page 74). Mariam and Martin [155] concluded, based on their spectrophotometric measurements, that about one part of $Ni(ADP)^-_{cl}$ (about 12%) is outersphere and that about four parts ($\sim$ 47%) are innersphere. It is evident that these equilibria deserve further study.

The consideration that Zn^{2+} or Cd^{2+} form macrochelates with GDP^{3-} and IDP^{3-} mainly by innersphere coordination with N7 originates from the same kind of data comparison [74].

Interesting observations were made about the $M(GDP-H)^{2-}$ and $M(IDP-H)^{2-}$ complexes formed between the metal ion and the (N1)H-deprotonated nucleotides. While there is no indication for macrochelation in any of the $M(NDP-H)^{2-}$ complexes of the alkaline earth metal ions, macrochelate formation with the divalent 3d

transition metal ions and with Cd^{2+} is quite pronounced, and larger than in the corresponding undeprotonated $M(NDP)^{-}$ complexes. In addition, for a 3d metal ion there is hardly a significant difference in base back-binding between the complexes of $M(GDP-H)^{2-}$ and $M(IDP-H)^{2-}$ (Section 2.5.7 on page 102), whereas the corresponding $M(GDP)^{-}_{cl}$ and $M(IDP)^{-}_{cl}$ species form to different extents. In analogy to what was observed for the corresponding $M(GMP-H)^{-}$ and $M(IMP-H)^{-}$ complexes [89], an additional interaction, next to the one with N7, between the (C6)O and the metal ion is expected to be responsible for the enhanced stability of the $M(NDP-H)^{2-}$ complexes of the 3d transition metal ions. This interaction could be of an innersphere or of an outersphere kind, as schematically shown in Figure 2.26 on page 108.

The most fascinating aspect of these results is most probably the following one: if one compares the formation degrees of $M(AMP)_{cl}$ and $M(ADP)^{-}_{cl}$ [105] with the corresponding values for $M(ATP)^{2-}_{cl}$ [65], and the ones of the 5′-mono-, 5′-di-, and 5′-triphosphates of guanosine and inosine [59,65] (see Table 3.1), respectively, one makes the remarkable observation that for nearly all metal ions considered, the formation degree of the macrochelated species for a given metal ion and purine-nucleobase residue, is identical within the error limits. This means, macrochelate formation is independent of the number of phosphate groups present in the ligands and in the coordination spheres of the metal ions.

The above observation is even more surprising when one considers the stabilities of the M(Nu) complexes, which are determined to the very largest part by the coordination of the metal ions to the phosphate residues: the stability differences between the M(NMP) and $M(NDP)^{-}$ complexes amount to about 1 to 2.4 log units, whereas those between the $M(NDP)^{-}$ and $M(NTP)^{2-}$ complexes are in the order of about 1 log unit!

On the basis of the results collected in Table 3.1, one can see that while for a given metal ion the degree of macrochelate formation does not depend on the length of the phosphate chain, whereas the percentage of macrochelates formed

increases by going from adenosine to inosine, to guanosine 5′-phosphates. Hence, for the extent of macrochelate formation, mainly the properties of the N7 site are responsible, at least as long as the coordination sphere of the metal ion considered is not yet saturated, while the length of the phosphate chain is mainly responsible for the overall complex stability.

Table 3.1: Extent of macrochelate formation in some metal ion complexes of purine nucleoside 5′-mono, 5′-di-, and 5′-triphosphates as determined by potentiometric pH titrations in aqueous solution, at 25 °C; I = 0.1 M, $NaNO_3$.[a]

Nu	%Mg(Nu)$_{cl}$	%Ca(Nu)$_{cl}$	%Mn(Nu)$_{cl}$	%Cu(Nu)$_{cl}$	%Zn(Nu)$_{cl}$	ref.
AMP^{2-}	13±10	0	15±11	50± 7	44±12	[105]
ADP^{3-}	13± 9	9± 8	21± 7	54± 5	31± 9	[105][b]
ATP^{4-}	17±10	15±12	17±15	67± 3	28±10	[65][c]
IMP^{2-}	22±10	13±12	32±10	77± 4	65± 6	[59]
IDP^{3-}	9± 9	13±13	22± 9	64± 9	44± 8	[b]
ITP^{4-}	17±11	19±13	48± 8	86± 3	50± 7	[65][c]
GMP^{2-}	31± 7	24±10	44± 9	89± 2	80± 3	[59]
GDP^{3-}	21± 9	29±10	42± 9	75± 3	63± 4	[b]
GTP^{4-}	21±11	24±10	63± 3	97± 1	68± 4	[65][c]

[a] The error limits given are *three times* the standard error of the mean value or the sum of the probable systematic errors, whichever is larger. [b] From Section 2.5.6 on page 94. [c] From Section 2.4.2 on page 57.

The large differences between the stability constants measured for the metal ion complexes of nucleoside mono-, di-, and triphosphates for a given metal ion and purine nucleobase residue, demonstrate that, for example, upon hydrolysis of the terminal γ-phosphate group of the ATP substrate the resulting product can relatively easily be replaced in the coordination sphere of the metal ion because its binding affinity is drastically reduced. One might recall that the free energy ΔG° is connected with the stability constant by the equation $\Delta G^\circ = -2.3\,RT \log K$, and that

1 log unit of a stability constant corresponds at 25 °C approximately to a change in free energy of 6 kJ mol^{-1}. These high-energy binding sites of the phosphate residue are in contrast with the weak structuring interactions as they occur at N7 of the nucleobase moieties: a stability difference log Δ of 0.1 log unit gives rise to a formation degree of about 20% for the macrochelated $M(Nu)_{cl}$ species (see, e.g., Table 2.16 on page 97), yet the change in the free energy involved, which creates the special structure, corresponds only to about 0.6 kJ mol^{-1}. On the other hand, it is evident that if 20% of a substrate is in the correct conformation/orientation needed by the enzyme for a reaction, this is more than enough, especially as equilibration is fast with all these metal ions. Finally, one may mention that not only Pt(II) species bind preferentially to the N7 site of purines [137,139,196] but that this holds for Mn^{2+} and Zn^{2+} as well [113,140]. In fact, there are indications [57] that N7 of ATP might interact with Zn^{2+} in a RNA polymerase reaction during the catalytic process [197,198]. Understanding the solution properties of metal ion-nucleotide complexes should help to appreciate their role in enzymatic reactions.

In studying the intramolecular stacking properties of the $Cu(arm)^{2+}$ complexes (with arm = bpy or phen), it has been proven (see Section 2.6 on page 109) that intramolecular stacks between the aromatic rings of arm and the purine residues of ADP [154], GDP or IDP, can be formed not only in the $Cu(arm)(NDP)^{-}$ complexes but also in their monoprotonated Cu(arm)(H;NDP) species, where the proton is at the terminal β-phosphate group. The stacking tendency of the nucleobase residue remains practically unaffected by the protonation of the phosphate group (*cf.* Table 2.27 on page 141).

From the results listed in Table 2.27 it is evident that the length of the phosphate residue has no significant effect on the formation degree of the intramolecular stacks. Of course, the absolute stabilities of the complexes differ [58,59,106], but the position of the intramolecular-stacking equilibrium is within the error limits identical. Moreover, stack formation in the Cu(phen)(Nu) complexes of the purine nucleotide, is slightly favoured over that in the Cu(bpy)(Nu) complexes, and the

same applies to the Cu(arm)(H;Nu) complexes: the larger phen is able to stack somewhat better with the purine residue than bpy. Such a tendency does not exist in the Cu(arm)(Py) complexes (Py = UMP^{2-}, UDP^{3-}, or UTP^{4-}; Table 2.28 on page 142): since the uracil residue consists only of a single ring, it may stack with bpy as well as with phen. The stacking tendency of the one-ring uracil residue is considerably smaller than that of the two-ring purine residues (*cf.* Tables 2.27 and 2.28). The stacking tendency of a nucleobase moiety in a nucleotide complex depends therefore on the nature of the nucleobase itself, and not on the denticity of the phosphate residue, or on its length.

This kind of adduct formation is relevant in recognition reactions in nature: e.g. in protein-nucleotide/nucleic acid interactions the role of bpy or phen may be taken over by the phenyl or indole moieties of phenylalanyl or tryptophanyl residues, respectively.

The acid–base and Cu^{2+}-binding properties of GDP have been further investigated in low polarity solvents, using mixtures of 30 and 50% 1,4-dioxane in water. Indeed, by now it is well established that in proteins [80,81,199] and the active-site cavities of enzymes [82] the *effective* or *equivalent solution* dielectric constant is reduced compared to the situation in bulk water; *i.e.*, the activity of water is decreased [83] due to the presence of aliphatic and aromatic amino acid side chains at the protein–water interface. Estimates for the dielectric constant (ε) in such locations range from about 30 to 70 [80,82,199], compared to approximately 80 of bulk water. Hence, by employing aqueous solutions that contain about 20–50% 1,4-dioxane, one may simulate to some extent the situation in active-site cavities [170]: the dielectric constants of these mixed solvents are about 60 and 35, respectively [82,200–202]. This study aimed at answering the question *To what extent are metal ion-complex equilibria affected by these effects?* A decreasing solvent polarity considerably favours phosphate-complex stability, and this effect can be quite drastic: for example, the stability of $Cu(GDP)^{-}$ increases by a factor of about 3 by going from water ($\log K^{\mathrm{Cu}}_{\mathrm{Cu(GDP)}} = 5.85 \pm 0.04$) to a 50% water-dioxane

mixture (log $K^{Cu}_{Cu(GDP)}$ = 6.36±0.05); in the case of Cu(GMP), this effect is even more pronounced, the stability of the complex increases by a factor of about 100 by going from water (log $K^{Cu}_{Cu(GMP)}$ = 3.86±0.04) to the 50% water-dioxane mixture (log $K^{Cu}_{Cu(GMP)}$ = 5.85±0.09; see Table 2.30 on page 151). The overall stability of the Cu(AMP), $Cu(ATP)^{2-}$, Cu(GMP), $Cu(GDP)^{-}$ complexes, which is mainly determined by the metal ion affinity of the phosphate residues, increases considerably for all four complexes with increasing amounts of 1,4-dioxane.

With these considerations in mind, it is fascinating to consider the percentages of the macrochelated species formed in dependence of the percentage of dioxane present in the aqueous solution (*cf.* Table 2.32 on page 155). The formation degree of $Cu(AMP)_{cl}$ passes through a minimum at about 30% (v/v) dioxane-water, despite the fact that the overall complex stability of Cu(AMP) [84] increases rather "regularly" in going from water to water containing 50% 1,4-dioxane (Table 2.32). The overall stability of $Cu(ATP)^{2-}$ is only little affected by the change in solvent composition, whereas the formation degree of its macrochelate decreases quite significantly [101]. The formation degree of $Cu(GMP)_{cl}$ increases with increasing amounts of 1,4-dioxane, while the percentage of $Cu(GDP)^{-}_{cl}$ formed seems to decrease to a constant value of about 60% upon addition of 1,4-dioxane to the aqueous solution.

The overall stability of all these complexes behaves largely as predicted for simple phosphate-metal ion complexes [195], whereas their structural changes are quite unpredictable.

There must then be a combination of two opposing effects resulting from the addition of 1,4-dioxane to an aqueous solution containing the complexes [58,59]. It could be, for example, that low amounts of 1,4-dioxane lead to a hydrophobic (lipophilic) solvation of the purine moiety of the nucleotides by the ethylene groups of 1,4-dioxane, and that in this way the N7 binding site is shielded to some extent. Upon addition of larger amounts of dioxane to the aqueous solution no further

shielding occurs but the activity of water decreases to the point where poor solvation results for those metal-ion sites not occupied by the phosphate group(s) of the nucleotides; consequently this poorer solvation leads to an increased affinity of these metal ion sites for other ligating groups, *i.e.*, for N7. Should this explanation be correct then for $Cu(ATP)^{2-}_{cl}$ and $Cu(GDP)^{-}_{cl}$ such a minimum should be observable at higher dioxane concentrations [58,59] though it might as well be that in the case of $Cu(GDP)^{-}$ this minimum has already been reached with the formation degree of 60% for the $Cu(GDP)^{-}_{cl}$ complex in 30 and 50% (v/v) water-dioxane. Unfortunately, at least in the case of the Cu^{2+}-ATP systems, the reactants become insoluble at higher dioxane concentrations, preventing such a study [59,101] and with Cu^{2+}-GDP no such experiments have been attempted up to now.

Chapter 4

Experimental Section

4.1 Materials and equipment

The sodium salts of GTP, ITP, CTP, UTP, and ADP were purchased from Sigma Chemical Co. (St. Louis, MO, US) and from Sera Histochemical, Gamba (Heidelberg, Germany); the ones of GDP and IDP were from Sigma Chemical Co. (St. Louis, MO, US). The results collected for the nucleotides from the different sources did not differ. The content of free inorganic phosphate initially present in the ligands (determined with molybdate reagent [203,204]; for more details see [47]) was below 3% for the nucleoside 5′-triphosphates and ADP, and amounted to about 2% in GDP and IDP.

Acetone (*pro analysi*), 1,4-dioxane (extra pure), the disodium salt of 1,2-diaminoethane-N,N,N′,N′-tetraacetic acid (Na_2H_2EDTA), the nitrate and perchlorate salts of Na^+, Mg^{2+}, Ca^{2+}, Sr^{2+}, Ba^{2+}, Mn^{2+}, Co^{2+}, Ni^{2+}, Cu^{2+}, Zn^{2+} and Cd^{2+}, as well as 2,2′-bipyridine, 1,10-phenanthroline, $HClO_4$, HNO_3, NaOH (titrisol), potassium hydrogen phthalate, potassium dihydrogen phosphate, ammoniumheptamolybdate $(NH_4)_6Mo_7O_{24}\cdot 4H_2O$, (all *pro analysi*) were from Merck KGaA (Darmstadt, Germany).

The buffer solutions [pH 4.00 or 4.64, 7.00, and 9.00; based on the NBS scale, now US National Institute of Standards and Technology (NIST)] were from Metrohm AG (Herisau, Switzerland). In those instances where the titrations were started at

a low pH (about 2.2), or were pursued up to a high pH (10 or higher), two additional buffer solutions of pH 2.01 and 9.98 (25 °C, based on the same scale), were employed, respectively. They were purchased from Merck KGaA (Darmstadt, Germany). The N_2 (99.999%, Carbagas, Basel, Switzerland) used during the titrations was led through the following sequence of solutions: Vanadium(III) with Zn in HCl, concentrated H_2SO_4, and solid NaOH, to purify it from eventual traces of O_2, H_2O, or CO_2.

The stock solutions of the nucleotides were freshly prepared daily dissolving the substance in deionized, ultrapure (MILLI-Q 185 PLUS-system from Millipore S. A. 67120 Molsheim, France) and CO_2-free water (CO_2 was removed by boiling the water under N_2) and the exact concentration of the solutions used in the experiments was each time determined by titration with NaOH.

The titre of the NaOH solutions used for the titrations was established with potassium hydrogen phthalate and the exact concentrations of the stock solutions of the divalent metal ions were determined by potentiometric pH titrations of their EDTA complexes.

The pH titrations were carried out with a Metrohm E536 potentiograph equipped with an E655 dosimat and an EA121 or 6.02002.100 (JC) combined macro glass electrode that was calibrated with the above specified buffer solutions.

All calculations were carried out with IBM-compatible desk computers with 80-486 or Pentium processors (connected with Epson Stylus 1000ESC/P 2 printers and a Hewlett-Packard Deskjet 1600 C Color Smart printer or a Hewlett-Packard 7475A plotter) by a curve-fitting procedure using a Newton–Gauss nonlinear least squares program [205].

The direct pH-meter readings were used to calculate the acidity constants, *i.e.*, these are so-called practical, mixed or Brønsted constants [99]. Their negative logarithms given for aqueous solutions at I = 0.1 M and 25 °C may be converted into the corresponding concentration constants by subtracting 0.02 log unit from the listed pK_a values [99]. This conversion term contains both the junction potential

of the glass electrode and the hydrogen ion activity [99,206]. The ionic product of water and the mentioned conversion term do not enter in the calculations because *differences* in NaOH consumption between solutions with and without ligand are evaluated [153]. No conversion is needed for the stability constants of the metal ion complexes, which are as usual concentration constants.

In the case of the nucleoside 5′-triphosphates, the experiments had been done by Dr. N. A. Corfù, Prof. Dr. Y. Kinjo and Dr. R. Tribolet, but they were evaluated only now [65,93]. Part of the experiments for the binary and ternary complexes of ADP were done by Dr. S. A. A. Sajadi; these experiments were now re-evaluated and completed by additional measurements; the final values refer to the average of all results [105,154].

4.2 Determination of the acidity constants

For the determination of the acidity constants, aqueous solutions of HNO_3 and $NaNO_3$ (or $HClO_4$ and $NaClO_4$, respectively), in the presence and absence of ligand, were titrated under N_2 (in all instances, I = 0.1 M, 25 °C) with NaOH. As already pointed out, the differences in NaOH consumption between solutions with and without ligand were evaluated.

Calculations of acidity constants were done with a curve fitting procedure using a Newton–Gauss non–linear least-squares program by employing every 0.1 pH unit the difference in NaOH consumption between the two mentioned titrations (for more details about the program, see the description of "POTENTIO" in [205]).

4.2.1 Acidity constants of the nucleoside 5′-triphosphates

Under the experimental conditions used (most measurements were made with solutions being 5×10^{-4} M in nucleotide concentration) no self-stacking occurs [67, 73,91]; therefore the properties of the monomeric species are studied.

There was no difference between the results of the re-evaluated data obtained

from earlier experiments, which were carried out in the presence of $NaClO_4$ (see [64]) and those carried out more recently (N. A. Corfù, Y. Kinjo, R. Tribolet) using $NaNO_3$ as background electrolyte.

The pH of the aqueous stock solutions was adjusted to about 8.2 with UTP, 8.5 with CTP, and to 8.0 with GTP and ITP, *i.e.*, to a pH value at which the phosphate group is fully deprotonated in all instances.

The acidity constants $K^{\mathrm{H}}_{\mathrm{H_2(NTP)}}$ (equation 2.2 on page 18), $K^{\mathrm{H}}_{\mathrm{H(NTP)}}$ (loss of the last phosphate-bound proton, equation 2.3), and $K^{\mathrm{H}}_{\mathrm{NTP}}$ (deprotonation of N1, equation 2.4, Section 2.1.1 on page 17) of $H_2(NTP)^{2-}$ for GTP and ITP were determined by titrating an aqueous solution of HNO_3 or $HClO_4$ in the presence and absence of NTP under N_2 with 1 or 1.5 ml of NaOH. Three sets of experiments, as specified in the table, were carried out and the constants were evaluated within the pH ranges specified below.

	$[H^+]$ M	[NTP] M	V_{tot} ml	[NaOH] M	V_{NaOH} ml	I M
(*i*) HNO_3	10^{-3}	5×10^{-4}	50	0.05	1.5	0.1 ($NaNO_3$)
(*ii*) $HClO_4$	1.6×10^{-3}	1.2×10^{-3}	25	0.05	1	0.1 ($NaClO_4$)
(*iii*) HNO_3	2×10^{-2}	2.8×10^{-3}	20	0.2	2	0.1 ($NaNO_3$)

In the case of GTP, the first set (*i*) was evaluated in the pH range 3.5–10.0, giving values for all three constants. The neutralization degrees are: 78–100% for the $H_2(GTP)^{2-}$ / $H(GTP)^{3-}$ equilibrium, 3–100% for the $H(GTP)^{3-}$ / GTP^{4-}, and 6–73% for the $GTP^{4-}/(GTP-H)^{5-}$ equilibrium. For ITP the pH range 4.8–10.4 was used, giving results for the second and third constants. From the second set (*ii*) values for all three constants were obtained for both NTPs in the pH range 3.5–8.5, and from the third set (*iii*) the first two constants were calculated for both NTPs in the pH range 2.1–7.0. The lowest and highest pH values considered in the evaluation of the constants correspond to neutralization degrees of about 45–100% for

the equilibrium $H_2(ITP)^{2-}/H(ITP)^{3-}$, of about 1–100% for the $H(ITP)^{3-}/\ ITP^{4-}$, and of about 9–95% for the $ITP^{4-}/(ITP-H)^{5-}$ equilibrium. The final results (see Table 2.1 on page 20) are the averages of 14 titrations for $K^{H}_{H_2(ITP)}$ and of more than 40 (on average 50) titrations for the other constants.

The acidity constants $K^{H}_{H_2(CTP)}$ and $K^{H}_{H(CTP)}$ (equations 2.2 and 2.3, Section 2.1.1) of $H_2(CTP)^{2-}$ were determined by titrating 50 ml of aqueous 1.3×10^{-3} M HNO_3 (I = 0.1 M, $NaNO_3$; 25 °C) in the presence and absence of 5×10^{-4} M CTP under N_2 with 1.5 ml of 0.05 M NaOH. Evaluations were carried out in the pH range 3.6–8.3. The averaged results from 15 titrations were identical to the values published previously for these acidity constants [88].

The acidity constants $K^{H}_{H(UTP)}$ and K^{H}_{UTP} (equations 2.3 and 2.4 on page 18) were determined exactly under the same conditions as given above for $H_2(CTP)^{2-}$ but the calculations were in this case carried out in the pH range 4.8–10.0. In a further set of experiments 25 ml of aqueous 1.6×10^{-3} M $HClO_4$ (I = 0.1 M, $NaClO_4$; 25 °C) were titrated in the presence and absence of 1.2×10^{-3} M UTP under N_2 with 1 ml of 0.055 M NaOH and evaluated for the same two acidity constants in the pH range 4.8–8.5. The final results (see Table 2.1 on page 20) are the averages of at least 14 independent pairs of titrations.

4.2.2 Acidity constants of the nucleoside 5′-diphosphates

Under the experimental conditions chosen (ligand concentrations varying between 1.7×10^{-3}–6×10^{-4} M) self-stacking of the nucleotides is negligible [74], *i.e.*, the results presented definitely refer to the monomeric species.

The pH of the aqueous stock solutions was adjusted to about 8.0 with all nucleoside 5′-diphosphates studied. Their acidity constants were determined by titrating with NaOH an aqueous solution of HNO_3 (I = 0.1 M, $NaNO_3$; 25 °C) in the presence and absence of the ligand, under N_2. The differences in NaOH consumption between such a pair of titrations were used for the evaluation of the constants.

The acidity constants $K^{H}_{H_2(ADP)}$ (deprotonation of N1, equation 2.6, Section

2.2.1) and $K^{\mathrm{H}}_{\mathrm{H(ADP)}}$ (loss of the last phosphate-bound proton equation 2.7 on page 27) of $H_2(ADP)^-$ were determined from two different sets of experiments:

	[HNO_3] M	[ADP] M	V_{tot} ml	[NaOH] M	V_{NaOH} ml	I M
(*i*)	2.2×10^{-3}	6×10^{-4}	50	0.06	2	0.1 ($NaNO_3$)
(*ii*)	5.4×10^{-2}	3×10^{-4}	50	0.03	1	0.1 ($NaNO_3$)

The experiments were evaluated for both constants in the pH ranges 3.0–8.1 (set (*i*)) and 4.0–8.1 (set (*ii*)), corresponding initially to about 11% neutralization for the equilibrium $H_2(ADP)^-/H(ADP)^{2-}$ and at the end to about 98% neutralization for $H(ADP)^{2-}/(ADP)^{3-}$. The two acidity constants, $K^{\mathrm{H}}_{\mathrm{H_2(ADP)}}$ (equation 2.6) and $K^{\mathrm{H}}_{\mathrm{H(ADP)}}$ (equation 2.7 on page 27), result from more than 100 independent pairs of titrations (Table 2.2 on page 28).

Values for $pK^{\mathrm{H}}_{\mathrm{H_2(IDP)}}$ (equation 2.10), $pK^{\mathrm{H}}_{\mathrm{H(IDP)}}$ (loss of the last phosphate-bound proton, equation 2.11), and $pK^{\mathrm{H}}_{\mathrm{IDP}}$ (deprotonation of N1, equation 2.12 on page 30, Section 2.2.2) of $H_2(IDP)^-$ were determined using again two experimental settings, as described in the following Table:

	[HNO_3] M	[IDP] M	V_{tot} ml	[NaOH] M	V_{NaOH} ml	I M
(*i*)	1.4×10^{-2}	1.7×10^{-3}	25	0.10	3.5	0.1 ($NaNO_3$)
(*ii*)	3.0×10^{-3}	6×10^{-4}	50	0.06	3	0.1 ($NaNO_3$)

The first set of four experiments was evaluated in the pH range 2.3–10.0, the second one between pH 2.7–10.0, corresponding initially to about 76% neutralization for the equilibrium $H_2(IDP)^-/H(IDP)^{2-}$ in the first instance, or about 89% neutralization of the same equilibrium when considering the second pH range. The equilibrium $H(IDP)^{2-}/IDP^{3-}$ had a neutralization degree of 1–100%, while the $IDP^{3-}/(IDP{-}H)^{4-}$ equilibrium reached a final neutralization degree of 89%. All

three constants were calculated from the data collected from both experimental sets. The final results (see Table 2.2 on page 28) are based on more than 40 independent pairs of titrations.

The acidity constants $K^{\mathrm{H}}_{\mathrm{H_2(GDP)}}$ (equation 2.10), $K^{\mathrm{H}}_{\mathrm{H(GDP)}}$ (loss of the last phosphate-bound proton, equation 2.11), and $K^{\mathrm{H}}_{\mathrm{GDP}}$ (deprotonation of N1, equation 2.12, Section 2.2.2 on page 30) of $H_2(GDP)^-$ were determined by titrating 50 ml of aqueous 3×10^{-3} M HNO_3 in the presence and absence of 6×10^{-4} M GDP under N_2 with 3 ml of 0.06 M NaOH. Evaluations were carried out in the pH range 2.7–10.0, corresponding to an initial neutralization degree of about 53% for the $H_2(GDP)^-/H(GDP)^{2-}$ equilibrium; to 3–100% neutralization degree for the $H(GDP)^{2-}/GDP^{3-}$ equilibrium, and to about 5–73% for the $GDP^{3-}/(GDP-H)^{4-}$ equilibrium. The final results (Table 2.2 on page 28) are based on 50 independent pairs of titrations.

4.3 Determination of the stability constants of the complexes

Titrations were done pairwise (in the presence and absence of ligand, L = NTP^{4-} or NDP^{3-}) under N_2. Again, the differences in NaOH consumption between solutions with and without ligand were evaluated. The stability constants were determined under the same conditions as described for the acidity constants (Section 4.2; see Tables 4.1 and 4.2), with the exception of the ones for the Sr^{2+} and Ba^{2+} complexes of CTP and UTP (see below). In all these experiments, part of $NaNO_3$ or $NaClO_4$ was replaced by $M(NO_3)_2$ or $M(ClO_4)_2$, respectively (I = 0.1 M, $NaNO_3$ or $NaClO_4$; 25 °C), where M^{2+} = Mg^{2+}, Ca^{2+}, Sr^{2+}, Ba^{2+}, Mn^{2+}, Co^{2+}, Ni^{2+}, Cu^{2+}, Zn^{2+}, or Cd^{2+}.

The stability constants were computed for each pair of titrations with a curve-fitting procedure by taking into account the species H^+, H_2L, HL, L, M^{2+}, M(H;L), and ML [207]. The data were collected every 0.1 pH unit from either the lowest pH which could be reached in the experiment or from a formation degree of about

2–6% for ML to either a neutralization degree of about 90% for the species HL, or the beginning of the hydrolysis of $M(aq)^{2+}$. In the latter case, the collection of data was therefore stopped before the onset of the formation of hydroxo complexes, which was evident from the titrations without ligand: the titration curves deviate from the ones that contain only the acid solution—without ligand and without metal ions—as soon as hydrolysis starts. The constants were calculated using the program "SASI1", explained in detail in [205].

In the following Tables 4.1 and 4.2, the nucleotide, acid, and NaOH concentrations are specified for the NTP and NDP studied, respectively.

In the case of the NTPs, the M^{2+}/NTP ratio was 1:1 throughout.

Table 4.1: Conditions under which the stability constants of the M^{2+} (M^{2+} = Mg^{2+}, Ca^{2+}, Sr^{2+}, Ba^{2+}, Mn^{2+}, Co^{2+}, Ni^{2+}, Cu^{2+}, Zn^{2+}, or Cd^{2+}) complexes of GTP^{4-} and ITP^{4-} were studied. The potentiometric pH titrations were carried out in aqueous solution at 25 °C; I = 0.1 M[a]

	$[H^+]$	[NTP]	$[M^{2+}]$	V_{tot}, ml	[NaOH]	V_{NaOH}, ml
[b]	10^{-3}	5×10^{-4}	5×10^{-4}	50	0.05	1.5
[c]	1.6×10^{-3}	1.2×10^{-3}	1.2×10^{-3}	25	0.05	1.0

[a] All the concentrations are given in [mol/l]. [b] $[H^+] = [HNO_3]$, I = 0.1 M, $NaNO_3$. [c] $[H^+] = [HClO_4]$, I = 0.1 M, $NaClO_4$.

The stability constants of the protonated species were not always well defined by the experimental data and in some instances they had to be estimated. In order to treat all the data in an homogeneous way the constants for ML were obtained as follows: once the stability constant of the protonated complexes were calculated or estimated, all calculations were repeated by keeping this value fixed and letting all the other parameters vary. The effect that the value of $K^{M}_{M(L\cdot H)}$ can have on the results of K^{M}_{ML} was considered in the error limits of the latter constant; by keeping $K^{M}_{M(L\cdot H)}$ constant—once with the lower and once with the upper error limit—and

by repeating the calculations for $K^{\mathrm{M}}_{\mathrm{ML}}$, this effect was determined. However, it is not overwhelming, as the degree of formation of the M(L·H) species is usually relatively low in the pH range where that of the ML complexes is high.

Table 4.2: Conditions under which the stability constants of the M^{2+} (M^{2+} = Mg^{2+}, Ca^{2+}, Sr^{2+}, Ba^{2+}, Mn^{2+}, Co^{2+}, Ni^{2+}, Cu^{2+}, Zn^{2+}, or Cd^{2+}) complexes of ADP, GDP, and IDP were studied. The potentiometric pH titrations were carried out in aqueous solution at 25 °C; I = 0.1 M ($NaNO_3$)[a]

$[H^+]$	[NDP]	M^{2+}/NDP[b]	V_{tot}, ml	[NaOH]	V_{NaOH}, ml
[c] 2.2×10^{-3}	6.0×10^{-4}	1:1 – 10:1	50	0.06	2
[c] 5.4×10^{-4}	3.0×10^{-4}	1:1 – 10:1	50	0.03	1
[d] 3.0×10^{-3}	6.0×10^{-4}	1:1 – 3:1	50	0.06	3

[a] All the concentrations are given in [mol/l]; $[H^+]$ = $[HNO_3]$. [b] The metal-to-ligand ratio varies in the range given. The ratios used with each metal ion are specified further in the text. [c] The two different sets of experiments were used to determine the stability constants of the M(H;ADP) and $M(ADP)^-$ complexes. [d] This set of experiments was used to determine the stability constants of the M(H;GDP), $M(GDP)^-$, $M(GDP-H)^{2-}$, M(H;IDP), $M(IDP)^-$, and $M(IDP-H)^{2-}$ complexes.

For the complexes of nucleotides with the alkaline earth ions it was possible to reach a neutralization degree of about 90%, while with the other metal ions, more prone to hydrolysis, the titrations were stopped at lower pH values. Details on the pH ranges used in the evaluations are given in the next sections.

All the constants given (see Section 2.4 on page 48 for the triphosphates; Section 2.5.1 on page 65 and Section 2.5.4 on page 80, for the diphosphates) are the average of at least 5 independent pairs of titrations.

4.3.1 Stability constants of nucleoside 5′-triphosphate complexes

There was no difference between the results of the re-evaluated data obtained from experiments carried out in the presence of $NaClO_4$ (see [64]) and those carried out in $NaNO_3$ as background electrolyte. As divalent metal ions promote the dephosphorylation of NTPs, although with a different effectiveness [47], the two reactants were only mixed in the last minute before the titration, which was usually completed within 15 minutes: in this way dephosphorylation was minimized.

The stability constants $K^{\mathrm{M}}_{\mathrm{M(NTP\cdot H)}}$ (equation 2.20) and $K^{\mathrm{M}}_{\mathrm{M(NTP)}}$ (equation 2.21 on page 49) were determined for ITP and GTP under the same conditions as described for the acidity constants (see Section 4.2.1 on page 169), and as schematically summarized in Table 4.1.

The stability constants of the Sr^{2+} and Ba^{2+} complexes of CTP and UTP were determined under the following conditions: [HNO_3] = 1.9×10^{-3} M; [NTP] = 5×10^{-4} M; volume 50 ml; [NaOH] = 0.05 M (2 ml); I = 0.1 M, $NaNO_3$; 25 °C.

The stability constants $K^{\mathrm{M}}_{\mathrm{M(NTP\cdot H)}}$ could only be determined for the M^{2+}/CTP and, in part, for the M^{2+}/GTP systems because $pK^{\mathrm{H}}_{\mathrm{H_2(NTP)}}$ is rather low, especially for ITP and UTP. Therefore, for these two last systems only estimates, with relatively large error limits, could be given for the stabilities of their $M(NTP\cdot H)^-$ complexes. These estimates were partly based on comparisons with related ligands [59,88,106].

The final stability constants (see Table 2.3 on page 52) [65] are the results from the averages of at least eight independent pairs of titrations, on average ten titration pairs were carried out for each system.

The pH values at which the evaluations for the GTP and ITP complexes were started in the individual calculations depended on the lowest pH that could be reached in the titrations (differences are due to the different experimental conditions): in every instance a pH corresponding to a formation degree varying between 3.5–6% for the ML species was considered; the single exception were the complexes of Cu^{2+}, which were formed to a much higher extent already at the pH

where the titrations started.

For the complexes of GTP with the alkaline earth metal ions, evaluations were done up to pH 7.3, *i.e.*, in a pH range corresponding to a formation degree of about 5–45% for the ML species in the case of Sr^{2+} and 5–39% for the complexes formed with Ba^{2+}. Formation degrees of about 70% and 60% were reached for the complexes with Mg^{2+} and Ca^{2+}, respectively. The highest formation degree reached for the protonated species, M(H;L), was 15% for complexes of the first two metal ions, and 13% in the case of Mg(H;L) and Ca(H;L). In all four cases, the stability constants of the protonated species, $K^{\mathrm{M}}_{\mathrm{M(NTP\cdot H)}}$, could be calculated, yet, due to the big scattering in the experimental values the error limits are rather large.

The data obtained for the Mn^{2+}, Co^{2+}, and Ni^{2+} systems were evaluated from a pH corresponding to a formation degree of about 5% of the ML species, to about 86% (85% in the case of Co^{2+}), or pH 6.4. The maximum formation degrees reached for the protonated species were about 35% for $Mn(H;GTP)^{-}$, 41% for $Co(H;GTP)^{-}$ and 48% for $Ni(H;GTP)^{-}$.

The stability constant of the $Cu(H;GTP)^{-}$ complex had to be estimated (hence the high error limit), while $K^{\mathrm{Cu}}_{\mathrm{Cu(GTP)}}$ could be well determined from the experimental data using a pH range corresponding to a formation degree of about 30–93% for the ML species (calculations were carried out up to pH 5.2, where no hydrolysis had started yet). The highest formation degree reached for the protonated species was about 63% in the pH range covered under the experimental conditions.

For the Zn^{2+} and Cd^{2+} complexes calculations were carried out up to pH 6.1, corresponding to formation degrees of 5–85% and 5–87%, respectively. In both instances, the constant $K^{\mathrm{M}}_{\mathrm{M(GTP\cdot H)}}$ could be evaluated, even if in the case of Zn^{2+} big scattering between the experimental values led to large error limits. The maximum formation degrees for the protonated species were about 37% for Zn(H;GTP) and about 55% for Cd(H;GTP).

The stability constants of the complexes of ITP with the alkaline earth metal

ions were evaluated up to pH 6.8, corresponding to a formation degree of about 5–67% for $Mg(ITP)^{2-}$; the maximum formation degree of $Mg(H;ITP)^{-}$ being about 9.7%. The formation degree of the $Ca(ITP)^{2-}$ complex amounted to 5–55% in the pH range considered, and the maximum formation degree reached for the monoprotonated species was about 9.8%. The formation degree of the complexes formed with Sr^{2+} and Ba^{2+} varied between 5–35% in the case of the first metal ion, and between 5–30% with Ba^{2+}. The maximum formation degree of the protonated species was about 8.2% in both instances.

Formation degrees of up to about 84%, 76% and 74% were reached for the complexes with Mn^{2+}, Co^{2+}, and Ni^{2+}, respectively. They were evaluated in the pH range corresponding to the lowest point reached in the titrations, up to pH 6.4 in the case of Mn^{2+} and to pH 6.0 with Co^{2+} and Ni^{2+}. The highest formation degree of the protonated species, M(H;L), was 28% for $Mn(H;ITP)^{-}$ and about 25% for the $Co(H;ITP)^{-}$ and $Ni(H;ITP)^{-}$ species.

$K^{Cu}_{Cu(ITP)}$ could be evaluated from the experimental data in a pH range corresponding to a formation degree of about 30–93% for the ML species (calculations were carried out up to pH 5.5, where no hydrolysis had started yet). The highest formation degree reached for the protonated species was about 51% in the pH range covered under the experimental conditions.

Data collected for the $Zn(ITP)^{2-}$ complex could be evaluated up to pH 6.2, corresponding to formation degrees of about 5–84%. The highest formation degree of the protonated complex was about 28%.

The stability constant of the Cd^{2+} complex was evaluated from the lowest point reached in the single titrations, up to pH 6.0, corresponding to a maximum formation degree of about 85% for the ML species. The highest formation degree of the $Cd(H;ITP)^{-}$ complex was about 45%.

4.3.2 Stability constants of nucleoside 5′-diphosphate complexes

The stability constants $K^{M}_{M(NDP\cdot H)}$ (equations 2.26 and 2.34) and $K^{M}_{M(NDP)}$ (equation 2.27 on page 66, and equation 2.35 on page 81), of the binary complexes of the nucleoside 5'-diphosphates with the divalent metal ions specified above, were determined under the same conditions as described for the acidity constants (see Section 4.2.2 on page 171), except that the background electrolyte was partly replaced by $M(NO_3)_2$, to keep I = 0.1 M. In the case of IDP, stability constants were determined under the same conditions as described under point (*ii*) in Section 4.2.2. All the experimental conditions are schematically collected and specified in Table 4.2 on page 175.

With ADP, the M^{2+}-to-ligand (M:L) ratios usually employed were 1:1 and 2:1 for all metal ion systems, except that in the case of the alkaline earth metal ions, because of the low stability of their complexes, also the ratios 3:1, 5:1, and 10:1 were used for the Ca^{2+}, Sr^{2+} and Ba^{2+} systems; for the Mg^{2+} system a 8:1 ratio was employed in addition. With Mn^{2+}, Co^{2+}, Ni^{2+}, and Zn^{2+}, the M:L ratio was usually 1:1, one experiment with each metal ion was carried out using a 2:1 ratio; with Ni^{2+} and Zn^{2+} a 3:1 ratio was used once, and with Zn^{2+} one experiment was carried out using a 4:1 ratio as well. In all other experiments M:L ratios of 1:1 were employed. With Cu^{2+} a proportion of 1:1 was used throughout, with the exception that in two of the 33 experiments carried out a 2:1 M:L ratio was used. For Cd^{2+} M:L ratios of 1:1, 1.5:1, 2:1 (in one instance, 3:1) were used. Depending on the experimental conditions in which the titrations were carried out, the evaluation of the curves started at different pH values, *i.e.*, at formation degrees for the ML species ranging from about 2.6 to 5.5%.

In the case of Mg^{2+}, 23 experiments were carried out and the curves were evaluated up to a pH of about 6.6. $K^{Mg}_{Mg(ADP\cdot H)}$ could only be evaluated in 4 instances: the four experiments were part of those done under the same conditions as described in (*i*) for the acidity constants (see Section 4.2.2 on page 171) —the titration started at a relatively low pH— and high M:L ratios (10:1 and 8:1) were used. The maximum

formation degree of the protonated species was about 2.3% with the 1:1 ratio and it reached about 16% with the highest metal-to-ligand ratio. The value of $K^{\mathrm{Mg}}_{\mathrm{Mg(ADP)}}$ was obtained from the average of 23 independent pairs of titrations. The pH range in which the evaluations were carried out corresponds to a formation degree for the $Mg(ADP)^-$ complex of about 5–35% (5–88% when M:L=10:1). The excess of metal ion had no influence on the value of the stability constant, showing that only 1:1 complexes were formed.

In the case of Ca^{2+} and Sr^{2+}, $K^{\mathrm{M}}_{\mathrm{M(ADP{\cdot}H)}}$ was estimated, as the formation degree of the protonated complex was too low and no reliable results could be obtained from the experimental data. Thirty independent experiments were carried out with Ca^{2+} and 36 with Sr^{2+}. The experiments were evaluated up to pH 7.1. In the pH range considered, the formation degree of the $Ca(ADP)^-$ complex varied between about 3–25% (3–80% with the highest ratio) and for the $Sr(ADP)^-$ species, between 3–11% (3–55% with M:L=10:1). The maximum formation degree for the Ca(H;ADP) complex was 1.6% (M:L=1:1) or 13% (M:L=10:1); for Sr(H;ADP) the values are 0.83% (M:L=1:1) or 7.4% (M:L=10:1).

Twenty-six independent experiments were carried out with Ba^{2+}, and in 12 instances it was possible to evaluate $K^{\mathrm{Ba}}_{\mathrm{Ba(ADP{\cdot}H)}}$; as in the case of Mg^{2+}, these 12 experiments were part of those done under the same conditions as given in the first line of Table 4.2 on page 175, and as described in (*i*) of Section 4.2.2, and using high M^{2+}-to-ligand ratios (10:1 and 5:1). As the formation degree of the protonated complex is rather small (maximum reached: 0.69% and 6.2% with M:L=1:1 and 10:1, respectively), there was a big scatter in the results, therefore a relatively high error limit results for the constant $K^{\mathrm{Ba}}_{\mathrm{Ba(ADP{\cdot}H)}}$ (see Table 2.9 on page 67). $K^{\mathrm{Ba}}_{\mathrm{Ba(ADP)}}$ was obtained from the average of 26 independent pairs of titrations. The agreement within the individual results of this constant was very good, yet the large error of $K^{\mathrm{Ba}}_{\mathrm{Ba(ADP{\cdot}H)}}$ was considered in the error limit of $K^{\mathrm{Ba}}_{\mathrm{Ba(ADP)}}$. The formation degree for the $Ba(ADP)^-$ complex was about 10% (M:L=1:1) or 52% (M:L=10:1).

The data collected for Mn^{2+}, Co^{2+}, and Ni^{2+} could be evaluated up to pH 6.8

(no hydrolysis problems arose). In the pH range considered, the formation degrees of the complexes were in the order of about 5–69% for $Mn(ADP)^{-}$, 5–59% for $Co(ADP)^{-}$ and 5–59% for $Ni(ADP)^{-}$. The highest formation degrees reached for the M(H;ADP) complexes were 8.1% for Mn(H;ADP), 4.7% for Co(H;ADP), and 6.9% for Ni(H;ADP). The final constants result from the average of 15 independent pairs of titrations in the case of $K^{\mathrm{Mn}}_{\mathrm{Mn(ADP)}}$ (12 for $K^{\mathrm{Mn}}_{\mathrm{Mn(ADP{\cdot}H)}}$); 16 such titrations were averaged to give $K^{\mathrm{Co}}_{\mathrm{Co(ADP)}}$ (8 for $K^{\mathrm{Co}}_{\mathrm{Co(ADP{\cdot}H)}}$), and 10 to give both $K^{\mathrm{Ni}}_{\mathrm{Ni(ADP)}}$ and $K^{\mathrm{Ni}}_{\mathrm{Ni(ADP{\cdot}H)}}$.

The data collected for complexes formed between Zn^{2+} and ADP could be evaluated up to pH 6.0, and the formation degrees of the various species are 1–6.9% for Zn(H;ADP) (about 20% with the 4:1 M:L ratio) and 4–57% (about 89% when M:L=4:1) for $Zn(ADP)^{-}$. The final constant $K^{\mathrm{Zn}}_{\mathrm{Zn(ADP)}}$ results from the average of 11 independent pairs of titration (10 were averaged to give $K^{\mathrm{Zn}}_{\mathrm{Zn(ADP{\cdot}H)}}$).

Due to hydrolysis problems, data for the Cu^{2+}-complexes could be collected only up to pH 5.6, corresponding to a formation degree of the $Cu(ADP)^{-}$ species of about 83%. The maximum formation degree reached for the Cu(H;ADP) complex was about 8.9%. There were relatively large differences in the experimental values obtained for log $K^{\mathrm{Cu}}_{\mathrm{Cu(ADP{\cdot}H)}}$, consequently a large error resulted for this constant. The value for $K^{\mathrm{Cu}}_{\mathrm{Cu(ADP)}}$ is the average of 33 independent pairs of titrations and the one for $K^{\mathrm{Cu}}_{\mathrm{Cu(ADP{\cdot}H)}}$ of 10 such titrations. The large error of this last constant was taken into account in the error limit of $K^{\mathrm{Cu}}_{\mathrm{Cu(ADP)}}$.

With Cd^{2+}, calculations were carried out up to pH 6.1, corresponding to formation degrees of the $Cd(ADP)^{-}$ species of about 5–70%; the highest formation degree reached for the Cd(H;ADP) complex was in the order of 10%. Sixteen independent pairs of titrations were averaged to give the final value for $K^{\mathrm{Cd}}_{\mathrm{Cd(ADP)}}$ and 8 to give $K^{\mathrm{Cd}}_{\mathrm{Cd(ADP{\cdot}H)}}$.

The stability constants ($K^{\mathrm{M}}_{\mathrm{M(ADP)}}$) of the complexes formed with the deprotonated ligand, ADP^{3-}, result form the average of at least ten independent pairs of titrations (on average 21 such titrations were carried out for each metal ion). The

stability constants ($K^{\mathrm{M}}_{\mathrm{M(ADP\cdot H)}}$) of the protonated complexes were not always accessible, as the formation degree of these species is very low in some instances, values had to be estimated on the basis of the few results that could be obtained, and on the comparison with related ligands [59,88,106]. This was especially the case with the alkaline earth ions. In those instances in which these constants were accessible, they were evaluated from at least 8 independent pairs of titrations (on average 10). The number of titrations done, the pH range used in the calculation for each constant and the formation degrees for the species involved in the equilibria have been specified above [105].

In the case of IDP and GDP the acidity constant $\mathrm{p}K^{\mathrm{H}}_{\mathrm{M(NDP)}}$ (deprotonation of the (N1)H site in the $\mathrm{M(NDP)}^{-}$ complex, equation 2.38 on page 81) for the formation of the $\mathrm{M(NDP{-}H)}^{2-}$ complex could in addition be evaluated in many cases. In the fitting-procedure this species had to be taken into account, in addition to the $\mathrm{(NDP{-}H)}^{4-}$ species, and to the ones listed at the beginning of Section 4.3 (page 173). The M:L ratio was 1:1 with all metal ions, with the exception of the alkaline earth ions, where ratios of 1:1, 2:1 or, in some instances, even 3:1 were employed due to the low stability of their complexes. Despite the relatively high metal-to-ligand ratio, these data could be evaluated to get the final value for $\mathrm{p}K^{\mathrm{H}}_{\mathrm{M(NDP)}}$, as their values agreed well with the ones calculated with the data collected using a M^{2+}:L=1:1 ratio.

The stability constants of the protonated complexes of IDP, $K^{\mathrm{M}}_{\mathrm{M(IDP\cdot H)}}$, had to be estimated, as in most instances the buffer depression was too low to get any reliable results. With Ni^{2+}, Cd^{2+}, and Cu^{2+}, it was nevertheless possible to evaluate this constant, and the results obtained were within the error limits identical with the estimations.

Complexes of the alkaline earth ions and IDP were evaluated in the pH range 2.7–10.0. The formation degrees of the species formed within that pH range are: about 5–38% (5–57% with the 2:1 ratio) for $\mathrm{Mg(IDP)}^{-}$, 0.8–20% (1–30% with

M:L=2:1) for $Mg(IDP-H)^{2-}$. The maximum formation degree reached for the protonated Mg(H;IDP) complex was 2.2% (4.4%). The formation degrees of the complexes of Ca^{2+} varied between about 5–25% (5–41% with M:L=2:1) for $Ca(IDP)^{-}$, and 0.9–27% (1.0–32%) for $Ca(IDP-H)^{2-}$. The maximum formation degree of the Ca(H;IDP) species was 1.8% (3.5%). Complexes of Sr^{2+} had formation degrees varying between about 5–11% (5–20% with M:L=2:1) and 1.0–13% (1.0–23%), respectively, in the pH range considered for the evaluation of the constants. The maximum formation degree of the species Sr(H;IDP) was 0.92% (1.8%). With Ba^{2+}, the formation degree of the $Ba(IDP)^{-}$ complex varied between about 5–9.3% (5–17%), the one of the species $Ba(IDP-H)^{2-}$ between 1.0–11% (1.0-20%), and the maximum formation degree of the protonated species was 0.74% (1.5%).

Complexes formed with Mn^{2+} were evaluated in the pH range 2.7–8.3, and the corresponding formation degrees were 5–69% for $Mn(IDP)^{-}$, and 1.0–26% for $Mn(IDP-H)^{2-}$. The maximum formation degree of Mn(H;IDP) was 9.4%.

With Co^{2+}, the experiments could be evaluated up to pH 8.0; the formation degrees of the various species were 5–64% for $Co(IDP)^{-}$ and 1.1–32% for $Co(IDP-H)^{2-}$. The highest formation degree reached for Co(H;IDP) was 7.8%.

The stability constants for the complexes of Ni^{2+} with IDP, were calculated in the pH range 2.7–7.8, corresponding to formation degrees of 5–64% for the $Ni(IDP)^{-}$ complex and of about 4.6–33% for $Ni(IDP-H)^{2-}$; the highest formation degree of the protonated Ni(H;IDP) species was 11%.

Complexes formed with Cu^{2+} were evaluated in the pH range 2.7–5.8, corresponding to a formation degree of 5–75% for the $Cu(IDP)^{-}$ complex. The highest formation degree of the Cu(H;IDP) species was about 25%.

Complexes of Zn^{2+} were evaluated in the pH range 2.7–7.3, their formation degrees corresponded in this pH range to about 5–59% for the $Zn(IDP)^{-}$ species and to 0.2–11% for $Zn(IDP-H)^{2-}$. The maximum formation degree reached for the Zn(H;IDP) complex was 11%.

In the case of Cd^{2+}, the experimental data could be evaluated from 2.7 up to

pH 7.6, corresponding to formation degrees of 5–74% for $Cd(IDP)^{-}$, 0.8–22% for $Cd(IDP-H)^{2-}$, and to a maximum formation degree of the protonated species of about 18%.

In the case of Ba^{2+}, the final results are based on the average of 4 independent pairs of titrations; the constants for the Mn^{2+} complexes are based on 6 independent pairs of titrations, while in all other instances 5 such titrations were averaged (the results are listed in Table 2.13 on page 83).

Only stability constants of the protonated complexes of the alkaline earth ions and of Mn^{2+} with GDP had to be estimated: all other constants could be evaluated from the experiments. In the case of $K^{\mathrm{Mn}}_{\mathrm{Mn(GDP\cdot H)}}$ the results obtained from some of the titrations were identical, within the error limits, with the estimated values. Experiments were carried out under the same conditions as described for the acidity constants (Section 4.2.2, page 171), and as summarized in Table 4.2 on page 175. The M:L ratios were 1:1, 2:1 or 3:1 with the alkaline earth ions, 1:1 in all other instances.

Experiments with Mg^{2+}, Ca^{2+}, Sr^{2+}, or Ba^{2+} were evaluated in the pH range 2.7–10.0. This corresponds to formation degrees of about 5–43% with a M:L ratio of 1:1, for $Mg(GDP)^{-}$ (with M:L=2:1, the observed formation degree was 5–63%), 0.9–23% (0.9–22with M:L=2:1, where the calculations were stopped at pH 9) for $Mg(GDP-H)^{2-}$, and a maximum formation degree of about 2.2% (4.2% with M:L=2:1) for the Mg(H;GDP) species. Formation degrees of the Ca^{2+} complexes varied between 2.5–30% with M:L=1:1 (between about 5–59% with M:L=3:1) for $Ca(GDP)^{-}$, between 0.5–16% (0.9–14% with M:L=3:1, where the pH range considered was 2.7–8.8) for $Ca(GDP-H)^{2-}$. The highest formation degree of the protonated species, Ca(H;GDP), was about 1.8% with the lowest metal-to-ligand ratio and about 5.1% with the highest one (3:1). In the case of Sr^{2+} and Ba^{2+} in 1:1 ratios formation degrees of about 5–13% (5–31% with Sr:GDP=3:1) and 5–11% (5–23% with Ba:GDP=3:1), respectively for the $M(GDP)^{-}$ species and of 1.0–12% (1.0–22% with Sr:GDP=3:1) for the $Sr(GDP-H)^{2-}$ and 0.6–11% (1.0–27% when

M:L=3:1) for the $Ba(GDP-H)^{2-}$ were reached. The highest formation degree of the protonated complexes was 0.9% in both instances when M:L=1:1 and 2.7% for Sr(H;GDP) and 2.2% for Ba(H;GDP) when M:L=3:1.

Data for Mn^{2+} were evaluated in the pH range 2.7–8.5, corresponding to formation degrees of about 5–70% for $Mn(GDP)^{-}$, and 0.5–16% for $Mn(GDP-H)^{2-}$, while the highest formation degree reached for Mn(H;GDP) was 8.7%.

Complexes with Co^{2+} were evaluated in the pH range 2.7–7.8, corresponding to formation degrees of about 5–70% for $Co(GDP)^{-}$, 0.5–11% for $Co(GDP-H)^{2-}$, and a maximum formation degree of about 11% for the protonated Co(H;GDP) species.

Complexes formed with Ni^{2+} were evaluated in the pH range 2.7–7.7, corresponding to a formation degree of about 5–75% for the $Ni(GDP)^{-}$ species, 0.9–10.6% for $Ni(GDP-H)^{2-}$, and a maximum formation degree of about 25% for Ni(H;GDP).

In the case of Cu^{2+}, it was not possible to evaluate the acidity constant for the deprotonation of (N1)H in presence of the metal ion, $pK^{H}_{M(GDP)}$, because hydrolysis started before the species $Cu(GDP-H)^{2-}$ could form. Evaluations could be carried out in the pH range 2.7–5.5, corresponding to a formation degree of about 5–85% for the $Cu(GDP)^{-}$ complex. The highest formation degree that was reached for the protonated Cu(H;GDP) species was 36%.

The stability constants for the complexes of Zn^{2+} with GDP were calculated in the pH range 2.7–7.0; the formation degrees are about 5–75% for the $Zn(GDP)^{-}$ complex and about 0.9–4.0% for the $Zn(GDP-H)^{2-}$ species, while the highest formation degree of the protonated species, Zn(H;GDP) is about 15%.

Complexes formed with Cd^{2+} were evaluated in the pH range 2.7–7.6, corresponding to formation degrees of 5–81% for $Cd(GDP)^{-}$ and 0.7–13% for the $Cd(GDP-H)^{2-}$ species. The highest formation degree of the Cd(H;GDP) complex was about 27%.

The final stability constants (see Table 2.13 on page 83) result from the average

of at least 5 independent pairs of titrations carried out for each metal ion system.

4.3.3 Stability constants of ternary complexes of nucleoside 5′-diphosphates

The stability constants log $K^{\mathrm{M}}_{\mathrm{M(H;NDP)}}$ and log $K^{\mathrm{M}}_{\mathrm{M(NDP)}}$, where M = $Cu(bpy)^{2+}$ or $Cu(phen)^{2+}$, of the complexes formed between nucleoside 5′-diphosphates and Cu^{2+}, 2,2′-bipyridine (bpy) or 1,10-phenanthroline (phen), were determined by applying the same conditions as described for the acidity constants (Section 4.2.2 on page 171), and as given in the following Table 4.3. The Cu^{2+}/NDP system was always titrated together with the ternary complexes. The M:L ratios were 1:1 in all the experiments. Under the experimental conditions the formation of the $Cu(arm)^{2+}$ complexes is practically complete due to their high stability [85,86], and indeed titrations containing only HNO_3 or HNO_3 plus Cu^{2+}/arm were identical in the lower pH range and therefore the evaluation of the titration data of the ternary systems could be done in the same way as described for the binary ones.

Table 4.3: Conditions under which the stability constants of the M^{2+} (M^{2+} = $Cu(bpy)^{2+}$ or $Cu(phen)^{2+}$) complexes of ADP^{3-}, GDP^{3-}, and IDP^{3-} were studied. The potentiometric pH titrations were carried out in aqueous solution at 25 °C; I = 0.1 M ($NaNO_3$)[a]

$[H^+]$	[NDP]	M^{2+}/NDP	V_{tot}, ml	[NaOH]	V_{NaOH}, ml
[b] 2.2×10^{-3}	6.0×10^{-4}	1:1	50	0.06	2
[b] 5.4×10^{-4}	3.0×10^{-4}	1:1	50	0.03	1
[c] 3.0×10^{-3}	6.0×10^{-4}	1:1	50	0.06	3

[a] All the concentrations are given in [mol/l]; $[H^+] = [HNO_3]$. [b] The two different sets of experiments were used to determine the stability constants of the M(H;ADP) and $M(ADP)^-$ complexes. [c] This set of experiments was used to determine the stability constants of the M(H;GDP), $M(GDP)^-$, M(H;IDP), and $M(IDP)^-$ complexes.

In the case of ADP, the final results (see Table 2.21 on page 112) [154] are the

averages of at least eleven independent pairs of titrations. The constants were evaluated up to pH 5.3 (corresponding to a formation degree of 90% of the Cu(arm)(ADP)$^-$ complexes), starting from a pH whose exact value depended on the experimental conditions used, and that corresponded to a formation degree of about 6% of the Cu(arm)(ADP)$^-$ species. The highest formation degree of the protonated ternary complexes was about 26% for Cu(phen)(H;ADP) and 36% for Cu(bpy)(H;ADP).

It was not possible to experimentally determine the values for the constants of the M(H;IDP) complexes; these had to be estimated. To evaluate $K^{\mathrm{M}}_{\mathrm{M(IDP)}}$, data points were collected between pH 2.7–5.8, corresponding to formation degrees of 25% (lower values were not reached under the given conditions) to 98% of Cu(bpy)(IDP)$^-$; in the pH range 2.7–5.6, the formation degree of Cu(phen)(IDP)$^-$ is 25%–98%. The protonated species had maximum formation degrees of 15% and 25%, respectively. The final results (Table 2.21) are the average of at least five independent pairs of titrations.

All stability constants of the ternary complexes of GDP could be determined, although in the case of the protonated species big scattering in the values led to large error limits for some constants. Experiments were evaluated in the pH range 2.7-5.5, corresponding to formation degrees of 15–96% for the species Cu(arm)(GDP)$^-$, with a maximum formation degree of the protonated species, Cu(arm)(H;GDP) of about 50% with Cu(bpy)$^{2+}$, and of about 58% with Cu(phen)$^{2+}$. The final results (Table 2.21 on page 112) are the average of at least 5 independent pairs of titrations. The high error limits of $\log K^{\mathrm{M}}_{\mathrm{M(H;IDP)}}$ (estimated) and of $\log K^{\mathrm{M}}_{\mathrm{M(H;GDP)}}$ were taken into account in the evaluation of $\log K^{\mathrm{M}}_{\mathrm{M(IDP)}}$ and $\log K^{\mathrm{M}}_{\mathrm{M(GDP)}}$, respectively, and are reflected in the error limits of the latter constants. The scattering in the values for $\log K^{\mathrm{M}}_{\mathrm{M(NDP)}}$ was actually rather small.

4.4 Determination of the equilibrium constants for 5′-GDP in water/ 1,4-dioxane mixtures

The titration apparatus was calibrated with the aqueous buffer solutions listed in Section 4.1 (page 167). The given acidity constants are so-called practical, mixed or Brønsted constants; no corrections were applied for the change in solvent from water to the dioxane–water mixtures, though correction factors have been published for such [208–210] and related mixtures [211]. The stability constants presented are, as usual, concentration constants. Experiments were carried out under the same conditions as used for the study of GDP in aqueous solution (Section 4.2.2). Similarly, for the experiments with water containing 30 or 50% (v/v) 1,4-dioxane, the M:L ratio was always 1:1.

For each pair of titrations, data were evaluated every 0.1 pH unit in the pH range 2.7–10.7 for the determination of the acidity constants. The final results for the acidity constants, $pK^{H}_{H_2(GDP)}$, $pK^{H}_{H(GDP)}$, and pK^{H}_{GDP} are the result of at least eight independent pairs of titrations. Experiments were carried out in the presence and absence of Cu^{2+}, $Cu(phen)^{2+}$, or $Cu(bpy)^{2+}$. The onset of the formation of hydroxo complexes was evident from the titrations without ligand. The stability constants of the Cu(H;GDP) and $Cu(GDP)^{-}$ complexes were determined from four independent pairs of titrations.

4.5 Statistical treatment of the experimental results

All the constants given are the result of the average of several experiments. The arithmetic mean is always considered. Errors were calculated according to the error propagation theory of Gauss. In the following, a brief summary of the mathematical expressions needed for their evaluation is given.

4.5.1 Arithmetic mean

The arithmetic mean $\overline{x}$ represents the average value of n individual measurements. It is given from the sum of the observed values divided by the sum of the number of observations [212,213]:

$$\overline{x} = \frac{\sum_{i=1}^{n} x_i}{n}$$

The standard deviation σ defines the deviation of the single values from $\overline{x}$ and is defined as:

$$\sigma(\overline{x}) = \sqrt{\frac{\sum_{i=1}^{n}(\overline{x} - x_i)^2}{(n-1)}}$$

The so called standard error depends on the following expression:

$$\Delta(\overline{x}) = \frac{\sigma(\overline{x})}{\sqrt{n}} = \sqrt{\frac{\sum_{i=1}^{n}(\overline{x} - x_i)^2}{n(n-1)}}$$

These formulas are used in the program "Mean", that is used to calculate the error limits of the measured acidity and stability constants. The error limits are set equal to a value corresponding to 3Δ (but at least 0.01 logarithmic units).

4.5.2 Error propagation according to Gauss

The error of a variable c, that is calculated from two or more quantities affected by an error, x_i, $c = f(x_i)$, follows from Gauss' theory of error propagation [212, 213]:

$$\Delta c = \sqrt{\sum_{i=1}^{n} \frac{\delta f(x_i)^2}{\delta x_i} \Delta x_i^2}$$

For addition and subtraction of the two quantities *a* and *b*, holds:

$$\Delta c = \sqrt{\Delta a^2 + \Delta b^2}$$

The multiplication of a number *a* (affected by an error Δa) by a number *b* (which error is represented by Δb) gives a product *c*, affected by the error Δc, which follows from

$$\Delta c = \sqrt{b^2 \cdot \Delta a^2 + a^2 \cdot \Delta b^2}$$

The division of the same number *a* by *b*, gives the quantity *c*, the error, Δc, of which follows from

$$\Delta c = \sqrt{\frac{\Delta a^2}{b^2} + \frac{a^2 \cdot \Delta b^2}{b^2}}$$

Abbreviations

19Mer	19 base-pairs oligomer
Ac^-	acetate
Ado	adenosine
ADP^{3-}	adenosine 5′-diphosphate
AMP^{2-}	adenosine 5′-monophosphate
arm	heteroaromatic nitrogen base, e.g., bpy or phen
Asn	asparagine
Asp	aspartic acid
ATP^{4-}	adenosine 5′-triphosphate
BPA	bis(2-pyridyl)amine
bpy	2,2′-bipyridine
CDP^{3-}	cytidine 5′-diphosphate
CTP^{4-}	cytidine 5′-triphosphate
CoA	coenzyme A
Cyd	cytidine
$dGMP^{2-}$	2′-deoxyguanosine 5′-monophosphate
ΔG	Gibbs free energy of activation
DNA	deoxyribonucleic acid

$dTDP^{3-}$	thymidine [=1-(2′-deoxy-β-D-ribofuranosyl)thymine] 5′-diphosphate
$dTMP^{3-}$	thymidine 5′-monophosphate
$dTTP^{3-}$	thymidine 5′-triphosphate
FAD	flavin adenine dinucleotide
$G1P^{2-}$	glycerol 1-phosphate
G-proteins	guanine nucleotide-binding proteins
Gly	glycine
GDP^{3-}	guanosine 5′-diphosphate
GMP^{2-}	guanosine 5′-monophosphate
2′-GMP	guanosine 2′-monophosphate
GTP^{4-}	guanosine 5′-triphosphate
Guo	guanosine
His	histidine
I	ionic strength
Ino	inosine
IDP^{3-}	inosine 5′-diphosphate
IMP^{2-}	inosine 5′-monophosphate
ITP^{3-}	inosine 5′-triphosphate
ITPase	inosine triphosphate pyrophosphatase
K_a	general acidity constant
L	general ligand
Lys	lysine
M^{2+}	general divalent metal ion

$MeDP^{3-}$	methyl diphosphate
$MeMP^{2-}$	methyl monophosphate
$MePP^{3-}$	methyl phosphonylphosphate
NAD^{+}	nicotinamide adenine dinucleotide
NDP^{3-}	nucleoside 5′-diphosphate
$NPhP^{2-}$	4-nitrophenyl phosphate
NMP^{2-}	nucleoside 5′-monophosphate
Ns	nucleoside
NTP^{4-}	nucleoside 5′-triphosphate
Nu	nucleotide
phen	1,10-phenanthroline
PhP^{2-}	phenyl phosphate
PuNTP	purine-nucleoside 5′-triphosphate
PyNTP	pyrimidine-nucleoside 5′-triphosphate
Ras	product of the ras (rat sarcoma) gene
$R\text{-}DP^{3-}$	diphosphate monoester with a non-coordinating residue R
$RibMP^{2-}$	D-ribose 5′-monophosphate
$R\text{-}MP^{2-}$	(mono)phosphate monoester with a non-coordinating residue R
RNA	ribonucleic acid
RNase	ribonuclease
Ser	serine
Thd	thymidine
Thr	threonine

tRNA	transfer ribonucleic acid
$TuMP^{2-}$	tubercidin 5′-monophosphate (= 7-deaza-AMP^{2-})
Tyr	tyrosine
UDP^{3-}	uridine 5′-diphosphate
UMP^{2-}	uridine 5′-monophosphate
Urd	uridine
UTP^{4-}	uridine 5′-triphosphate

In formulas like M(H;GDP) the H^+ and the NDP^{3-} are separated by a semicolon to facilitate reading, yet they appear within the same parentheses to indicate that the proton is at the ligand without defining its location.

Formulas like $(GDP-H)^{4-}$ indicate that the ligand has lost a proton without defining the site from which it was released. These formulas should be read as GDP^{3-} *minus* H^+.

Species written without a charge either do not carry one or represent the species in general (*i.e.*, independent of their protonation degree); which of the two possibilities applies is always clear from the context.

Bibliography

[1] O. T. Avery, C. M. MacLeod, and M. McCarty, *J. Exp. Med. 79*, 137–158, **1944**.

[2] D. Voet and J. G. Voet, eds., *Biochemie (1st. edition, corrected version)*. VCH Verlagsgesellschaft mbH, Weinheim, 1994, pp. 790–791.

[3] J. D. Watson and J. Tooze, eds., *The DNA Story*. W. H. Freeman and Co., San Francisco, 1981, pp. 1–605.

[4] L. Stryer, ed., *Biochemistry (3rd. edition)*. W. H. Freeman and Co., New York, 1988, pp. 1–1089.

[5] E. Hammarsten, *Biochem. Z. 144*, 383–466, **1924**.

[6] R. B. Martin and Y. H. Mariam, *Met. Ions Biol. Syst. 8*, 57–124, **1979**.

[7] R. Tribolet and H. Sigel, *Eur. J. Biochem. 163*, 353–363, **1987**.

[8] M. Singer and P. Berg, eds., *Gene und Genome*. Spektrum Akademischer Verlag GmbH, Heidelberg, Berlin, New York, 1991, pp. 1–896.

[9] D. Voet and J. G. Voet, eds., *Biochemie (1st. edition, corrected version)*. VCH Verlagsgesellschaft mbH, Weinheim, 1994, pp. 743–771.

[10] D. Voet and J. G. Voet, eds., *Biochemie (1st. edition, corrected version)*. VCH Verlagsgesellschaft mbH, Weinheim, 1994, pp. 733–742.

[11] A. Sigel and H. Sigel, eds., *Metal Ions in Biological Systems, Vol. 32: Interactions of Metal Ions with Nucleotides, Nucleic Acids, and their Constituents*. Dekker, New York, 1996, pp. 1–814.

[12] A. S. Mildvan, *Magnesium 6*, 28–33, **1987**.

[13] S. Doublié, S. Tabor, A. M. Long, C. C. Richardson, and T. Ellenberger, *Nature 391*, 251–258, **1998**.

[14] H. Pelletier, M. R. Sawaya, A. Kumar, S. H. Wilson, and J. Kraut, *Science 264*, 1891–1903, **1994**.

[15] J. W. Arndt, W. Gong, X. Zhong, A. K. Showalter, J. Liu, C. A. Dunlap, Z. Lin, C. Paxson, M.-D. Tsai, and M. K. Chan, *Biochemistry 40*, 5368–5375, **2001**.

[16] H. R. Boume, D. A. Sanders, and F. McCormick, *Nature 348*, 125–132, **1990**.

[17] C. A. Parent and P. N. Devreotes, *Science 284*, 765–770, **1999**.

[18] S. W. Jeong and S. R. Ikeda, *Proc. Natl. Acad. Sci. USA 97*, 907–912, **2000**.

[19] M. Groysman, C. Shifrin, N. Russek, and S. Katzav, *FEBS Lett. 467*, 75–80, **2000**.

[20] M. Barbacid, *Ann. Rev. Biochem. 56*, 779–827, **1987**.

[21] C. Allin and K. Gerwert, *Biochemistry 40*, 3037–3046, **2001**.

[22] L. Tong, A. M. de Vos, M. V. Milburn, and S.-H. Kim, *J. Mol. Biol. 217*, 503–516, **1991**.

[23] H. M. Berman, J. Westbrook, Z. Feng, G. Gilliland, T. N. Bhat, H. Weissig, I. N. Shindyalov, and P. E. Bourne, *The Protein Data Bank. Nucl. Acids Res. 28*, 235–242, **2000**.

[24] M. Rohrer, T. F. Prisner, O. Brügmann, H. Käss, M. Spoerner, A. Wittinghofer, and H. R. Kalbitzer, *Biochemistry 40*, 1884–1889, **2001**.

[25] T. Maier, F. Lottspeich, and A. Bock, *Eur. J. Biochem. 230*, 133–138, **1995**.

[26] C. Liu, Y. Suo, and T. S. Leyh, *Biochemistry 33*, 7309–7314, **1994**.

[27] P. Karran and T. Lindahl, *J. Biol. Chem. 253*, 5877–5879, **1978**.

[28] M. O. Bradley and N. A. Sharkey, *Nature 274*, 607–608, **1978**.

[29] B. S. Vanderheiden, *J. Cell. Physiol. 99*, 287–301, **1979**.

[30] R. Seifert, U. Gether, K. Wenzel-Seifert, and B. K. Kobilka, *Mol. Pharmacol. 56*, 348–358, **1999**.

[31] J. F. Klinker and R. Seifert, *Biochem. Pharmacol. 54*, 551–562, **1997**.

[32] B. Zachara and J. Lewandowski, *Biochim. Biophys. Acta 353*, 253–259, **1974**.

[33] S. Lin, A. G. McLennan, K. Ying, Z. Wang, S. Gu, H. Jin, C. Wu, W. Liu, Y. Yuan, R. Tang, Y. Xie, and Y. Mao, *J. Biol. Chem. 276*, 18695–18701, **2001**.

[34] S. L. Holmes, B. M. Turner, and K. Hirschhorn, *Clin. Chim. Acta 97*, 143–153, **1979**.

[35] S. Shuman and B. Moss, *J. Biol. Chem. 263*, 6220–6225, **1988**.

[36] T. Auer, J. J. Sninsky, D. H. Gelfand, and T. W. Myers, *Nucleic Acids Res. 24*, 5021–5025, **1996**.

[37] M. Saparbaev and J. Laval, *Proc. Natl. Acad. Sci. USA 91*, 5873–5877, **1994**.

[38] G. Dianov and T. Lindahl, *Nucleic Acids Res. 19*, 3829–3833, **1991**.

[39] C. Auclair, A. Guyette, A. Levy, and I. Emerit, *Arch. Biochem. Biophys. 278*, 238–244, **1990**.

[40] W. Vormittag and W. Brannath, *Mut. Res. 476*, 71–81, **2001**.

[41] H. Sigel, F. Hofstetter, R. B. Martin, R. M. Milburn, V. Scheller-Krattiger, and K. H. Scheller, *J. Am. Chem. Soc. 106*, 7935–7946, **1984**.

[42] B. Albert, D. Bray, J. Lewis, M. Raff, K. Roberts, and J. Watson, eds., *Molecular Biology of the Cell (3rd. edition)*. Garland, New York, 1994, p. 89.

[43] P. D. Boyer, *Angew. Chem. Int. Ed. Engl. 37*, 2296–2307, **1998**.

[44] J. E. Walker, *Angew. Chem. Int. Ed. Engl. 37*, 2308–2319, **1998**.

[45] P. D. Boyer, *Biochemistry 26*, 8503–8507, **1987**.

[46] S. Löbau, J. Weber, and A. E. Senior, *Biochemistry 37*, 10846–10853, **1998**.

[47] H. Sigel, *Coord. Chem. Rev. 100*, 453–539, **1990**.

[48] J. J. G. Tesmer, R. K. Sunahara, R. A. Johnson, G. Gosselin, A. G. Gilman, and S. R. Sprang, *Science 285*, 756–760, **1999**.

[49] J. H. van de Sande, L. P. McIntosh, and T. M. Jovin, *EMBO J. 1*, 777–782, **1982**.

[50] T. K. Chiu and R. E. Dickerson, *J. Mol. Biol. 301*, 915–945, **2000**.

[51] J. Nickol and D. C. Rau, *J. Mol. Biol. 228*, 1115–1123, **1992**.

[52] W. Han, M. Dlakic, Y. J. Zhu, S. M. Lindsay, and R. E. Harrington, *Proc. Natl. Acad. Sci. USA 94*, 10565–10570, **1997**.

[53] G. Parkin, *Chem. Commun.*, 1971–1985, **2000**.

[54] J. P. Slater, A. S. Mildvan, and L. A. Loeb, *Biochem. Biophys. Res. Commun. 44*, 37–43, **1971**.

[55] G. L. Eichhorn, *Met. Ions Biol. Syst. 10*, 1–21, **1980**.

[56] F. Y.-H. Wu and C.-W. Wu, *Met. Ions Biol. Syst. 15*, 157–192, **1983**.

[57] F. Y.-H. Wu, W.-J. Huang, R. B. Sinclair, and L. Powers, *J. Biol. Chem. 267*, 25560–25567, **1992**.

[58] H. Sigel, *Chem. Soc. Rev. 22*, 255–267, **1993**.

[59] H. Sigel and B. Song, *Met. Ions Biol. Syst. 32*, 135–205, **1996**.

[60] L. D. Pettit and H. K. J. Powell, "*IUPAC Stability Constants Database*." Release 3, Version 4.02. Academic Software, Timble, Otley, West Yorkshire (UK), 1999.

[61] R. M. Smith and A. E. Martell, "*NIST Critically Selected Stability Constants of Metal Complexes.*" Reference Database 46, Version 6.0. US Department of Commerce, National Institute of Standards and Technology, Gaithersburg, MD (USA), 2001.

[62] K. Murray and P. M. May, *"Joint Expert Speciation System (JESS)."* Version 6.0. Joint venture by the Division of Water Technology, CSIR, Pretoria, South Africa, and School of Mathematical and Physical Sciences, Murdoch University, Murdoch (Western Australia), 1999.

[63] H. Sigel, *J. Am. Chem. Soc. 97*, 3209–3214, **1975**.

[64] H. Sigel, *J. Inorg. Nucl. Chem. 39*, 1903–1911, **1977**.

[65] H. Sigel, E. M. Bianchi, N. A. Corfù, Y. Kinjo, R. Tribolet, and R. B. Martin, *Chem. Eur. J. 7*, 3729–3737, **2001**.

[66] B. Albert, D. Bray, J. Lewis, M. Raff, K. Roberts, and J. Watson, eds., *Molecular Biology of the Cell (3rd. edition)*. Garland, New York, 1994, pp. 1–1294.

[67] O. Yamauchi, A. Odani, H. Masuda, and H. Sigel, *Met. Ions Biol. Syst. 32*, 207–270, **1996**.

[68] U. Heinemann and W. Saenger, *Nature 299*, 27–31, **1982**.

[69] S. Yoshizawa, G. Kawai, K. Watanabe, K. Miura, and I. Hirao, *Biochemistry 36*, 4761–4767, **1997**.

[70] W. A. Beard, D. D. Shock, X.-P. Yang, and S. F. DeLauder, *J. Biol. Chem. 277*, 8235–8242, **2002**.

[71] R. Marmorstein, M. Carey, M. Ptashne, and S. C. Harrison, *Nature 356*, 408–414, **1992**.

[72] P. O. P. Ts'o, I. S. Melvin, and A. C. Olson, *J. Am. Chem. Soc. 85*, 1289–1296, **1963**.

[73] K. H. Scheller, F. Hofstetter, P. R. Mitchell, B. Prijs, and H. Sigel, *J. Am. Chem. Soc. 103*, 247–260, **1981**.

[74] K. H. Scheller and H. Sigel, *J. Am. Chem. Soc. 105*, 5891–5900, **1983**.

[75] J. H. Phillips, Y. P. Allison, and S. J. Morris, *Neuroscience 2*, 147–152, **1977**.

[76] H. Holmsen and H. J. Day, *Ser. Haematol. IV*, 28–58, **1971**.

[77] A. Pletscher, M. Da Prada, K. H. Berneis, H. Steffen, B. Lütold, and H. G. Weder, *Adv. Cytopharmacol. 2*, 257–264, **1974**.

[78] M. Da Prada, K. H. Berneis, and A. Pletscher, *Life Sci. 10*, 639–646, **1971**.

[79] C. F. Naumann and H. Sigel, *J. Am. Chem. Soc. 96*, 2750–2756, **1974**.

[80] N. K. Rogers, G. R. Moore, and M. J. E. Sternberg, *J. Mol. Biol. 182*, 613–616, **1985**.

[81] G. Iversen, Y. I. Kharkats, and J. Ulstrup, *Mol. Phys. 94*, 297–306, **1998**.

[82] H. Sigel, R. B. Martin, R. Tibolet, U. K. Häring, and R. Malini-Balakrishnan, *Eur. J. Biochem. 152*, 187–193, **1985**.

[83] L. de Meis, *Biochim. Biophys. Acta 973*, 333–349, **1989**.

[84] G. Liang and H. Sigel, *Inorg. Chem. 29*, 3631–3632, **1990**.

[85] G. Anderegg, *Helv. Chim. Acta 46*, 2397–2410, **1963**.

[86] H. Irving and D. H. Mellor, *J. Chem. Soc.*, 5222–5237, **1962**.

[87] S. A. A. Sajadi, B. Song, and H. Sigel, *Inorg. Chim. Acta 283*, 193–201, **1998**.

[88] H. Sigel, R. Tibolet, R. Malini-Balakrishnan, and R. B. Martin, *Inorg. Chem. 26*, 2149–2157, **1987**.

[89] H. Sigel, S. S. Massoud, and N. A. Corfù, *J. Am. Chem. Soc. 116*, 2958–2971, **1994**.

[90] Y. Kinjo, L.-n. Ji, N. A. Corfù, and H. Sigel, *Inorg. Chem. 31*, 5588–5596, **1992**.

[91] N. A. Corfù, R. Tribolet, and H. Sigel, *Eur. J. Biochem. 191*, 721–735, **1990**.

[92] N. A. Corfù and H. Sigel, *Eur. J. Biochem. 199*, 659–669, **1991**.

[93] H. Sigel, E. M. Bianchi, N. A. Corfù, Y. Kinjo, R. Tribolet, and R. B. Martin, *J. Chem. Soc., Perkin Trans. 2*, 507–511, **2001**.

[94] S. S. Massoud and H. Sigel, *Inorg. Chem. 27*, 1447–1453, **1988**.

[95] R. B. Martin, *Met. Ions Biol. Syst. 32*, 61–89, **1996**.

[96] R. B. Martin, *Acc. Chem. Res. 18*, 32–38, **1985**.

[97] C. F. Moreno-Luque, E. Freisinger, B. Costisella, R. Griesser, J. Ochocki, B. Lippert, and H. Sigel, *J. Chem. Soc., Perkin Trans. 2*, 2005–2011, **2001**.

[98] R. M. Smith, A. E. Martell, and Y. Chen, *Pure Appl. Chem. 63*, 1015–1080, **1991**.

[99] H. Sigel, A. D. Zuberbühler, and O. Yamauchi, *Anal. Chim. Acta 255*, 63–72, **1991**.

[100] R. Tribolet and H. Sigel, *Eur. J. Biochem. 170*, 617–626, **1988**.

[101] R. Tribolet, R. Malini-Balakrishnan, and H. Sigel, *J. Chem. Soc., Dalton Trans.*, 2291–2303, **1985**.

[102] R. B. Martin, *Science 139*, 1198–1203, **1963**.

[103] R. B. Martin, *Met. Ions Biol. Syst. 9*, 1–39, **1979**.

[104] H. Sigel, S. S. Massoud, and R. Tribolet, *J. Am. Chem. Soc. 110*, 6857–6865, **1988**.

[105] E. M. Bianchi, S. A. A. Sajadi, B. Song, and H. Sigel, *Chem. Eur. J. 9*, 881–892, **2003**.

[106] S. A. A. Sajadi, B. Song, F. Gregàň, and H. Sigel, *Inorg. Chem. 38*, 439–448, **1999**.

[107] A. Saha, N. Saha, L.-n. Ji, J. Zhao, F. Gregàň, S. A. A. Sajadi, B. Song, and H. Sigel, *J. Biol. Inorg. Chem. 1*, 231–238, **1996**.

[108] R. Phillips, P. Eisenberg, P. George, and R. J. Rutman, *J. Biol. Chem. 240*, 4393–4397, **1965**.

[109] W. S. Sheldrick, *Acta Cryst. B 37*, 1820–1824, **1981**.

[110] K. Burger and L. Nagy, in *Biocoordination Chemistry* (K. Burger ed.), Ellis Horwood, London, 1990, pp. 236–283.

[111] N. S. Poonia and A. V. Bajaj, *Chem. Rev. 79*, 389–445, **1979**.

[112] H. Einspahr and C. E. Bugg, *Met. Ions Biol. Syst. 17*, 51–97, **1984**.

[113] K. Aoki, *Met. Ions Biol. Syst. 32*, 91–134, **1996**.

[114] G. Liang, D. Chen, M. Bastian, and H. Sigel, *J. Am. Chem. Soc. 114*, 7780–7785, **1992**.

[115] H. Sigel and L. E. Kapinos, *Coord. Chem. Rev. 200–202*, 563–594, **2000**.

[116] S. S. Massoud and H. Sigel, *Eur. J. Biochem. 179*, 451–458, **1989**.

[117] H. Sigel, N. A. Corfù, L.-n. Ji, , and R. B. Martin, *Comments Inorg. Chem. 13*, 35–59, **1992**.

[118] A. Szent-Györgyi in *Units of Biological Structure and Function* (O. H. Gaebler ed.), Academic Press, New York, 1956, pp. 393–397.

[119] R. S. Taylor and H. Diebler, *Bioinorg. Chem. 6*, 247–264, **1976**.

[120] A. Peguy and H. Diebler, *J. Phys. Chem. 81*, 1355–1358, **1977**.

[121] L. A. Herrero and A. Terrón, *J. Biol. Inorg. Chem. 5*, 269–275, **200**.

[122] M. D. Reily, T. W. Hambley, and L. G. Marzilli, *J. Am. Chem. Soc. 110*, 2999–3007, **1988**.

[123] P. Annen, S. Schildberg, and W. S. Sheldrick, *Inorg. Chim. Acta 307*, 115–124, **2000**.

[124] R. B. Martin and H. Sigel, *Comments Inorg. Chem. 6*, 285–314, **1988**.

[125] H. Sigel, D. Chen, N. A. Corfù, F. Gregàň, A. Holý, and M. Strašàk, *Helv. Chim. Acta 75*, 2634–2656, **1992**.

[126] R. Cini, M. C. Burla, A. Nunzi, G. P. Polidori, and P. F. Zanazzi, *J. Chem. Soc., Dalton Trans.*, 2467–2476, **1984**.

[127] C. V. Grant, V. Frydman, and L. Frydman, *J. Am. Chem. Soc. 122*, 11743–11744, **2000**.

[128] J. A. Cowan, *Inorg. Chem. 30*, 2740–2747, **1991**.

[129] H. Irving and R. J. P. Williams, *Nature 162*, 746–747, **1948**.

[130] H. Irving and R. J. P. Williams, *J. Chem. Soc.*, 3192–3210, **1953**.

[131] H. Sigel and D. B. McCormick, *Acc. Chem. Res. 3*, 201–208, **1970**.

[132] H. Sigel and D. B. McCormick, *Biochim. Biophys. Acta 148*, 655–664, **1967**.

[133] L. E. Kapinos, A. Holý, J. Günter, and H. Sigel, *Inorg. Chem. 40*, 2500–2508, **2001**.

[134] H. Sigel, *Eur. J. Biochem. 165*, 65–72, **1987**.

[135] G. P. P. Kuntz and G. Kotowycz, *Biochemistry 14*, 4144–4150, **1975**.

[136] J. Reedijk, *Chem. Commun.*, 801–806, **1996**.

[137] J. P. Whitehead and S. J. Lippard, *Met. Ions Biol. Syst. 32*, 687–726, **1996**.

[138] P. M. Takahara, C. A. Frederick, and J. S. Lippard, *J. Am. Chem. Soc. 118*, 12309–12321, **1996**.

[139] B. Lippert ed., *Cisplatin: Chemistry and Biochemistry of a Leading Anticancer Drug*. Wiley-VHCA, Zürich, Weinheim, 1999, pp. 1–563.

[140] E. Sletten and N. Å. Frøystein, *Met. Ions Biol. Syst. 32*, 397–418, **1996**.

[141] J. E. Wedekind and D. B. McKay, *Nature Struct. Biol. 6*, 261–268, **1999**.

[142] M. Katahira, M. H. Kim, T. Sugiyama, Y. Nishimura, and S. Uesugi, *Eur. J. Biochem. 255*, 727–733, **1998**.

[143] P. Chartrand, N. Usman, and R. Cedergren, *Biochemistry 36*, 3145–3150, **1997**.

[144] H. Sigel, *Pure Appl. Chem. 70*, 969–976, **1998**.

[145] H. Sigel, *Biol. Trace Elem. Res. 21*, 49–59, **1989**.

[146] H. Sigel and N. A. Corfù, *Eur. J. Biochem. 240*, 508–517, **1996**.

[147] M. M. Taqui Khan and A. E. Martell, *J. Am. Chem. Soc. 84*, 3037–3041, **1962**.

[148] C. M. Frey and J. E. Stuehr, *J. Am. Chem. Soc. 94*, 7787–8904, **1972**.

[149] C. M. Frey and J. E. Stuehr, *J. Am. Chem. Soc. 100*, 139–145, **1978**.

[150] M. M. Khalil, *J. Chem. Eng. Data 45*, 70–74, **2000**.

[151] B. Song, J. Zhao, R. Griesser, C. Meiser, H. Sigel, and B. Lippert, *Chem. Eur. J. 5*, 2374–2387, **1999**.

[152] H. Sigel and B. Lippert, *Pure Appl. Chem. 70*, 845–854, **1998**.

[153] M. Bastian and H. Sigel, *J. Coord. Chem. 23*, 137–154, **1991**.

[154] E. M. Bianchi, S. A. A. Sajadi, B. Song, and H. Sigel, *Inorg. Chim. Acta 300-302*, 487–498, **2000**.

[155] Y. H. Mariam and R. B. Martin, *Inorg. Chim. Acta 35*, 23–28, **1979**.

[156] J. Sari and J. Belaich, *J. Am. Chem. Soc. 95*, 7491–7496, **1973**.

[157] K. Hotta, J. Brahms, and M. Morales, *J. Am. Chem. Soc. 83*, 997–998, **1961**.

[158] H. Sigel and R. B. Martin, *Chem. Rev. 82*, 385–426, **1982**.

[159] Y. Kinjo, R. Tribolet, N. A. Corfù, and H. Sigel, *Inorg. Chem. 28*, 1480–1489, **1989**.

[160] L. G. Marzilli, B. de Castro, and C. Solorzano, *J. Am. Chem. Soc. 104*, 461–466, **1982**.

[161] M. Quirós, J. M. Salas, M. P. Sánchez, J. R. Alabart, and R. Faure, *Inorg. Chem. 30*, 2916–2921, **1991**.

[162] G. Frommer, H. Preut, and B. Lippert, *Inorg. Chim. Acta 193*, 111–117, **1992**.

[163] T. Kohzuma, H. Masuda, and O. Yamauchi, *J. Am. Chem. Soc. 111*, 3431–3433, **1989**.

[164] B. Fischer, J. Strähle, and M. Viscontini, *Helv. Chim. Acta 74*, 1544–1554, **1991**.

[165] K. Yamanouchi, J. T. Huneke, J. H. Enemark, R. D. Taylor, and J. T. Spence, *Acta Crystallogr. B35*, 2326–2330, **1979**.

[166] H. Sigel, *Angew. Chem. Int. Ed. Engl. 14*, 394–402, **1975**.

[167] S. S. Massoud, R. Tribolet, and H. Sigel, *Eur. J. Biochem. 187*, 387–393, **1990**.

[168] S. S. Massoud and H. Sigel, *Chimia 44*, 55–57, **1990**.

[169] M. S. Lüth, L. E. Kapinos, B. Song, B. Lippert, and H. Sigel, *J. Chem. Soc., Dalton Trans.*, 357–365, **1999**.

[170] H. Sigel, *Pure Appl. Chem. 61*, 923–932, **1989**.

[171] H. Sigel, K. H. Scheller, and R. M. Milburn, *Inorg. Chem. 23*, 1933–1938, **1984**.

[172] R. Malini-Balakrishnan, K. H. Scheller, U. K. Häring, R. Tribolet, and H. Sigel, *Inorg. Chem. 24*, 2067–2076, **1985**.

[173] H. Sigel, B. E. Fischer, and B. Prijs, *J. Am. Chem. Soc. 99*, 4489–4496, **1977**.

[174] H. Sigel, *Inorg. Chem. 19*, 1411–1413, **1980**.

[175] R. Griesser and H. Sigel, *Inorg. Chem. 9*, 1238–1243, **1970**.

[176] H. Sigel, P. R. Huber, R. Griesser, and B. Prijs, *Inorg. Chem. 12*, 1198–1200, **1973**.

[177] B. Song, S. A. A. Sajadi, F. Gregàň, N. Prónayová, and H. Sigel, *Inorg. Chim. Acta 273*, 101–105, **1998**.

[178] P. R. Mitchell and H. Sigel, *J. Am. Chem. Soc. 100*, 1564–1570, **1978**.

[179] P. R. Mitchell, B. Prijs, and H. Sigel, *Helv. Chim. Acta 62*, 1723–1735, **1979**.

[180] W. S. Sheldrick, *Z. Naturforsch. 37b*, 863–871, **1982**.

[181] D. Chen, M. Bastian, F. Gregáň, A. Holý, and H. Sigel, *J. Chem. Soc., Dalton Trans.*, 1537–1546, **1993**.

[182] L. E. Kapinos, B. Song, and H. Sigel, *Chem. Eur. J. 5*, 1794–1802, **1999**.

[183] N. A. Corfù and H. Sigel, results to be published.

[184] J. B. Orenberg, B. E. Fischer, and H. Sigel, *J. Inorg. Nucl. Chem. 42*, 785–792, **1980**.

[185] H. Sigel, *Coord. Chem. Rev. 144*, 287–319, **1995**.

[186] H. Sigel, *Pure Appl. Chem. 71*, 1727–1740, **1999**.

[187] H. Sigel, B. Song, C. A. Blindauer, L. E. Kapinos, F. Gregàň, and N. Prónayová, *Chem. Commun.*, 743–744, **1999**.

[188] H. Winkler and S. W. Carmichael, in *The Secretory Granule* (A. M. Poisner and J. M. Trifaró, eds.), Elsevier Biomedical Press, Amsterdam, 1982, pp. 3–79.

[189] N. A. Thorn, J. T. Russel, and M. Treiman, in *The Secretory Granule* (A. M. Poisner and J. M. Trifaró, eds.), Elsevier Biomedical Press, Amsterdam, 1982, pp. 119–151.

[190] S. S. Massoud and H. Sigel, *Inorg. Chim. Acta 159*, 243–252, **1989**.

[191] D. Chen, F. Gregàň, A. Holý, and H. Sigel, *Inorg. Chem. 32*, 5377–5384, **1993**.

[192] H. Sigel, R. Malini-Balakrishnan, and U. K. Häring, *J. Am. Chem. Soc. 107*, 5137–5148, **1985**.

[193] K. A. Connors and S.-r. Sun, *J. Am. Chem. Soc. 93*, 7239–7244, **1971**.

[194] B. Farzami, Y. H. Mariam, and F. Jordan, *Biochemistry 16*, 1105–1110, **1977**.

[195] G. Liang, N. A. Corfù, and H. Sigel, *Z. Naturforsch. 44b*, 538–542, **1989**.

[196] M. J. Bloemink and J. Reedijk, *Met. Ions Biol. Syst. 32*, 641–685, **1996**.

[197] D. Chatterji and F. Y.-H. Wu, *Biochemistry 21*, 4657–4664, **1982**.

[198] D. Chatterji, C.-W. Wu, and F. Y.-H. Wu, *J. Biol. Chem. 259*, 284–289, **1984**.

[199] D. C. Rees, *J. Mol. Biol. 141*, 323–326, **1980**.

[200] G. Åkerlöf and O. A. Short, *J. Am. Chem. Soc. 58*, 1241–1243, **1936**.

[201] G. Åkerlöf and O. A. Short, *J. Am. Chem. Soc. 75*, 6357, **1953**.

[202] F. E. Critchfield, J. A. Gibson, Jr., and J. L. Hall, *J. Am. Chem. Soc. 75*, 1991–1992, **1953**.

[203] A. A. Hirata and D. Appleman, *Anal. Chem. 31*, 2097–2099, **1959**.

[204] P. W. Schneider and H. Brintzinger, *Helv. Chim. Acta 47*, 1717–1733, **1964**.

[205] C. Blindauer, *Untersuchungen zu Stabilität, Struktur und Reaktivität von Metallionenkomplexen einiger antiviraler Nucleotid-Analoga*. PhD thesis, University of Basel, Institute of Inorganic Chemistry, 1998.

[206] H. M. Irving, M. G. Miles, and L. D. Pettit, *Anal. Chim. Acta 38*, 475–488, **1967**.

[207] H. Sigel, R. Griesser, and B. Prijs, *Z. Naturforsch. 27b*, 353–364, **1972**.

[208] Y. K. Agrawal, *Talanta 20*, 1354–1356, **1973**.

[209] L. G. V. Uitert and C. G. Haas, *J. Am. Chem. Soc. 75*, 451–455, **1953**.

[210] L. G. V. Uitert and W. C. Fernelius, *J. Am. Chem. Soc. 76*, 5887–5888, **1954**.

[211] R. G. Bates, *Determination of pH: Theory and Practice*. Wiley, New York, 1973, pp. 243–249.

[212] L. Sachs, *Statistisches Auswertungsmethoden*. Springer-Verlag, Berlin, second ed., 1969.

[213] P. D. Bevington, *Data Reduction and Error Analysis for the Physical Sciences*. Mc Graw Hill, New York, 1969.

Summary

Nucleotides and metal ions are involved in the basic metabolic processes of life, participating as substrates in enzymatic reactions in the form of metal ion complexes. Hence, their acid–base and metal-ion coordinating properties were intensely studied in the past years. However, these studies were mainly devoted to nucleoside 5′-monophosphates, and to ATP. Only little information exists on nucleoside 5′-diphosphates and GTP or ITP. Considering their importance in biochemical reactions, and the recently growing interest on G-proteins, which utilize guanosine 5′-triphosphate, a systematic investigation on their coordinating properties is needed.

In this study, mainly based on potentiometric pH titrations in aqueous solution at 25 °C and I = 0.1 M ($NaNO_3$), the acidity constants of purine-nucleoside 5′-di- and 5′-triphosphates (adenosine 5′-diphosphate; guanosine and inosine 5′-di- and 5′-triphosphates, here designated as Nu) and the stability constants of their 1:1 complexes formed with ten metal ions (M^{2+} = Mg^{2+}, Ca^{2+}, Sr^{2+}, Ba^{2+}, Mn^{2+}, Co^{2+}, Ni^{2+}, Cu^{2+}, Zn^{2+}, or Cd^{2+}) have been determined.

Nucleotides are composed of three units, each of them with potential binding sites for protons and metal ions. In this work, only the properties of the phosphate groups and the nucleobase residues have been investigated in detail, since the sugar moiety interacts with metal ions or releases protons only under special conditions or in the strongly alkaline pH range.

Analysis of the collected equilibrium constant data reveals that the stability of all these complexes is largely governed by the metal ion affinity of the phosphate residue. While for the complexes formed with the divalent ions of the second half

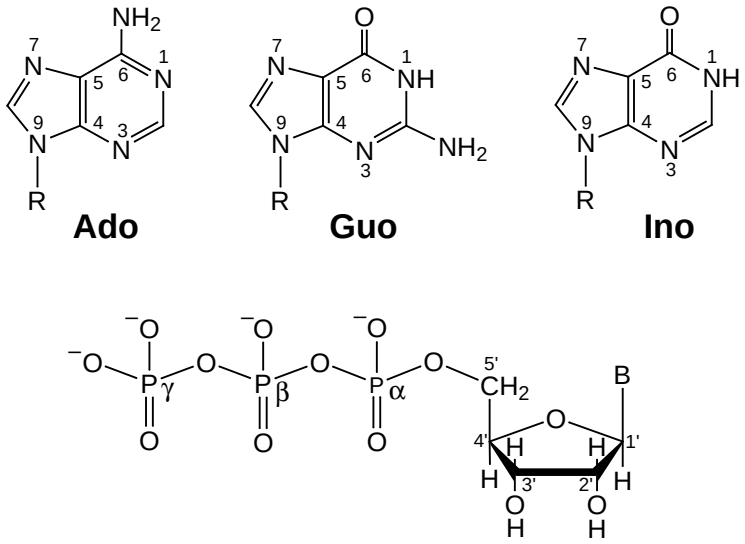

Figure 1: Chemical structure of the purine-nucleotides 5′-mono-, di-, or triphosphates (R = ribosyl 5′-mono-, 5′-di-, or 5′-triphosphate); Ado = adenosine; Guo = guanosine; Ino = inosine. The ribosyl 5′-triphosphate residue is shown in the lower part of the figure, where B represents one of the three bases given above.

of the 3d series, including Zn^{2+} and Cd^{2+}, macrochelate formation is an important property in all the M(Nu) species considered, with GDP, GTP and ITP, the formation of macrochelated species is considerable with all the metal ions studied, including the alkaline earth ions. These macrochelates are formed by the interaction of the phosphate-coordinated metal ion with N7 of the purine moiety. Analysis of the isomer ratio between the open and macrochelated species shows that the formation degree of the latter increases in the series $M(AP)_{cl} < M(IP)_{cl} < M(GP)_{cl}$ (where AP, IP, or GP represents the nucleoside phosphate, *i.e.*, NMP^{2-}, NDP^{3-}, or NTP^{4-}). Moreover, it is observed that, for a given metal ion and nucleobase residue, the formation degrees of such macrochelates are identical within the error limits, that is, independent of the number of phosphate groups present in the ligands and in the coordination sphere of the metal ions, e.g., $M(GMP)_{cl} \simeq M(GDP)^{-}_{cl} \simeq M(GTP)^{2-}_{cl}$. These results clearly indicate that the properties of the N7 site are mainly responsible for the extent of macrochelate formation, at least as long as the

coordination sphere of the metal ion is not saturated.

Comparison of the formation degrees of $M(Nu)_{cl}$ as determined from stability constant measurements with the formation degrees determined by methods that monitor only innersphere binding reveals that macrochelated species of (at least) two kinds occur: one in which the phosphate-coordinated metal ion is innersphere bound and one in which the interaction is of an outersphere type and occurs via hydrogen bonding of a metal ion-coordinated water molecule to N7.

Another kind of interaction has been quantified between the 3d metal ions, as well as Zn^{2+} and Cd^{2+} (with the exception of Cu^{2+}, which forms hydroxo complexes at a relatively low pH) and the guanine and hypoxanthine residues of GDP and IDP: after deprotonation of the (N1)H site of the nucleobase, $M(GDP-H)^{2-}$ and $M(IDP-H)^{2-}$ complexes are formed. An enhanced stability is measured for these complexes, compared to what would be expected on the basis of a pure electrostatic attraction, as is observed for the complexes of the alkaline earth metal ions. An additional interaction, next to the one with N7, between the (C6)O, carrying part of the negative charge created upon deprotonation of N1, and the metal ion is expected to be responsible for this additionally enhanced stability. This interaction could again be of an innersphere or an outersphere kind, and a schematic representation of the possible structures of one of these complexes is shown in Figure 2.

For the correct positioning of the metal ion during an enzymatic reaction involving nucleotides, the anchoring process of the nucleotide substrate in the active site of the enzyme is essential. This recognition process is governed by hydrogen bonding and nucleobase stacking with suitable amino acid side-chain residues of the protein. Here, the interactions between the purine-nucleoside 5′-diphosphates and two low molecular-weight ligands (arm = 2,2′-bipyridine, bpy, or 1,10-phenanthroline, phen; see Figure 3) have been investigated. The heteroatomic amines (arm) can simulate the role that phenyl or indole moieties of phenylalanyl or tryptophanyl residues play in protein-nucleotide interactions. The advantage of these amines is that they allow a detailed quantification of the intramolecular stacking interaction

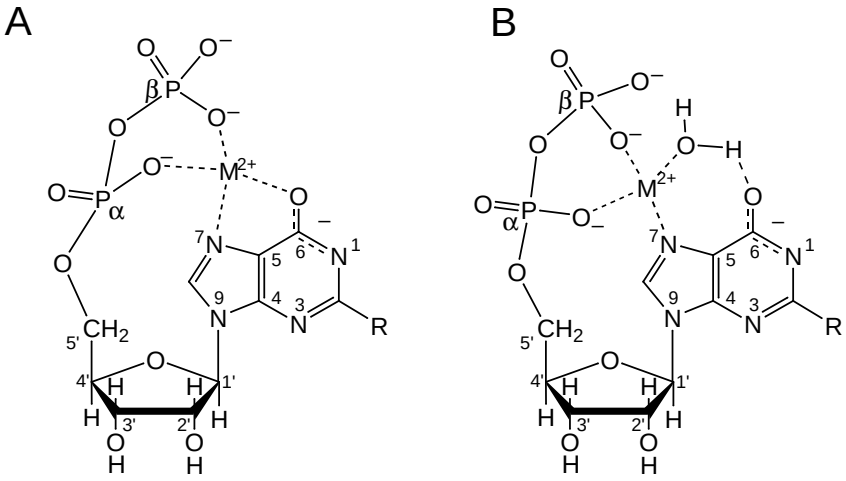

Figure 2: Schematic and simplified structures for the macrochelated N1-deprotonated innersphere (A) and outersphere (B) isomers of M(GDP−H)$^{2-}$ (R = NH_2) and M(IDP−H)$^{2-}$ (R = H).

between the aromatic rings of the Cu(arm)$^{2+}$ species and the nucleobase residue of the nucleotide.

The analysis of the stability constants measured for these complexes allowed the quantification of their isomeric distribution.

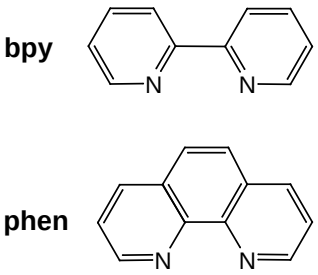

Figure 3: Structures of 2,2′-bipyridine (bpy) and 1,10-phenanthroline (phen).

Intramolecular stacks are shown to form not only between the aromatic rings of arm and the purine residue of ADP^{3-}, GDP^{3-}, and IDP^{3-}, but also in their mono-protonated Cu(arm)(H;NDP) complexes, where the proton sits at the terminal β-phosphate group. Indeed, the stacking tendency of the nucleobase residue remains

practically unaffected by the phosphate protonation. Moreover, the comparison of the data collected now with those existent on purine-nucleoside 5′-mono- and 5′-triphosphates shows that the length of the phosphate residue has no significant effect on the formation degree of the intramolecular stacks: the absolute stabilities of the complexes differ, but the position of the intramolecular stacking equilibrium is, within the error limits, identical.

Stack formation in the Cu(phen)(Nu) complexes is slightly favoured over that in the Cu(bpy)(Nu) complexes: the larger phen stacks somewhat better with the purine residue than bpy. Such a tendency does not exist in the Cu(arm)$^{2+}$ complexes of the uridine nucleotides: the single ring of the uracil residue may stack with bpy as well as with phen, and its stacking tendency is considerably smaller than that of the two-ring purine residues.

One can then conclude that the stacking tendency of a nucleobase moiety in a nucleotide complex does not depend on the denticity or the length of the phosphate chain, but on the nature of the nucleobase.

The acid–base and Cu^{2+}-binding properties of GDP have been further investigated in aqueous–organic solvent mixtures. At the protein-water interface and in the active-site cavities of enzymes, the effective dielectric constant is reduced compared to the situation in bulk water, due to the presence of aliphatic and aromatic amino acid side chains in the proteins. By using mixtures of 30 and 50% 1,4-dioxane in water, dielectric constants of about 60 and 35 are reached, values that are comparable with the estimates of the dielectric constants at the protein-water interface or in the active sites of enzymes, that range from about 30 to 70. By employing such solvent mixtures, the situation in these locations may be simulated to some extent.

Some general conclusions can be made comparing the data collected for this work with those found in the literature: a decreasing solvent polarity generally increases the basicity of the phosphate group(s) and favours phosphate-metal ion complex stability, as shown by the (sometimes drastic) increase of the stability constant values.

In Figure 4 the percentages of macrochelated species involving Cu^{2+} and four different nucleotides are plotted as a function of the percentage of 1,4-dioxane added to the aqueous solution. It is evident that the addition of dioxane to the aqueous solution of the complexes alters the extent of macrochelate formation considerably, and not in an easily predictable manner!

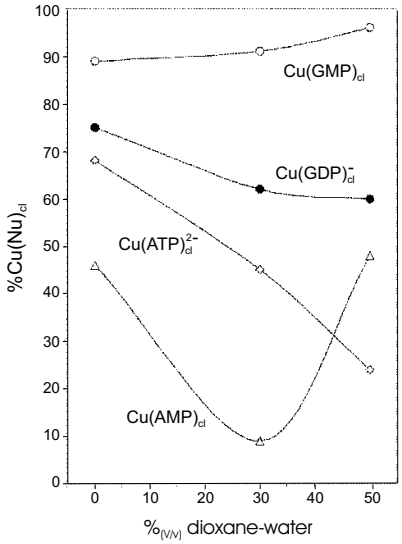

Figure 4: Formation degree of the macrochelates in the binary Cu(AMP), $Cu(ATP)^{2-}$, Cu(GMP), and $Cu(GDP)^{-}$ complex systems as a function of the percentage of 1,4-dioxane added to the aqueous reagent mixtures (I = 0.1 M, $NaNO_3$; 25 °C).

More research efforts are needed to clarify better the stability and structure of metal ion-nucleotide complexes in aqueous organic solvent mixtures. Very little is known about the variation in the formation degree of the various isomers if the polarity of the solvent changes, and nothing is known about the effect of this polarity change on the extent of inner-/outersphere complexation and about the possibility that in low dielectric constant environments the hydroxy groups of sugars may begin to participate in complex formation. Considering that in nature in most (or all) reactions that involve nucleotides metal ions are present, more studies are highly desirable.